NASA CONTRACTOR REPORT

NASA CR-1244

HYDROGEN-OXYGEN ELECTROLYTIC REGENERATIVE FUEL CELLS

by M. Klein and R. Astrin

Prepared by
ELECTRO-OPTICAL SYSTEMS, INC.
Pasadena, Calif.
for Lewis Research Center

NATIONAL AERONAUTICS AND SPACE ADMINISTRATION • WASHINGTON, D. C. • FEBRUARY 1969

HYDROGEN-OXYGEN ELECTROLYTIC REGENERATIVE FUEL CELLS

By M. Klein and R. Astrin

Prepared under Contract No. NAS 3-2781 by
ELECTRO-OPTICAL SYSTEMS, INC.
Pasadena, Calif.

for Lewis Research Center

NATIONAL AERONAUTICS AND SPACE ADMINISTRATION

For sale by the Clearinghouse for Federal Scientific and Technical Information
Springfield, Virginia 22151 – CFSTI price $3.00

FOREWORD

The work described herein, which was done by Electro-Optical Systems, Inc., was performed under NASA Contract NAS 3-2781 with Mr. D. G. Soltis, Space Power Systems as Project Manager. The report was originally issued as Electro-Optical Systems Report EOS-4110.

CONTENTS

CONTENTS (contd)

ILLUSTRATIONS

ILLUSTRATIONS (contd)

ILLUSTRATIONS (contd)

ILLUSTRATIONS (contd)

ILLUSTRATIONS (contd)

SECTION 1

INTRODUCTION

One of the promising concepts for advancing the technology of electrochemical energy storage devices is the electrolytically regenerative fuel cell. To develop this concept into useable hardware for orbital and interplanetary space applications, Electro-Optical Systems, Inc., has been conducting a research and development program to define the design and operational parameters and the problem areas involved. This effort has been conducted under the sponsorship and technical direction of the Space Power Systems Office, Lewis Research Center, National Aeronautics and Space Administration.

This report reviews the progress made on the development of the regenerative hydrogen-oxygen fuel cell under contract NAS3-2781 during the period 20 June 1963 through 30 September 1967.

The regenerative hydrogen-oxygen cell is basically a combination of a hydrogen-oxygen primary fuel cell and a water electrolysis cell in one compact package. The research and development program was based on a capillary matrix fuel cell concept in which the electrolyte containing the water of reaction is absorbed in a matrix located between the fuel cell electrodes. During the charge mode of operation, water contained within this matrix is electrolyzed, producing hydrogen at the anode and oxygen at the cathode. As the gases are evolved, they are fed through manifolds to integral tanks. During discharge, the stored gases are reacted at the electrodes to form water which returns to, and is absorbed

by, the matrix. The same electrodes serve as the reacting surface for both the charge and discharge modes of operation. Concentrated aqueous potassium hydroxide, contained in the matrix, serves as the electrolyte and as the source of water for electrolysis. The quantity of electrolyte employed is such that the solution is totally absorbed by the matrix and no free liquid exists within the system. With the integral gas tankage, there is no flow of materials in and out of the unit, and it can be operated as a sealed container similar to conventional secondary batteries.

Such a device offers advantages in the areas of watt-hour per pound, high ambient temperature operation, and comparable cycle life to that which could be obtained from existing secondary batteries. The program contained a number of modifications and additions to the statement of work. The detailed statement of work is shown in the appendix.

As initially conceived, Phase I of the development program was divided into three tasks. The first task was an analytical investigation of a complete power package including a silicon solar cell power source, a hydrogen-oxygen fuel cell, a power conditioner and required accessories. Both component and total system weights were calculated as a function of orbital altitude and power level. The second task involved the design and fabrication of a multicell, 75-watt 6-cell device suitable for scaling up to higher voltage levels. The third task consisted of the testing and experimental evaluation of the cell to determine its operational characteristics. As a result of technical difficulties encountered in the initial phase, single cell testing was undertaken to improve the cell components and performance. Phase II consisted of investigations to optimize the fuel cell electrodes, investigation of the asbestos matrix, and the development of a substitute matrix material for the regenerative fuel cell. Simultaneously with these tasks the design, development, building, and testing of additional 6-cell units,

and a 500-watt, 600-watt-hour, 34-cell unit capable of yielding approximately 15 watt-hours per pound were accomplished.

Section 2 is a summary of the activities accomplished during this program, and Section 3 presents the design analysis of the fuel cell, Sections 4, 5, 6, and 7 describe the development of the single cell, 6-cell, and 34-cell units. These latter sections present the evolutionary progress made in the various aspects of the program; however, the chronological order of events does not follow the report format since the multicell testing and component developments were interspersed with the single cell activities of the program. Figure 1 shows the schedule of major task efforts over the past five years.

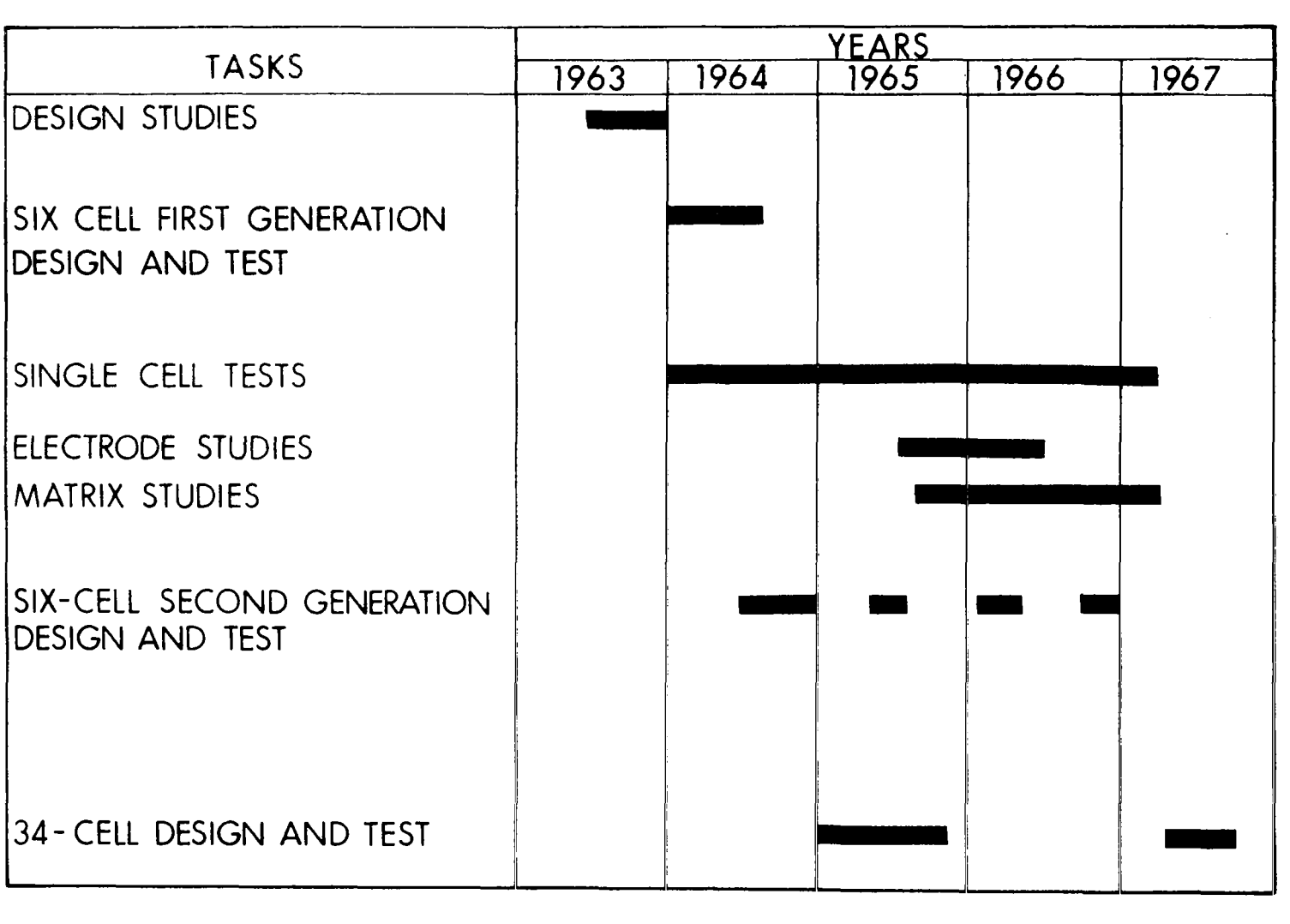

Figure 1. Program Schedule

SECTION 2

SUMMARY

A research and development program to develop an eletrolytic regenerative hydrogen-oxygen fuel cell was conducted under contract NAS3-2781. The program concentrated on the development of a capillary matrix bipolar pile fuel cell stack with integral gas storage tankage. Tasks were undertaken to select and develop electrodes and matrix materials for the regenerative fuel cell. A cell stack employing an American Cyanamid AB-6 oxygen electrode, a potassium titanate matrix, and a hydrogen electrode consisting of a platinized sintered porous nickel plaque was found to comprise the best cell construction. Such cells were cycled on a 35-minute discharge/65-minute charge test regime and attained lifetimes in the 500 to 1000 cycle range with minimal deterioration.

A 500-watt 34-cell prototype, assembled at the end of the program, was subjected to a limited number of test cycles and yielded approximately 15 watt hours per pound. The program demonstrated the potential of the regenerative hydrogen-oxygen fuel cell concept and it is apparent that increases in cycle life and energy density can be achieved with additional development.

SECTION 3

DESIGN ANALYSIS

The entire program was initiated with a design analysis task to determine the weight and performance capabilities of the regenerative fuel cell under a range of operating conditions. This analysis and all the subsequent work were based on a capillary matrix fuel cell in which water was stored in the matrix between the hydrogen and oxygen electrodes. Figure 2 is a schematic of the construction principles of this cell. The design employs a bipolar plate (which contains integral manifold channels) upon which hydrogen and oxygen electrodes are attached. The matrix is between the electrodes. A ring spacer is employed to obtain the desired compression on the matrix. Integral manifolding allows the hydrogen and oxygen gases to flow out the back side of the electrodes, through the manifolds, and into their respective gas storage compartments. In the integral gas storage tank concept, the fuel cell stack is placed within the gas storage tanks, and is used to separate the hydrogen and oxygen compartments.

Typically, the matrix is placed between the electrodes, and is compressed during cell assembly. This compression severely decreases cross leakage of hydrogen and oxygen through the matrix and causes a partial penetration of the electrolyte into each of the electrodes.

During charge, i.e., the electrolysis mode of operation, water is decomposed from the matrix at the rate of 0.336 gram per ampere hour of charge, Limitations exist as to the extent of charging, aside from

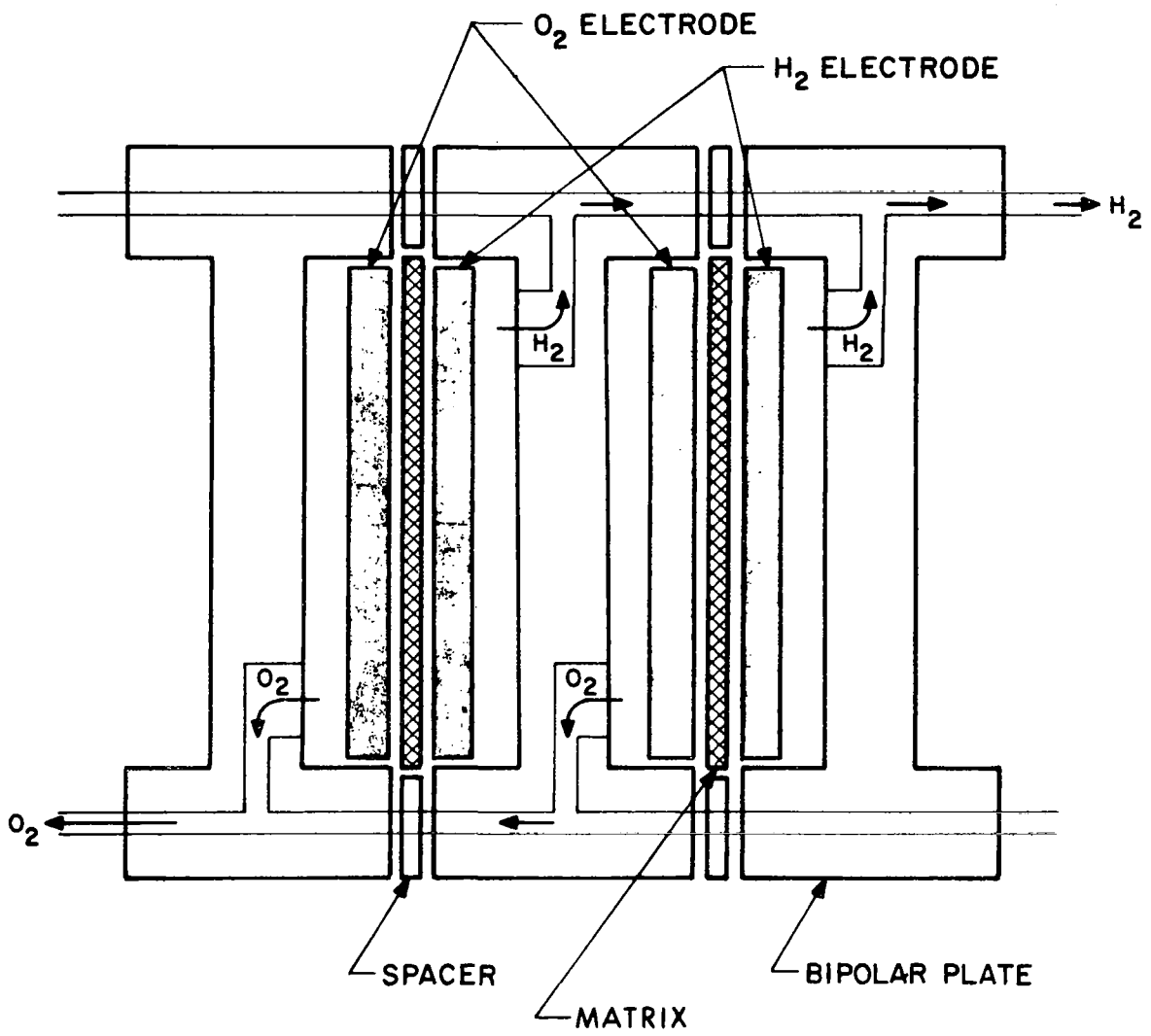

Figure 2. Cell Construction Details

the obvious one of increased resistance due to loss of ionic conductivity. If charge is continued, cross leakage of hydrogen and oxygen through the matrix becomes appreciable. This cross leakage results in water formation chemically at the electrodes.

As discharge proceeds, water is formed that is absorbed by the asbestos matrix. Here, too, limitations exist since excessively rapid formation of water will result in flooding of the reaction zones and a decrease in performance. The effects and limitations of the system, in regard to drying out toward the end of charge and flooding toward the end of discharge are mass-transport rate-dependent processes. Slower rates of charge and discharge allow the use of higher capacities without encountering performance degradation.

Since the electrodes serve both in the charge (electrolysis) and discharge (fuel cell) mode, their design criteria are somewhat different from those of an electrode used exclusively for either of the above operations. From a purely electrolysis standpoint, it is desirable to have a nearly flooded system; whereas for the primary fuel cell mode, a somewhat dryer reacting surface, maximizing the triphase reaction area, is desirable. These two criteria are in conflict. Therefore, a design compromise had to be made for use in a regenerative mode, as to electrolyte quantity within the matrix, concentration of electrolyte, matrix compression, and electrode structure.

Based on these criteria the initial design analysis was made. The first generation design employed stearic acid as a thermal storage material which absorbed heat during the discharge portion and rejected heat during the charge portion to enable the fuel cell to perform at a constant operating temperature.

3.1 WEIGHT RELATIONSHIPS

The system analysis had been made by first relating the component weights to the fuel cell electrode area, and then relating the latter to the pertinent operating parameters of the system. After this part of the analysis was completed, the weight relationships were programmed into an IBM computer, and all parameters pertinent to the problem were varied systematically. For a given orbit and discharge power, the optimum current density for minimum system weight can be determined. From this current density, the number and size of the cells was calculated. The results of this analysis are given below.

3.2 RESULTS OF THE OPTIMIZATION STUDIES

The expressions for the weight totals were programmed into an IBM-1620 computer. Orbital altitudes of 300, 1000, 5000, 10,000, and 22,400 miles were used with current densities of 10, 20, 40, 60, 80, 100, 120, 140, 160, 180 and 200 mA/cm^2. The appropriate number of cells was used according to the step function in Fig. 3. Calculations for only two different output power levels were used. Figure 4 shows the electrode diameter as a function of the discharge current density necessary to give either 100, 500, or 1000 watts for an output of 28 volts. For power levels above 500 watts the appropriate number of 500-watt modules can be used and each component weight will scale up almost exactly in proportion to the discharge power.

One feature which is immediately evident is that the optimum current density (i.e., the current density which yields minimum system weight) ranges from 80 mA/cm^2 at the lowest orbit to 120 mA/cm^2 at the highest. The reason for this is due mostly to the much lower solar panel weight

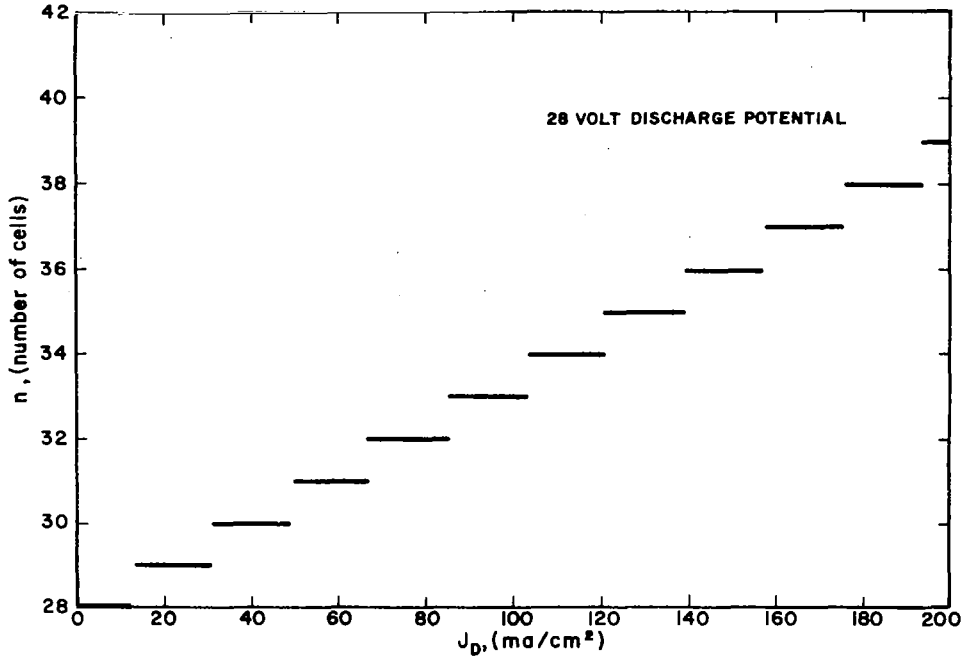

Figure 3. No. of Cells Required as a Function of Current Density

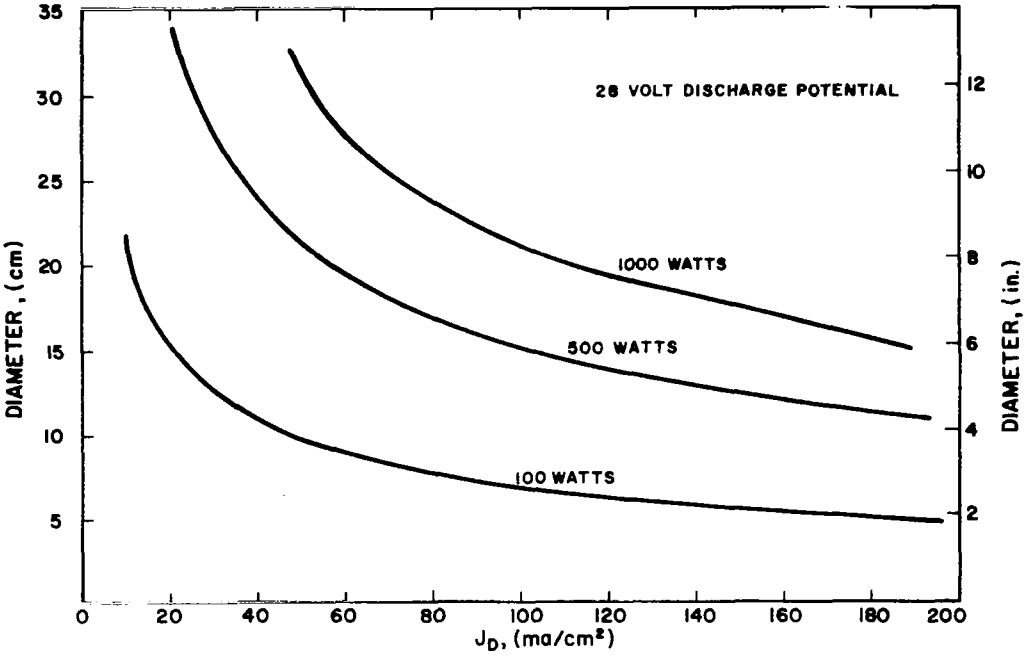

Figure 4. Electrode Size versus Current Density

at the higher orbits. This allows operation at higher current densities while paying only a negligible penalty for the lower efficiencies. The solar panel weight drops off sharply with increasing altitude because of the rapidly decreasing value of the fraction of the orbit during which the fuel cell is discharging. At the highest orbit, the fuel cell is hardly on more than a trickle charge even for the highest discharge current densities. The charging potential would be even lower than that assumed here, since a linear charge polarization curve was used for all charge as well as for all discharge current densities. However, this refinement would yield a negligible correction to the panel weight.

Another fact which is immediately evident is that system weight is only a weak function of discharge current density within rather broad limits. In the design of a fuel cell this leaves a wide latitude in the selection of a discharge current density. It will very likely prove desirable to operate at somewhat less than the optimum current density in order to build in a large overload factor.

It was also quite noticeable that the thermal storage material (stearic acid, in this case) adds considerable weight to the system, particularly at the higher orbital altitudes. More thermal storage is necessary in higher orbits because of the greater variation between heat generation on discharge and heat generation on charge, when the heat generation is often negative. It should be remembered that the curves showing auxiliary weights really represent the weight of stearic acid plus its container, except for the power conditioner. The latter adds a constant 0.91 kg (2 lb) for the 100-watt system or 3.2 kg (7 lb) for the 500-watt system.

In terms of energy/weight ratios, it can be seen that for minimum system weight, the 100-watt fuel cell will yield 11.5 watt-hr/lb at the lowest orbit and 25.3 watt-hr/lb at the highest. The corresponding figures for

the 500-watt system are 13.1 and 29.0. If the thermal storage system is used, the fuel cell energy/weight ratio is considerably reduced, especially for the higher orbits. The figure for the 100-watt system in the 300-mile orbit becomes 7 watt-hr/lb; and for the 500-watt system in the 22,400-mile orbit, 13 watt-hr/lb.

3.3 HEAT BALANCE STUDIES

Heat generation and heat transfer analyses were performed to determine the necessity of supplying either external heating or cooling to the assembly for testing within the laboratory (earth environment rather than space environment). The results of these analyses are presented below.

3.3.1 HEAT GENERATION

Heat generation within the fuel cell is attributed to two causes; the first is cell polarization, and the second is the entropy change for the hydrogen-oxygen reaction. During discharge, the heat generation rate for a single cell is given by the following relationship:

$$Q = \Delta V \cdot I + T \cdot \Delta S \cdot I \cdot k$$

where

Q = heat generation (watts)

ΔV = polarization loss (volts), equal to the difference between the theoretical open circuit voltage 1.23 volts, and the operating cell voltage, i.e., 0.7 to 1.0 volts.

I = cell current (amps)

T = temperature (^{o}K)

S = entropy change for the hydrogen-oxygen reaction, cal/mol/^{o}K)

k = conversion factor to express the second term in the right hand side of the equation in terms of watts. The constant is the product of two other conversion

factors which consist of the following:

$$k = \frac{\text{watt-hr}}{\text{cal}} \times \frac{\text{mols } H_2O}{\text{amp-hr}}$$

$$k = (1.163 \times 10^{-3}) \times (.0189) = 2.2 \times 10^{-5}$$

Based on a single cell performance data, the following values may be substituted in the above equation to obtain the heat generation per cell during discharge at 19 amps and charge at 9.6 amps.

ΔV = 0.43 volt discharge, 0.31 volt charge

I = 19 amps discharge, 9.6 amps charge

T = $70^{o}C = 343^{o}K$

ΔS = 39 cal/mol/^{o}K

k = 2.2×10^{-5}

The heat generation is thus found to be 13.8 watts for discharge and 0 watts for charge for a single cell. For the six-cell assembly the rates will be six times the unit cell rate and correspond to values of 82.8 watts for discharge and again 0 watts for charge.

The rate of heat generation in the six-cell assembly has been calculated for other current loads, and the results are given in Fig. 5. Inspection of this figure indicates that the heat generation during discharge is always positive and varies in a near linear manner with current. For charge, however, it is noted that the heat generation is slightly negative at low currents and becomes positive at higher currents. At low charge currents, then it may be said that the assembly will absorb heat from the surroundings.

3.3.2 HEAT TRANSFER

For ambient test conditions, heat may be transferred from the assembly by both convection and radiation. The rates of heat transfer by these

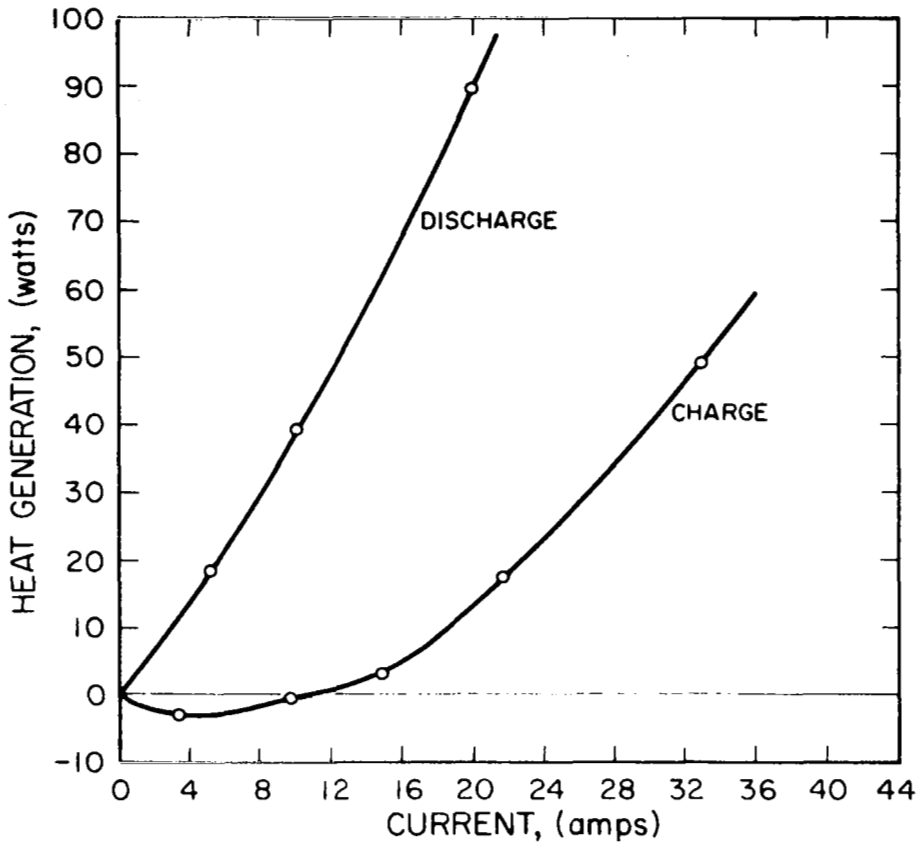

Figure 5. Heat Generation in Six Cell Prototype

mechanisms are given by the following equations:

$$Q_C = h\,A\,\Delta t; \quad h = 0.5\left(\frac{\Delta t}{D}\right)^{.25}$$

$$Q_R = \sigma A \epsilon \left[\left(\frac{T_c + 460}{100}\right)^4 - \left(\frac{T_a + 460}{100}\right)^4\right]$$

where:

Q_C = heat transfer by natural convection, Btu/hr

h = coefficient of heat transfer, Btu/hr/ft^2/^{o}F

A = external surface area of assembly

Δt = temperature difference between assembly and ambient, ^{o}F

D = diameter of assembly, inches

Q_R = heat transfer by radiation, Btu/hr

σ = constant, 0.171

ϵ = emissivity

T_c = temperature of assembly, ^{o}F

T_a = ambient temperature, ^{o}F

The values of the heat transfer rates by convection and radiation may be calculated on the basis of an assumed ambient temperature of 25^{o}C (76^{o}F) and fuel cell assembly temperature of 70^{o}C (157^{o}F).

$$\Delta t = (157-76) = 81\,^oF$$

$$D = 8 \text{ inches}$$

$$\therefore h = 0.5\left(\frac{81}{8}\right)^{.25} = 0.885$$

$$\therefore Q_c = 0.885 \times 2.47 \times 76 = 177 \text{ Btu/hr} = 52 \text{ watts}$$

The emissivity can, of course, be varied by application of various types of coatings to the surface of the assembly. The value of the emissivity for an unpolished nickel-plated surface (which will be the case if no additional coatings are applied to the assembly) is

given as 0.11. The rate of heat transfer by radiation is thus found to be:

$$Q_R = 0.171 \times 2.46 \times 0.11 \left[\left(\frac{617}{100} \right)^4 - \left(\frac{536}{100} \right)^4 \right]$$

$$Q_R = 24.5 \frac{\text{Btu}}{\text{hr}} = 7 \text{ watts.}$$

If the assembly is coated with a suitable black paint with emissivity of 0.9, the rate of heat transfer by radiation is found to be 194 Btu/hr or 65 watts.

The total heat transfer from the assembly "Q_T" is equal to the sum of the transfer rates by convection Q_c and radiation Q_R. For the assumed cell and ambient temperatures above, the value of Q_T is found to be 59 watts for ϵ = 0.11 and 127 watts for ϵ = 0.9.

Calculations have also been carried out for the total heat transfer rate at various assumed cell temperatures. The results of these calculations are given in Fig. 6 for the two assumed emissivities above, and for a fixed ambient temperature of 76°F. If the cycle times were long enough, the results of this graph could be used to estimate the steady-state temperature of the fuel cell as a function of load. For example, at a discharge current of 10 amps, the heat generation rate is found to be 40 watts (see Fig. 5). For an emissivity value of 0.11 the results in Fig. 6 indicate that the steady-state temperature corresponding to a heat dissipation rate of 40 watts is 133°F.

3.3.3 THERMAL CAPACITY

The fuel cell assembly contains a quantity of stearic acid which serves as a thermal storage material. The function of the thermal storage medium is to provide for isothermal cell operation during cycling in

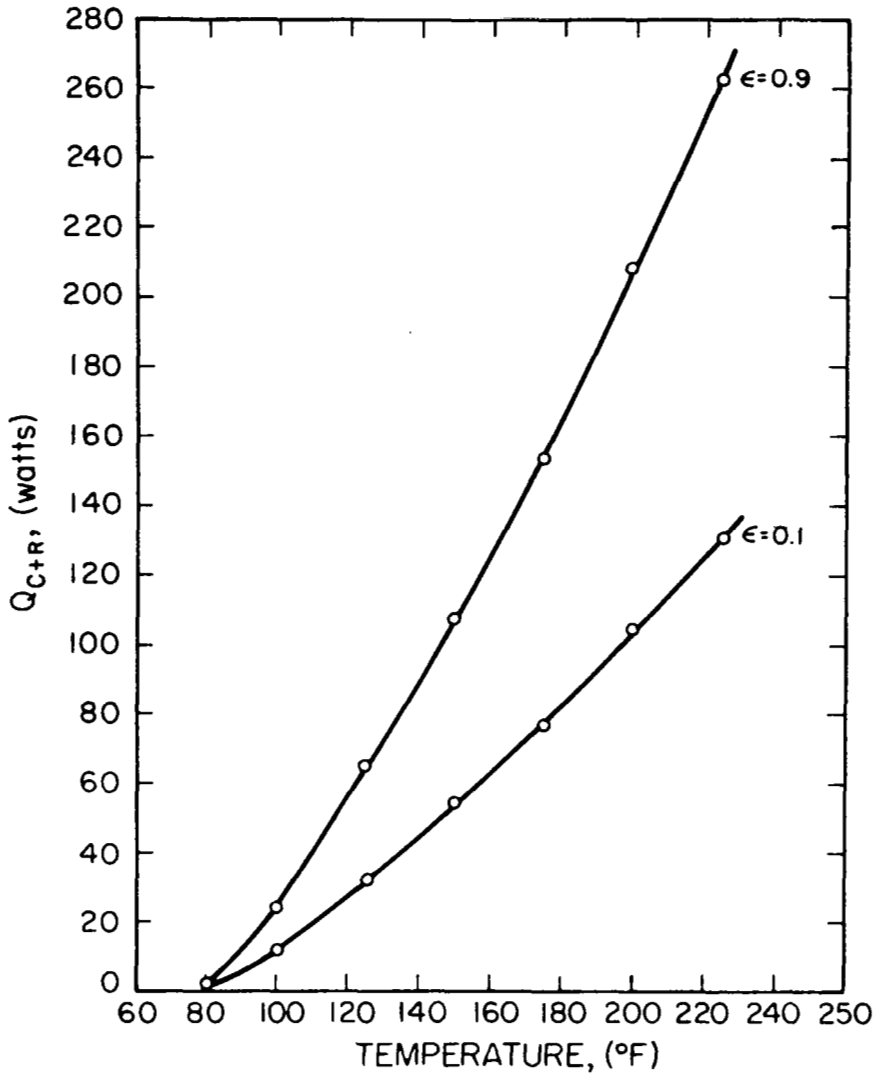

Figure 6. Heat Transfer From Six Cell Prototype by Convection and Radiation

a space environment. The stearic acid would absorb that fraction of the total heat which is not dissipated by radiation during discharge, and would supply that heat to the cell to balance the radiation losses during charge.

The amount of stearic acid is approximately 30 $in.^3$, and its density is 0.80 g/cm^3. The weight of stearic acid is therefore 393 grams. The heat of fusion of this material is 47.6 cal/g and the total thermal capacity is 18,400 cal or the equivalent of 21.4 watt-hr of electrical energy.

3.3.4 HEAT BALANCE

The results of the three preceding sections may now be employed to estimate the net heat transfer from the fuel cell for the case of cycling at ambient conditions. Let us assume that the assembly is initially at 70°C, is uninsulated, that the stearic acid is in the frozen (solid) state, and finally that the cell is fully charged. The net heat transfer for a cycle beginning under these conditions may be determined as follows:

A.	Total cycle time	=	1.890 hr
B.	Discharge time	=	0.625 hr
C.	Charge time	=	1.265 hr
D.	Rate of heat generation during discharge	=	82.8 watts
E.	Rate of heat generation during charge	=	0 watts
F.	Total heat generated during discharge	=	51.7 W-hr
G.	Heat absorbed by stearic acid during discharge	=	21.4 W-hr
H.	Heat to be rejected during discharge	=	30.3 W-hr

I.	Total heat generated during charge	= 0 W-hr
J.	Rate of heat transfer by convection	= 52 watts
K.	Heat transfer by convection during discharge	= 32.4 W-hr
L.	Heat transfer by convection during charge	= 65.8 W-hr
M.	Rate of heat transfer by radiation	= 7 watts (ϵ = 0.11) 57 watts (ϵ = 0.9)
N.	Heat transfer by radiation during discharge	= 4.4 W-hr (ϵ = 0.11) 35.6 W-hr (ϵ = 0.9)
O.	Heat transfer by radiation during charge	= 8.9 W-hr (ϵ = 0.11) 72.0 W-hr (ϵ = 0.9)
P.	Heat supplied by stearic acid during charge	= 21.4 W-hr
Q.	Total heat rejection during discharge	= 36.8 W-hr (ϵ = 0.11) 68.0 W-hr (ϵ = 0.9)
R.	Total heat rejection during charge	= 74.7 W-hr 137.8 W-hr
S.	Net heat lost during discharge	= 6.5 W-hr (ϵ = 0.11) 37.7 W-hr (ϵ = 0.9)
T.	Net heat lost during charge	= 53.3 W-hr (ϵ = 0.11) 116.4 W-hr (ϵ = 0.9)

These results indicate a net loss of heat from the assembly during both discharge and charge. For isothermal operation at 70°C under ambient test conditions, it will therefore be necessary to supply additional heat to the assembly or to provide extra insulation. It is anticipated that the heating tapes that will be used to initially heat the cell to 70°C will provide the required extra insulation needed.

SECTION 4

SINGLE CELL STUDIES

4.1 SINGLE CELL DESIGN

Five 6-inch electrode diameter fuel cells were designed and fabricated. These cells contain features similar to those used on the multicell unit, but do not contain pressure balancing mechanisms. Therefore, the hydrogen and oxygen tank volumes within the cells had to be carefully balanced prior to use in the regenerative mode of operation.

A single cell unit consists of two circular plates of Monel containing gas cavities in an approximate 2 to 1 volume ratio. Machined into these cavities are grooves for electrode backup plates and electrodes of the same, i.e. 6-inch diameter, that are utilized in the multicell unit. The two halves are bolted together by a series of bolts along the periphery. Sealing is accomplished by the of O-rings. A glass-reinforced epoxy spacer is employed between the two plates to provide electrical insulation between the positive and negative sides of the cell. The insulating spacer thus provides the spacing between the two plates and also fixes the compression on the asbestos matrix. Since the diameter of the matrix is somewhat larger than the 6-inch electrodes, the peripheral edge of the matrix is compressed against the cell halves inside the insulating spacer, effectively preventing leakage around the matrix. Assembly was accomplished by stacking one end plate, backup plate, electrode, matrix, second electrode, and second backup plate, and then bolting the entire assembly together.

Certain fittings, valves, and instrumentation are attached to each of the chambers for pressure measurement and for flushing the unit. Major cell components were fabricated out of Monel to minimize corrosion problems. Since the cell does not contain a volume balancing mechanism to assure a 2 to 1 volume ratio, it was necessary to adjust the volumes by adding external tubing to the cell. The entire cell was set up in an oven that contained lead-ins for electrical and flushing gas connections. Figure 7 is a photo of the assembled single cell and Fig. 8 is an assembly drawing of the unit giving details of the internal construction.

Each cell was provided with both a total and a differential pressure transducer. A pressure switch which removes the cell from the charge circuit when the pressure reaches a pre-set level was also employed in each cell.

4.2 TESTING AND EVALUATION

The single cells were used to test and evaluate various electrodes, matrixes, and matrix materials. Other variables investigated using single cells included electrolyte, spacing, matrix/electrolyte balance, and corrosion of materials. Most important, the single cells provided convenient vehicles in which great progress was made in increasing the cycle life and reliability of the hydrogen-oxygen regnerative fuel cell.

Table I is a complete list of all the single cells built, with construction variables and results obtained. The following sections describe test condition variables and results of these tests.

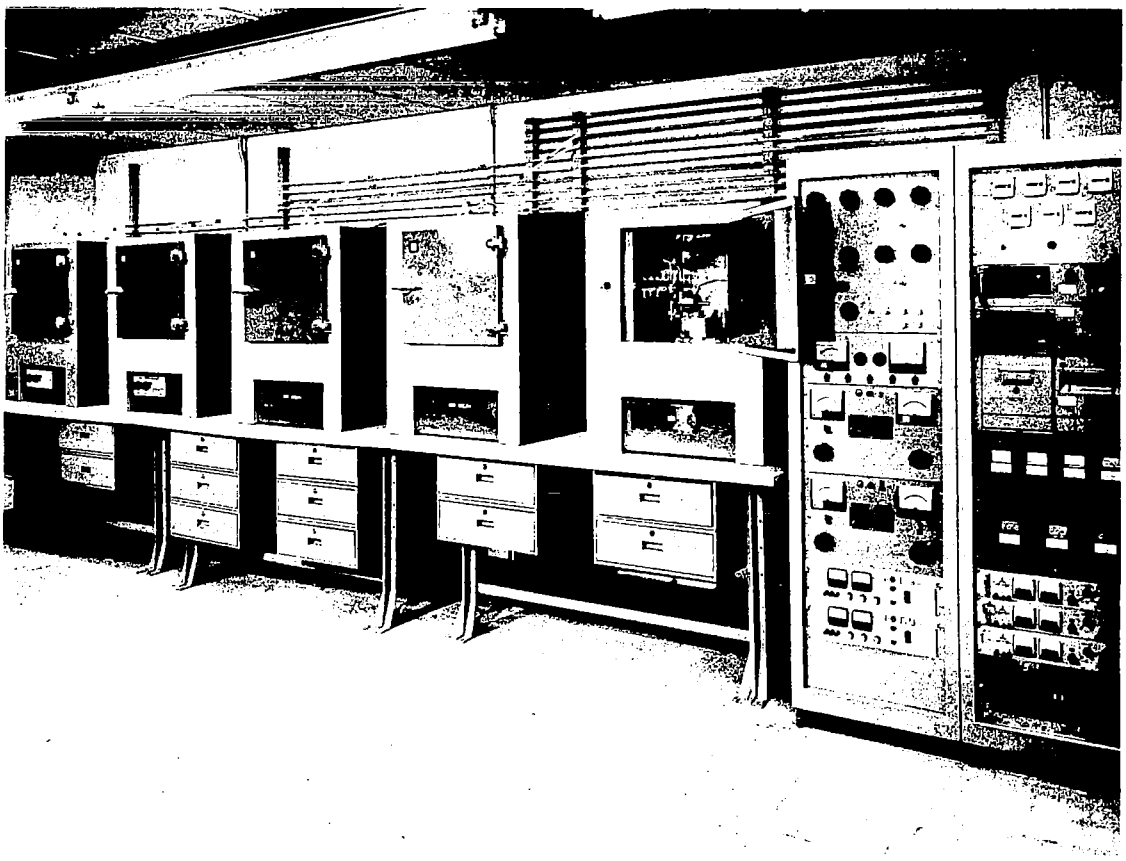

Figure 7. Single Fuel Cell Test Station

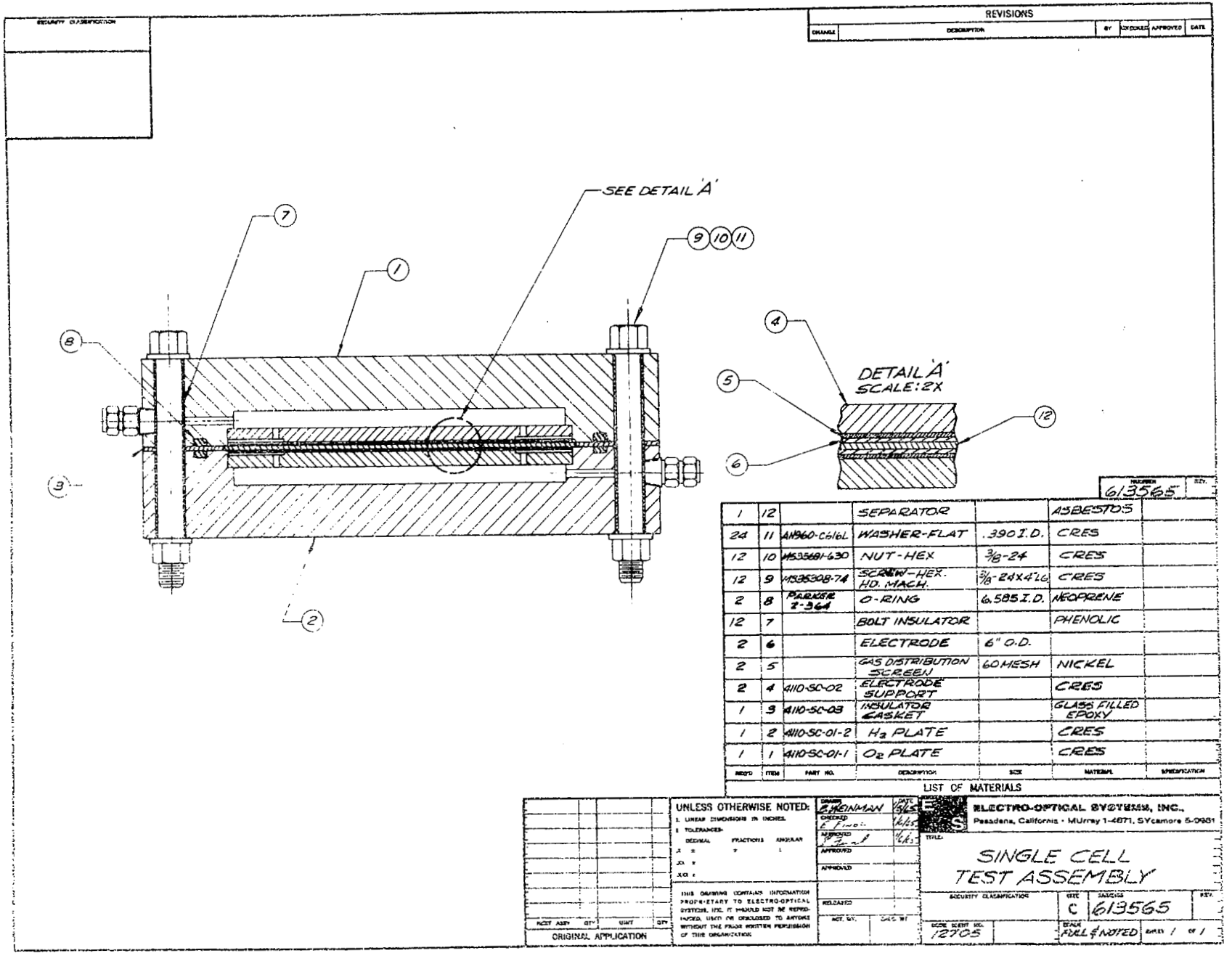

ITEM	QTY	PART NO.	DESCRIPTION	SIZE	MATERIAL	SPECIFICATION
1	12		SEPARATOR		ASBESTOS	
24	11	AN960-C616L	WASHER-FLAT	.390 I.D.	CRES	
12	10	MS35681-630	NUT-HEX	3/8-24	CRES	
12	9	MS35308-74	SCREW-HEX. HD. MACH.	3/8-24X4"LG	CRES	
2	8	PARKER 2-364	O-RING	6.585 I.D.	NEOPRENE	
12	7		BOLT INSULATOR		PHENOLIC	
2	6		ELECTRODE	6" O.D.		
2	5		GAS DISTRIBUTION SCREEN	60 MESH	NICKEL	
2	4	4110-SC-02	ELECTRODE SUPPORT		CRES	
1	3	4110-SC-03	INSULATOR GASKET		GLASS FILLED EPOXY	
1	2	4110-SC-01-2	H_2 PLATE		CRES	
1	1	4110-SC-01-1	O_2 PLATE		CRES	

Figure 8. Single Cell - Test Assembly

TABLE I

SUMMARY OF SINGLE CELL TESTS

Cell No.	O_2 Electrode #		H_2 Electrode #		Mat Thickness Inches and Grade	Mat Dry Wt.	KOH %	KOH Wt.	Comments	Results
	#	Catalyst	#	Catalyst						
1	2	10 mg Pt/ cm^2	1	10 mg Pt/ cm^2	0.050-0.020 Electrolytic	30.3	25.4	18.2		Used cell to balance volumes and check out test circuit.
2	4	"	3	"	0.050-0.020 Electrolytic	29.0	25.4	20.3		Cycled cell 7 times. Stopped test due to excessive internal leakage.
3	4	"	3	"	0.050- Electrolytic	29.9	25.4	20.9		In initial test differential transducer failed and cell had to be reassembled.
4	4	"	3	"	0.050-0.020 Electrolytic	30.2	25.4	21.1		Did not cycle cell due to inability to hold pressure differential across mat.
5	4	"	3	"	0.050-0.020 Electrolytic	30.9	25.4	21.6		Cycled 4 times. Discontinued due to internal leakage.

TABLE I

SUMMARY OF SINGLE CELL TESTS (Cont'd)

Cell #	O_2 Electrode #		H_2 Electrode #		Mat Thickness Inches and Grade	Mat Dry Wt.	KOH %	KOH Wt.	Comments	Results
	#	Catalyst	#	Catalyst						
6	4	10 mg Pt/ cm^2	3	10 mg Pt/ cm^2	0.050-0.020 Electrolytic	30.0	25.4	21.0	Placed Spacers behind gas feed ports.	Cycled 3 times. Discontinued due to internal and external leakage.
7	1	"	2	"	0.020-0.030-0.020 Electrolytic	31.6	25.4	23.3		Cycled 12 times. Stopped test due to low discharge voltage on 10th, 11th, and 12th cycle. Possibly caused by gas leakage and cell drying out.
8	1	"	2	"	0.020-0.020-0.020 Electrolytic	27.0	25.4	23.3		Cycled cell 4 times. Stopped test due to low discharge voltage.
9	6	"	5	"	0.020-0.020-0.020 Electrolytic	27	25.4	23.3	All following cells contained grooves in back-up plates.	Cycled 7 times, left on stand 3 days at temp. After stand exhibited low voltage on discharge.
10	4	"	3	"	Commercial Grade 0.035-0.035	31	25.4	24.3		Cell test stopped due to excessive internal leakage

TABLE I

SUMMARY OF SINGLE CELL TESTS (Cont'd)

Cell #	O_2 Electrode # Catalyst	H_2 Electrode # Catalyst	Mat Thickness Inches and Grade	Mat Dry Wt.	KOH %	KOH Wt.	Comments	Results
11	8 10 mg Pt/ cm^2	7 10 mg Pt/ cm^2	0.035- 0.004- 0.035 Commerical Grade	34	25.4	28	0.004 mat layer was Visking celluosic membrane	Cell had excessive intem al resistance.
12	1 "	2 "	0.020- 0.030- 0.020 Electrolytic	31.8	25.4	23.5		Cycled 2 times left on stand at temp. 2 days. Gave degraded performance.
13	6 "	5 "	0.020- 0.030- 0.020 Pure asb. fuel cell millboard	29.1	25.4	23.3	Added water to the cell by pressuriz-ing and discharging.	Cycled 14 times. No deter-ioration noted but cell had low discharge voltage.
14	- 10 mg Pt/ cm^2 + 10 mg Pd cm^2	20 mg Pt/ cm^2	0.020- 0.030- 0.020 Electrolytic	31	25.4	23.3		Gave improved initial dis-charge voltage but deter-iorated after 7 cycles.
15	- "	- "	0.020- 0.020- 0.020 Electrolytic	26.8	25.4	21.25	Following cells operated in horizontal position.	Cycled 7 times, showed deterioration with time.

TABLE I

SUMMARY OF SINGLE CELL TESTS (Cont'd)

Cell #	O_2 Electrode #		H_2 Electrode #		Mat Thickness Inches and Grade	Mat Dry Wt.	KOH %	KOH Wt.	Comments	Results
	#	Catalyst	#	Catalyst						
16	-	10 mg Pt/ cm^2 + 10 mg Pd cm^2	-	20 mg Pt/ cm^2	0.020-0.020-0.020 Electrolytic	26.8	25.4	21.25	Same electrodes as above without washing.	Shows initial good performance but deteriorated with cycling.
17	-	"	-	"	Pure 0.060	28.0	25.4	26.5	After 5th cycle added water remtly. to improve performance.	Cycled 10 times. Cell had low discharge voltage.
18	19	"	20	"	Pure 0.050	22	25.4	32		Cycled 325 times 50 hours continuous operation. Exhibited slow deterioration with cycling. Final KOH 10.5%.
19		20 mg. Pt/ cm^2		20 mg. Pt/ cm^2	Pure 0.050 F.C.	21.5	35	36.5		Cycled 2 times. Cell flooded.
20	9	"	10	"	Pure 0.050 F.C.	22	40	35		Cell flooded.
21		10 mg. Pt/ 10 mg. Pd.		20 mg. Pt/ cm^2	Pure 0.050 F.C.	22	40	29		Cell cycled 3 times. Allowed to set overnight then cycled and found to show no deterioration.

TABLE I

SUMMARY OF SINGLE CELL TESTS (Cont'd)

Cell#	Electrode # # Catalyst	Electrode# # Catalyst	Mat Thickness Inches and Grade	Mat Dry Wt.	KOH %	KOH Wt.	Comments	Results
22	20 mg. Pt/ cm^2	20 mg. Pt/ cm^2	Pure 0.050 F.C.	22	40	29		Cell used to check out new test set-up.
23	9 mg. Pt/ cm^2	9 mg. Pt/ cm^2	Pure 0.050 F.C.	22	40	29	Commercial Electrodes Type AB-4	Cycled 7 times. High charge voltage 1.7-1.9 volts. Discharge voltage degraded with time. Final KOH 33%
24	9 mg. Pt/ cm^2	20 mg.Pt/ cm^2	Pure 0.050 F.C.	22	40	29	Used Type AB-4 as O_2 Electrode	Cycled 11 times. High charge voltage 1.6-1.7 volts. Discharge degraded with time. Final KOH 37%.
25	46 20 mg.Pt/ cm^2	45 20 mg. Pt/ cm^2	Pure 0.050 F.C.	22	40	29		Tested cell at 125°C Tested cell at high current discharge.
26	46 20 mg.Pt/ cm^2	45 20 mg. Pt/ cm^2	Pure 0.050	22	40.5	21		Used to check KOH loss. Final KOH 34.3%.
27	46 "	45 "	"	24.0	40.5	31.5	Used 0.045 Spacer	Cell had pressure drop on first discharge.

TABLE I

SUMMARY OF SINGLE CELL TESTS (Cont'd)

Cell #	O_2 Electrode #	O_2 Catalyst	H_2 Electrode #	H_2 Catalyst	Mat Thickness Inches and Grade	Mat Dry Wt.	KOH %	KOH Wt.	Comments	Results
28	46	20 mg.Pt./ cm^2	45	20 mg.Pt./ cm^2	Pure 0.050	24.2	40.5	31.5	Used 0.045 Spacer	Cell improved capacity.
29	46	"	45	"	Pure 0.052	23	40.5	33	"	"
33		30 mg.Pt./ cm^2		20 mg.Pt./ cm^2	Pure 0.050	22	40.5	24		Cell used to test increased O_2 catalyst Performance was not improved and test will be re-run.
38		20 mg.Pt./ cm^2		20 mg.Pt./ cm^2	Pure 2X 0.030	26.5	40.5	36.4		Cell gave increased capacity but exhibited internal leakage.
44	76	"	77	"	Pure .050	22	40.5	29		Cell cycled 41 times. Final KOH 26.7% Exhibited poor Faradaic eff. throughout test. No obvious deterioration.
45	32	"	57	"	"	22	40.5	29		Cell used to balance and check out 2nd single cell.

TABLE I

SUMMARY OF SINGLE CELL TESTS (Cont'd)

Cell #	O_2 Electrode #	O_2 Electrode Catalyst	H_2 Electrode #	H_2 Electrode Catalyst	Mat Thickness Inches and Grade	Mat Dry Wt.	KOH %	KOH Wt.	Comments	Results
46	72	20 mg. Pt./ cm^2	73	20 mg. Pt./ cm^2	Pure .060	26.5	40.5	35	No screen behind electrodes Stnl. Steel	Cycled 10 times Stopped test due to large differential pressure swings. Final KOH 34.3%.
47	72	"	73	"	Pure .060	26.5	40.5	32	Stainless Steel Cell	Cycled 43 times. Cell exhibited large differential pressures and fall off in voltage at end of discharge. Final KOH 37.8%.
48	88	"	91	"	Pure .060	26.5	40.5	31		Cell cycled 209 times. Exhibited gradual degradation in performance between 100th and 200 cycle. Cell shorted at 209th cycle.
49	92	10 mg. Pt/ cm^2 10 mg. Pd/ cm^2	96	20 mg. Pt./ cm^2	.060 F.C.	26.6	40.5	31		Cycled 30 times. Developed internal short due to gas mixing caused by leak in ΔP gauge.

TABLE I

SUMMARY OF SINGLE CELL TESTS (Cont'd)

Cell #	O_2 Electrode #		H_2 Electrode #		Mat Thickness Inches and Grade	Mat Dry Wt.	KOH %	KOH Wt.	Comments	Results
	#	Catalyst	#	Catalyst						
50	89	10 mg Pt/cm^2 10 mg Pd/cm^2	100	20 mg. Pt/cm^2	.060 F.C.	26.5	40.5	35	Used no gas distrb. back-up screens	Cell had large differential pressure swings, voltage fell off at end of discharge, cycles two times.
51	103	"	95	"	.060 F.C.	26.4	40.5	31		Cycled 18 times, cell had gas mixing due to leak in ΔP gauge.
52	89	"	100	"	.060 F.C.	26.5	40.5	31	Cell tested at 150°C.	Cycled 3 times external plumbing developed leaks due to high temperature.
53	96	20 mg.Pt/	95	20 mg. Pt/	.060 + .015	32.6	44.5	38.2	.045 span one back-up screen behind O_2 electrode	Cell dryed out and recombined at end of charge and voltage fell off at end of discharge. Final KOH 38.2%
54	96	"	95	"	"	32.75	40.7	38.4	"	" Final KOH 34%
55	96	"	95	"	0.060	26.5	40.7	31.0	Wet Asbestos placed in gas compartments.	Cell performed poorly on charge and discharge.

TABLE I

SUMMARY OF SINGLE CELL TESTS (Cont'd)

Cell #	O_2 Electrode #		H_2 Electrode #		Mat Thickness Inches and Grade	Mat Dry Wt.	KOH %	KOH Wt.	Comments	Results
	#	Catalyst	#	Catalyst						
56	110	10 mg. Pt./cm^2 10 mg. Pd/cm^2	102	10 mg. Pt./cm^2 10 mg. Pd/cm^2	0.060	26.5	40.7	31.0	Wet Asbestos placed in gas compartments.	Wet mat in gas compartments did not transfer water to the cell to improve performance.
57	123	20 mg. Pt./cm^2	122	20 mg. Pt./cm^2	0.060	27	40.7	31.6	Electrodes made on new automatic process.	Performance poorer than with manual processed electrodes.
58	123	"	124	"	0.060	26.5	41.7	31.0	Automatic electrode on O_2 side only.	Performance better than cell No. 57 but still worse than the standard cell.
59	126	"	125	"	0.060 0.015	33.1	40.7	41	No gas distribution screen behind electrode.	Cell developed leakage, test discontinued.
60	123	"	129	"	0.060	27	40.7	32.5	Subjected cell to storage at 150°C.	After the 150°C storage, cell performance slightly degraded.

TABLE I

SUMMARY OF SINGLE CELL TESTS (Cont'd)

Cell #	O_2 Electrode#		H_2 Electrode#		Mat Thickness Inches and Grade	Mat Dry Wt,	KOH %	Wt.	Comments	Results
	#	Catalyst	#	Catalyst						
61	125	20 mg. Pt./ cm^2	126	20 mg. Pt./ cm^2	0.030 0.015 0.030	32.5	40.7	42	No gas distribution behind electrodes.	Improved capacity slightly.
62	125	"	126	"	0.030 0.015 0.015	32.5	40.7	40	"	"
63	-	"	-	"	0.060	27.5	40.7	31.2	Bishop electrodes	High voltage on charge. Fair on discharge.
64	124	"	123	"	0.060 0.015	33.0	40.7	40	Automatic electrode on H_2 side.	Cell used to check out new setup.
65	125	"	126	"	0.060	26.5	40.7	35	Used second set of electrodes behind the standard electrodes.	Cell developed leakage. Test discontinued.
66	124	"	123	"	0.060 0.015	40.9	40.7	48	Capacity improvement test.	Attained $>$18AH on discharge, current efficiency $<$80%.

TABLE I

SUMMARY OF SINGLE CELL TESTS (Cont'd)

Cell#	O_2 Electrode#		H_2 Electrode#		Mat Thickness Inches and Grade	Mat Dry Wt	KOH %	KOH Wt.	Comments	Results
	#	Catalyst	#	Catalyst						
67	Bish.	20 mg. Pt./ cm^2	Bish.	20 mg. Pt./ cm^2	0.060	27.35	40.7	31.9	Retest of Bishop electrode.	Attained > 21AH on discharge, current efficiency > 85%.
68	125 + old	"	126 + old	"	0.060	27.29	40.7	35	Capacity improvement test. No back-up screen -.045 Spacer	No improvement in capacity.
69	125	"	126 + old	"	0.060	25.9	40.7	35	Repeat of 68 with 2 electrodes on H_2 only.	No improvement in capacity.
70	139	20 mg. Pt./ cm^2	151	20 mg. Pt./ cm^2	0.060	26.1	40.7	30.5	First attempt at thermal steriliz-ation cycle.	KOH loss accelerated performance poor after sterilization -O cathode mechani-cally degraded. Other cell components OK.
71	125	"	126 + old	"	0.060	26.2	40.7	35	Repeat of 69.	No improvement in capacity.

TABLE I

SUMMARY OF SINGLE CELL TESTS (Cont'd)

Cell#	O_2 Electrode#		H_2 Electrode#		Mat Thickness Inches and Grade	Mat Dry Wt.	KOH %	KOH Wt.	Comments	Results
	#	Catalyst	#	Catalyst						
72	AA-1	9 mg. Pt./ cm^2	214	20 mg Pt./ cm^2	0.060	27.0	40.5	31	Cyanamid Electrode on O_2 side.	Cell leaked due to poor "O" ring seal.
73	AA-1	"	217	"	0.060	27.0	40.5	31.1	"	Tantalum screen dissolved in electrolyte
74	AA-1	"	214	"	0.060		40.5	31	"	"
75	AA-1	"	217	"	0.060	27.5	40.5	31	"	"
76	AB-4	"	217	"	0.060	27.2	40.5	36	"	Cell cycled showed gradual deterioration Final KOH 31.4, 30.5
77	AB-40	40 mg. Pt/ cm^2	114	20 mg. Pt./ cm^2	0.060	2	40.5	31	"	Showed good peak performance but water sensitive. 31.6 31.4 Final KOH
78	AB-40	"	112	"	0.060	27.1	40.5	31	"	
79	217	"	214	"	0.060	27.2	40.3	31	KOH washed mat	Cell not cycled 5.2 35.2 Final KOH
80	AB-4	9 mg. Pt./ cm^2	211	"	0.060	27.0	40.3	33		Cell showed rapid deterioration
81	217	20 mg. Pt/ cm^2	214	"	0.060	27.1	40.3	31	Mat KOH washed	

TABLE I

SUMMARY OF SINGLE CELL TESTS (Cont'd)

Cell No.	O_2 Electrode #	O_2 Electrode Catalyst	H_2 Electrode #	H_2 Electrode Catalyst	Mat Thickness Inches and Grade	Mat Dry Wt.	KOH %	KOH Wt.	Comments	Results
82	235	20 mg.Pt./ cm^2	234	20 mg.Pt./ cm^2	0.060	27.2	40.3	31	Reference electrode	Reference Electrode shorted out.
83	108	"	118	"	0.060	27.1	40.3	31	Used electd. from S/N 107	Poor performance
84	216	"	118	"	0.060	27.1	40.3	31	Used Hydrogen electd. New oxygen electrode	Good performance
85	136	20 mg.Pt./	137	"	2X.030	27	40.3	31	Used HgO Ref. between mat.	Cycled 7 times, obtain individual electrode.perform.
86	219	40 mg.Pt./ cm^2	211	"	0.060	28	40.3	31	Automatic process oxygen electrode.	Showed no improvement.
87	219	"	211	"	0.060	27.6	40.3	31	Repeat of cell #86	Cycled 16 times. Showed no improvement in performance.
88	Felt Metal	20 mg.Pt./ cm^2	213	"	0.060	27	40.3	31	Felt metal oxygen	Cycled 17 times good initial perform.
89	208	"	133	"	2X.030	27.2	40.3	31	Used HgO Ref. between mat.	Cycled 45 times Obtain individual electrode perform.
90	Felt Metal	40 mg.Pt./ cm^2	137	"	.060	27	40.3	31	Felt Metal Oxygen	Cycled 11 times poor performance.

TABLE I

SUMMARY OF SINGLE CELL TESTS (Cont'd)

Cell#	O_2 Electrode#		H_2 Electrode#		Mat Thickness Inches and Grade	Mat Dry Wt.	KOH %	KOH Wt.	Comments	Results
	#	Catalyst	#	Catalyst						
91	Felt Metal	20 mg.Pt./	213	20 mg.Pt./	.060	27.1	40.3	31	Repeat of cell 88	Cycle 39 times. Showed gradual decay in performance.
92		9 mg. Pt./ cm^2	215	20 mg.Pt./ cm^2	2x.030	27	40.3	31	Cyanamid Oxygen electd. with gold plated screen.	Final KOH 26.2%,26.9% 130 cycles. Cell showed gradual degradation in performance.
93		"	213	"	.060	27.5	40.3	31	"	Final KOH 27.8%, 28.4% 38 cycles. Cell showed initial poor performance on charge.
94		20 mg. Pt./ cm^2		"	.060	27.1	40.3	31	Bishop platinized oxygen electrode	Final KOH 35.3% 35.6% 21 cycles. Showed initial good performance, but degraded slowly.
95		40 mg.Pt./ cm^2	213	"	.060	26.0	40.3	31	"	Final KOH 29.4%, 48 cycles. Increased catalyst did not improve performance.
96		9 mg.Pt./	213	"	. 060	27.3	40.3	31	Same electrodes as Cell #93	Final KOH 29.6%, 29.7%. Cycled 37 poor initial performance

TABLE I

SUMMARY OF SINGLE-CELL TESTS (Cont'd)

Cell#	O_2 Electrode#		H_2 Electrode#		Mat Thickness Inches and Grade	Mat Dry Wt.	KOH %	KOH Wt.	Comments	Results
	#	Catalyst	#	Catalyst						
97		9 mg. Pt./ cm^2	215	20 mg. Pt./	.060	27.0	40.3	31	Same electrodes as cell No. 92	Final KOH 25.7, 25.8%. Cycled 95 times. Initial good performance. Gradual degradation with cycling.
98		9 mg. Pt./ cm^2	215	20 mg.Pt./ cm^2	0.060	27.1	39.9	31	Oxygen electrode Cyanamid	125 cycles 30 at high rate, 95 at low rate.
99	216	20 mg.Pt./ cm^2	206	20 mg.Pt./ cm^2	0.060	27.2	39.9	31.1		100 cycles. Showed good performance.
100	2 ea.	9 mg.Pt./ cm^2	215	20 mg.Pt./ cm^2	0.060	27.0	39.9	31.1		60 cycles sensitive to water content.
101	2 ea.	9 mg.Pt./ cm^2	215	20 mg.Pt./ cm^2	0.060	27.1	39.9	31.0		15 cycles. Same performance as cell 100.
102		20 mg.Pt./	210	20 mg.Pt./	0.060	26.2	39.7	31	O_2 electrode Ni plaque (gold-coated and platinized)	Cells shorted out after 5 cycles.
103	Aul	7-10 mg. Pt./cm^2	206	20 mg.Pt./ cm^2	0.060	28.0	39.7	31		174 cycles degraded gradually.

TABLE I

SUMMARY OF SINGLE-CELL TESTS (Cont'd)

Cell#	O_2 Electrode#		H_2 Electrode#		Mat Thickness Inches and Grade	Mat Dry Wt.	KOH %	KOH Wt.	Comments	Results
	#	Catalystl	#	Catalyst						
104	-	9 mg.Pt./ cm^2	-	9 mg.Pt./ cm^2	0.060	27.5	29.7	31		100 cycles degraded gradually.
105	A_u7	7-10 mg. Pt/cm^2	-	20 mg.Pt./ cm^2	0.060	27.3	39.9	31	Oxygen electrode gold-plated felt metal	Cycled 46 times. Poor performance.
106	-	9 mg.Pt./ cm^2	-	9 mg.Pt./ cm^2	Reused from cell No. 104				Repeat of No. 104	Cycled 46 times. Internal reaction
107	A_u6	7-10 mg. Pt/cm^2	206	20 mg.Pt/ cm^2	0.060	27.1	39.7	31	Porous nickel plaque (gold-coated and platinized	Cycled 42 times. Fair performance. Internal reaction during weekend.
108	A_u6	11	206	20 mg.Pt/ cm^2	0.060	27.1	39.7	31	Repeat of Cell No. 107	Cycled 6 times Internal short. Good performance.
109	A_u4	Porous-sintered Ni plq. coated and plat. by Bishop 20 mg Pt/ cm^2	-	20 mg.Pt/	0.060	27.4	39.7	31		Cycled 44 times. Fair performance. Gradual degradation

TABLE I

SUMMARY OF SINGLE-CELL TESTS (Cont'd)

Cell#	O_2 Electrode#		H_2 Electrode#		Mat Thickness Inches and Grade	Mat Dry Wt.	KOH %	KOH Wt.	Comments	Results
	#	Catalyst	#	Catalyst						
110	A_u5	Ni-felt mtl.plq. gold-coated and plat. by Bishop 20 mg.Pt/cm^2	-	20 mg.Pt./cm^2	0.060	28.0	39.7	31.0		Cycled 50 times. Fair performance.
111	A_u3	" " Bishop	-	20 mg.Pt/cm^2	0.060	28.0	39.7	31.0		Different pressure. Transducer failed.
112	A_u4	-	-	20 mg.Pt/cm^2	0.060	27.6	39.7	31.0	Repeat of Cell No. 109	Cycled 18 times. Poor performance.
113	A_u6	Porous Ni plq.gold-coated plat.7-10 mg.Pt/cm^2	206	20 mg.Pt/cm^2	0.060	29.7	39.7	31.0		78 cycles.
114	A_u	" "	-	Porous Ni plq. No catalyst	0.060	27.0	39.7	31.0		Just changed cell to see effect of Ni on asbestos.
115	-	20 mg.Pt/cm^2	-	20 mg.Pt/cm^2	0.060	27.1	39.7	31.0	1 layer of cellophane on hydrogen electrode.	8 cycles. Very poor performance

TABLE I

SUMMARY OF SINGLE-CELL TESTS (Cont'd)

Cell#	O_2 Electrode#		H_2 Electrode#		Mat Thickness Inches and Grade	Mat Dry Wt.	KOH % Wt.		Comments	Results
	#	Catalyst	#	Catalyst						
116	A_u4	7.5 mg $Pt./cm^2$	208	20 mg.Pt./ cm^2	2 layers Webril 1 layer cello-phane	12.0	39.7	35.0	-	1 Cycle. Cell shorted
117	A_u12	7.5 mg Pt/cm^2	216	20 mg. Pt/ cm^2	0.060	26.8	39.7	31.0		121 cycles. Good initial performance degraded slowly.
118	A_u10	7.5 mg	217		0.060	27.2	39.7	31.0	Oxygen electrode felt metal substrate	Cycled 6 times. Poor performance.
119	Am Cy	9 mg. Pt/ cm^2	Am. Cy.	9 mg. Pt/ cm^2	0.060	27.1	39.7	31.0		61 cycles. Gradual degradation.
120	Am. Cy.	9 mg.Pt/ cm^2	Am. Cy.	9 mg. Pt/ cm^2	0.060	27.2	39.7	31.0		50 cycles. Gradual degradation.
121	(Same as Cell 120)				-	-	-	-	Repeat of No.120 with washed O_2 electrode	5 cycles. Poor performance.
122	(Same as Cell 120				-	-	-	-	Repeat of Cell No. 119 with washed O_2 electrode	4 cycles. Poor performance.

TABLE I

SUMMARY OF SINGLE-CELL TESTS (Cont'd)

Cell#	O_2 Electrode#		H_2 Electrode#		Mat Thickness Inches and Grade	Mat Dry Wt.	KOH %	KOH Wt.	Comments	Results
	#	Catalyst	#	Catalyst						
123	(Same as Cell 120)				-	-	-	-	Repeat of Cell No. 121 with washed H_2 electrode	2 cycles. Poor performance.
124	(Same as Cell 120)				-	-	-	-	Repeat of Cell No. 122 with washed H_2 electrode	2 cycles. Poor performance.
125	Am. Cy.	9 mg.Pt./ cm^2	Am.	9 mg.Pt./ cm^2	.060	27.0	40.0	31.0	Electrodes from Cell 124.	Cycled 25 times. Poor performance.
126	A_u8	7 mg.Pt./ cm^2	A_u14	7 mg.Pt./ cm^2	-	-	40.0	31.0	Acid washed mat.	Very poor performanee
127	Am. Cy.	9 mg.Pt./ cm^2	Am. Cy.	9 mg.Pt./ cm^2	-	28	40.0	31.0	Acid-KOH washed mat.	Good initial performance. Δp transducer failed during 3rd cycle.
128	Am. Cy.	"	Am. Cy.	"	Same as Cell	No. 125			Repeat of 125 with new O_2 electrode Same mat H_2 electrode.	Good performance. 16 cycles. Internal reaction over weekend.
129	Am. Cy.	"	Am. Cy.	"	.060	27.5	40.0	31.0	Electrodes from cell 123. New mat.	Cycled 84 times. Fair performance. Gradual degradation developed a short.

TABLE I

SUMMARY OF SINGLE-CELL TESTS (Cont'd)

Cell#	O_2 Electrode#		H_2 Electrode#		Mat Thickness Inches and Grade	Mat Dry Wt.	KOH %	KOH Wt.	Comments	Results
	#	Catalyst	#	Catalyst						
130	Am. Cy.	9 mg.Pt./ cm^2	Am. Cy.	9 mg.Pt./ cm^2	.060	27.2	40.0	31.0	Electrolyzed KOH	29 cycles, initial. Fair performance.
131	Am. Cy.	"	Am. Cy.	"	-	-	-	-	Electrode from 127. Thin acid washed mat.	Internal reaction during flushing.
132	Am. Cy.	"	Am. Cy.	"	.060	27.5	40.0	31.0	Same electrode as 131.	Used to check damage to electrode Poor performance.
133	Am.	"	Am.	"	.060	26.5	40.0	31.0	Same electrode from cell No. 130	Poor performance.
134	Am. Cy.	"	Am. Cy.	"	.060	27.0	40.0	31.0	Electrode from cell 128. Electrolyzed KOH.	Cycled 72 times. Fair performance, gradual degradation.
135	Am. Cy.	"	Am. Cy.	"	.060	28.0	40.0	31.0	Electrolyzed KOH	75 cycles. Gradual degradation.

TABLE I

SUMMARY OF SINGLE-CELL TESTS (Cont'd)

Cell#	O_2 Electrode#		H_2 Electrode#		Mat Thickness Inches and Grade	Mat Dry Wt.	KOH %	KOH Wt.	Comments	Results
	#	Catalyst	#	Catalyst						
136	Am. Cy.	9 mg. Pt./	Am. Cy.	9 mg. Pt./	.060	26.8	40.0	31.0	Electrolyzed KOH.	10 cycles. Stopped test due to gas leakage.
137	A_u22	7 mg.Pt./ cm^2	A_u30	7 mg.Pt./ cm^2	.060	28.0	40.0	31.0	-	Poor performance.
138	A_u25	"	A_u31	"	-	-	-	-	-	25 cycles. Fair performance.
139	A_u19	14 mg.Pt./ cm^2	A_u18	14 mg.Pt./ cm^2	.060	26.7	40.0	31.0	-	20 cycles. Fall off in performance at end of discharge.
140	Am. Cy.	9 mg.Pt./ cm^2	Am. Cy.	9 mg.Pt./ cm^2	0.060	27.0	40	31.0	Electrodes Cell 136	Not subjected to test due to gas leakage.
141	A_u14	15 mg.Pt./ cm^2	A_u18	15 mg.Pt./ cm^2	0.060	27.5	40	29	Electrodes from Cell 139.	400 cycles test discontinued
142	Am. Cy.	9 mg.Pt./ cm^2	Am. Cy.	9 mg.Pt./ cm^2	0.060	27.5	40	31.0	Electrodes from Cell 134.	Cycled 46 times. Developed internal reaction and short. Gradual degradation.
143	Am. Cy.	9 mg.Pt./ cm^2	Am. Cy.	9 mg.Pt./ cm^2	0.060	27.0	40	31.0	Electrodes from Cell 135.	Shorted out during 12th cycle.

TABLE I

SUMMARY OF SINGLE-CELL TESTS (Cont'd)

Cell#	O_2 Electrode#		H_2 Electrode#		Mat Thickness Inches and Grade	Mat Dry Wt.	KOH %	KOH Wt.	Comments	Results
	#	Catalyst	#	Catalyst						
144	Am. Cy.	9 mg.Pt./ cm^2	Am. Cy.	9 mg.Pt./ cm^2	0.060	27.5	40	31.0	Electrodes from Cell 140.	9 Cycles. Fair performance.
145	Am. Cy.	"	Am. Cy.	Nickel plaque	0.060	27.3	40	31.0	-	Charged for 1-1/2 hours.
146	Am. Cy.	Nickel Plaque	Am. Cy.	9 mg. Pt./ cm^2	0.060	26.8	40	31.0	-	Charged for 1-1/2 hours.
147	Mod. Am.	9 mg. Pt./ cm^2 + 7 mg. Pt./ cm^2	Am.	9 mg.Pt./ cm^2	0.060	27.5	40	31.0	Electro deposited Pt on top of Am. Cy. electrode.	Flat good initial performance. 53 cycles gradual degradation.
148	Am. Cy.	9 mg.Pt./ cm^2	Am. Cy.	Nickel Plaque	0.060	27.4	40	33.0	-	Charged for 2 hours.
149	-	Nickel Plaque	Am. Cy.	9 mg.Pt./ cm^2	0.060	28,0	40	33.0	-	Charged for 2 hours.
150	Mod. Am. Cy.	9 mg.Pt./ cm^2 + 15 mg.Pt./ cm^2	Am. Cy.	9 mg.Pt./ cm^2	0.060	27.0	40	31.0	Electro deposited Pt on top of Am. Cy. electrode	Cycled 11 times. Fair performance.

TABLE I

SUMMARY OF SINGLE-CELL TESTS (Cont'd)

Cell#	O_2 Electrode#		H_2 Electrode#		Mat Thickness Inches and Grade	Mat Dry Wt.	KOH % Wt.		Comments	Results
	#	Catalyst	#	Catalyst						
151	Mod. Am.	9 mg.Pt./cm^2 + 7 Mg.Pt./cm^2	Am. Cy.	9 mg.Pt./cm^2	0.060	27.0	40	31.0	Electrodes from Cell 147	-
152	Am. Cy.	9 "	"	"	0.060	27.0	40	31.0	Electrodes from Cell 150.	Cycled 7 times. Fair performance.
153	A_u26	14 mg.Pt./cm^2	A_u 36	14 mg.Pt./cm^2	0.060	27.0	40	30.0	-	2 cycles. Poor performance.
154	"	"	"	"	0.060	27.0	40	30.0	Electrodes from Cell 153.	2 cycles. Slight improvement.
155	Mod. Am. Cy.	9 mg.Pt./cm^2 + 14 mg.Pt./cm^2	Au 40	14 mg.Pt./cm^2	0.060	26.5	40	31.0	Pt.Am.Cy. O_2 electrode Nickel plq. hydrogen	2 cycles. Poor performance.
156	Au 26	14 mg.Pt./cm^2	A_u 36	14 mg.Pt./cm^2	0.060	27.0	40	31.0	Electrodes from Cell 154.	2 cycles. Poor performance.
157	Mod. Am. Cy.	9 mg.Pt./cm^2 + 15 mg.Pt./cm^2	A_u 40	14 mg.Pt./cm^2	0.060	27.0	40	31.0	Electrodes from Cell 155	1 cycle. Poor performance.

TABLE I

SUMMARY OF SINGLE-CELL TESTS (Cont'd)

Cell#	O_2 Electrode#		H_2 Electrode#		Mat Thickness Inches and Grade	Mat Dry Wt.	KOH %	KOH Wt.	Comments	Results
	#	Catalyst	#	Catalyst						
158	Bish	7 mg.+ 15 mg.Pt./ cm^2	-	15 mg.Pt./ cm^2	0.060	27.5	40	31.0	Electroplated Bishop O_2 electrode	8 cycles. Good performance.
159	Mod. Am.	9 + 15 mg.Pt./cm^2	A_u Cy.	9 mg.Pt./ cm^2	0.060	27.0	40	31.0	O_2 Electrode from Cell 157.	17 cycles. Poor performance.
160	A_u 26	14 mg.Pt./ cm^2	-	14 mg.Pt./ cm^2	0.060	27.09	40	31.09	O_2 electrode from No.156 Quick change of electrode and mat.	Very poor discharge. 1 cycle.
161	Bish	7 mg.+ 15 Mg.Pt./ cm^2	-	15 mg.Pt./ cm^2	0.060	27.09	40	31.09	Electrodes were run in No. 158.	12 cycles. Poor performance.
162	Au 46	14 mg.Pt./ cm2	Au 45	14 mg.Pt./ cm2	.30 (Two of them)	27.09	40	31.0	Continuous concentra-taion cell with reference.	Ran 6 days. Internal reaction during night.
163	A_u 48	14 mg.Pt./ cm^2	A_u 49	14 mg.Pt./ cm^2	.30 (Two)	26.5	40	31.0	Cycling con-centration cell.	Ran 34 cycles. Volt-age went up to 10 on one side and 11 on other.
164	Au 47	14 mg.Pt./ cm^2	-	14 mg.Pt./ cm^2	Same mat From 160	-	-	-	Put new O_2 electrode in cell No. 160	17 cycles. Ran poor.

TABLE I

SUMMARY OF SINGLE-CELL TESTS (Cont'd)

Cell#	O_2 Electrode#		H_2 Electrode#		Mat Thickness Inches and Grade	Mat Dry Wt.	KOH %	KOH Wt.	Comments	Results
	#	Catalyst	#	Catalyst						
165	A_u 43	14 mg.Pt./ cm^2	A_u 44	14 mg.Pt./ cm2	.30 (Two)	27.1	40	31.09	Cycling concentration cell.	Gradual degradation.
166	-	EOS elect. with gold over.	-	Old washed gold.	.060	27.5	40	31.09	-	Improved with performance. 130 cycles.
167	A_u 42	14 mg. Pt./ cm^2	A_u 43	14 mg.Pt./ cm^2	.030 (Two)	27.0	40	31.0	Concentration cell.	Ran 6 days, turn off due to high voltage ref.
168	A_u 47	"	-	"	.060	27.0	40	31.0	Electrodes from Cell No. 164	130 cycles. Ran poor.
169	57	EOS regular	56	EOS	.060	27.0	40	31.0		105 cycles. Ran fair.
170	64	14 mg.Pt./ cm2	65	14	FC Asb. .060	27.0	40	31.09	Cont.Conc. cell.	Run for 456 hours to 1V. end Point. Final KOH 26.25%.
171	Am. Cy.	7 mg.Pt./ cm2	Am.	7 mg.Pt./ cm2	.060	27.2	40	31.0	Concentration cell.	30 cycles. Voltage went up 1 Volt.
172	Chem Cell	Std.	Chem Cell	-	.060	27.1	40	31.0		Runs poor.
173	A_u 52	14 mg.Pt./ cm^2	A_u 51	14 mg.Pt./ cm2	3 layers .020 K.T. paper	21.5	40	31.0	Cycling concentration cell.	Cycled 200 times to .95V end point.

TABLE I

SUMMARY OF SINGLE-CELL TESTS (Cont'd)

Cell#	O_2 Electrode#		H_2 Electrode#		Mat Thickness Inches and Grade	Mat Dry Wt.	KOH %	KOH Wt.	Comments	Results
	#	Catalyst	#	Catalyst						
174	Chem Cell	with Hydrophobic	Chem Cell	with Hydrophobic	.060	27.2	40	31.09		Did not run.
175	-	20 mg.Pt./ cm^2	-	20 mg.Pt./ cm^2	FC Asb. .060	27.1	40	31.0	O_2 electrode pasted Pt Black on Nickel screen	Cycled 10 times. Poor performance Final KOH 29.15%
176	72	"	59	"	4 layers (.020) ACCO I	21.5	40	31.0	Am. Cy. Asb. Matl.	Cycled 4 times low discharge voltage. Final KOH 27.85%
177	Am. Cy.	9 mg.Pt./ cm^2	Am. Cy.	9 mg.Pt./ cm^2	FC Asb. .060	26.8	40	31.0	Acid washed electrodes.	Cycled 3 times. Good performance. Disassembled to replace mat. Final KOH 32.75%
178	A_u 61	20 mg.Pt./ cm^2	A_u 138	20 mg.Pt./ cm^2	FC Asb. .060	27.0	40	31.0	Tested as a Primary FC	Ran poor due to water transport difficulties.
179	A_u 58	"	Au 57	"	"	"	"	"	Tested as a Primary FC Pt. Nickel plaque elect.	Ran poor due to water transport difficulties.
180	Am. Cy.	9 mg.Pt./ cm^2	Am. Cy.	9 mg.Pt./ cm^2	FC Asb. Acid washed	30.0	40	31.0	Electrodes used in Cell 177.	Cycled 45 times Cell exhibited poor eff., fair perform. Final KOH 32%.

TABLE I

SUMMARY OF SINGLE-CELL TESTS (Cont'd)

Cell#	O_2 Electrode#		H_2 Electrode#		Mat Thickness Inches and Grade	Mat Dry Wt.	KOH %	KOH Wt.	Comments	Results
	#	Catalyst	#	Catalyst						
181	Am. Cy.	9 mg. Pt./ cm^2	Am. Cy.	9 mg.Pt./ cm^2	3 layers .020 KT paper	-	-	-	New O_2 electrode Old H_2 electrode Cycle conc. cell.	Cycled 32 times to 1 V. Showed gradual increase.in voltage. Final KOH 32.9%.
182	85	20 mg.Pt./ cm^2 nickel plaque	86	20 mg.Pt./ cm^2 nickel plaque	75% KT 25% FC Asb.	20	40	32		Developed internal short on 12th cycle. Good performance Final KOH 35.2%
183	Am. Cy.	9 mg.Pt./ cm^2	Am. Cy.	9 mg.Pt./ cm^2	FC Asb. Acid Washed	30	40.15	31	Cont. conc.	Ran 140 hours to .95 V. Showed gradual rise in voltage. Final KOH 36.3%.
184	Am. Cy.	"	Am. Cy.	"	"	25	40.15	31	Cont.conc. cell. Electrodes from cell 180	Ran 72 hours to 1.2 V. Showed gradual rise in voltage. Final KOH 30 5%.
185	A_u 90	14 mg.Pt./ cm^2	A_u 91	14 mg.Pt./ cm^2	75% KT 25% FC Asb.	20.0	40	36	-	426 cycles slow gas cross leakage at 418 cycles.
186	Am. Cy.	9 mg.Pt./ cm^2	Am. Cy.	9 mg.Pt./ cm^2	"	20.0	40	31	Cycling conc cell.	320 cycles to 1.1 volts.

TABLE I

SUMMARY OF SINGLE-CELL TESTS (Cont'd)

Cell#	O_2 Electrodes#		H_2 Electrodes#		Mat Thickness Inches Dry Grade	Mat Dry Wt.	KOH %	Wt.	Comments	Results
	#	Catalyst	#	Catalyst						
187	Am. Cy.	9 mg.Pt./ cm^2	Am. Cy.	9 mg.Pt./ cm^2	100% KT	17.5	40.14	31	Old electrodes cont. conc. cell.	Ran 27 hours to 1.1 V Had high initial voltage rose rapidly. Final KOH 35.6%.
188	Am. Cy.	"	Am Cy.	"	100% KT	20.0	40	31	Cont. conc. cell. Old electrodes.	High initial voltage. Test discontinued.
189	"	"	"	"	"	19.9	40	31	-	Short in assembly.
190	"	"	"	"	"	19.5	40.15	31.0	Cont. O_2 Cell test	700 hours to 1.1 volts.
191	Felt Metal	14 mg.Pt./ cm^2	Felt Metal	14 mg.Pt./ cm^2	"	19.5	40.15	34.0	Cont. O_2 Conc. Cell test	840 hours to 1.1 volts.
192	Plat. gold screen	20 mg.Pt./ cm^2	Plat. nickl. plq.	20 mg.Pt./ cm^2	90% KT 10% Ab	20	40.0	33.0		330 Cycles. Slow gas cross leakage at 327 cycles.
193	Plat. gold screen	"	"	"	" "	19.5	40.15	34.0	Cycling O_2 Conc. Cell Test	200 cycles to 1.1 volts.
194	Am. Cy.	9 mg.Pt./ cm^2	Am. Cy.	9 mg.Pt./ cm^2	100% KT	19.0	40.15	31.0	Used electrodes	Initial poor performance.
195	Am. Cy.	9 mg.Pt./ cm^2	Plat. nickl plq.	20 mg.Pt./ cm^2	90% KT 10% Ab	20.5	40.0	34.09		278 cycles, then developed high internal resistance

TABLE I

SUMMARY OF SINGLE-CELL TESTS (Cont'd)

Cell#	O_2 Electrode#		H_2 Electrode#		Mat Thickness Inches and Grade	Mat Dry Wt.	KOH %	Wt.	Comments	Results
	#	Catalyst	#	Catalyst						
196	Am. Cy.	9 mg.Pt./ cm^2	Plat. nickl plq.	20 mg. Pt./ cm^2	90% KT 10% Ab	20.0	40.15	34.0		60 cycles, slow gas cross leakage at 60th cycle.
197	Plat gold screen	25 mg.Pt./ cm^2	"	"	90% KT 10%Ab	20.0	40.15	34.0		Volume balance problem. Test discontinued.
198	Plat. gold screen	"	Plat Ni plq.	"	"	19.6	-	-	-	952 cycles, gradual degradation.
199	Am. Cy.	9 mg.Pt./ cm^2	Plat. Ni. plq.	"	"	24.5			O_2 electrode from Cell 196	Test stopped at 405 cycles, due to poor perform.
200	Am. Cy.	"	173	"	"	24.59	40.15	34.09		Test discontinued due to cell imbalance.
201	Plt. 92 gold Screen	25 mg.Pt./ cm^2	Plt. 93 gold Screen	25 mg.Pt./ cm^2	Teflon Cloth Mat		40.0	32	O_2 cycling Conc. Cell	When started cell voltage rose to 1.5 V. Discontinued
202	Am. Cy.	9 mg.Pt./ cm^2	Plat Ni Plq.	20 mg.Pt./ cm^2	90% KT 10% Ab	20.09			O_2 electrodes from cell 195	387 cycles, cell developed internal. short.
203	Am. Cy.	9 mg.Pt./ cm^2 Extra Pt.	172 Plt. nkl.plq.	"	90% KT 10% Ab with Teflon	22.59	40.0	34		30 cycles. Fair performance.
204	Am. Cy.	9 mg.Pt./ cm^2	127 Pt.Nkl. plq.	"	100% KT	250	40.15	33.0		Slow gas cross leakage.

TABLE I

SUMMARY OF SINGLE-CELL TESTS (Cont'd)

Cell#	O_2 Electrode#		H_2 Electrode#		Mat Thickness Inches and Grade	Mat Dry Wt.	KOH % Wt.	Comments	Results
	#	Catalyst	#	Catalyst					
205	Am. Cy.	9 mg.Pt./ cm^2	Plat. Ni Plq.	20 mg.Pt./ cm^2	90% KT 10% Ab	25.0			52 cycles, developed slow recombination.
206	Am. Cy.	"	"	"	"	20		O_2 electrode used in cells 196, 199	700 cycles gradual degradation.
207	Am. Cy.	"	"	"	"	20		O_2 electrode from cell 202	25 cycles, developed slow recombination.
208	Am. Cy.	"	"	"	"	24.5		Electrode from 6-cell 110	21 cycles. Good performance.
209	Plat. Ni Plq	20 mg.Pt./	"	20 mg.Pt./	"	22.0		H_2 concentration cell.	Discontinued test after 1415 hours final voltage 0.223.
210	Am. Cy.	9 mg.Pt./ cm^2	Plat. Ni Plq.	"	90% KT 10% Ab.	21.5		Electrodes from 6-cell 110	Ran poorly.
211	Am. Cy.	"	Plat. Ni Plq.	"	90 KT 10 ppl**	21.5			50 good cycles, then developed slow gas recombination.
212	Am. Cy.	40 mg.Pt./ cm^2	Plat. Ni	"	90 KT 10 Asb.	22.0			418 cycles, then developed slow recombination last 17 cycles.

** ppl= polypropylene

TABLE I

SUMMARY OF SINGLE-CELL TESTS (Cont'd)

Cell#	O_2 Electrode#		H_2 Electrode#		Mat Thickness Inches and Grade	Mat Dry Wt.	KOH % Wt.	Comments	Results
	#	Catalyst	#	Catalyst					
213	Am. Cy.	9 mg. Pt./ cm^2	Plat. Ni Plq	20 mg.Pt./ cm^2	90 KT 10 ppl**	22.0		O_2 electrode was used in Cell 211	119 cycles, then developed slow recombination.
214	Am. Cy.	"	"	"	90 KT 10 Asb	21.5		O_2 electrode used in cells 196, 199 and 206.	464 cycles, then developed slow gas recombination.
215	Am. Cy.	"	"	"	90 KT 10 ppl	21.5		Used electrodes	30 cycles, then developed slow gas recombination.
216	Am. Cy.	"	Am. Cy.	9 mg. Pt./ cm^2	90 KT 10 ppl	21.5		New electrodes	209 cycles; developed recombination
217	Am. Cy.	40 mg.Pt./ cm^2	Plat. Ni Plq.	20 mg.Pt./ cm^2	90 KT 10 Asb	24 1		Used electrds. from cell 212	432 cycles; recombination.
218	Plat Ni Plq.	20 mg.Pt./ cm^2	Plat. Ni Plq	"	"	21		Electrolyte wt: 35 gm H_2 concentration cell.	1272 hour total
219	Am. Cy.	9 mg.Pt./ cm^2	Plat. Ni Plq.	"	90 KT 10 Asb.	21.3		Electrolyte wt: 50 gm. No backup screens	Poor performance

** ppl = polypropylene

TABLE I

SUMMARY OF SINGLE-CELL TESTS (Cont'd)

Cell#	O_2 Electrode#		H_2 Electrode#		Mat Thickness Inches and Grade	Mat Dry Wt.	KOH % Wt.	Comments	Results
	#	Catalyst	#	Catalyst					
220	Am. Cy.	9 mg.Pt./ cm^2	Plat Ni Plq.	20 mg.Pt./ cm^2	0.060 Asb.	27.3		Electrolyte wt: 50 gm	High impedance cell
221	Am. Cy.	"	"	"	0.060 Asb.	26.1		Electrolyte wt: 50 gm No backup screens	Poor performance
222	Am. Cy.	"	"	"	90 KT 10 Asb.	(1)13.6 (2)13		Two matrixes; Electrolyte: 50 gm. No backup screens Matrix: membrane (poly-ethylene)	Ran poorly; 5 cycles
223	Am. Cy.	"	"	"	90 KT 10 ppl**				40 cycles; recomb-ination developed on cycle 22.
224	Am. Cy.	"	"	"	90 KT 10 ppl	21.4		Electrolyte: 30% KOH, 37 gm.	Discontinued after 24 cycles; recombin-ation developed.
225	Am. Cy.	"	"	"	90 KT 10 Asb.	21.7		Electrolyte: 49% KOH, 37 gm.Used electrodes from 6-cell unit.	10 cycles good. Matrix was subsequen-tly damaged by H_2 leak.

** ppl = polyproplene

TABLE I

SUMMARY OF SINGLE-CELL TESTS (Cont'd)

Cell#	O_2 Electrode#		H_2 Electrode#		Mat Thickness Inches and Grade	Mat Dry Wt.	KOH % Wt.	Comments	Results
	#	Catalyst	#	Catalyst					
226	Am. Cy.	9 mg.Pt./ cm^2	Plat Ni Plq.	20 mg.Pt./ cm^2	90 KT 10 Asb	(1)13.8 (2)14		Electrolyte: 40.3% KOH; 40 gm. Polyethylene membrane. New electrodes. 0.040 separator	4 cycles; poor performance.
227	Am. Cy.	"	"	"	"	(1)14.1 (2)13.6		Electrolyte: 40.3% KOH 40 gm total (20 gm/Matrix) 0.5-inch spacer.	Damaged matrix with large differential.
228	Am. Cy.	"	"	"	"	(1)13.2 (2)13.2		Matrix of woven teflon cloth. Elect. 40.3% KOH; 40 gm total (20 gm/matrix) 0.5-inch spcr.	39 cycles; poor performance.

TABLE I

SUMMARY OF SINGLE-CELL TESTS (Cont'd)

Cell No.	Matrix Layers H_2	Matrix Layers O_2	Matrix Comp. %	Membrane Comp. & %	Separator Thick (Mils)	Electrolyte H_2 Wt.	Electrolyte O_2 Wt.	Electrode Comments	Results	KOH Analysis
229	13.3g	13.5g	90/10 KT & AB	100 FSC	.050	20.0g	20.0g	New	Complete test run at 115°C 347 cyls. Cycle 1-275 good; 276-347 poor, (degradation of matrix due to high oven temp.)	H_2 20.9% Ended O_2 21.2% test at 150 psi.
230	13.3g	13.2g	90/10 KT & AB	Irradiated Polyethylene 100%.	050	20.0g	20.0g	New	44 cycles poor charge pressure (350 psi), discharge press. as low as 70 psi (poor perform.)	H_2 Ended O_2 test at 70 psi.
231	13.5g	13.7g	90/10 KT & AB	"	060	25.0g	20.0g	New	96 cycles, cycles 1-25 good; 26-96 poor (poor performance)	H_2 31.5% Ended O_2 34.15% test at 175 psi.
232	13.4g	13.6g	"	Irradiated Teflon 100%.	050	20.0g	20.0g	New	3 cycles; test discontinued due to high impedance (poor performance)	H_2 29.9% Ended O_2 28.4% test at 100 psi.
233	14.1g	13.5g	"	"	050	20.0g	20.0g	Used in run 232	22 cycles (poor performance throughout test)	Ended test at 170 psi.
234	13.9g	13.7g	"	Irradiated Polyethylene 100%	060	25.0g	20.0g	Used in run 230	5 cycles-differential pressure transducer failed - recombination of gases due to hole in mat (discontinued test)	Ended test at 50 psi.

NOTE: O2 Electrode-Cyanamid 9 mg/cm^2 H2 Electrode-Plat Nickel Plaque 20 mg/cm^2
Electrolyte KOH % - 40.3

TABLE I

SUMMARY OF SINGLE-CELL TESTS (Cont'd)

Cell No	Matrix Layers H_2	Matrix Layers O_2	Matrix Comp. %	Membrane Comp. & %	Separator Thick (Mils)	Electrolyte H_2 Wt.	Electrolyte O_2 Wt.	Electrode Comments	Results	KOH Analysis
235	13.6g	13.4g	90/10 KT & AB	Irradiated Polyethylene 100%	060	25.0g	20.0g	Used in run 230 & 234.	Oven temp. 150°C (one cycle) discontinued test.	Ended test at 150 psi
236	13.9g	13.6g	"	"	"	25.0g	20.0g	Used in run 230,234 & 235.	47 cycles (ran poorly throughout test)	Ended test at 190 psi
237	13.6g	13.5g	"	50/50 KT	050	25.0g	20.0g	Used in run 231	29 cycles (vol. imbalance) discontinued test (ran poorly)	Ended test at 150 psi
238	13.5g	13.5g	"	Microporous polyethylene 12cm	050	20.0g	20.0g	Used in run 232 & 233.	7 cycles (ran poorly) membrane develops leaks easily.	Ended test at 50 psi
239	13.3g	13.8g	"	50/50 KT & Teflon	060	20.0g	20.0g	Used in run 232,233, 238.	Discontinued test after 2079 cycles.	Final KOH 22.5%
240	One matrix 22.3g		95/5 KT & PP	None	040	25.0g	total	Used in run 231 & 237.	Only 25.0g of 40.2% KOH; impedance: 0.017 ohm (discontinued test) (polypropelene derived from polypropylene rope fiber)	Ended test at 100 psi

Note: O_2 Electrode - Cyanamid 9 mg/cm^2 H_2 Electrode - Plat. Nickel Plaque 20 mg/cm^2
Electrolyte KOH % 40.2
Cells #235 & 236 KOH % 40.3

TABLE I

SUMMARY OF SINGLE-CELL TESTS (Cont'd)

Cell No.	Matrix Layers H_2	Matrix Layers O_2	Matrix Comp. %	Membrane Comp.& %	Separator Thick (Mils)	Electrolyte H_2 Wt.	Electrolyte O_2 Wt.	Electrode Comments	Results	KOH Analysis
241	13.5g	13.9g	90/10 KT & AB	50/50 KT & Teflon	060	20.0g	20.0g	New	37 cycles; perform. poor; discontinued test due to high impedance.	Ended test at 130 psi.
242	13.2g	13.2g	90/10 KT & AB	50/50 KT & Teflon	060	20.0g	20.0g	Used in run 225 and SN No.100-11	Membrane soak period; 1 hr 31 cycles-cycles 1-30 good; cycle 31:explosion (recombination of gases due to hole in mat) discontinued test	H_2&O_2 33.15% Ended test at 30 psi.
243	One matrix 19.6g		95/5 KT & PP	None	040	34.0g total		Used in run 241.	Polypropylene derived from polypropylene rope fiber (one cycle),recombination of gases due to extremely porous matrix.	24.1% Ended test at 0 psi

Note: O_2 Electrode - Cyanamid 9 mg/cm^2 H_2 Electrode - Plat. Nickel Plaque 20 mg/cm^2
Electrolyte KOH % 40.2

Cell #241: O_2 Electrode - Plat.Nickel Plaque. 20 mg/cm^2
H_2 Electrode - Cyanamid 9 mg/cm^2

TABLE I
SUMMARY OF SINGLE-CELL TESTS (Cont'd)

Cell No.	Matrix Layers H_2	Matrix Layers O_2	Matrix Comp. %	Membrane Comp.&%	Separator Thick (Mils)	Electrolyte H_2 Wt.	Electrolyte O_2 Wt.	Electrode Comments	Results	KOH Analysis
244	13.5g	13.9g	95/5 KT & PP	FSC 100%	060	20.0g	20.9g	Used in run 229.	Performance good but not equal to that of the 50/50 KT & Teflon membrane (52 cyls. discontinued test due to large differential swing).	Ended test at 20 psi
245	13.7g	14.3g	90/10 KT & AB	50/50 KT & Teflon	060	20.0g	20.0g	Used in run 241 and 243.	Set up as a reproduction of run 239; differential pressure swing due to oxidation reduction. Statham differential pres. transducer failed; recombination of gas due to hole in mat, 27 cycles poor perform.	O_2 30.8% H_2 31.25% Ended test at 150 psi

Note: O_2 Electrode - Cyanamid 9 mg/cm^2 H_2 Electrode - Plat. Nickel Plaque 20 mg/cm^2
Electrolyte KOH % 40.2

TABLE I

SUMMARY OF SINGLE-CELL TESTS (Cont'd)

Cell No.	Electrodes	Matrix	KOH	Spacer (Mils)	Comments
246	Used EOS/Cyanamid	KT/Teflon (50-50) pasted membrane - untreated - sandwiched in 90/10 KT/asbestos	40g (40%)	60	Performance good cycles 1-150 -- discontinued after 257 cycles.
247	New EOS/	KT/Teflon (50-50) pasted membrane- untreated sandwiched in 90/10 KT/asbestos.	40g (40%)	60	HgO reference electrodes on each side of membrane -- test discontinued because of internal recombination.
248	New Cyanamid AB6	100% KT (washed)	34g (40%)	60	O_2 concentration cell. Final voltage = 0.922-0.93 at 18 amps. Test discontinued after 1730 hours. Final KOH 29.5%.
249	New EOS/ American Cyanamid	50% KT/50% Teflon pasted membrane treated 1/2 hour at 130°C in 40% KOH. Membrane sandwiched in 90% KT/10% asbestos mats.	40 gm of 40% KOH	60	Ran 163 cycles; recombination after overcharging. KOH analysis 31.0% on O_2 side, 29.5% on H_2 side.
250	Used in run 247 EOS/American Cyanamid	50% KT/50% Teflon pasted membrane untreated sandwiched in 90% KT/10% asbestos mats.	40 gm of 40% KOH	60	HgO reference electrodes; Run 330 cycles; test discontinued because of degradation in performance. Final KOH: 30.75% O_2 side 30.7% H_2 side.

TABLE I

SUMMARY OF SINGLE CELL TESTS (Cont'd)

Cell No.	Electrodes	Matrix	Electrolyte KOH	Spacer (Mils)	Comments
251	Used EOS/ American Cyanamid	50% KT/50% Teflon membrane treated in KOH at 130°C for 1/2 hour sandwiched between 95% KT/5% polypropylene mats.	40 gm of 40% KOH	60	Ran 594 cycles; test discontinued because of degradation in performance; Final KOH: 26.45% O_2 side 26.7% H_2 side.
252	New EOS/ American Cyanamid	50% KT/50% Teflon membrane treated 1/2 hour in KOH at 130°C. Sandwiched between 2 90% KT/10% asb. mats.	80 gm of 40% KOH	60	Completed 567 cycles; test discontinued because of degradation in performance.
253	From ref. cell 250	50% KT/50% Teflon pasted membrane (untreated) Sandwiched in two 90% KT/10% asb. mats	40	60	Test of reference cell 250 electrode after treatment in KOH and washed; ran 122 cycles; performance poor.
254	New EOS/ American Cyanamid treated in KOH one hour at 130°C.	50% KT/50% Teflon pasted membrane treated 0.5 hours in KOH at 130°C - Sandwiched between two 90% KT/10% asb. mats. All KT treated in KOH at 100 - 130°C and washed.	40	60	Discontinued test after 947 cycles. Final performance was borderline KOH analysis 31%.

TABLE I

SUMMARY OF SINGLE-CELL TESTS (Cont'd)

No.	Electrode	Matrix	Electrolyte KOH	Spacer (mils)	Comments
255	New American Cyanamid AB6	100% KT treated in KOH one hour between 100-130°C washed. Mat (70 mils) weighed 22.2 gm.	34	60	O_2 cycling concentration cell; ran 58 cycles; test discontinued.
256	New EOS/ American Cyanamid	50% KT/50% Teflon pasted membrane treated 0.5 hour in KOH at 130°C sandwiched between two 95% KT/5% polypropylene mats.	40		Discontinued testing because of performance degradation after 443 cycles KOH analysis 31.35%.
257	New EOS/ American Cyanamid	50% KT/50% Teflon pasted membrane (treated) Sandwiched between two 90% KT 10% asbestos mats.	40	60	O_2 cycling concentration cell; ran 59 cycles. Test ended.
258	New EOS/ American Cyanamid	50% KT/50% Teflon pasted membrane (treated) sandwiched between two 100% KT mats.	40	60	Cycle life total 13 cycles. Discontinued test due to recombination of gases.

TABLE I

SUMMARY OF SINGLE-CELL TESTS (Cont'd)

Cell No.	Electrode	Matrix	Electrolyte KOH	Spacer (inch)	Comments
259	H_2-EOS O_2 Cyanamid used	50% KT/50% Teflon pasted membrane treated in 40% KOH sandwiched between 100% KT mats.	40 gm of 40.2% KOH	0.060	Ran 35 cycles then cross gas leakage occurred. KOH analysis 32.6%.
260	H_2-EOS O_2-Cyanamid new, treated one hour in 40% KOH	50% KT50% Teflon sandwiched in two 90% KT/10% asb. mats.	40 gm of 40.2% KOH	0.060	Reverse cycling O_2 concentration cell. Total 56 cycles.

TABLE I

SUMMARY OF SINGLE CELL TESTS (Cont'd)

Cell No.	Electrodes	Matrix	Electrolyte	Spacer (Inch)	Comments
261	H_2-EOS Cyanamid new, treated one hour in 40% KOH	American Cyanamid CeO membrane sandwiched between two 90% KT/10% asb. mats.	40 gm of 40.2% KOH	0.060	Cycles 1-36 discharge 17.5 amp 80°C. " 37-64 " 25 amp 80°C. " 65-386 " " " 100°C. Cross gas leakage occurred after 386 cycles.
262	H_2-EOS O_2-Cyanamid new, treated one hour in 40% KOH.	New KT/Teflon matrix	51.5 gm of 39.7% KOH	0.060	Cross leakage of gases after 3 cycles.
263	H_2-EOS O_2-Cyanamid new, treated one hour in 40% KOH.	50% KT/50% Teflon membrane sandwiched between two 80% KT/20% ZrO mats.	40 gm of 39.7% KOH	0.060	Cycles 1-25 17.5 amp discharge at 80°C. Cycles 26-108 25 amp discharge at 80°C. 109-439 25 amp discharge at 100°C. Discontinued testing because of performance degradation. Total 439 cycles.
264	H_2-EOS O_2-Cyanamid new, treated.	New KT and Teflon matrix	33.2 gm of 39.7% KOH	0.060	After first cycle cross gas leakage occurred.
265	H_2-EOS O_2-EOS new, treated.	50% KT/50% Teflon membrane sandwiched in two 90% KT/10% asbestos mats.	40 gm of 40% KOH	0.060	Reversing current cycling H_2 gas concentration cell. Cell has run 1940 cycles. Test complete. Test temp. 80°C. Final KOH 34.8%.
266	H_2-EOS O_2-Cyanamid used.	New KT and Teflon structure sandwiched between two 90% KT/10% asb. mats.	65 gm of 40% KOH	0.060	Test discontinued after 746 cycles performance good until cycles 660 where the degradation became extreme. Test temp. 80°C. Final KOH 35%.

TABLE I

SUMMARY OF SINGLE-CELL TESTS (Cont'd)

Cell No.	Electrodes	Matrix	Electrolyte	Spacer (inch)	Comments
267	H_2-EOS cyanamid both new and treated in 40% KOH for one hour.	50-50 KT & Teflon membrane sandwiched between 2-90/10 KT & AB mats.	40 gm 39.7% KOH	0.060	Reference cell performance good up through cycle #81. Cycle #82 showed recombination of gases after which testing was discontinued. Total 82 cycles.
268	H_2-EOS O_2-Cyanamid both used in run #252.	KT and Teflon composite matrix with a 34 mesh teflon screen sealed between.	37.7 g of 40% KOH	0.060	Ran a total of 55 cycles cycles when recombination of gases occurred on charging.
269	H_2-EOS O_2-Cyanamid both used in Cell #254.	KT and Teflon composite matrix with a 100 mesh screen pasted with KT & teflon.	56.1 g of 40% KOH	0.060	Performance good through cycle 300. Subsequent cycles show a steady degradation in performance. Test discontinued after 670 cycles. Final KOH 35.5%.
270	H_2-EOS O_2 Cyanamid both used in run #263.	KT and Teflon complosite matrix with a 35 mesh screen sealed between.	47.7 gm of 40% KOH	0.060	Total 1/2 cycle. Discontinued testing due to recombination of gases.
271	H_2 EOS O_2 Cyanamid new electrodes.	50/50 KT and Teflon pasted membrane sandwiched 2-90/10 KT and AB mats.	40 g of 40.3% KOH	0.060	Reference cell. After total two cycles fast self discharge.

TABLE I

SUMMARY OF SINGLE-CELL TESTS (Cont'd)

Cell No	Electrodes	Matrix	Electrolyte	Spacer (inch)	Comments
272	H_2 EOS O_2-Cyanamid Both used in runs #263 and 270.	50/50 KT and Teflon pasted membrane sandwiched 2-90/10 KT and AB mats.	40 g of 40.3% KOH	0.060	Reference cell. After total three fast self discharge.
273	H_2 EOS O_2 Cyanamid New electrodes	50/50 KT and Teflon pasted membrane sandwiched between 2-90/10 KT and AB mats.	40 g of 40.3% KOH	0.060	Reference cell. After total 31 cycles fast self discharge.
274	H_2-EOS O_2-Cyanamid Both used in runs #263, #270, and 272.	Pressed KT-Asbestos Teflon composite 0.060" thick.	47.0g of 40.3% KOH	0.050	Excellent performance through cycle #394. Subsequent cycles show degradation in performance. Total cycles 1120, Test discontinued.
275	H_2-EOS O_2 Cyanamid Both used in runs #272 and 273.	50/50 KT and Teflon pasted membrane is sandwiched between 2-90/10 KT and AB mats.	45.3g of 40.3% KOH	0.060	Reference cell performance good up through cycle #43. Cycle #44 cell began to self discharge.
276	H_2 EOS O_2 Cyanamid Both new and treated for one hour in 40% KOH.	80/20 KT and Teflon composite membrane sandwiched between 2-90/10 KT and AB mats.	45.1g of 40.3% KOH	0.060	Duplication of cell #266. Ran 1102 cycles test. Cell charged in reverse.

TABLE I

SUMMARY OF SINGLE-CELL TESTS (Cont'd)

Cell No.	Electrode	Matrix	Electrolyte	Spacer (inch)	Comments
277	H_2-EOS O_2-Cyanamid Both new and treated for one hour in 40% KOH.	50/50 KT and Teflon pasted membrane between 2-90/10 KT and AB mats.	44.5g of 40.3% KOH	0.060	Reference Cell. Cycle 5 through 13. Showed a fast self discharge. Test discontinued.
278	H_2-EOS O_2-Cyanamid Both new and treated for one hour in 40% KOH.	50/50 KT and Teflon pasted membrane sandwiched between 2-80/20 KT and Teflon rolled composites.	37.2g of 40% KOH.	0.060	Duplication of run #269. Cross leakage of gases.
279	H_2-EOS O_2-Cyanamid Both new and treated for one hour in 40% KOH	50/50 KT and Teflon pasted membrane sandwiched between 2-80/20 KT and Teflon rolled composites.	25.8g of 40% KOH	0.060	Duplication of run #269. Cross leakage of gases.
280	H_2-EOS O_2-Cyanamid Both used in run #277.	50/50 KT and Teflon pasted membrane sandwiched between 2-90/10 KT and AB mats.	45.3 g of 39.5% KOH	0.060	Reference cell. Cell demonstrated good performance through cycle 86, then would not recharge, gross gas recombination. 0.015" nickel wire was substituted for 0.020" nickel wire.

TABLE I

SUMMARY OF SINGLE-CELL TESTS (Cont'd)

Cell No.	Electrode	Matrix	Electrolyte	Spacer (inch)	Comments
281	H_2 EOS O_2 Cyanamid Both used in run 279	50/50 KT and Teflon pasted membrane sandwiched between 2-80/20 KT and Teflon rolled composited.	24.3g of 40% KOH	0.040	Duplication of run #269. Cross leakage of gases.
282	H_2 EOS O_2 Cyanamid Both used in runs 279 and 281.	Pressed KT, asb. Teflon composite 27.5 gm mat.	52.0 g of 39.5% KOH	0.050	Same matrix as cell 274. Cell has run 488 cycles steady. Performance degradation. Test discontinued.
283	H_2 EOS O_2 Cyanamid Both new.	Pressed KT and polypropylene composite 27.1 gm mat.	44 gm of 39.5% KOH	0.060	Cross gas leakage occurred after first cycle.
284	H_2 EOS O_2 Cyanamid Both new.	50% KT/50% Teflon pasted, membrane sandwiched between two 90% KT/10% asbestos mats.	43.5 gm of 39.5% KOH	0.060	Reference cell. Reference electrode wires 10 mils in thickness. Cell showed poor cycling performance. Recombination of gases on cycles 215. Test discontinued.
285	H_2 EOS O_2 Cyanamid Both used in Cell 283.	Pressed KT, poly-propylene and Teflon composite. 23.1 gm mat.	40.0 gm of 39.7% KOH	0.060	Cross gas leakage occurred during first cycle.
286	H_2 EOS O_2 Cyanamid Both new	Pressed KT, asb. and Teflon composite 31.8 gm mat.	40.0 gm of 39.7%	0.060	Cycles 1, through 49 show good performance. Cycle 50, recombination of gases. Test ended.

TABLE I

SUMMARY OF SINGLE-CELL TESTS (Cont'd)

Cell No	Electrode	Matrix	Electrolyte	Spacer (inch)	Comments
287	H_2 EOS O_2 Cyanamid Both new.	Pressed KT, asbestos and Teflon composite 31.8 gm mat.	40.0 gm of 39.7% KOH	0.060	Ran 24 cycles, test discontinued. Cell self-discharges.
288	H_2 EOS O_2 Cyanamid used in runs #283 and 285.	Pressed KT, asbestos and Teflon composite 27.3 g mats.	45.0 g of 39.5% KOH	0.060	Cell ran 859 cycles. Test discontinued because of obvious recombination of gases.
289	H_2 EOS O_2 Cyanamid used in run #287.	50/50 KT and Teflon pasted membrane sandwiched between two 90/10 KT and Teflon mats. Total matrix weight 27.8 g.	45.5 g of 39.5% KOH	0.060	Cell was run 969 cycles. Test discontinued.
290	H_2-EOS O_2 Cyanamid Both new.	Pressed KT, asbestos and Teflon composite 27.3 g mat.	45.5 g of 39 % KOH	0.060	Cycles 1 through 30 demonstrated good performance. Cycle 31, recombination of gases. Test discontinued.

4.3 ELECTRODES

The electrodes were first fabricated by depositing platinum black on sintered carbonyl nickel plaques obtained from Gould Battery Company. A measured amount of heated chloroplatinic acid in water solution was poured through the porous plaques. The plaques were set in a buchner funnel and the solution was sucked through into a vacuum flask. The solution was reheated and repoured over the plaque until all the platinum was deposited. The platinum loading originally used was 10 mg Pt/cm^2 plaque. Figure 9 shows the performance of single cell 7 using this type of catalyst loading. Figure 10 shows a typical E-I curve of a cell using these electrodes at 125°C.

To improve the discharge voltage characteristics it was decided to increase the catalyst loading in the electrodes. For cell 14, an oxygen electrode containing 10 mg/cm^2 platinum catalyst, and 10 mg/cm^2 of palladium catalyst was used. The hydrogen electrode consisted of 20 mg/cm^2 of platinum. Initial performance of this cell was considerably better than that on all previous tests. Typical operating voltage on discharge with the original electrodes was approximately 0.7 volt. By increasing the catalyst loading, the cell operated at approximately 0.8 volt on discharge at the same current level. However, after cycling 7 to 8 times, this cell deteriorated in performance. Figures 11 and 12 show the performance and degradation of performance of cell 18 using these same electrodes. This fast degradation of performance has been shown to be caused by the asbestos matrix and will be discussed in the matrix section of this report.

A series of single cell tests were done to evaluate commercial platinized fuel cell electrodes. Cell 23 employed American Cyanamid AB-4 electrodes on both the hydrogen and oxygen positions. The initial discharge voltage at 16 amps was 0.8 to 0.82 volt, but the charge ranged between 1.7 to 1.9 volts. After six cycles, the

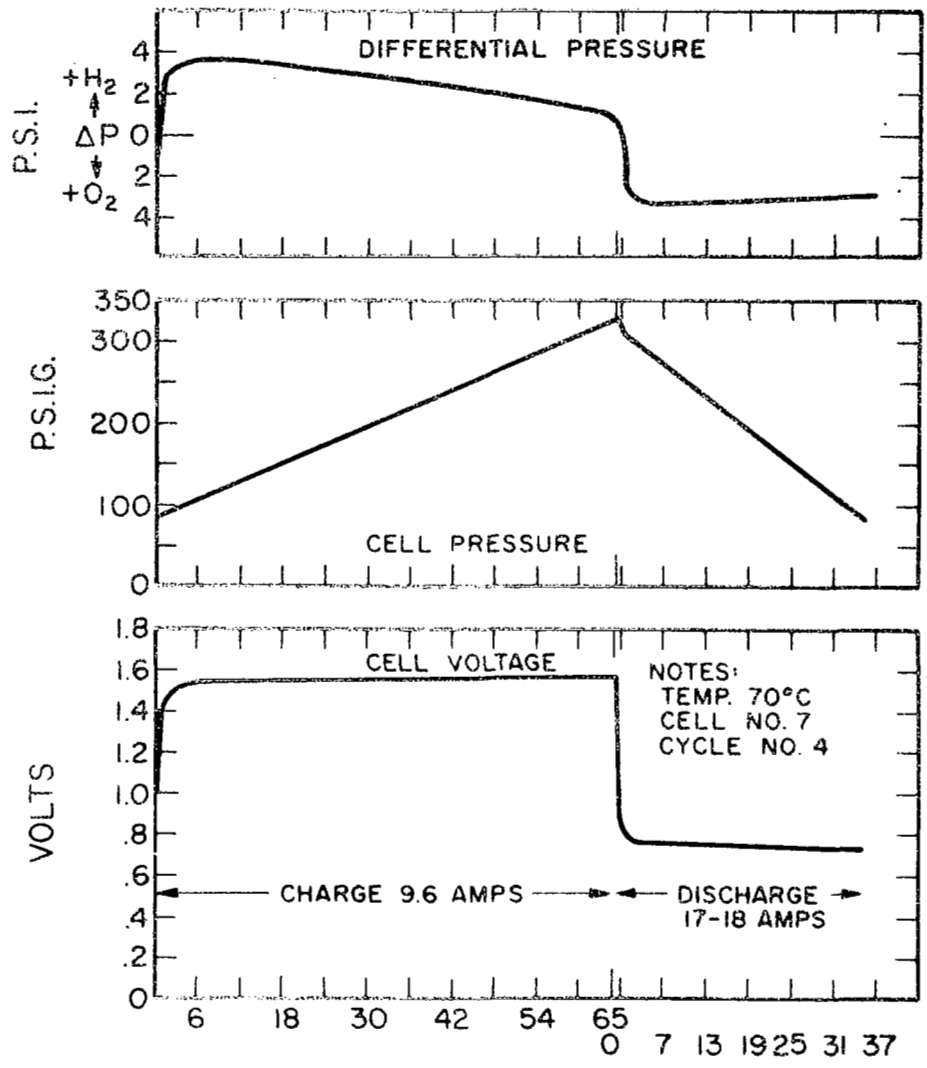

Figure 9. Cycling Data - Hydrogen-Oxygen Electrolytic Regenerative Fuel Cell

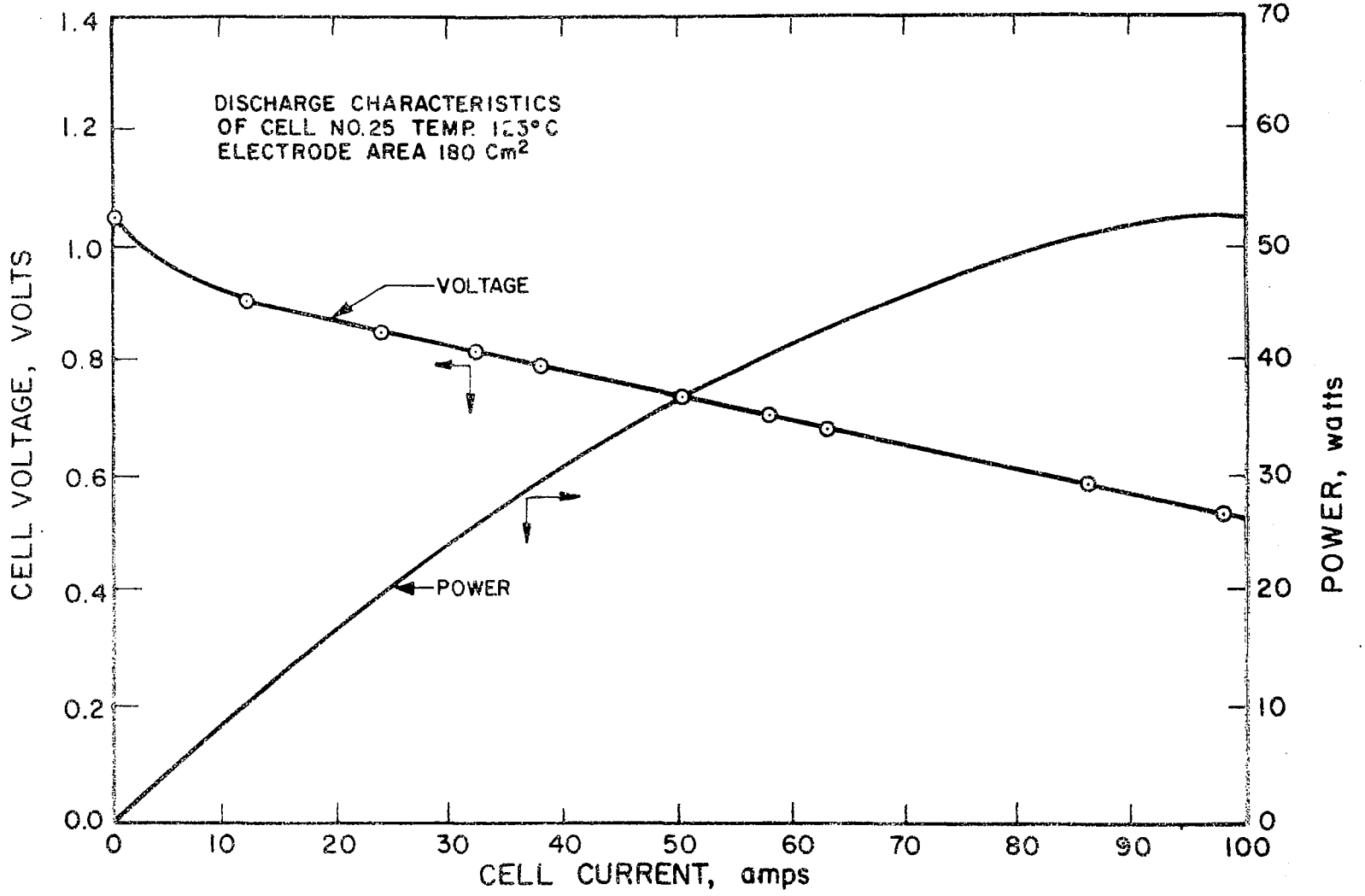

Figure 10. Cell No. 25 Discharge Characteristics

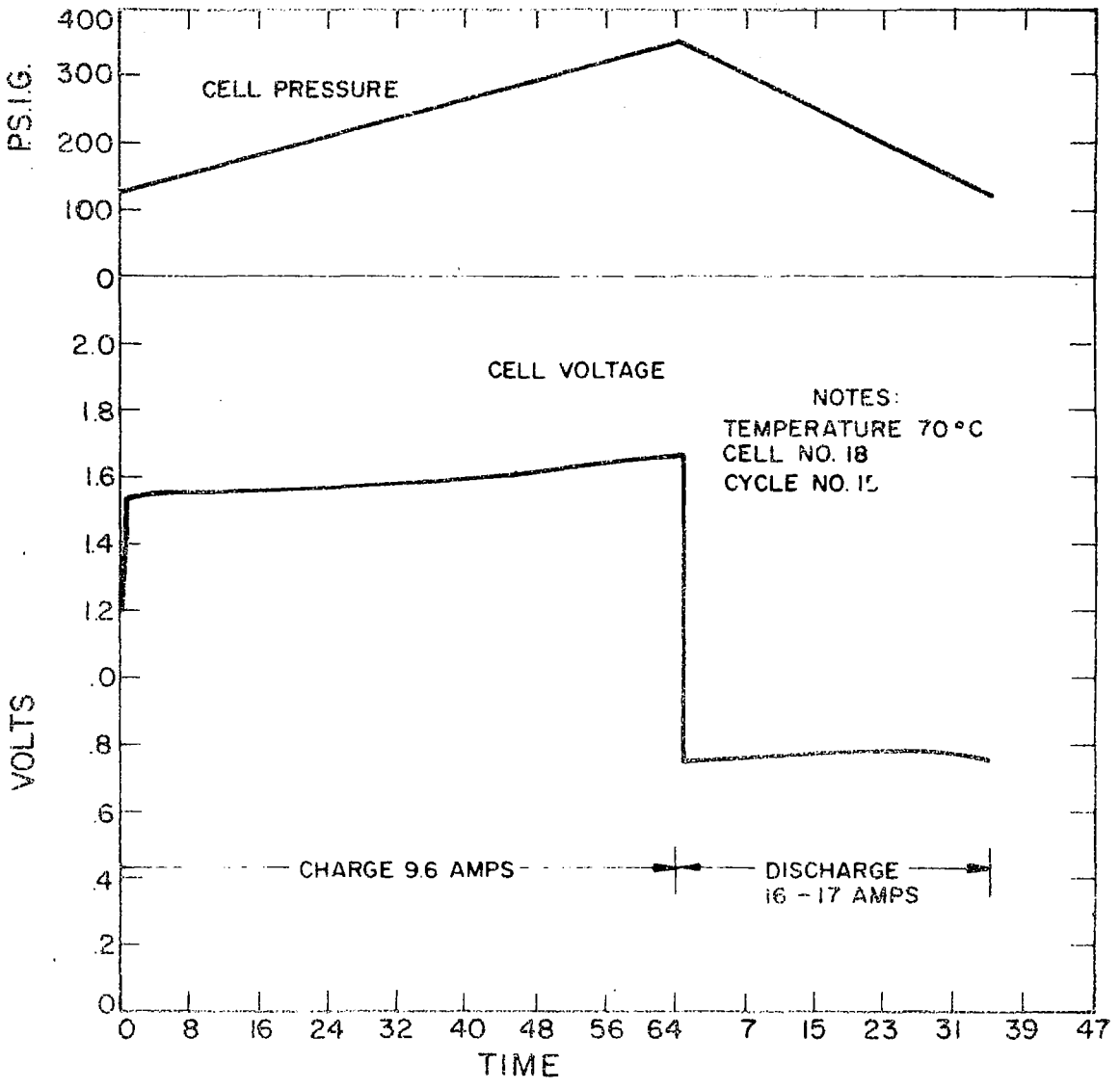

Figure 11. Cycling Data for Cell 18

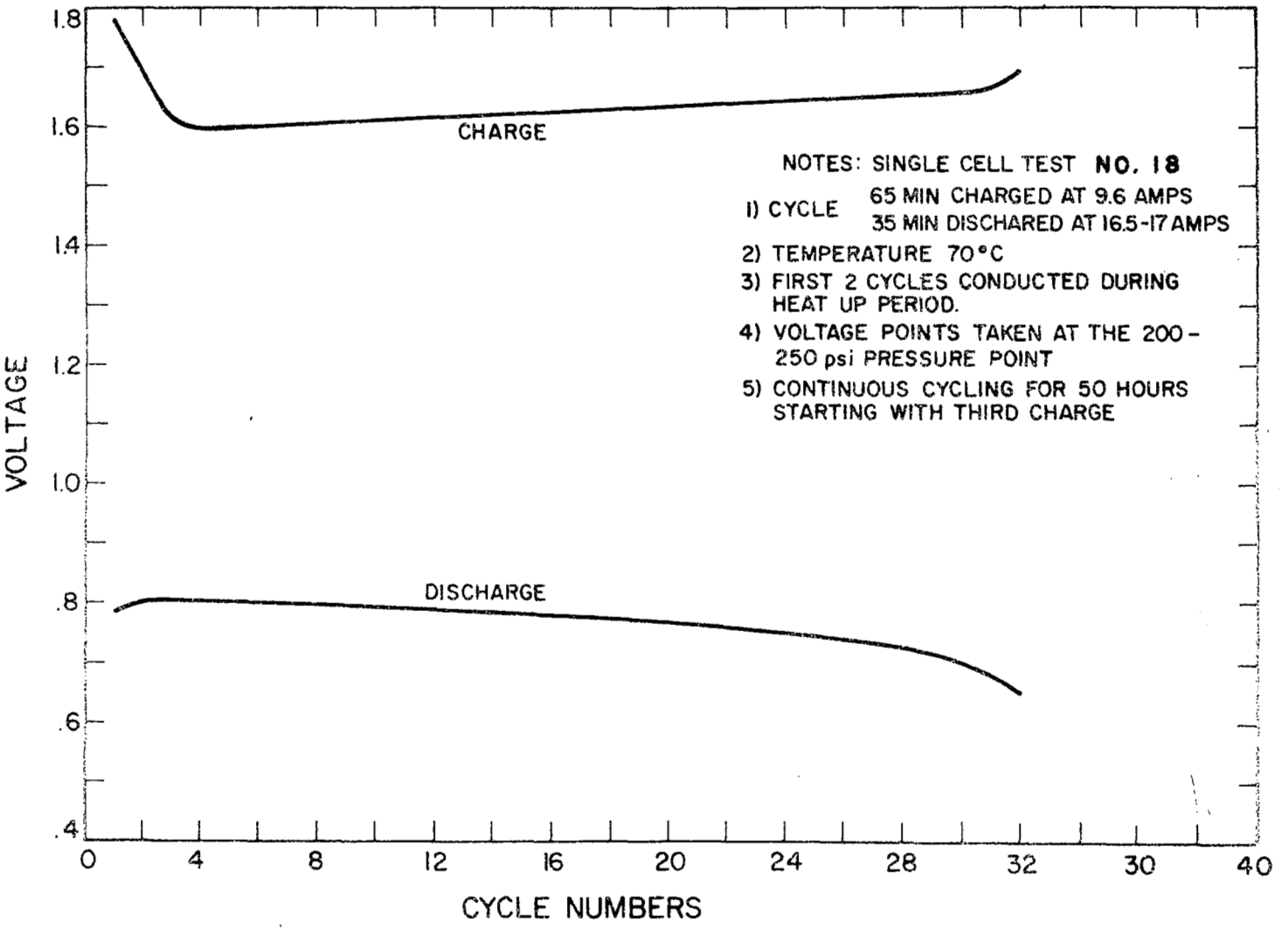

Figure 12. Effect of Cycling on Cell Voltage, Cell 18

discharge dropped to 0.76 to 0.78 volt.

Cell 24 utilized an AB-4 electrode on the oxygen side, and a standard EOS (20 mg/cm^2 platinum) hydrogen electrode. The discharge voltage at 16 amps initially was between 0.80 and 0.82 volt. The charge voltage ranged between 1.7 and 1.8 volts. After 11 cycles, the discharge voltage dropped to 0.78 volt. Cell 25 used EOS electrodes with a 20 mg Pt/cm^2 loading in both the hydrogen and oxygen positions. Figure 13 shows a comparison among cells 23, 24 and 25. At this time the EOS 20 mg Pt/cm^2 loading was adopted as the standard electrode and utilized on both positions.

The high porosity electrodes employed in the regnerative cell at this time had been prepared by manual application of the catalyst fluid to the basic electrode plaque. This procedure was both time consuming and subject to variations in quality. Since a 500-watt unit required 78 electrodes per assembly, this manual process was deemed unsuitable. Therefore, we set up an automated process for electrode preparation. The process consists of a recycling flow system in which the catalyst solution is pulled, via vacuum, through the nickel plaques in controlled pulses. The first electrodes made by the automated process were found not to be suitable. The problem was that the catalyst had been deposited as a loose surface coat that was mechanically unstable. Indications were that this was due to incorrect (too slow) cycle timing. A new cycle timer was purchased. At higher cycle rates, high performance electrodes were obtained.

Cell 57 was assembled to check out a new set of electrodes processed using the automatic electrode technique. The cell was cycled on the standard 65 minutes charge, 35 minutes discharge. Performance, as shown in Fig. 14, was slightly worse than that obtained with electrodes prepared in the manual process. The structural aspects of the electrodes were good. Apparently, the location of the catalyst within the porous

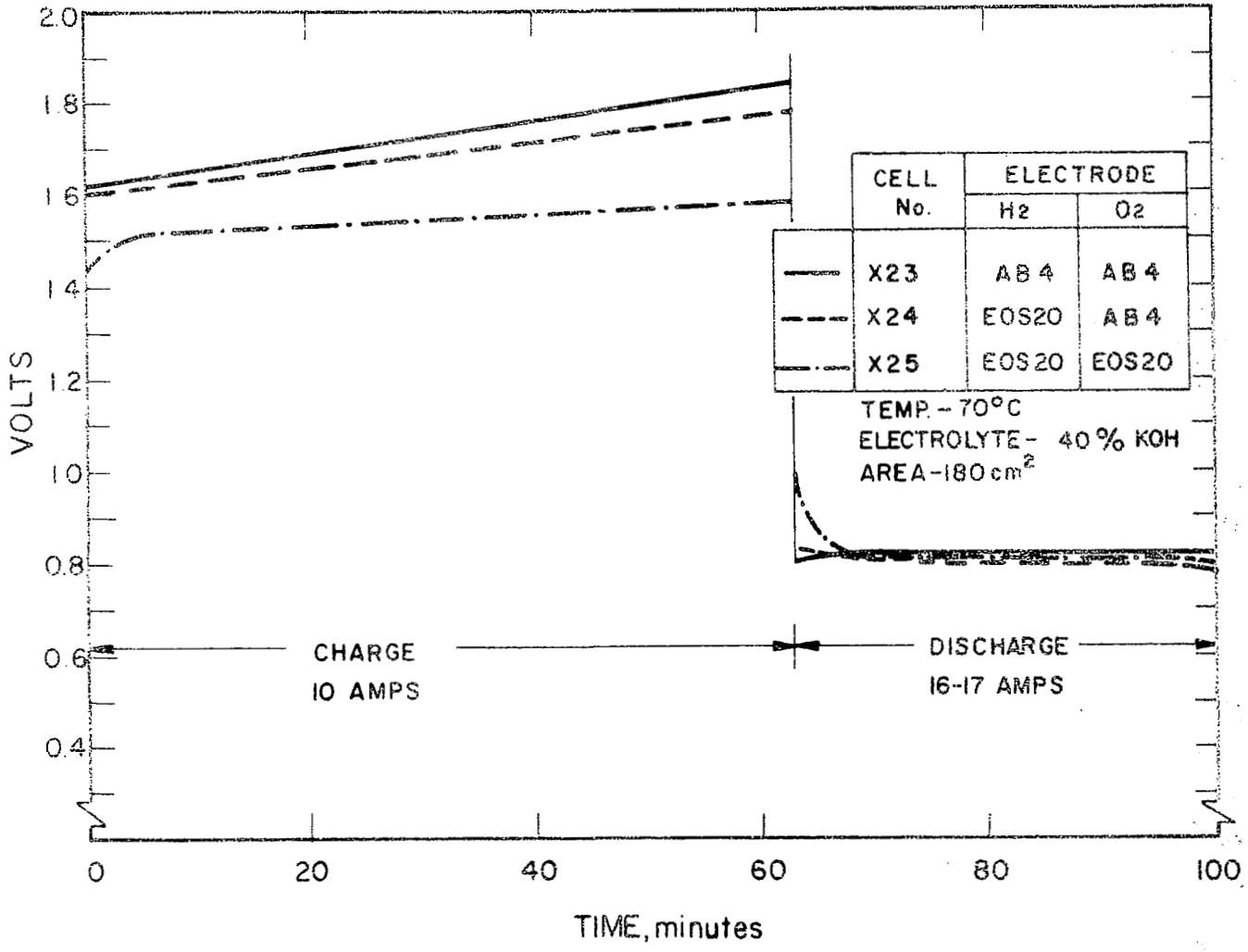

Figure 13. Comparison Between Commercial and EOS Electrodes

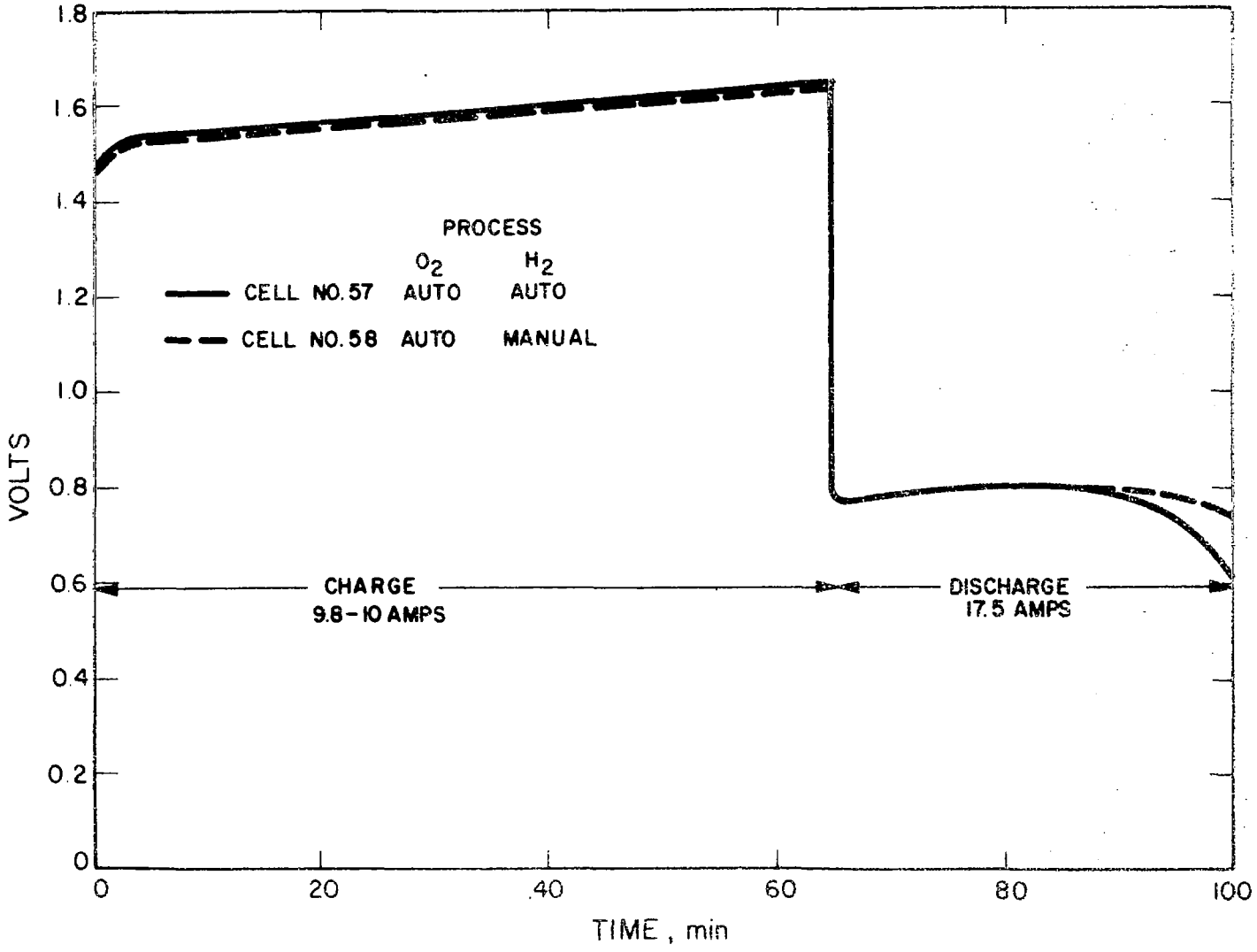

Figure 14. Performance Data of Automatic Processed Electrodes

nickel plaques is very critical. Visually, it appears that in our manual process, a heavier catalyst loading exists on the top of the electrode, the surface adjacent to the matrix, with a decreasing catalyst loading out to the back side. These electrodes appeared to have a more uniform distribution of loading, and possibly the actual reaction zone had a relatively low catalyst loading. The location of the catalyst in the automatic process can be adjusted somewhat by the cycle used in applying the catalyst.

Cell 58 was assembled with one of the "automatic" electrodes on the oxygen side as a comparison between "standard" cells and the cell containing two automatic processed electrodes. The performance of this cell was improved above the previous cell, but did not reach the levels of cells employing electrodes made by the manual process. Performance of this cell is also shown in Fig. 14.

Electrodes, supplied as samples by Bishop Metals, were used in cell 63. These electrodes were standard porous nickel plaques (the type used in EOS electrodes) that had been platinized by a Bishop proprietary process that impregnates the catalyst in the half of the electrode adjacent to the mat. The platinum catalyst loading of these electrodes was 20 mg/cm^2. On charge, the cell voltage rose rapidly to as high as 3 volts. However, on discharge, the performance was fair and an average plateau voltage of 0.75 volt was obtained. Measurements of the cell impedance indicated that the cell resistance was slightly higher than that of normal cells. Therefore, it was decided to discontinue the test, reassemble the cell, and re-run it to assure that performance obtained was reproducible.

Cell 67 was assembled to re-evaluate the Bishop platinum electrodes. As initially received, the electrodes contained what we believe to be acetic acid. In this condition, as described for cell 63, performance

was not satisfactory. Prior to re-use, the electrodes were thoroughly washed to eliminate reaction products between the KOH electrolyte and the "acetic acid". Performance was vastly improved in cell 67 as compared to the prior test. Figure 15 shows a discharge voltage of 0.87 volt and a lower charge voltage than cell 63.

Single cells 72, 73, 74 and 75 were set up to evaluate American Cyanamid type AA-1 electrodes. These electrodes consist of a platinum/Teflon mix that is coated on a tantalum wire screen. The catalyst loading is 9 mg/cm^2, and the electrode thickness is 0.015 in. In all the cell tests, the Cyanamid electrode was used on the oxygen side, and an EOS 20 electrode was used on the hydrogen side. A leak developed through a worn out spacer in cell 72, and this cell was never subjected to test.

Cells 73, 74, and 75 were cycled a limited number of times. Performances were very poor on both charge and discharge. Disassembly of the cells revealed that the tantalum screen within the electrode had been entirely dissolved in the alkaline electrolyte.

Cells 77 and 78 were assembled to determine if performance improvements could be obtained by using higher catalyst-loaded oxygen electrodes. The oxygen electrodes employed were American Cyanamid type AB-40, which consist of a nickel screen coated with a platinum/Teflon mix with 40 mg of platinum per square centimeter. The cells were cycled on a normal 100-minute cycle. Typical performance is shown in Fig. 16. As can be seen, the voltage of the cell took an initial dip when the discharge was started, rose to a high level, and then dipped off once again at the end of discharge. During the cycle, cell discharge voltages as high as 0.9 of a volt at 17.5 amperes were obtained. This performance exceeded all previous test results. However, this high performance level only occurred during a short portion of the discharge. Apparently the AB-40 electrode performance is very sensitive to water content. During

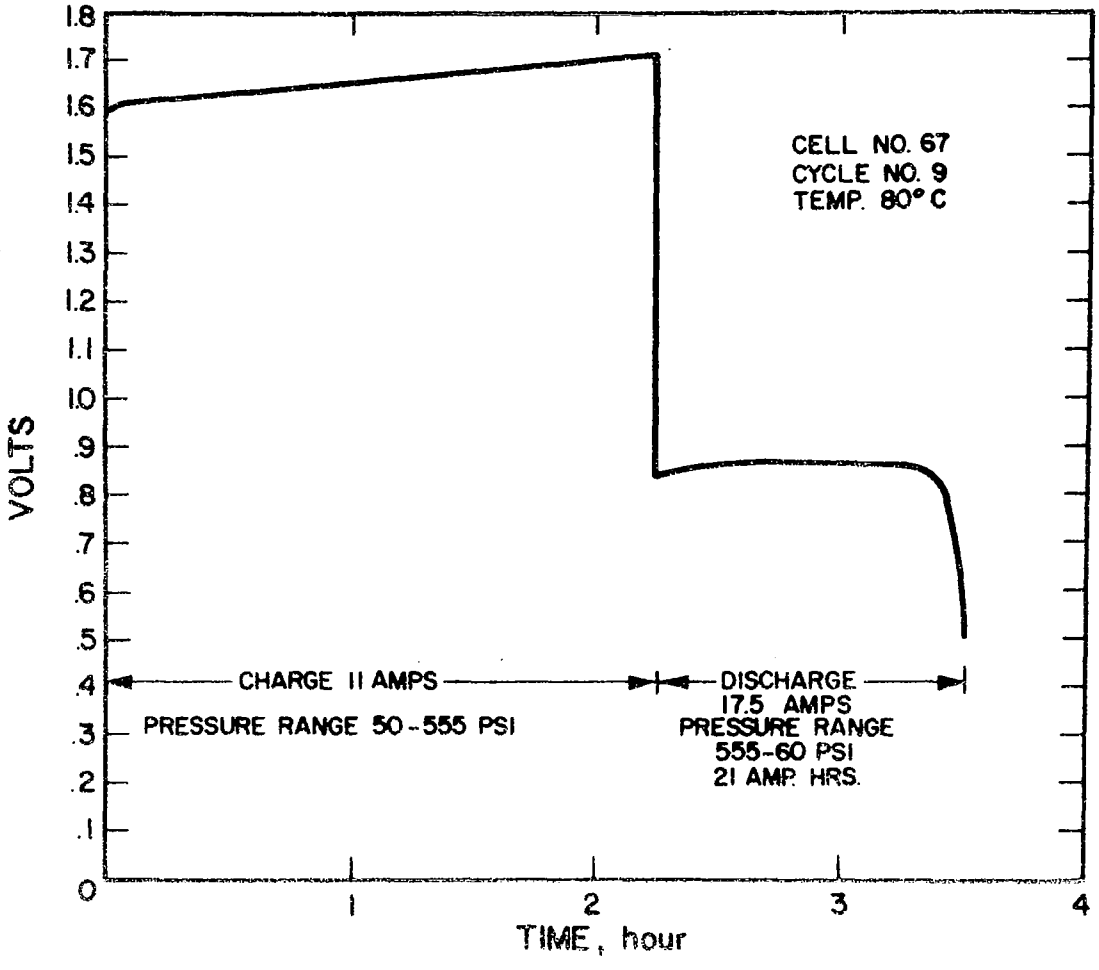

Figure 15. High Capacity Test

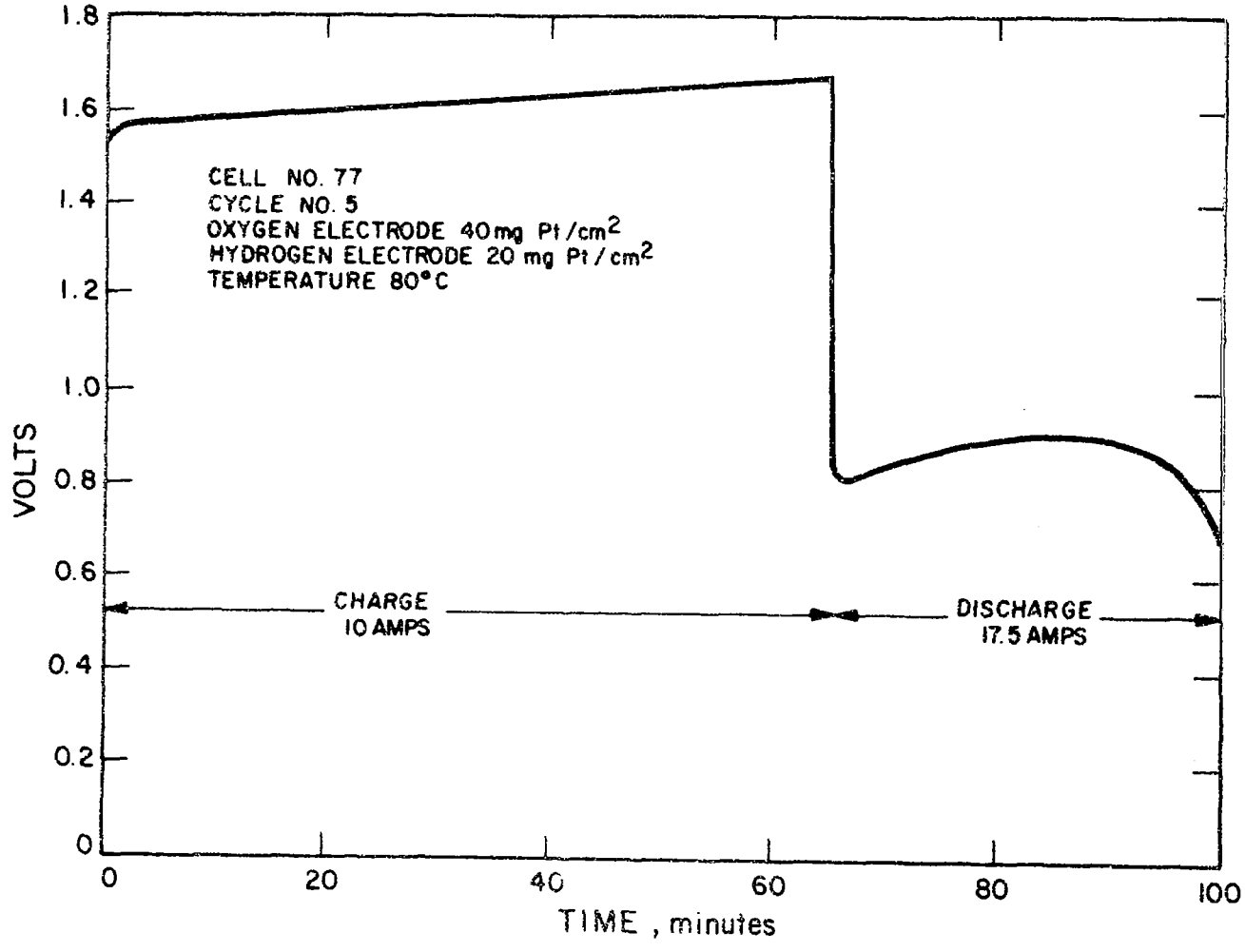

Figure 16. Performance Data of High Catalyst Loaded Oxygen Electrode

the middle of the discharge, the optimum liquid quantity occurs, and peak performance is obtained. For the rechargeable type fuel cell, where water is stored in a matrix, this sensitivity to liquid quantity is not desirable. Possibly different initial electrolyte quantities and compression ratios could alter the water sensitivity of these electrodes.

Cell 86 consisted of an oxygen electrode that had been catalyzed with 40 mg/cm^2 of platinum by our automatic electrode process. It was hoped that this cell would show improved performance due to the increased catalyst loading on the oxygen electrode. However, the electrical performance was no better than obtained with standard 20 mg/cm^2 platinum electrodes.

Cell 87 was a repeat of cell 86 using the same electrodes that had been washed in distilled water before the reassembly. This cell also showed no significant improvement of performance as compared to the standard electrodes.

Cell 88 was a test which included an oxygen electrode of the Huyck felt metal type that had been catalyzed with 20 mg of platinum per square cm. The felt metal employed was material received from NASA that was 0.022 inch thick, and was designated as 15 percent dense nickel. The substrate was catalyzed in the normal manner by manually recycling a hot solution of chloroplatinic acid through the plaque until 20 mg/cm^2 of platinum was picked up by the porous nickel structure. Performance of this cell is shown in Fig. 17. The Huyck plaque electrodes performed as well as our standard porous nickel plaque electrodes. Similarly, upon repeated cycling, this cell showed a gradual degradation of performance. The cell was cycled 17 times, disassembled, and the electrodes washed.

A new cell was assembled with the washed electrodes plus a new matrix, and was designated Cell 91. Initial cell performance was approximately of the same level as cell 88 when the test was stopped. On repeated cycling, the performance gradually degraded. Testing was stopped at the 39th cycle. Figure 17 also shows the performance on the 38th cycle of cell 91. The fact that the initial cell performance was

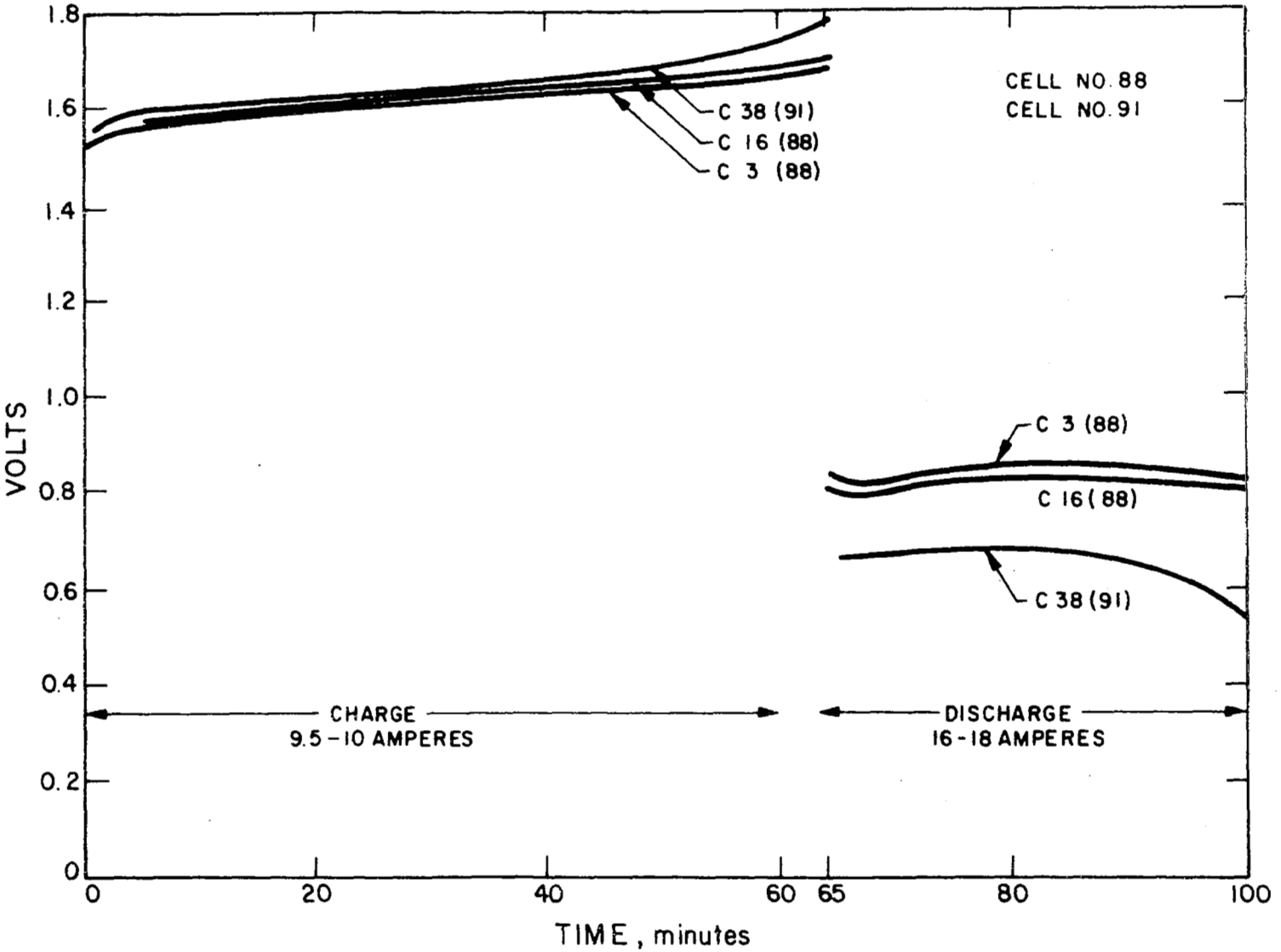

Figure 17. Performance of Felt Metal Electrodes

recovered after the electrodes were washed and assembled in a new cell indicated that the source of immediate performance degradation may not have been caused by the electrode.

In discussions with NASA/Lewis, and American Cyanamid technical personnel, it was revealed that gradual performance deteriorations with the AB-4 type electrodes had been encountered in primary hydrogen-oxygen fuel cells. In that case it was reasoned that a gradual oxidation of the nickel screen caused the degradation in performance. To overcome this deficiency, American Cyanamid fabricated experimental electrodes in which the nickel screen was gold plated, and they found that this considerably reduced performance deterioration. The phenomenon of the nickel substrate being oxidized would be greatly accelerated in a regenerative device, since oxidation occurs much more readily during the charge portion of the cycle. This mode of deterioration was in agreement with our thinking and was a primary reason for evaluating American Cyanamid electrodes as a method of eliminating porous nickel plaques, such as EOS electrodes. However, the high porosity nickel plaque electrode remains the best electrode from the standpoint of overall performance. Gold-plated nickel screen Cyanamid electrodes were then evaluated in single cell tests.

Cells 92 and 93 were assembled utilizing oxygen electrodes purchased from American Cyanamid. These were the standard AB-4 type containing 9 milligrams of platinum per square centimeter, except that the nickel substrate screen had been gold plated to minimize oxidation and corrosion. Cell 92 contained two 0.030 inch asbestos mats and was cycled 130 times on the standard 65 minute charge, 35 minute discharge test cycle. Figure 18 shows voltage performance of the cell at various cycles. As can be seen there was a gradual increase of the charging voltage, and a decrease in the discharge voltage as the cycling continued. The final electrolyte concentration within the asbestos mat was found to be between 26.2 and 26.9%. Examination

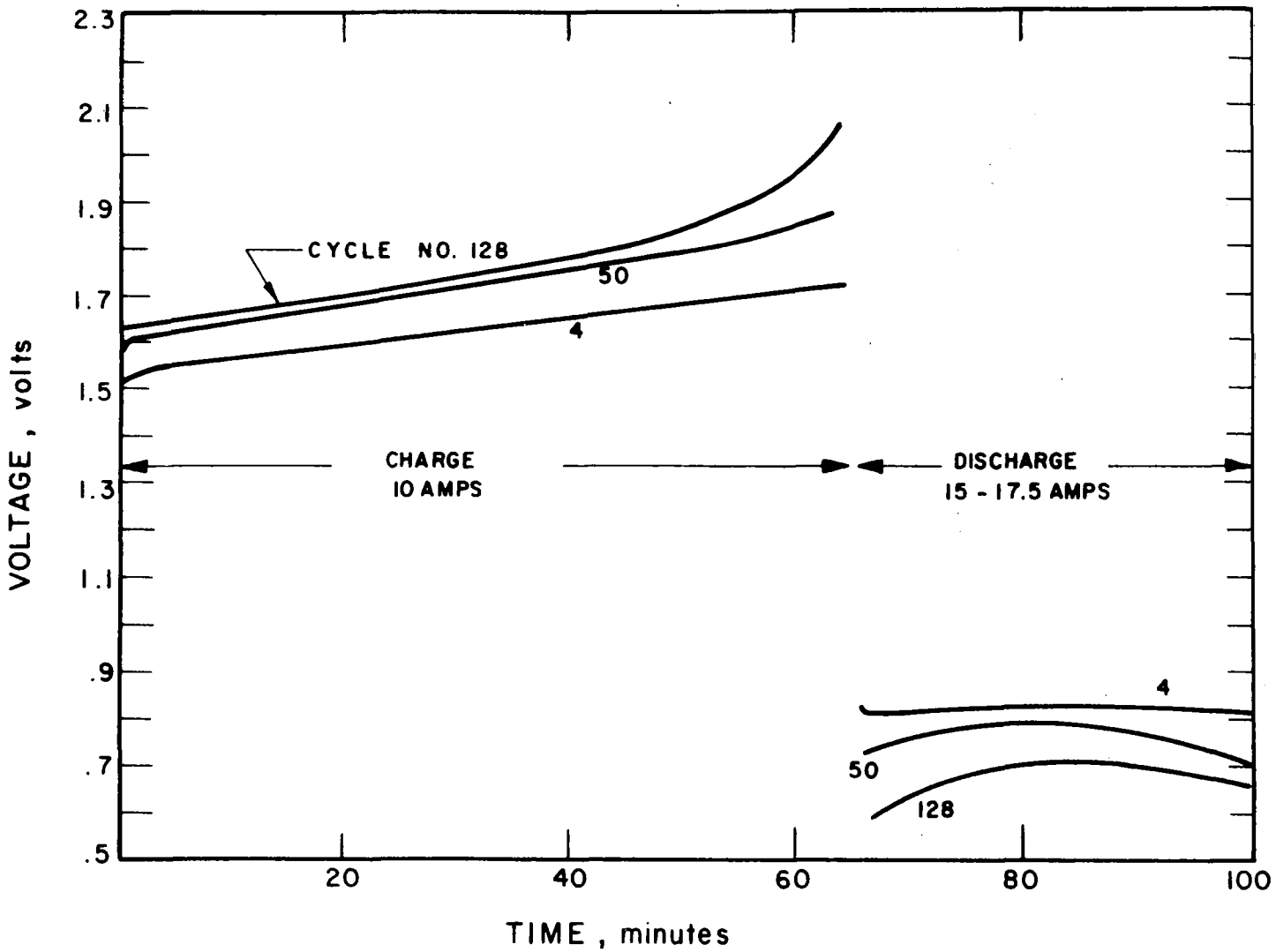

Figure 18. Cycling Performance of Cell No. 92

of the cell components after the cell was disassembled revealed no obvious changes in the electrodes. The gold plating on the nickel subscreen, wherever visible, looked impervious and firmly attached to the screen.

Cell 93 was similar to 92 except that one layer of 0.060 inch asbestos was used and cycled only 38 times. This cell showed good discharge performance (0.80 to 0.84 volt at 100 mA/cm^2), but the voltage during charge rose very rapidly to values as high as 2.0 volts. As cycling continued, the voltage on charge got progressively higher, and the discharge voltage fell off rapidly towards the end of discharge. The test was therefore discontinued. KOH concentration was found to be 27.8 and 28.4 percent on two samples extracted from the matrix.

Cell 94 consisted of an oxygen electrode that had been platinized to 20 mg/cm^2 by a proprietary process of the Bishop Company. The substrate of these electrodes consisted of porous sintered carbonyl nickel plaques of the type used in standard EOS electrodes. This cell was cycled 21 times. The initial performance of the cell was good, discharge voltage being approximately 0.82 volt (100 mA/cm^2) and charge voltage approximately 1.6 to 1.75 volts (55 mA/cm^2). However, as the cycling continued, a gradual increase in the charging voltage and a decrease in the discharge voltage accompanied by a substantial fall-off in discharge voltage at the end of discharge was observed.

Cell 95 consisted of an oxygen electrode that had been platinized by the Bishop Company to 40 mg/cm^2. This cell also exhibited good initial performance, and showed a gradual degradation of both charge and discharge voltage. However, the increased catalyst loading of the electrode did not improve performance above that obtained with the 20 mg/cm^2 loading as used in cell 94.

Cells 96 and 97 were repeats of cells 92 and 93, utilizing the same electrodes with fresh asbestos mats. Before the test, each of the electrodes was washed with hot distilled water and dried. Performance obtained with cell 96 was similar to that obtained with cell 93; i.e, the charge voltage rose rapidly to levels as high as 2.2 volts. Discharge performance was low, ranging between 0.5 and 0.7 volt. The cell was cycled 37 times. Cell 97 showed good initial performance, but gradually degraded with cycling. Voltage performance at various cycles is shown in Figure 19. The final KOH concentration in the matrix was found to be 25.7 percent.

Test results, using American Cyanamid electrodes, indicated that performance degradation can occur even though nickel is not present in the electrochemical reaction zone. Since these electrodes were apparently rejuvenated by a simple washing process, this indicated that either the asbestos/electrolyte interface was the cause of performance degradation, or some water-soluble catalyst poison was formed which was removed by washing. Since KOH was lost during cycling, the initial premise appeared to be more likely. This KOH loss factor was definitely accelerated by cyclical operation and indications were that increasing temperature also accelerated the loss. This loss factor is discussed later in the report.

Cell 100 consisted of two Cyanamid 9 mg/cm^2 platinum (gold-plated nickel screen) electrodes back to back on the oxygen side and standard EOS electrode on the hydrogen side. Purpose of the test was to determine if use of the back-to-back oxygen electrodes would reduce the sensitivity to water content, i.e, flooding out and drying observed with American Cyanamid electrodes when used in the regenerative fuel cell. The cell was cycled continuously for 60 times on the standard cycle. A typical cycle is shown in Fig. 20. As can be seen, even with the back-to-back oxygen electrodes, the cell exhibited a gradual rise in voltage at the end of charge

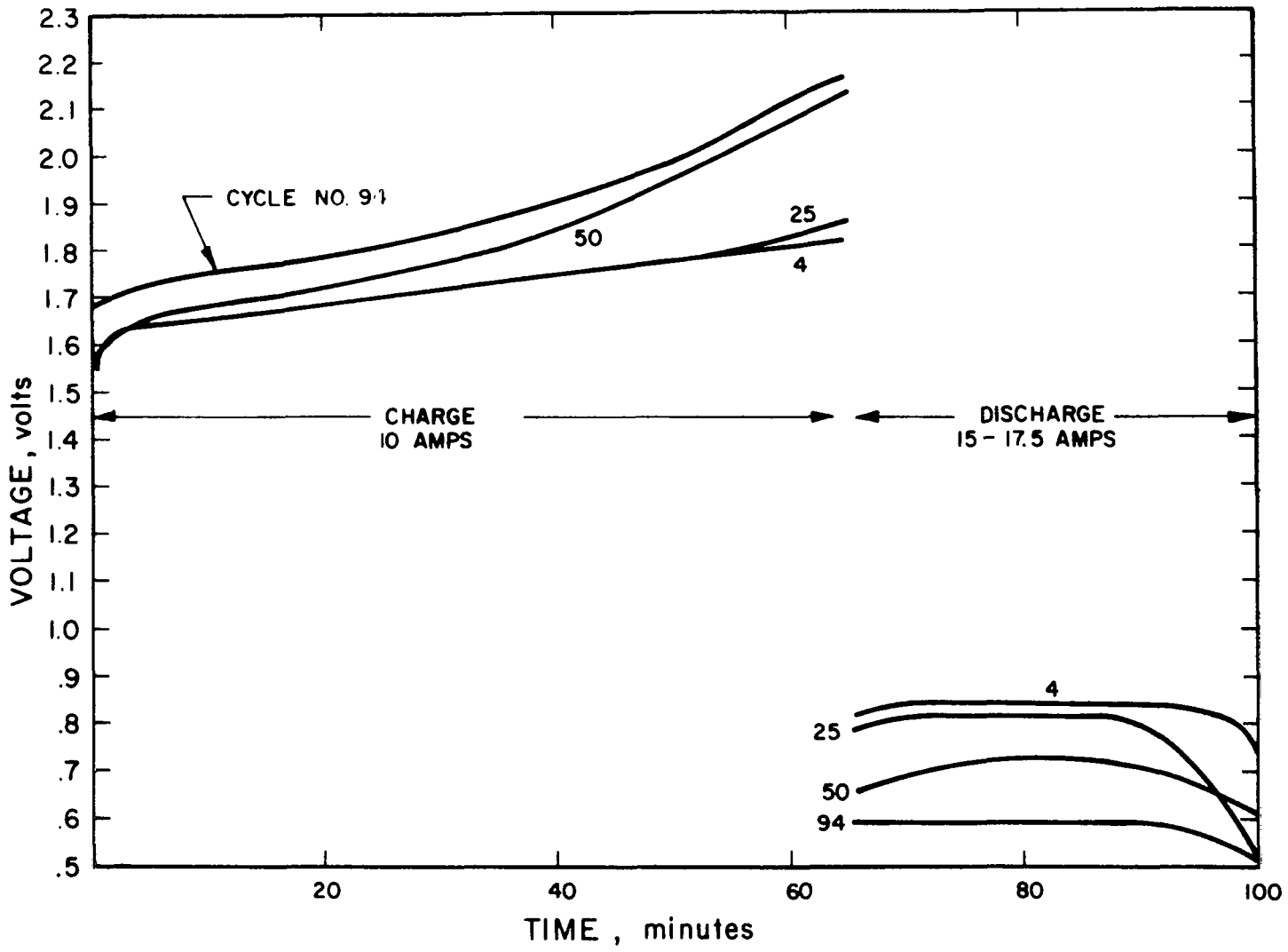

Figure 19. Cycling Performance of Cell No. 97

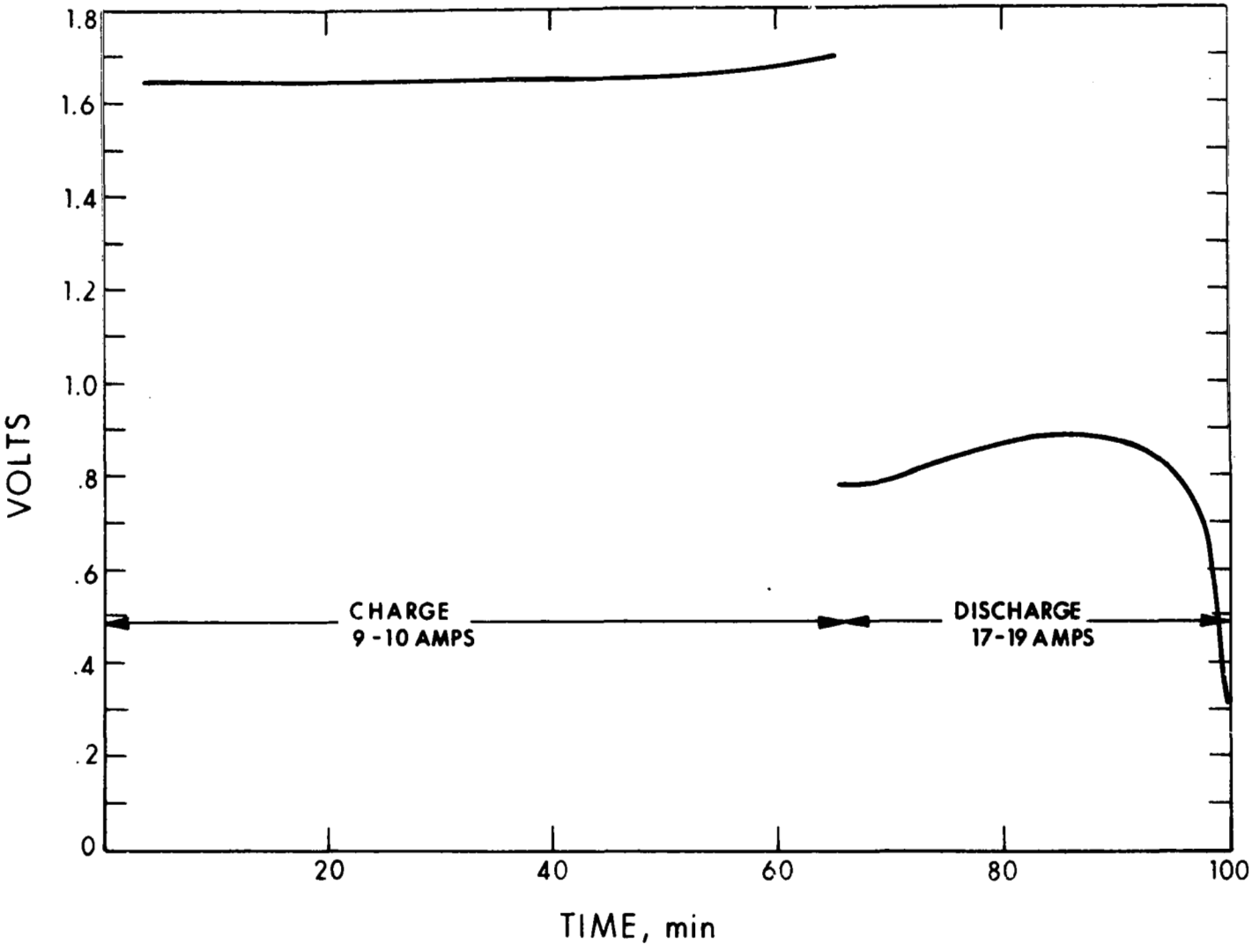

Figure 20. Performance Data of Two Cyanamid Electrodes Back-to-Back as Oxygen Electrodes

(indicating drying out, a dip in the voltage initially during discharge, and rapid fall-off in voltage toward the end of discharge, indicating flooding). However, during the middle of discharge, the performance of these electrodes was excellent.

Cell 101 was a repeat of cell 100 utilizing the same electrodes after they had been washed and employing a new matrix. The performance of the cell was virtually identical to that of the previous cell, and the test was stopped after 15 cycles.

Cell 102 consisted of a standard hydrogen electrode and a new type of oxygen electrode. This oxygen electrode was fabricated at EOS by gold plating and then platinizing a standard porus nickel plaque.

The procedure used in preparing these new electrodes was similar to that used in fabricating our standard type. The steps were as follows:

1. Plaques were washed and degreased.
2. A hot (190-200°F) electroless gold plating solution was continuously recycled through the plaque. The plating solution was a commercial material designated Aurolectroless-N, manufactured by Lee Ronal, Inc. It contained 1 troy ounce of gold per gallon. A quantity of 400cc of this solution was used per 6-inch-diameter electrode and contained 3.3 grams of gold.
3. After removal from the electroless bath, the electrodes were washed and then immersed in a gold cyanide electroplating bath. An electroplating of an additional 3.7 grams of gold was then put on the electrodes.
4. After removal from the gold electroplating bath, the electrodes were washed and immersed in a chloroplatinic acid plating bath. Platinum was plated on the electrode to an equivalent of 7.5 mg/cm^2.

Cell 102 was cycled five times and then developed an internal short. It was disassembled and examined. The short was found on the edge of the electrodes and was due most probably to poor assembly, The electrodes were washed, assembled with a new matrix, and designated cell 103. The performance of this cell at various cycles is presented in Fig. 21. As can be seen, during the first 150 cycles, only slight degradation was encountered; however, beyond that point a rapid rate of degradation was observed. Examination of the disassembled cell revealed no obvious cause for the degradation. This cell represented our initial attempt at fabricating such electrodes. It demonstrated that this approach is promising and warrents further study and perfection.

Cell 104 was installed with American Cyanamid H_2 and O_2 electrodes having 9 mg platinum per cm^2 on gold plated nickel screens. This test was set up to determine effects that occur without "free" nickel being present in the electrodes. The cell was cycled 100 times, during which a gradual degradation in performance was observed. The electrodes were then removed from the cell, washed, and replaced in the cell utilizing the same matrix. This cell was designated 106. Figure 22 presents the performances during various cycles of cells 104 and 106. As can be seen, washing the electrodes and rebuilding the cell resulted in somewhat improved performance. The improvement in performance by rebuilding the cell is inconclusive. It did, however, indicate the possibility of a water soluble catalyst poison, which accumulated on the electrodes with cycling, as a cause of gradual performance degradation. Cell 106 also degraded gradually, as shown in Fig. 22.

Cell 105 consisted of an oxygen electrode similar to the type used in cell 103 except that the electrode substrate was nickel felt metal as opposed to the sintered porous nickel plaque. This cell was cycled 46 times and showed relatively poor performance, discharging at approximately 0.7 volt per cell and charging in a range of 1.65 to 1.9 volts.

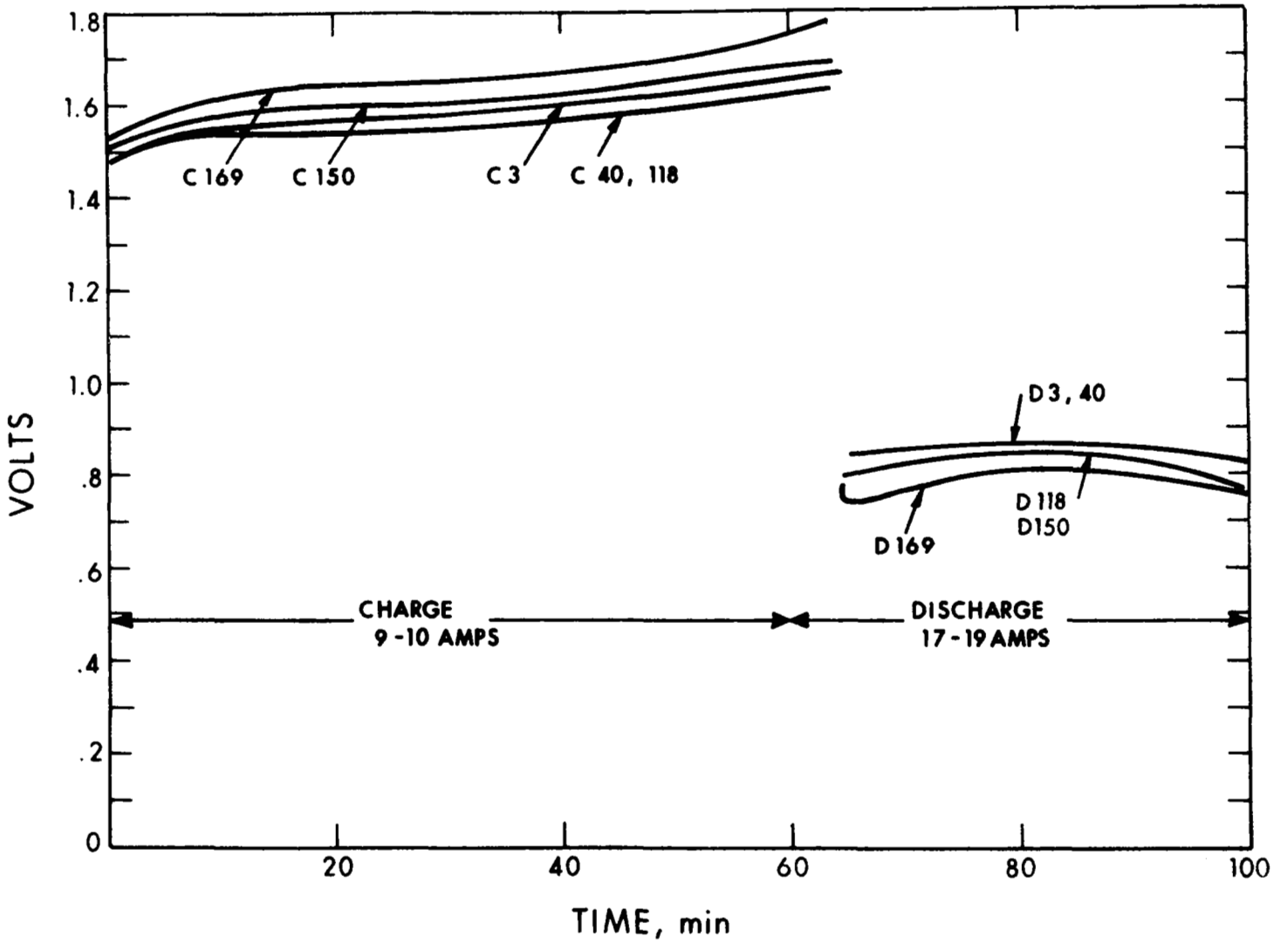

Figure 21. Cycling Performance of Cell No. 103

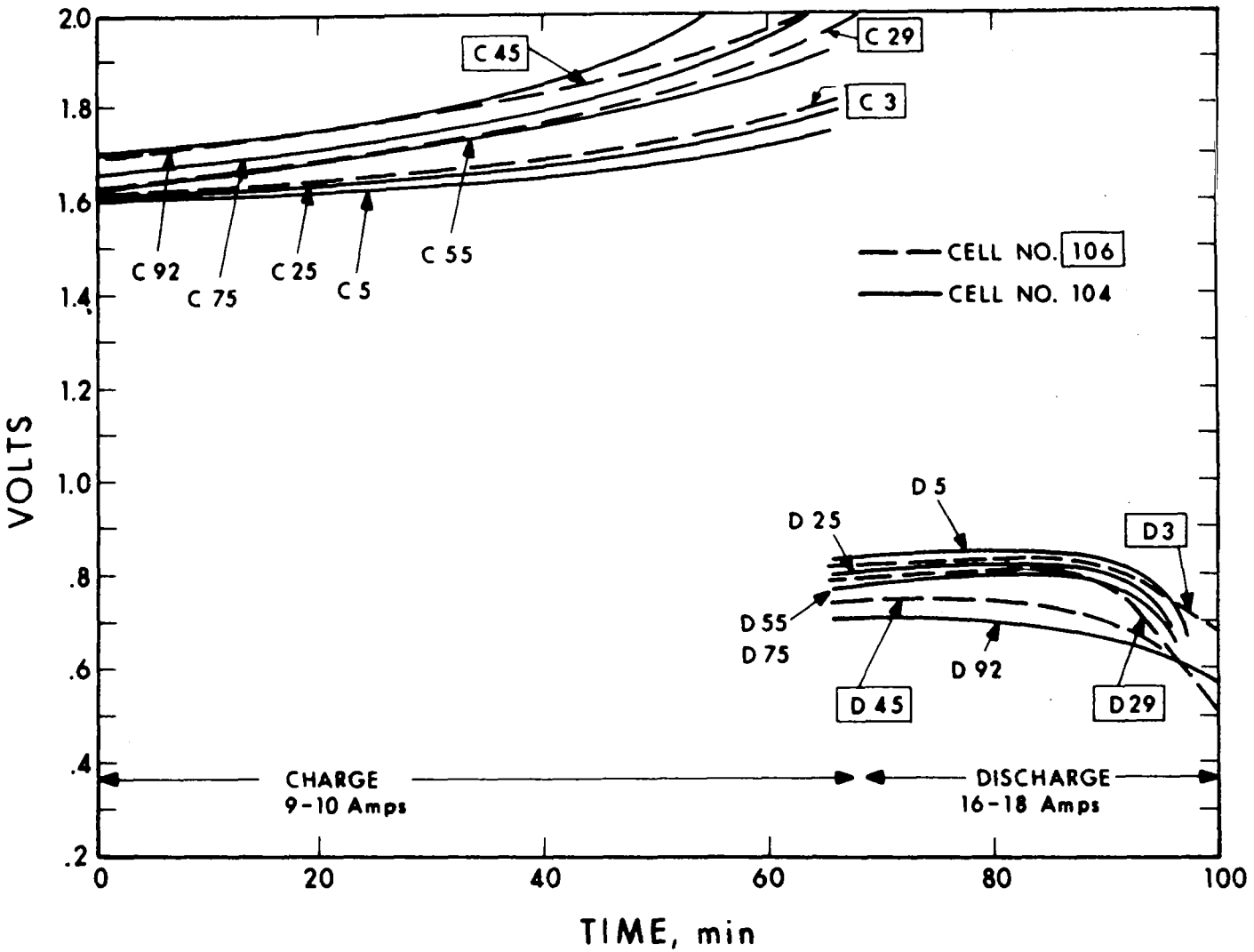

Figure 22. Cycling Performance of Cell Nos. 104 and 106

Cell 107 consisted of an oxygen electrode processed similarly to the electrode used in cell 103, i.e., a gold plated, platinized porous nickel plaque. This cell was cycled 42 times after which an internal reaction occurred within the cell causing a drastic drop in performance.

The electrodes were removed from cell 107 and were washed, reassembled with a new matrix, and designated cell 108. This cell was cycled six times, at which time an internal short developed within the cell. The performance data of cells 107 and 108 are shown on Fig. 23. As can be seen, performance recovered after the reassembly. Results of the rebuilding of cell 107 and the rebuilding of cell 103, described previously, seemed to indicate that an additional deteriorating factor within the cells existed besides the gradual oxidation of the porous nickel plaques as previously determined. This deterioration was thought to have been caused by an impurity from the electrolyte and/or the asbestos matrix.

Cells 109 and 111 consisted of porous sintered nickel plaques that were gold-coated at EOS and platinized by the Bishop Company, utilizing a proprietary platinizing process. Cell 109 was cycled 44 times and showed fair performance, discharging at 0.8 to 0.85 volt per cell and charging at 1.5 to 1.6 volts. A gradual increase in the charging voltage and decrease in the discharge voltage was observed through the cycling. Testing was stopped after 44 cycles. Cell 111 was not subjected to tests due to failure of the differential pressure transducer during the initial setup.

Cell 110 consisted of a felt metal nickel plaque that was gold-coated at EOS and platinized by the Bishop Company. This cell was cycled 50 times and then the test was discontinued. Performance of the cell was poor. At the end of discharge, there was a rapid fall-off in voltage, and, at the end of charge, there was a substantial rise in voltage.

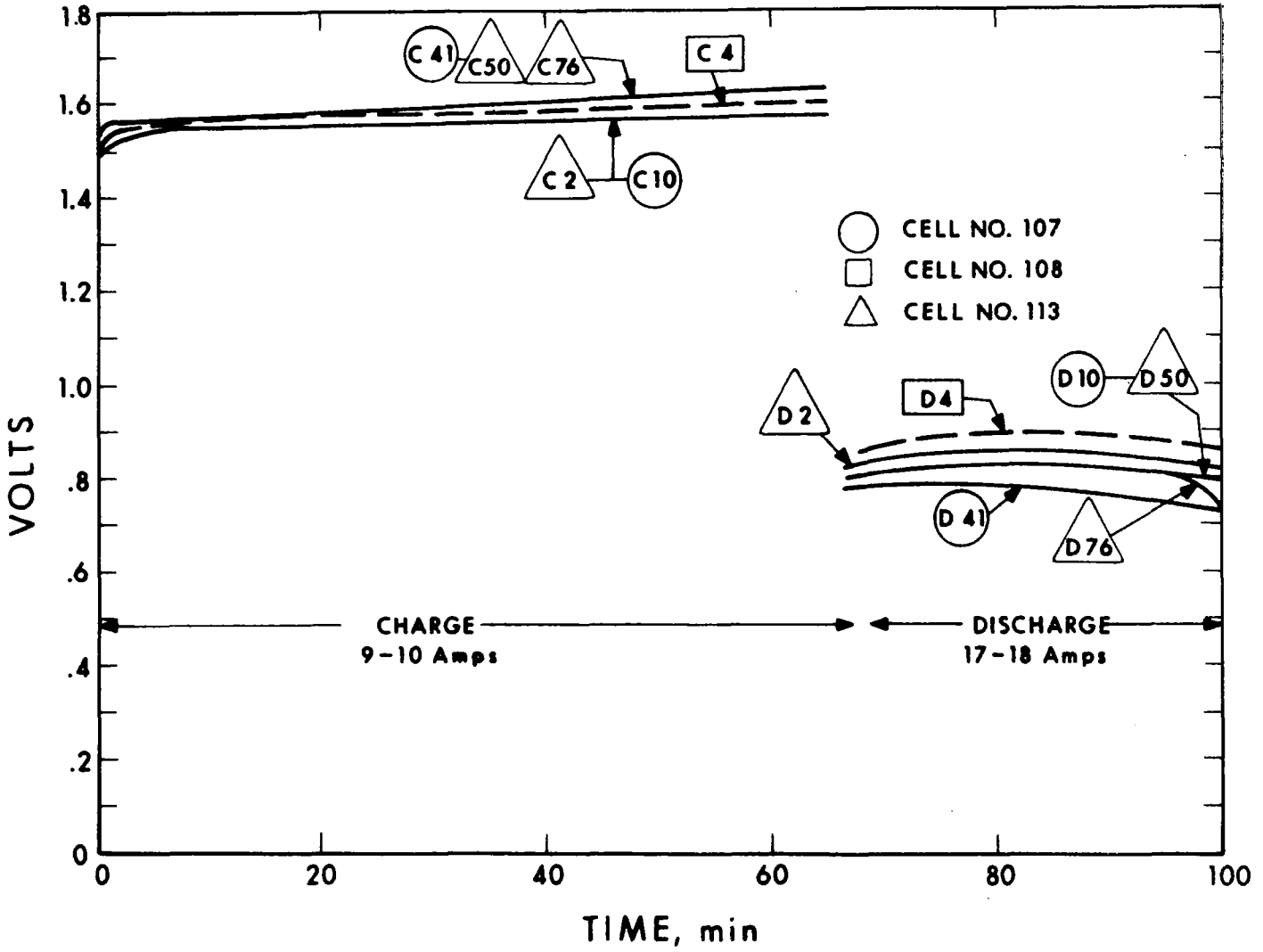

Figure 23. Cycling Performance of Rewashed Electrodes

Poor performances obtained from cells 105 and 110, employing nickel felt metal substructures, were disappointing and very different from results obtained with prior cells utilizing nickel felt metal samples obtained from the NASA contract monitor. Discussions held with technical representatives of Huyck Corporation revealed that there are two types of fiber structures, i.e, A10 and A30. The electrodes from cells 105 and 110 employed A30 fibers. The A10 fiber structures have a larger surface area and thus presumably a more active electrochemical area. It was therefore suggested that the original sample may have been the A10 type. It was also suggested that different densities of felt metal be evaluated as another variable. (All the previous work was done with 15 percent dense nickel felt metal.)

Cell 112 was a repeat of cell 109, utilizing the same electrodes, after they had been washed, with a new matrix. The cell was cycled 18 times. The initial performance was considerably improved over the performance obtained during the latter cycles in cell 109, once again demonstrating the ability to rejuvenate the cell by washing the electrodes and utilizing a new asbestos matrix.

Cell 113 was a repeat run using the electrodes from cells 108 and 107, after they were washed, plus a new matrix. This cell was cycled continuously 78 times. The data and performance for this cell are also presented in Fig. 23. Once again, the cell performance recovered initially in a new assembly and gradually degraded.

The series of tests with gold-plated electrodes indicated that nickel in the electrode structure was not the only cause of cell performance deterioration. A series of tests was therefore initiated to determine what aspects of the matrix and/or electrolyte were causing the degradation.

Examination of multi and single cells tested had consistently shown a gray-black discoloration of the asbestos mat adjacent to the hydrogen electrode. Although cell deterioration was not primarily due to hydrogen electrode failure, it was felt that this discoloration may have been the end product of some anodic reaction in the electrolyte and/or matrix. The oxygen electrode could then have been expected to be affected by the concurrent cathodic reaction.

Several tests, including cell 111, had been aborted during the first cycle. It was noted on these occasions that the gray discoloration occurred principally as the result of the charge mode of operation. Therefore emphasis was placed on testing of cells in the electrolysis mode.

Preliminary chemical analyses of the discoloration zone in the matrix (described in detail in subsection 6.5) showed that platinum was a principal constituent of the discolored zone. Since platinum in the matrix near the anode could not readily be conceived as the cause of cathode deterioration, other cause and effect systems were investigated. To eliminate possible effects of anode platinum, cell 114 was assembled with a non-gold-plated, non-platinum-catalyzed nickel plaque on the hydrogen side. This cell was subjected to charging at 10 amperes for approximately one hour, after which it was disassembled and examined. A slight gray discoloration adjacent to the anode was noted. This test indicated that platinum was not the only factor in the asbestos discoloration.

The next test, cell 115, was made to see if a semipermeable barrier between the anode and the matrix would stop formation of the gray-black deposit. The cell contained standard EOS electrodes with a conventional asbestos matrix, plus one layer of battery separator cellophane placed between the matrix and the hydrogen eelectrode. The addition of the cellophane layer increased cell resistance appreciably and the cell

could only be cycled at reduced current levels, i.e., approximately 5 amperes during charge and 10 amperes during discharge. The cell was cycled in such a manner for eight cycles and then disassembled. It was observed that there was virtually no discoloration of the cellophane or the asbestos matrix adjacent to the hydrogen electrode, indicating that the discoloration had been stopped by the cellophane.

Several interpretations of this test result are possible. It was obvious that the cellophane provided a barrier of the migration of particles from the anode to the matrix. (However, the question of whether such particles originated in the electrode or ionized materials remained in the matrix.) To eliminate one of these variables, several cells were assembled with Webril matrixes of varying thicknesses in place of the standard fuel cell grade asbestos. As anticipated, cells employing just Webril matrixes could not withstand minor differential pressures and were, therefore, not subjected to test.

Cell 116 consisted of two layers of Webril with one layer of cellophane in the center to enable the cell to hold a pressure differential. This cell was cycled once, after which it developed an internal short, probably due to a wire whisker protruding from the edge of one of the electrodes. No discoloration was noted on the Webril when the cell was disassembled.

Cell 117 consisted of gold-coated platinized oxygen electrode, as previously described, except that after the gold coating (and prior to the platinization) the electrode was fired in a hydrogen furnace for one hour at 1500°F. This firing was added to the electrode preparation procedure in an attempt to improve the adherence of the gold coating to the nickel substrate. The firing had the effect of essentially diffusing and alloying the gold layer into the upper surfaces of the nickel plaque. After removal from the furnace, the plaque surface

had changed from a dull gold color to a gray nickel color with a slight yellow tinge. The hydrogen electrode employed in the cell was a standard EOS electrode. The cell was put on a standard cycle and subjected to 121 continuous cycles. It showed good initial performance with a gradual degradation similar to that obtained in previous tests with cells employing gold-coated platinized porous nickel electrodes.

Cell 118 consisted of an oxygen electrode processed similarly to that used in cell 117, except that the porous substrate was nickel felt metal. This cell was cycled six times and showed relatively poor performance. The test was, therefore, discontinued. Poor performance of this felt metal substrate electrode was similar to that obtained with cells 105 and 110.

Cells 119 and 120 consisted of American Cyanamid hydrogen and oxygen electrodes containing 9 mg of platinum per cm^2 on a nickel screen that had been gold plated with a minimum of 100 micro-inches of gold to insure a pinhole-free surface. By the use of these type of electrodes, it was hoped to eliminate the deteriorations caused by the gradual oxidation of the nickel substrates, observed in some of the earlier work. By the elimination of this variable, it would then be possible to obtain a better understanding of the causes of other modes of degradation.

Cell 119 was cycled 61 times, then disassembled. The oxygen electrode was removed, washed, and reassembled with the same asbestos matrix and hydrogen electrode and designated cell 122. This cell was then cycled four times and disassembled. The hydrogen electrode was washed, reassembled with the same oxygen and asbestos matrix, and cycled two additional times (cell 124). The same procedure was followed for cell 121 and cell 125 was then assembled with a new matrix and both electrodes were washed.

Results of the testing with cells 119, 120, 121, 122, 123, 124, and 125 are shown in Figs. 24, 25 and 26. As can be seen, the initial cell performance was good and with cycling there was a gradual degradation of performance. Washing the oxygen electrode and rebuilding the cell had only a slight effect on improving the performance, and washing of the hydrogen electrode had no beneficial effect. These results were inconsistent with the results obtained from cells 104 and 106 in which both electrodes were washed and reassembled with the old matrixes. However, these types of tests were difficult to conduct since in the disassembly of the cell, it was possible that water was lost from the asbestos matrix and carbonates formed in the matrix due to CO_2 pickup from the air.

Cell 128 consisted of the same hydrogen electrode and asbestos mat as employed in cell 125. A new oxygen electrode of the American Cyanamid type was substituted for the old oxygen electrode. Initial performance of the cell was good and the cell was allowed to cycle continuously. During the sixteenth cycle, which occurred over the weekend, recorded data showed that the cell developed an internal short. Performance of this cell is also shown in Fig. 26. Recovery of this cell performance, by replacement of the oxygen electrode after a long successive series of tests, indicated that the major form of deterioration in cell performance might have been a result of deterioration of the oxygen electrode that cannot be recovered by washing.

Cell 134 contained the same electrodes as utilized in cell 128 with a new asbestos matrix. The cell was cycled continuously for 72 times, initially showing fair performance, and as cycling continued, a gradual degradation in voltage was noted. Figure 26 also shows the performance of this cell.

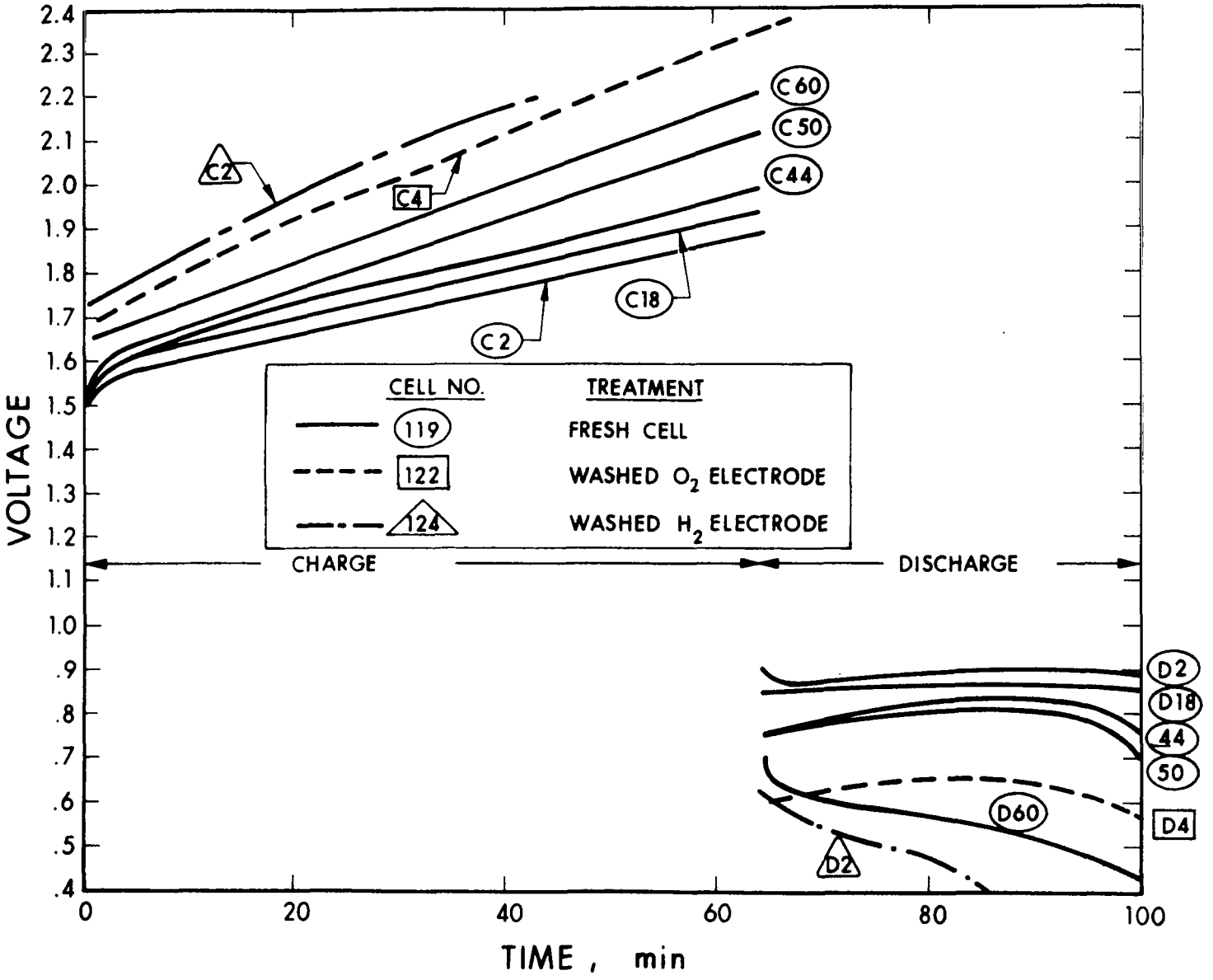

Figure 24. Cycling Performance With Washed Electrodes

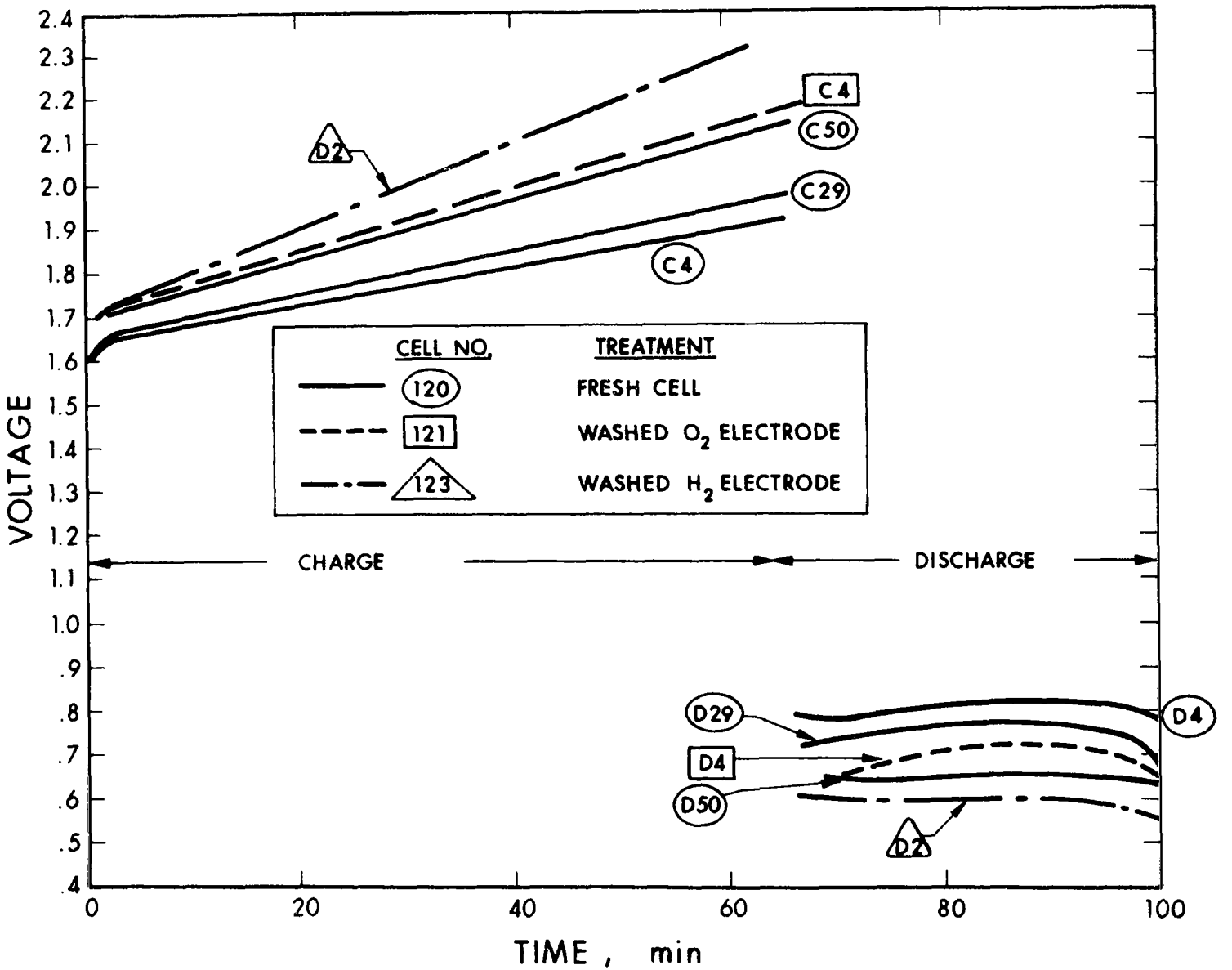

Figure 25. Cycling Performance With Washed Electrodes

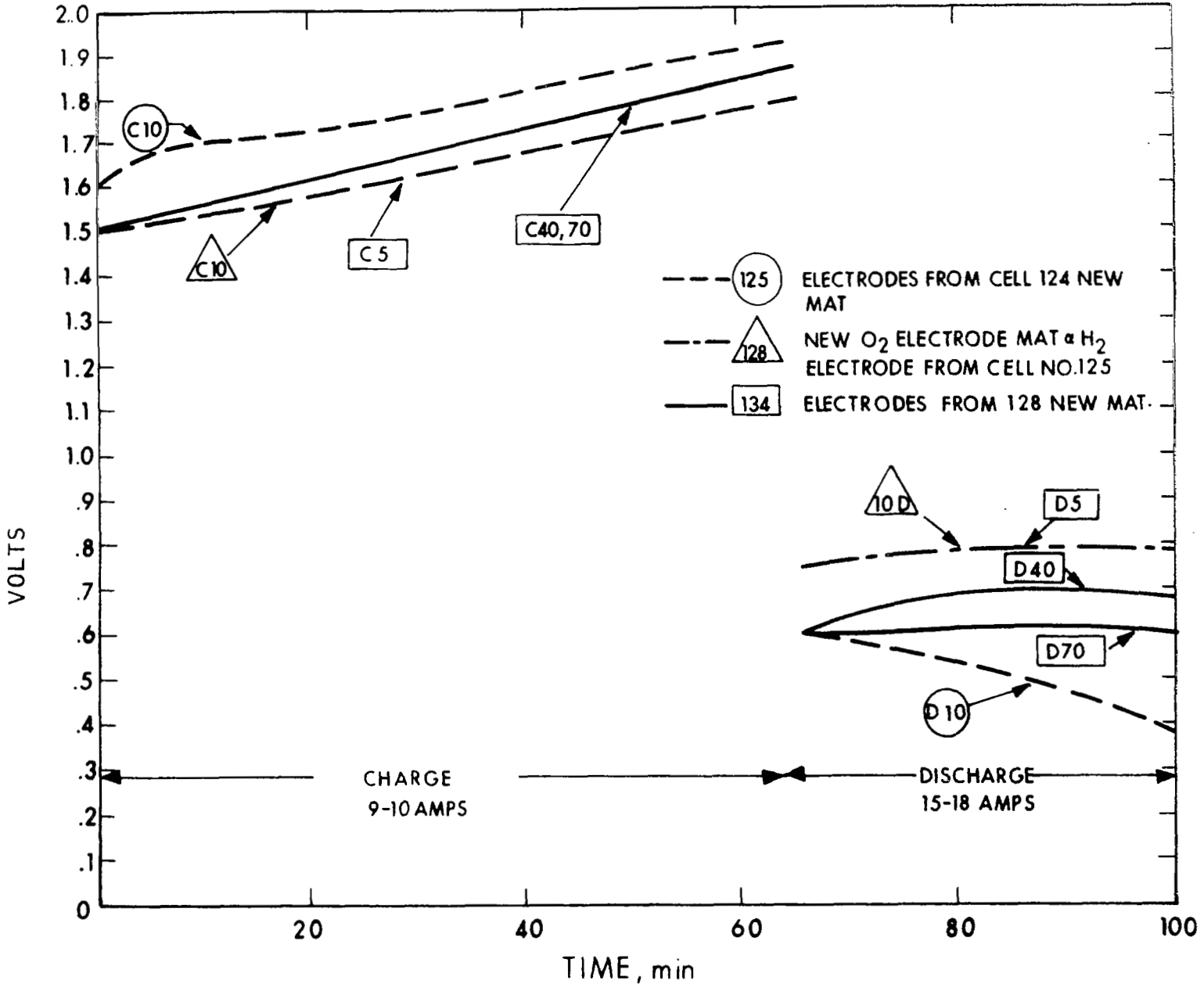

Figure 26. Cycling Performance of Used Electrodes

Cells 129 contained American Cyanamid electrodes that had been utilized in cells 123, 121, and 120. This cell was cycled 84 times continuously during which it showed a gradual degradation in performance. Initial performance was fair, discharging at 0.7 to 0.75 volt. The results of this cell were inconsistent with the result obtained from cell 124, which had electrodes of similar prior history. The lack of reproducibility between cells 125 and 129 indicated that differences existed in the cell active components. However, the conclusions drawn from cells 125 and 128, i.e., that the oxygen electrode does not recover performance after use, were reconfirmed.

To improve the voltage levels obtained with gold-coated platinized electrodes, a new set of electrodes was prepared using gold-coated porous nickel plaque subsequently platinized, but the platinum loading was doubled to 14 mg/cm^2. These electrodes were subjected to tests in cell 139. The cell was cycled 20 times. During discharge, initial voltage performance was satisfactory, 0.85 to 0.9, but as the discharge proceeded, voltage fell off rapidly, indicating flooding.

Cell 147 consisted of an American Cyanamid type AB-6 oxygen electrode that was modified at EOS by electrodepositing an additional 7 mg/cm^2 black platinum layer on one surface that was subsequently assembled in the cell adjacent to the asbestos matrix. The hydrogen electrode employed was a standard American Cyanamid type AB-6 electrode. This modification of the electrode was an attempt to increase the thickness of the electrode structure and make the electrodes less sensitive to matrix water content. As shown in Fig. 27, this electrode structure initially showed good flat performance, but as cycling continued, gradual degradation in the performance was observed. Previous tests with American Cyanamid electrodes showed considerably higher charging voltages, presumably due to a lack of availability of water in the electrode during the charge mode. Since the outer layer of electrodeposited platinum was not wet-proofed, this section of the electrode

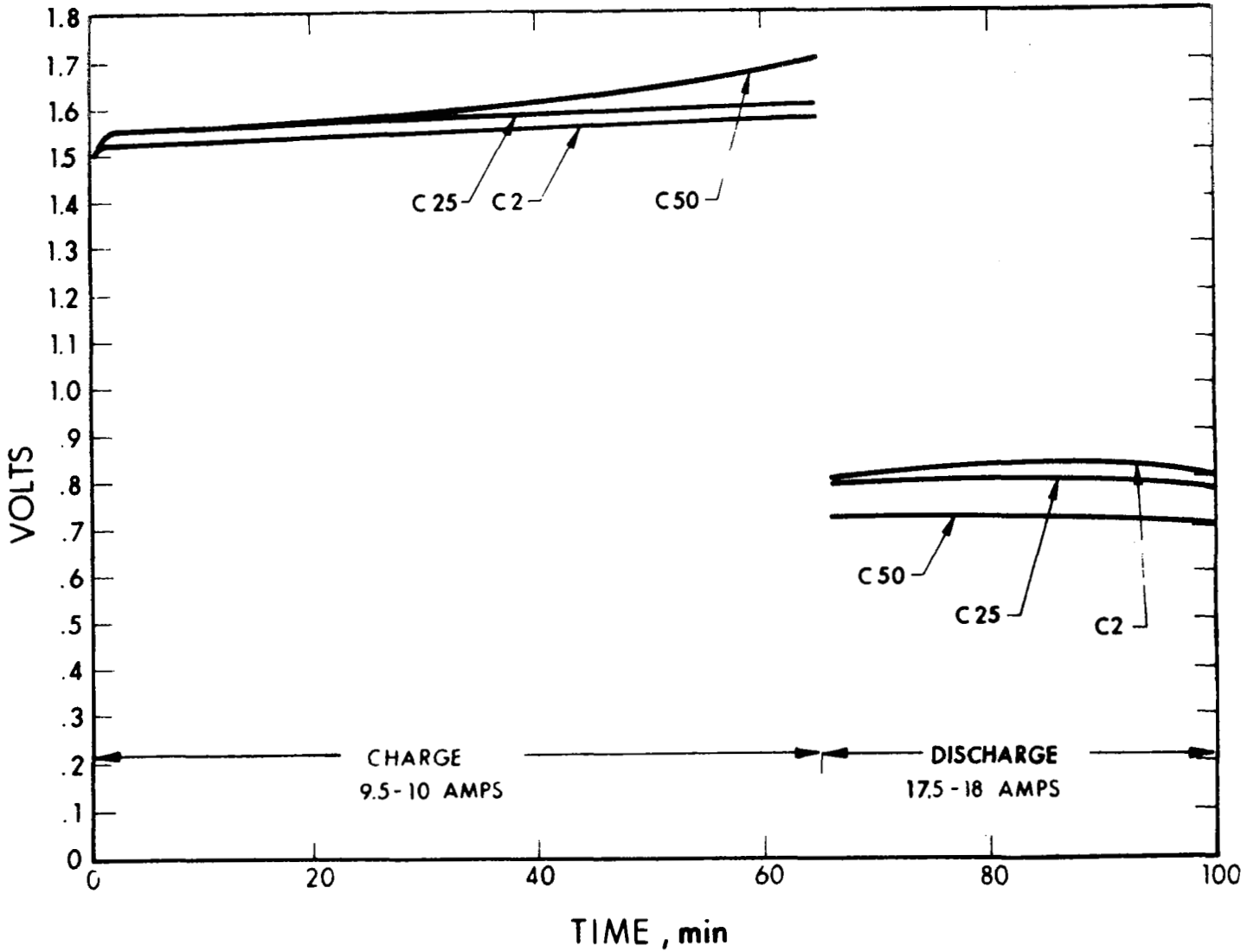

Figure 27. Cycling Performance of Modified Cell 147

probably contributed considerably to the lowering of the charge voltage. This type of electrode structure indicated a possible technique for increasing the performance capabilities of American Cyanamid type electrodes.

Cell 150 consisted of a modified American Cyanamid type AB-6 electrode of the type used in Cell 147 except that instead of 7 mg of platinum being electrodeposited on the electrode, 15 mg platinum per cm^2 were electrodeposited. Performance of this cell was mediocre, and cycling was stopped after the eleventh cycle. It was then hypothesized that the additional platinum possibly was blocking the lower active material and was not accomplishing any useful purpose.

Cell 151 consisted of the original modified American Cyanamid electrode that was used in cell 147. The electrodes were washed and reassembled with a new asbestos matrix. Initial performance of this cell indicated the same performance as that of cell 147. The cell was cycled intermittently for an additional 54 cycles with gradual degradation.

Cell 152 consisted of the modified American Cyanamid oxygen and hydrogen electrodes that were previously used in cell 150. The electrodes were washed and then assembled with a new asbestos matrix. The cell exhibited fair performance very similar to that obtained with cell 150. After seven cycles, the test was discontinued.

Cell 153 consisted of a new set of electrodes containing 14 mg platinum per cm^2 electrodeposited on porous nickel plaque that had been gold-coated. The cell was tested, and subjected to two cycles. Performance of the cell was extremely poor, operating at about 0.5 volt at 10 amps. Therefore, the cell was disassembled, the electrodes were washed, and the cell reassembled with a new asbestos matrix, in a new designated cell 154. This cell showed only a slight improvement in performance over the results of the previous cell. After two cycles, this test was also discontinued.

Cell 155 consisted of an oxygen electrode of the American Cyanamid type that had 15 milligrams of platinum electrodeposited on the surface assembled adjacent to the asbestos matrix. The hydrogen electrode was a porous nickel plaque that contained 15 milligrams of platinum electrodeposited on the surface assembled adjacent to the asbestos mat. This nickel plaque contained no gold-coating. The cell was subjected to test and exhibited poor performance. After two cycles, the test was discontinued.

Cell 156 consisted of the gold-coated platinized electrodes previously used in cell 154. The electrodes were washed and assembled in the cell with a new asbestos mat. This cell showed poor performance and after two cycles, the test was discontinued.

Cell 157 consisted of the modified American Cyanamid electrode and the platinized nickel electrode previously used in cell 155. These electrodes were washed and assembled with a new asbestos mat to see if the washing process would improve the performance. The cell showed very poor performance, and after one cycle the test was discontinued.

Cell 158 consisted of a porous nickel plaque oxygen electrode that was gold-coated at EOS and platinized by Bishop Metals to half the depth of the electrode with 7 mg platinum per cm^2. An additional 15 mg platinum per cm^2 was electrodeposited at EOS on the heavy platinum side which was assembled adjacent to the asbestos mat. The hydrogen electrode employed was a standard gold-coated platinized nickel plaque containing 15 mg platinum per cm^2. The cell showed good initial performance; however, the cell developed a leak and the test was discontinued after 8 cycles.

Cell 159 consisted of the modified American Cyanamid electrode employed in cell 157 on the oxygen side, an American Cyanamid electrode on the hydrogen side, and a new asbestos matrix. Performance was poor again, and the test was stopped after 17 cycles.

Cell 160 consisted of oxygen electrode AU26 which had been previously used on cell 156, unwashed, and a new hydrogen electrode and asbestos matrix. The cell was cycled one time and exhibited a very poor discharge, so the test was discontinued.

Cell 161 consisted of the oxygen and hydrogen electrodes that had been previously used in cell 158 with a new asbestos matrix. The electrodes were washed prior to the new assembly. The performance of the cell was flat in the charge and discharge mode, but the discharge voltage was poorer, approximately 0.6 of a volt. The cell was cycled 12 times, and then the test was discontinued.

Cell 164 consisted of the same hydrogen electrode and asbestos matrix that had been used previously in cell 160 with a new oxygen electrode. The cell was cycled 17 times. It exhibited poor performance, possibly due to the exposure of the asbestos matrix to CO_2 in the air during reassembly.

Cell 166 consisted of a new type of oxygen electrode that was platinized by manually recycling chloroplatinic acid through a porous nickel plaque until 20 mg of platinum per cm^2 was picked up by the electrode. The O_2 electrode was then coated with electroless gold by recycling the electroless solution through the plaque. This was an attempt to coat over those areas of nickel that had not been coated by the platinum. The cell was assembled with a previously used gold-coated platinized hydrogen electrode in a standard 60 mil asbestos matrix. The cell exhibited unusual performance. It initially operated at 0.5 to 0.6 volt and as cycling proceeded, discharge voltage performance increased gradually to a level of 0.75 volt. During additional cycling, the discharge voltage degraded gradually to approximately 0.6 volt. Throughout this test, the unit was cycled 130 times. Apparently, the gold layer initially had coated over the platinum and as testing continued (for some unknown reason), more catalyst area became available and performance improved.

Cell 168 consisted of the same electrodes as used in cell 164, unwashed, with a new asbestos matrix. The cell was cycled 130 times continuously and showed fair to poor performance, discharging at 0.65 to 0.75 volt.

Cell 169 consisted of hydrogen and oxygen electrodes fabricated by the standard EOS technique. The cell was cycled continuously for 105 times and showed a very slight degradation in performance during this period.

Cell 172 consisted of hydrogen and oxygen electrodes that had been purchased from the Chem. Cell Corp. for evaluation. These electrodes consisted of a gold-plated fine mesh nickel screen on which a mixture of black platinum and Teflon had been applied to form the reacting surface. The cell was put on the standard test cycle, but performance was such that cycling could not be carried out. These type electrodes appear very sensitive to the variations in water content that occur during the charge and discharge process of the secondary fuel cell. During one stage of the discharge, the voltage performance was good, i.e. approximately 0.85 volt at 17.5 amps, but the performance was poor at the beginning and end of discharge and charge, indicating flooding and drying of the electrodes. It appears that this type of electrode structure is not satisfactory for use in the RHO battery since it is apparently too thin and cannot tolerate the changes in moisture that are encountered with cycling.

Cell 174 consisted of a variation of a Chem. Cell electrode containing an added porous Teflon hydrophobic layer located adjacent to the asbestos matrix in the cell assembly. The water proofing layer is supposed to prevent drowning of the electrode as water is formed in the cell. However, it was found that the cell could not be subjected to test due to an extremely high internal impedance. This apparently was due to the nonwetting nature of the hydrophobic layer between the electrodes and the asbestos matrix. It is possible that the electrolyte-to-asbestos weight ratio and the asbestos compression ratio used in setting up this cell, which were originally optimized for EOS type electrodes, were not well suited for the Chem Cell type of structure.

The discrepancy in rate of degradation encountered thus far with the single cell tests pointed to a lack of consistency in the cell components or test method. The active cell components consist of electrodes, electrolyte, and asbestos matrix. High purity (pre-electrolyzed) electrolyte had been used in recent cell tests and this would certainly not be the cause of the lack of reproducibility. Both EOS and American Cyanamid type fuel cell electrodes had shown a lack of reproducibility in our performance tests. However, American Cyanamid had reported good reproducibility when using their electrodes in primary fuel cells. Further, it was believed that the process techniques and materials used in the fabrication of EOS type electrodes were reproducible. Therefore, the material that had potentially the greatest variability was the asbestos matrix. Fuel cell grade asbestos is fabricated from a variable mined ore which is pulped to remove large impurities, washed to remove water soluble impurities, and then processed into mats. Thin mats, i.e. 0.020 inch, are made on a "board" machine. Apparently more asbestos per unit thickness is applied to the board material as compared to the paper material. Since in the RHO battery, an 0·060 inch board was used as the matrix rather than the 0.020 inch paper used in primary cells, it appeared that we had 3 to 4 times the possible contamination present. Therefore, it was certainly possible that the more rapid rate of degradation of the RHO battery, compared to primary cells of the American Cyanamid type, was due to a higher quantity of asbestos impurity being present. Further, the unreproducibility could be attributed to the same factor.

At this point asbestos studies and concentration cell tests were initiated (see Subsections 4.5 and 4.6). These tests indicated that the matrix produced the immediate degradation in performance observed thus far. The asbestos matrix was replaced by a more stable potassium titanate matrix.

Cell 212 consisted of an American Cyanamid oxygen electrode containing platinum of 40 mg/cm^2 (as opposed to the standard type electrodes which contain 9 mg/cm^2). The matrix was 90 percent KT and 10 percent asbestos. The hydrogen electrode was the standard nickel porous plaque type. The cell was subjected to 418 charge/discharge cycles. The voltage performance at various cycles is shown in Fig. 28. As can be seen, there was a gradual degradation in performance with cycling. In addition, this cell exhibited the slow gas recombination which resulted in a rapid falloff in the voltage performance during discharge in the latter cycles. The electrodes were removed from this cell, unwashed, and preassembled with a new matrix consisting of the same type. This new cell (designated 217) was cycled continuously for 432 cycles to a point of slow gas recombination. The results shown in Fig. 29 indicate that an American Cyanamid electrode of 40 mg Pt/cm^2 has the same performance characteristics as the 9 mg Pt/cm^2 electrodes normally used.

Cell 216 consisted of the standard 9 mg Pt/cm^2 American Cyanamid electrodes for both the hydrogen and oxygen sides and a matrix of 90 percent KT, 10 percent asbestos. The American Cyanamid electrode was employed on the hydrogen side to see if its use would improve performance and life. The cycling results are shown in Fig. 30. As can be seen, a gradual deterioration of charge and discharge voltage was observed. This rate of degradation was greater than that normally obtained with the nickel plaque hydrogen electrode cells. The American cyanamid AB-6 electrode was made with a gold-plated screen and 9 mg Pt/cm^2. The AB-6 was adopted as our standard O_2 electrode. The carbonyl nickel plaques with 20 mg Pt/cm^2 are used as the standard H_2 electrode.

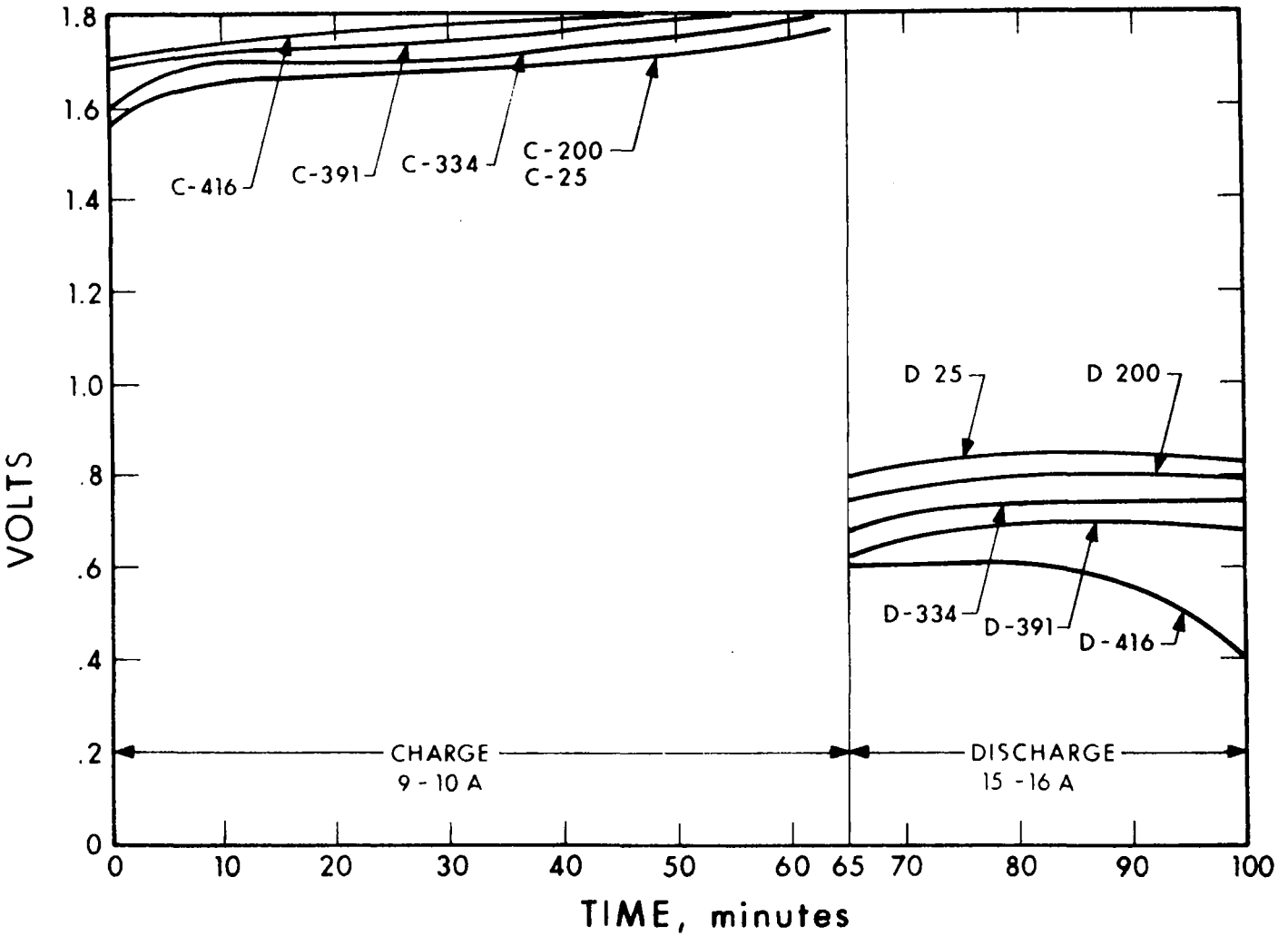

Figure 28. Cycling Performance of Cell 212

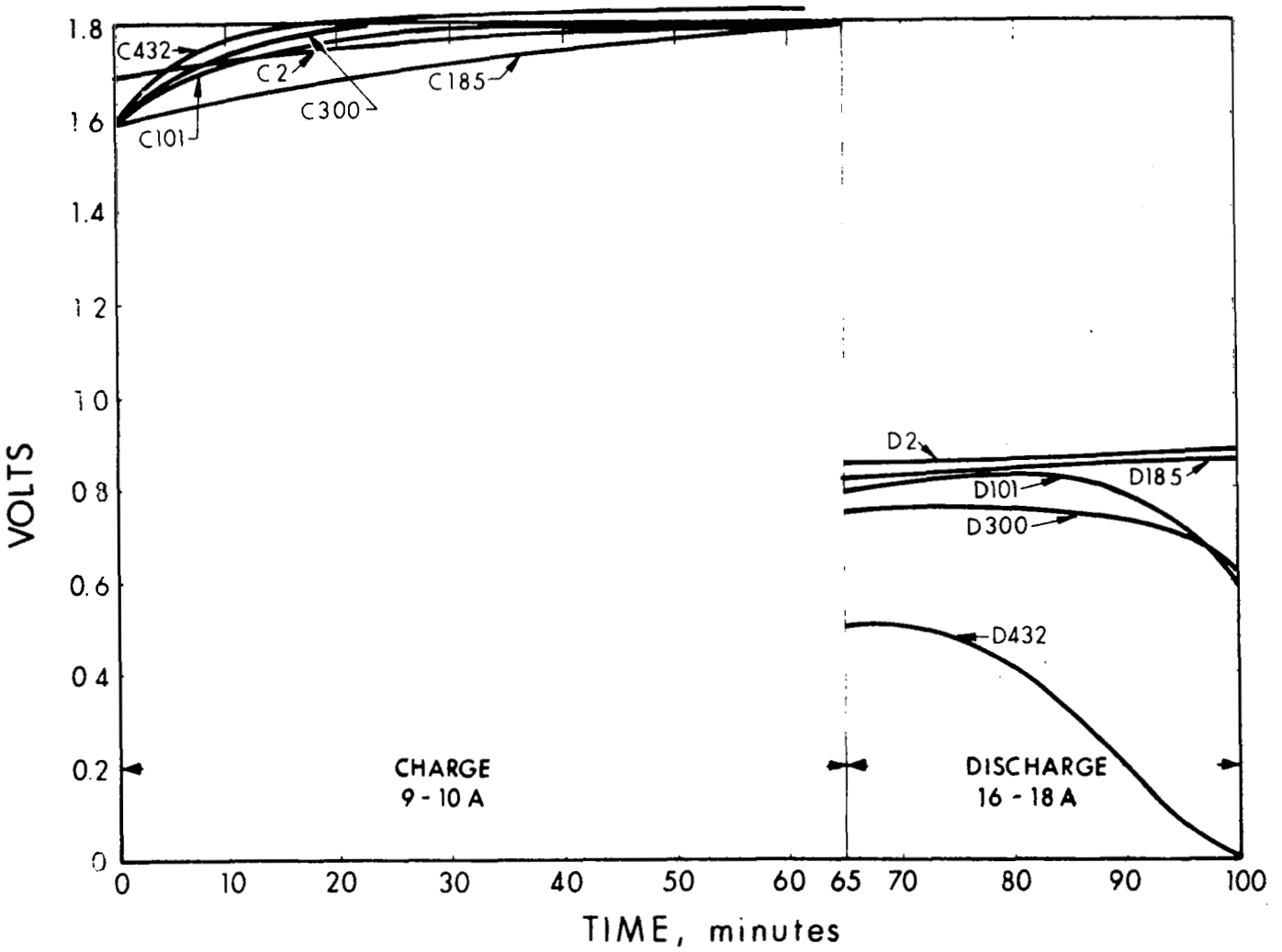

Figure 29. Cycling Performance of Cell 217

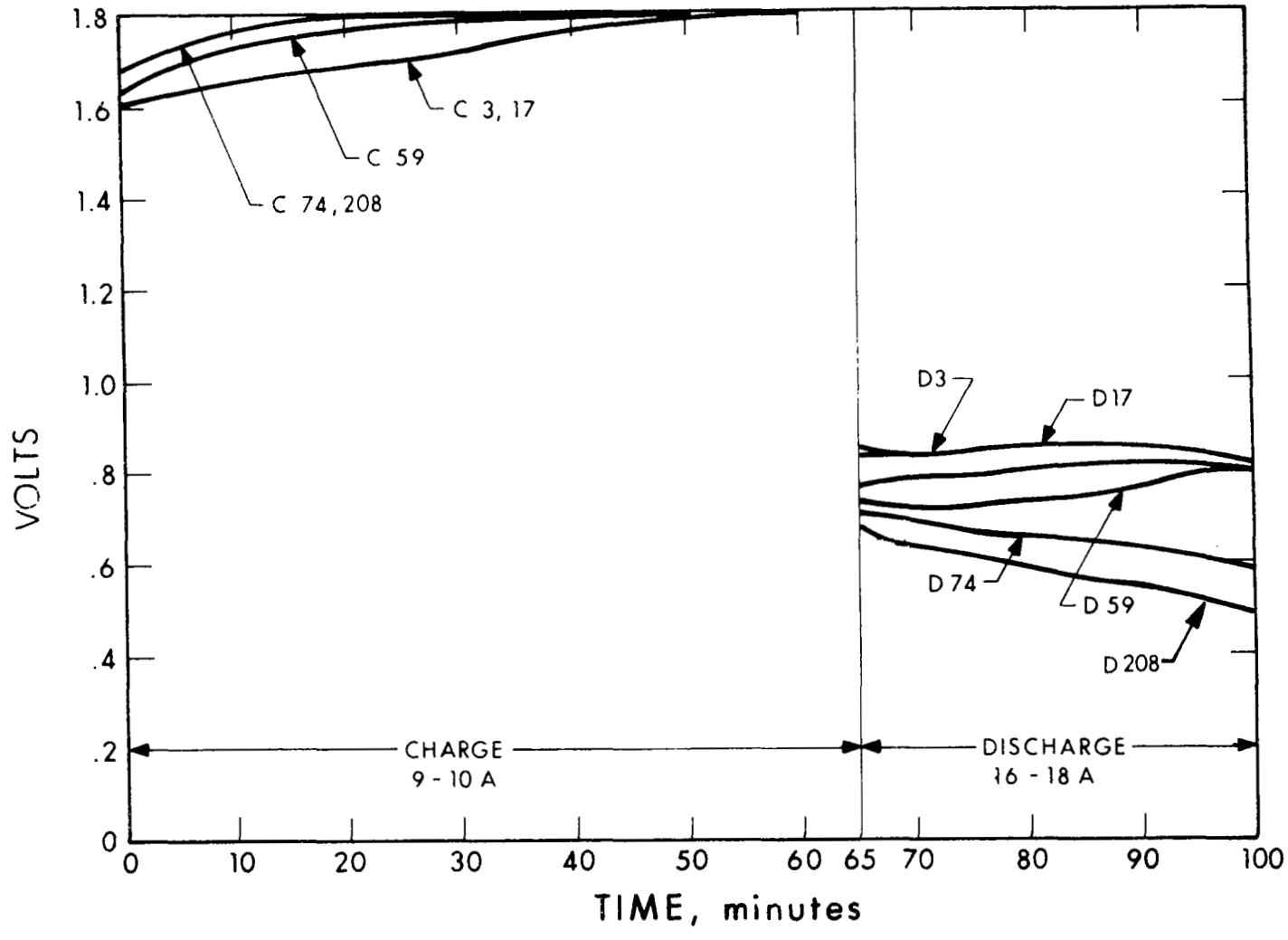

Figure 30. Cycling Performance of Cell 216

4.4 REFERENCE CELL

To characterize the American Cyanamid and EOS electrodes used in the EOS fuel cell, reference cell testing was initiated. Each cell contained an American Cyanamid AB-6 oxygen electrode and a standard EOS electrode (20 mg Pt/cm^2). The matrix was made of a pasted KT/Teflon membrane sandwiched between two 90-10 KT asbestos mats. On each side of the membrane was placed a mercuric oxide (HgO) reference electrode. The reference electrodes consisted of nickel screens on which HgO powder was pressed. Each screen had a nickel wire spotwelded on one end; the wire was fed out through the 60-mil insulating spacer.

Table II lists the reference cells and the cycle life of each. On cell 247, polarization curves were obtained at room temperature; the discharge curve is shown in Fig. 31, and the charge curve in Fig. 32. The data of Fig. 31 indicated that at room temperature the polarization losses were greatest at the O_2 electrode while discharging. Figure 32 indicated that at room temperature the increased polarization of the H_2 electrode limited the charging density to slightly above 100 mA/cm^2. This is probably due to activation polarization.

At 80°C greater charging densities are obtained. This is shown with cell 250. Polarization scans were done on cycles 2, 78, and 165. The cell pressure was kept between 180 and 270 psia. The results are shown in Figs. 33 and 34. Figure 34 shows that when the cell was charged, most of the polarization occurred at the O_2 electrode. The steep voltage rise between zero and 1 amp was caused by both the activation polarization of the O_2 electrode and the cell resistance. Since the cell resistance was 0.009 ohm, 0.009 volt could be attributed to cell impedance. Therefore, the major polarization loss was due to lack of activation on the O_2

TABLE II

REFERENCE CELL TESTS

Cell No.	Total Cycles	Comments
247	1	Cell charged backwards on second cycle.
250	318	Concluded test because of performance degradation final KOH 30.7%. Both electrodes used in cell 247.
267	81	Cases recombined during charge #82
271	2	Self discharge
272	1	Self discharge
273	30	Self discharge
275	43	Self discharge
277	5	Self discharge
280	86	Self discharge
284	215	Ran poorly - self discharge at 215 cycles.

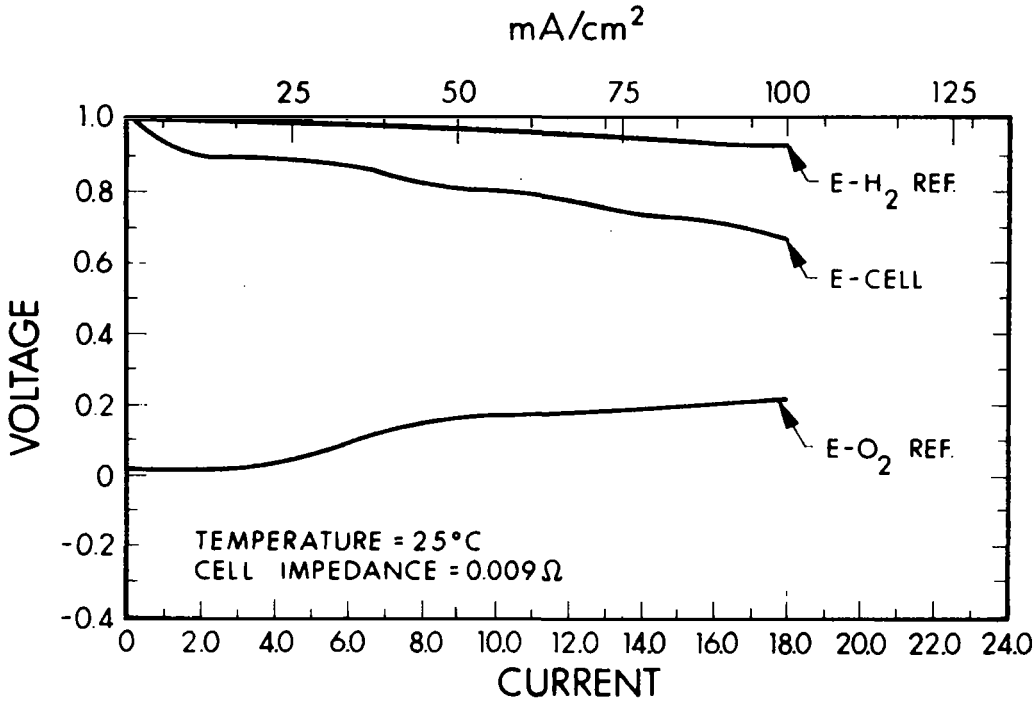

Figure 31. Discharge Polarization Curve, Cell 247

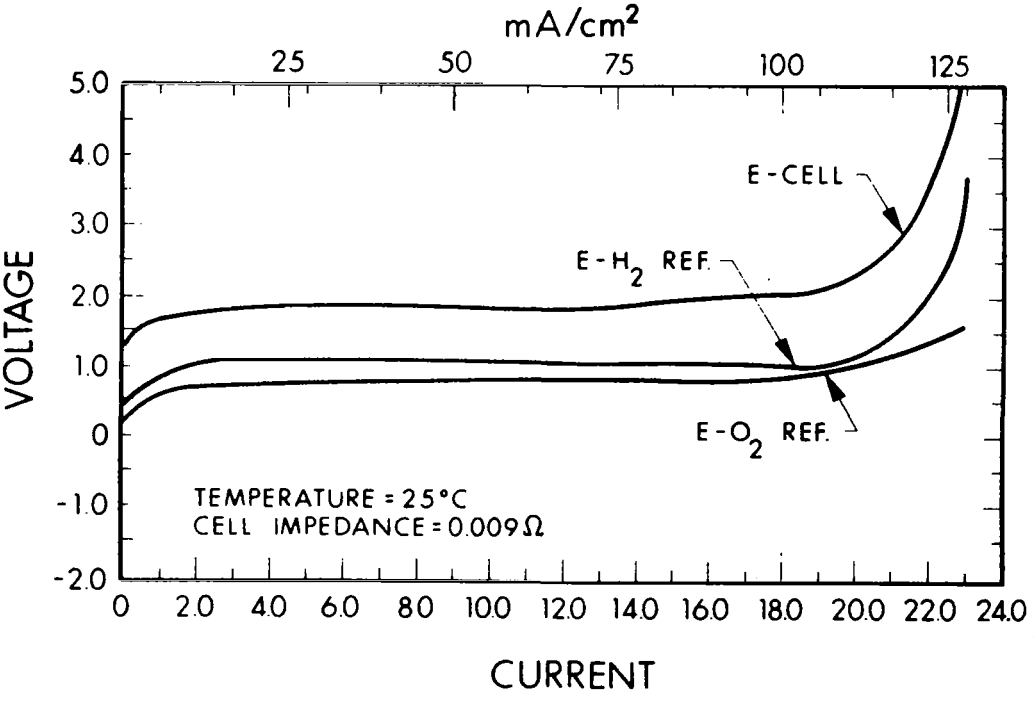

Figure 32. Charge Polarization Curve, Cell 247

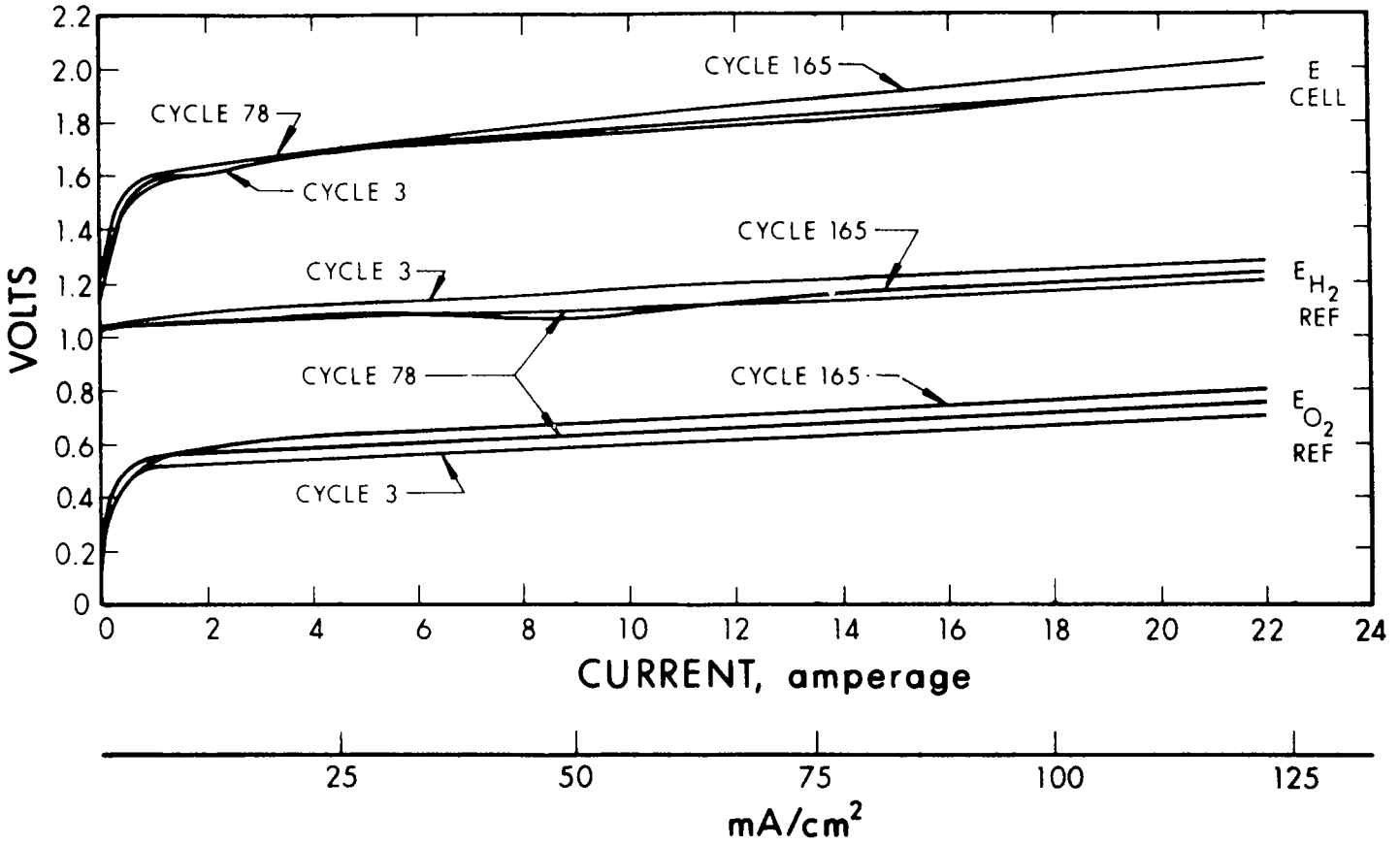

Figure 33. Charge Polarization at 80°C, Cell 250

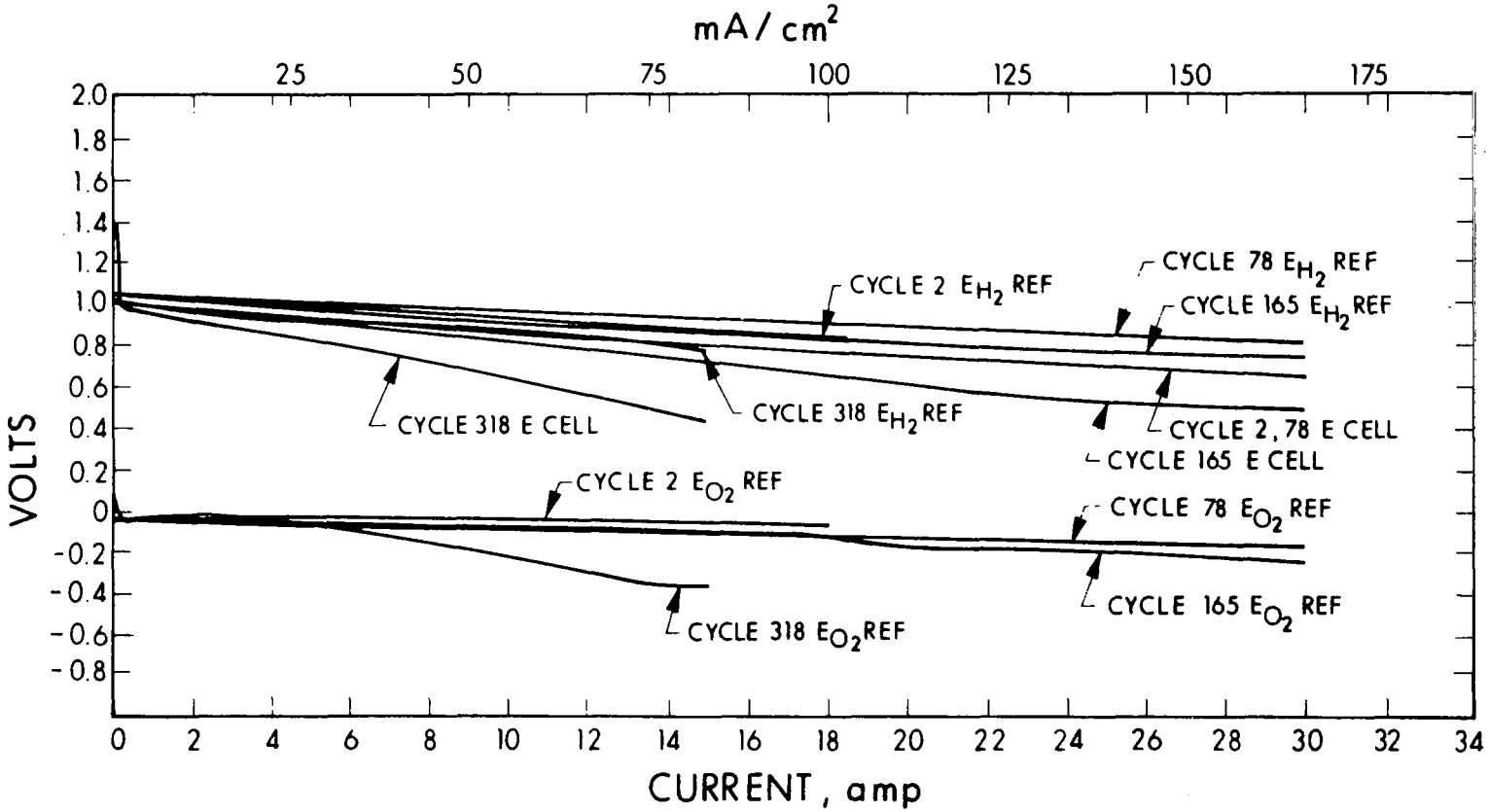

Figure 34. Cell 250, Discharge Polarization at 80°C

electrode as shown in Figs. 33 and 34. The O_2 electrode performance degraded with cycle life, whereas the H_2 electrode either remained the same or improved. Figure 34 shows that the polarization loss at both the H_2 and O_2 electrodes was about the same on the discharge mode.

The scans on reference cell 280 confirmed the results obtained above. Figures 35 and 36 show the initial polarization curves on charge and discharge for this cell. Figure 35 shows that the major polarization loss occurred at the O_2 electrode during charge. The largest component of polarization, a combination of activiation and IR effects, was shown by the initial steep rise of the O_2 reference curve. Figure 36 shows that the largest polarization loss was observed at the initial slope of the O2 reference curve, again showing activation polarization. After a current density of about 80 mA/cm^2, the polarization losses are equally contributed by both the H_2 and O_2 electrodes since then their slopes are nearly equal. Figures 37, 38, and 39 respectively show reference readings of cell 280 cycled at 18 amps charge and discharge, 10 amps charge and 10 amps discharge, 10 amps charge and 18 amps discharge. All the cycles were extended beyond the normal charge and discharge limits to observe the effects of drying and flooding on the electrodes. As can be seen in Figs. 37, 38, and 39 the largest effect caused by drying was an increase in the cell impedance. By again referring to these figures it was learned that during flooding the O_2 electrode was most adversely affected.

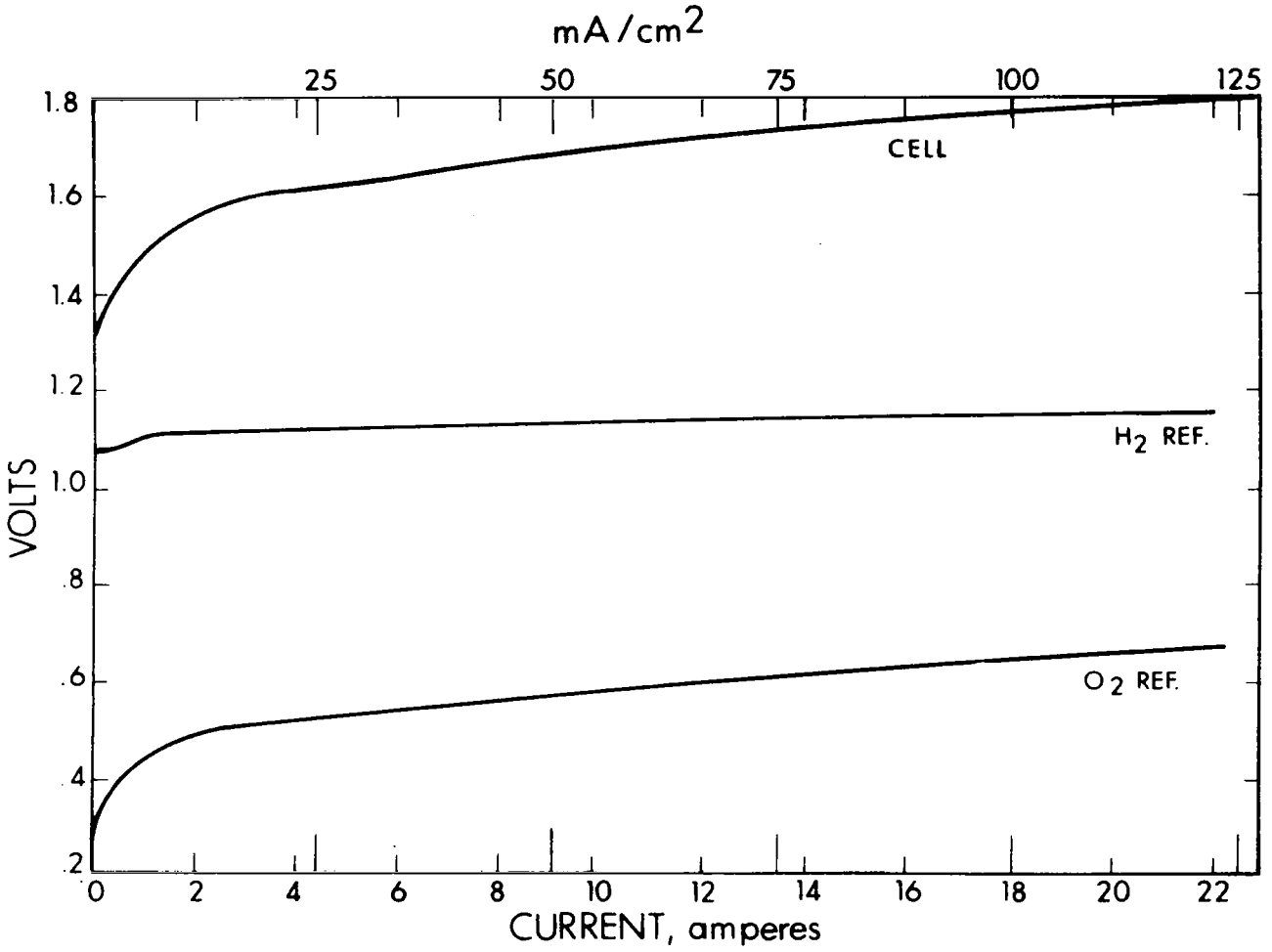

Figure 35. Charge Polarization of Reference Cell No. 280

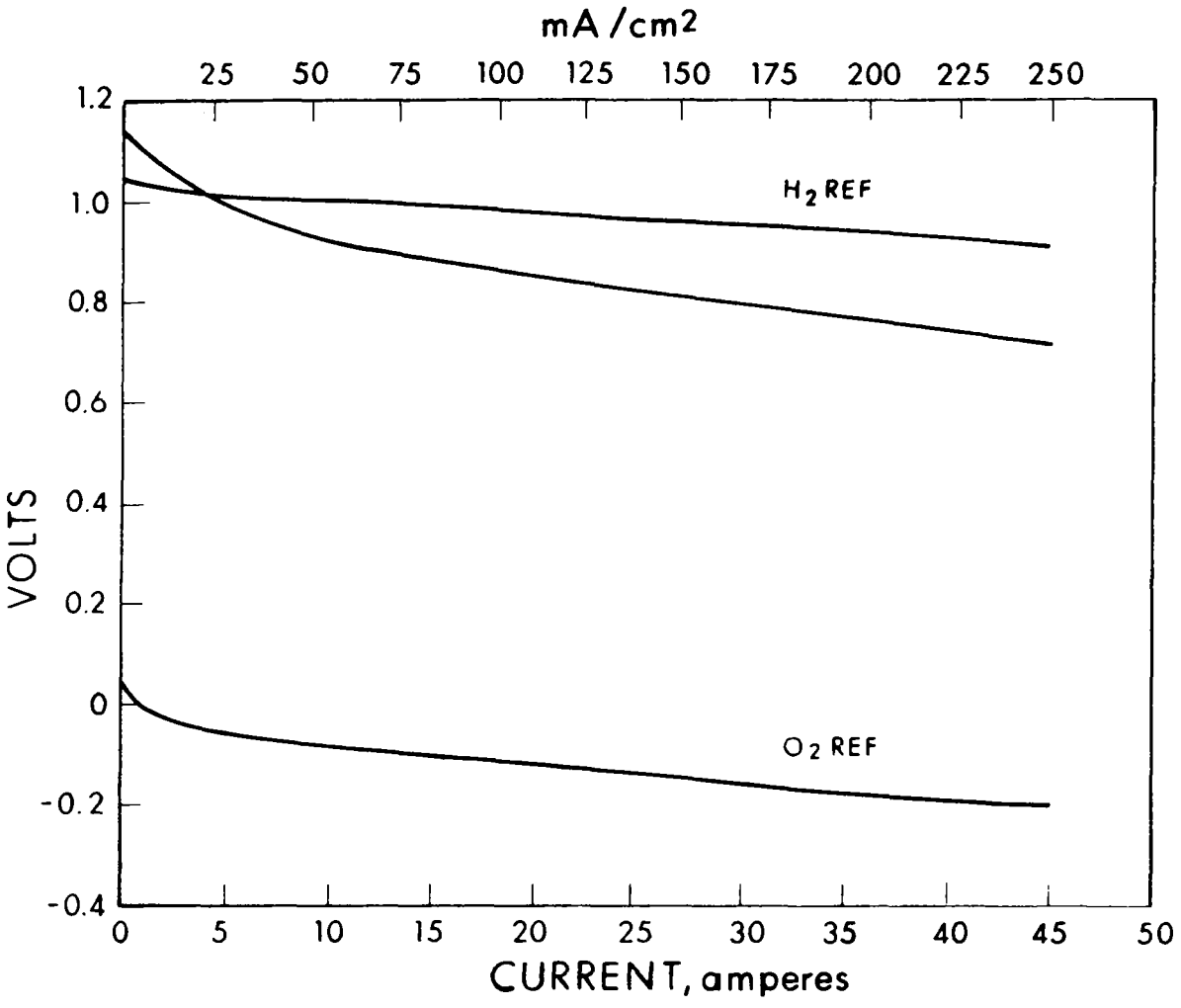

Figure 36. Discharge Polarization of Reference Cell No. 280

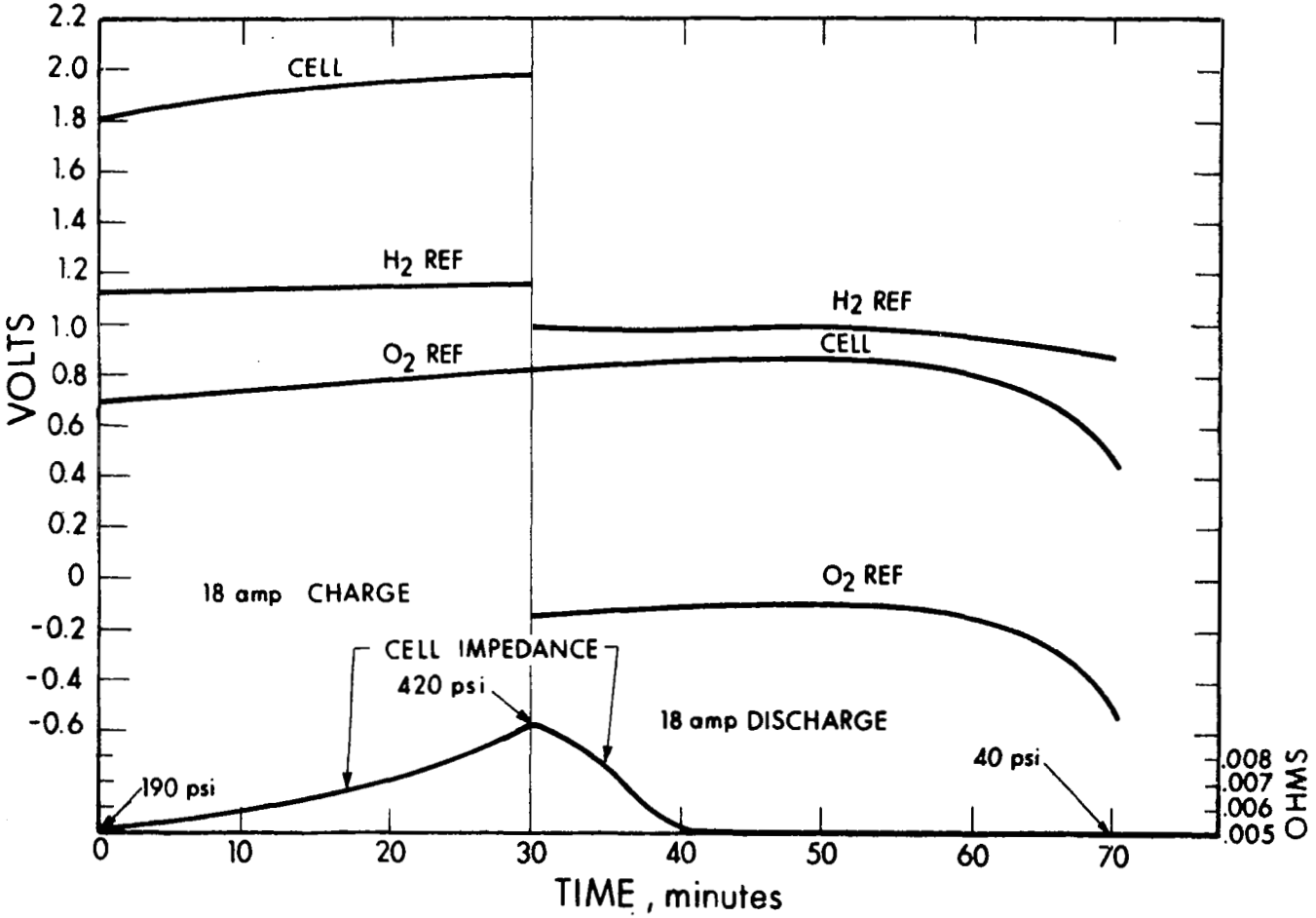

Figure 37. Reference Cell No. 280, Cycle No. 2

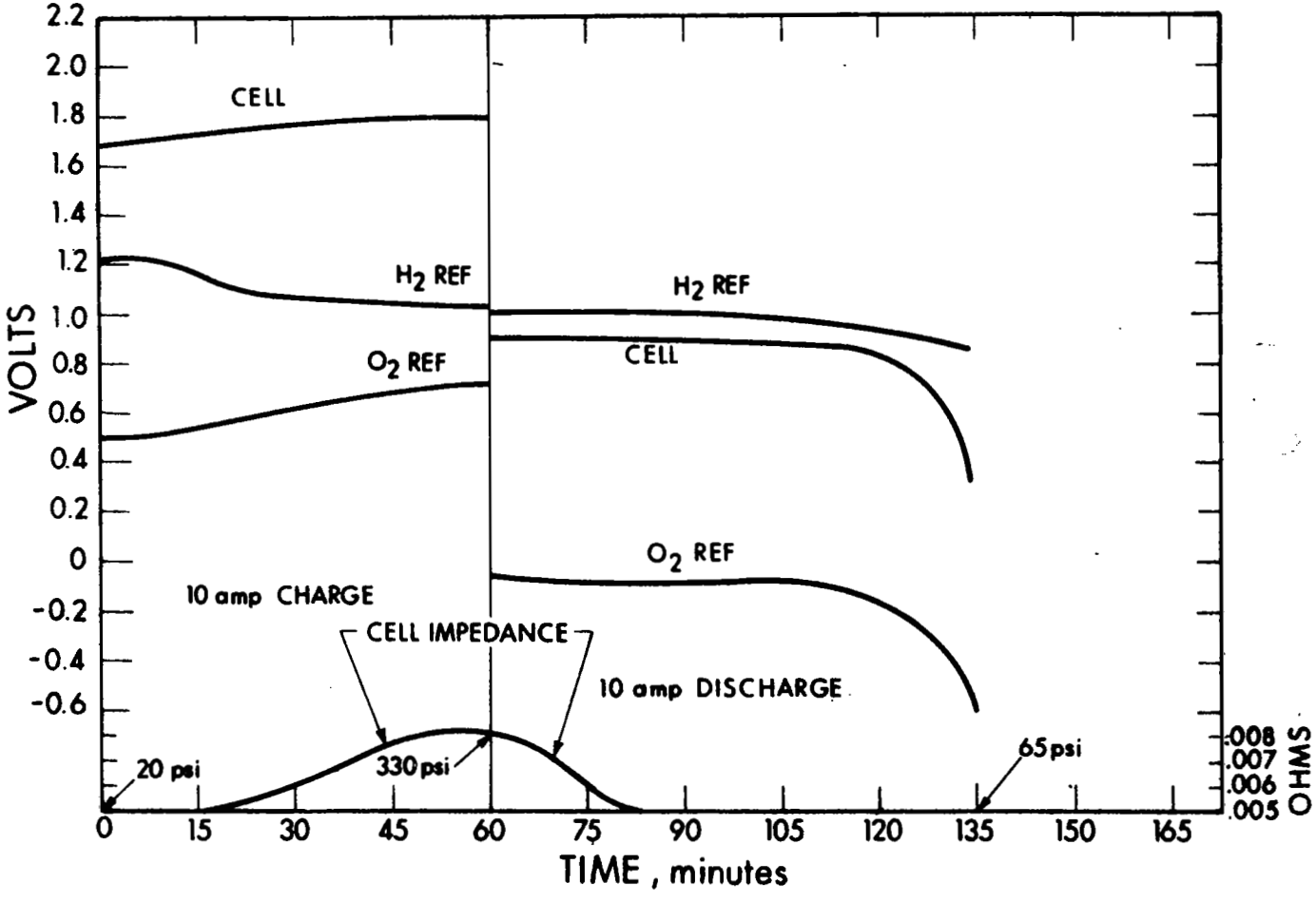

Figure 38. Reference Cell No. 280, Cycle No. 3

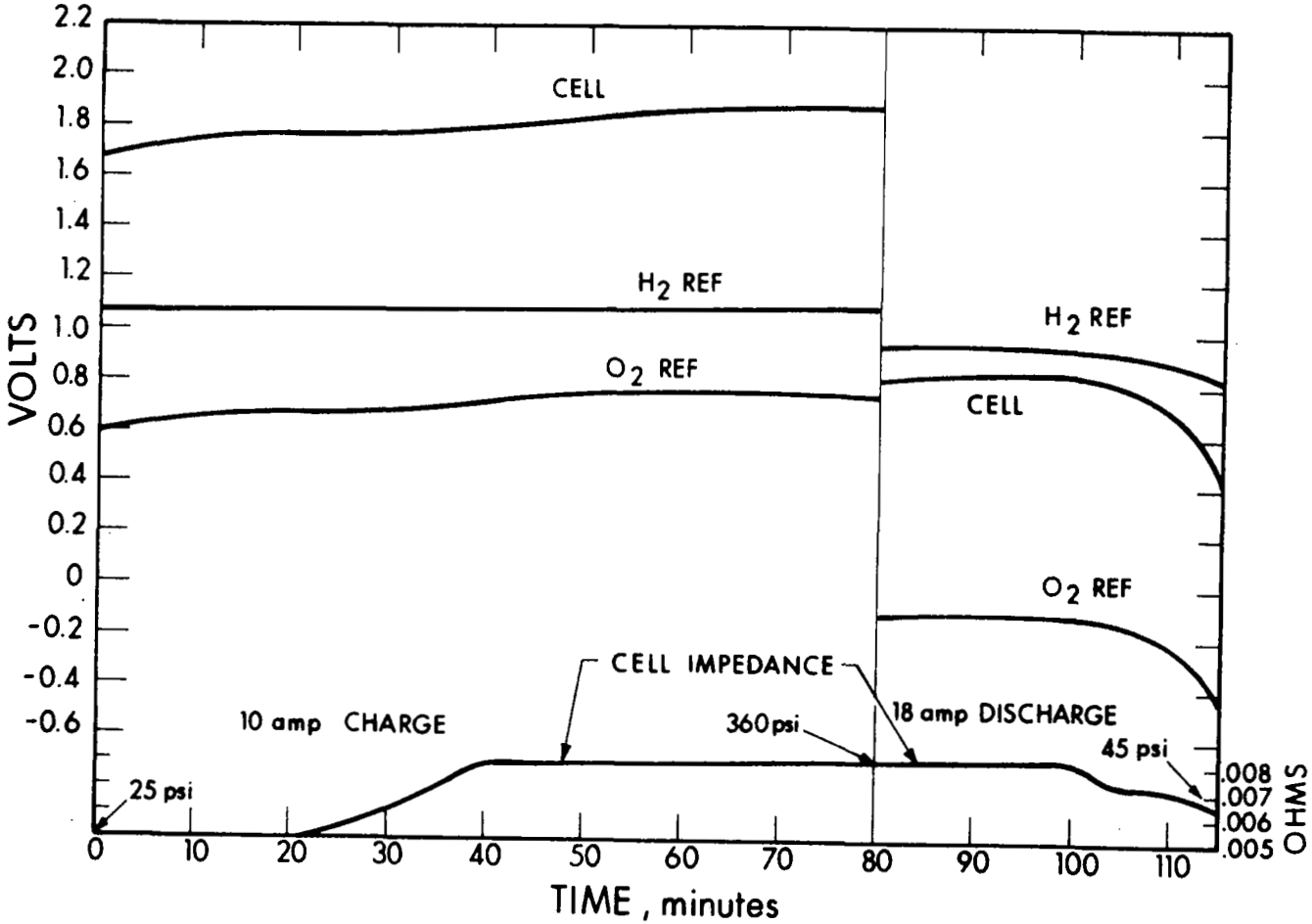

Figure 39. Reference Cell No. 280, Cycle No. 4

4.5 ASBESTOS STUDIES

To obtain a better understanding of the composition of the asbestos materials, and to determine what chemical changes occur within the material, samples were submitted to outside testing laboratories for a semi-quantitative spectrographic analysis.

Two different laboratories were used because of some questions concerning the results obtained from the first laboratory. The first submissions consisted of three different samples: (a) the pure asbestos material, (b) asbestos from a used mat adjacent to the oxygen electrode, and (c) asbestos from a used mat adjacent to the hydrogen electrode. The first results are shown in Table III. This data is presented as a weight ratio compared to magnesium in order to make it easier for relative comparisons.

Table IV shows the second set of data on four samples also on the basis of a ratio to magnesium content. Electrodes taken from these cells were washed and tested again with fresh asbestos mats to obtain further information.

Asbestos samples taken from the multicell unit serial number 1003-34 were submitted to an outside testing laboratory for a semi-quantitative spectrographic analysis. Two samples of used mats were prepared by mixing the asbestos in a blender to obtain a homogeneous mixture. A third sample was prepared utilizing a fresh asbestos mat by homogenizing it with distilled water. The results of this analysis are presented in Table V. The major difference between these and previous test results was the large percentage of calcium found in the asbestos mats. Prior spectrographic analyses showed calcium concentrations in the tenths of a percent range. However, the asbestos material used in these tests represented a newer lot of material

TABLE III

ASBESTOS SPECTROGRAPHIC ANALYSIS, FIRST TEST

	Pure Material	Sample Adjacent to Hydrogen Electrode	Sample Adjacent to Oxygen Electrode
Magnesium	1.00	1.00	1.00
Silicon	.86	.54	.58
Potassium	Nil	.71	1.315
Boron	.00153	.00022	.00038
Manganese	.0027	.00067	.0011
Aluminum	.0005	.00375	.0017
Iron	.0046	.0116	.0205
Platinum	Nil	.00125	.005
Calcium	.0039	.0396	.0115
Vanadium	.00016	.00006	.0001
Copper	.00021	.00003	.00016
Sodium	Nil	.00167	.028
Titanium	Nil	.000075	.000033
Nickel	Nil	.000067	.00017
Strontium	Nil	Trace	Trace
Chromium	.000023	.000017	.00009

TABLE IV

ASBESTOS SPECTROGRAPHIC ANALYSIS, SECOND TEST

	Pure Sample	Material with KOH	Sample Adjacent to Hydrogen Electrode	Sample Adjacent to Oxygen Electrode
Magnesium	1.00	1.00	1.00	1.00
Silicon	1.17	1.11	.84	1.00
Potassium	Nil	.67	.78	2.27
Boron	.00034	.00094	.00061	.0001
Manganese	.005	.0036	.0026	.0048
Aluminum	.0046	.0016	.0012	.00091
Iron	.0058	.0035	.0035	.0062
Platinum	.0008	Nil	.0007	.01
Calcium	.0062	.0038	.0035	.0018
Vanadium	Nil	.00009	.00007	.0001
Copper	Nil	.00025	.00025	.00011
Sodium	Nil	.0046	.0023	.057
Nickel	.0003	.00026	.00025	.012
Chromium	Trace	Trace	.00008	Trace

TABLE V

ASBESTOS SPECTROGRAPHIC ANALYSIS, THIRD TEST

	Pure Asbestos Sample (%)	Samples taken from Fuel Cell S/N 1003-34 (%)	
Ag	0.0005*	0.0005*	0.0005*
Al	0.08	0.09	0.01
As	0.05*	0.05*	0.05*
B	0.01	0.01	0.01
Ba	0.08*	0.08*	0.08*
Be	0.0001*	0.0001*	0.0001*
Bi	0.001*	0.001*	0.001*
Ca	8.5	7.	8.5
Cd	0.05*	0.05*	0.05*
Co	0.007*	0.007*	0.007*
Cr	0.008*	0.008*	0.008*
Cu	0.01	0.02	0.01
Fe	0.2	0.01	0.1
K	Not Detected	Rem. △	Rem. △
Li	0.1*	0.1	0.1*
Mg	21.	15.	5.
Mn	0.04	0.005	0.001
Mo	0.01*	0.01*	0.01*
Na	0.07*	0.15	0.1
Nb	0.01*	0.01*	0.01*
Ni	0.005*	0.05	0.07
Pb	0.007*	0.007*	0.007*
Sb	0.02*	0.02*	0.02*

TABLE V

ASBESTOS SPECTROGRAPHIC ANALYSIS, THIRD TEST (Cont'd)

	Pure Asbestos Sample (%)	Samples taken from Fuel Cell S/N 1003-34 (%)	
Si	16.5	8.5	3.5
Sn	0.005*	0.005*	0.005*
Sr	0.01	0.005	0.005
Ti	0.003*	0.003*	0.003*
V	0.005*	0.005*	0.005*
Zn	0.1*	0.1*	0.1*
Zr	0.003*	0.003*	0.003*
Pt	0.01*	0.17	0.13

*Less Than △ Plus Anion

Anion---Rem

received from Johns-Manville. Possibly there was a variation of the raw materials. Two samples of dry asbestos, one from the previous shipment and one from the newer lot, were then submitted to an analytical testing laboratory to confirm this point. The test results showed 2.9 percent calcium for the old lot and 3.3 percent calcium for the new lot. This was inconsistent with all prior spectrographic analyses. Thus far, we had submitted asbestos samples to three different laboratories for spectrographic analysis and had received a wide range of results on the major constituents. Therefore, it must be concluded that the spectrographic analysis techniques were incapable of indicating major constituent quantities of asbestos with any reasonable degree of accuracy.

To determine the effect of KOH impregnation of the mat on the analytical procedure, asbestos samples impregnated with 40 percent potassium hydroxide were analyzed per procedures recommended by Johns-Manville. Results of the analyses performed on asbestos without and with KOH are shown in Table VI. The major constituents weight percentages are in fair agreement from the two samples. The loss upon ignition is considerably different, apparently due to the potassium hydroxide. Weight percentages in this table were based on the dry weight of asbestos, i.e., without potassium hydroxide.

Analytical tests were conducted on samples of asbestos taken from cells that had been cycled to determine quantities of platinum in the mat. A new gravimetric procedure was used to make these determinations. A 1-in^2 sample, taken from the mat used in cell 103, yielded 26.3 milligrams of platinum. (The electrodes used in cell 103 consisted of a gold-coated platinized nickel plaque as the oxygen electrode and a platinized nickel plaque as the hydrogen electrode.)

TABLE VI

ASBESTOS ANALYSIS RESULTS, FOURTH TEST

	Standard Asbestos (%)	Asbestos Impregnated with KOH (%)
Loss upon ignition	17.39	38.8
S_i	18.25	16.7
M_yO_x	2.4	1.53
C_a	2.45	2.0
M_g	22.9	21.3

Similar tests were conducted on a mat sample from cell 106, which employed American Cyanamid type electrodes. The mat in this case yielded 13.6 milligrams of platinum from a 1-in.^{2} sample. These tests verified the previously reported results in that quantities of platinum migrated into the asbestos mat during cycling. The source of the platinum was determined to be the H_2 electrode, but the mechanism of migration was not determined as yet.

Since the platinum observed was distributed in the interior of the mat as well as adjacent to the H_2 electrode, simple mechanical abrasion could not have been the cause for its inclusion in the mat. This conclusion was verified by the observation that only minimal platinum inclusion, due to abrasion or other mechanical modes, occurred adjacent to the O_2 electrode. The mode of platinum migration was obviously, therefore, electrochemical, but the mechanism remains a mystery.

Another approach to eliminating possible asbestos contaminants was undertaken. This consisted of acid washing the asbestos mats as described below to remove chemically reactive species. Washing was accomplished by agitating the asbestos in glass beakers containing 20 percent HCl. After wet processing, the mats were dried and cut to 6-inch diameters. Surprisingly, the resultant mats were mechanically coherent.

Cell 126 consisted of electrodes fabricated by gold coating and platinizing porous nickel plaques and an asbestos mat that has been acid washed. The acid-washed asbestos mat was prepared by shredding two standard 6-inch mats in a beaker to which had been added 200 cm^3 of concentrated hydrochloric acid. Initial mixing of the acid with the asbestos resulted in considerable gassing due to the reaction of the acid with certain constituents of the mat. After one hour, the asbestos fibers were repeatedly washed with distilled water and then poured into a Buchner funnel in which the free liquid was vacuum

filtered from the fibers. This process was repeated until the filtrate water reached a pH of 7. For the final mat formation procedure, the asbestos fibers were mixed with distilled water to form a slurry and were poured into the Buchner funnel under vacuum to form an even layer of asbestos. The mat was then dried and cut to a 6-inch diameter. Initial performance of cell 126 with the acid-washed mat was very poor, discharging at approximately 0.5 to 0.6 volt and charging at 1.7 to 1.8 volts. Therefore, the test was discontinued. An examination of the cell components showed a reddish discoloration of the asbestos mat adjacent to the hydrogen electrode. It was concluded that all the acid had not been completely washed from the asbestos mat.

A new mat was prepared as described above. After completion of the distilled water washing of the mat, it was reshredded and mixed with 40 percent KOH and allowed to react for one hour. After the KOH treatment, the fibers were once again washed with distilled water until a pH of 7 was reached. The mat prepared in this manner was assembled in cell 127 with American Cyanamid electrodes on the hydrogen and oxygen sides. The cell was cycled three times and showed good performance. At the end of the third cycle, an instrumentation failure (the differential pressure transducer) caused the test to be stopped.

Cell 177 consisted of previously used American Cyanamid electrodes that were acid-washed in hydrochloric acid, then washed with water, soaked in potassium hydroxide, and again washed with distilled water to remove any possible impurities in the electrodes. The cell was assembled with a fuel cell type asbestos mat and subjected to three cycles to evaluate the effect of acid washing on the electrodes. The cell exhibited good performance.

At the end of three cycles, the test was discontinued to replace the fuel cell mat with an acid-washed asbestos mat which was then designated cell 180. The cell was cycled on a standard test cycle of 65 minutes

charge, 35 minutes discharge for 45 cycles, at which time the test was discontinued. During cycling, the charge and discharge voltage levels were good, except that at the end of discharge, there was considerable fall-off in voltage, indicating drowning of the electrodes. Difficulties were had in getting the cell pressure above 250 psig, indicating that gas leakage and recombination were occurring as the mat was drying out. Due to this difficulty, the end of discharge pressure was noted to continually decrease. Analysis of a sample of electrolyte squeezed from the mat revealed a final KOH concentration of 32.9 percent.

Because of the results above, the acid-treated asbestos mats were deemed unsuitable for the fuel cell. However, the technique of forming mats on the Buchner funnel led to the fabrication of more suitable matrixes.

Another type of asbestos was tested in cell 176 which contained hydrogen and oxygen electrodes fabricated by the standard EOS technique. The mat consisted of four 0.020-inch layers of ACCO No. 1 asbestos manufactured by the American Cyanamid. Four layers of material were used to prevent possible cross leakage in the mat, since this asbestos material has a higher porosity and lower bubble-through pressure than conventional fuel cell grade asbestos. The cell was cycled and exhibited low discharge voltage in a range of 0.6 to 0.7 volt. The charge voltage was good, 1.5 to 1.6 volts. The test was stopped after four cycles due to the low discharge voltage. Visual examination of the mat material showed a gray discoloration throughout the mat. An analysis of a sample of electrolyte squeezed from the mat revealed a final KOH concentration of 27.85 percent, indicating that this type of asbestos also reacted within the cell environment. The ACCO No. 1 asbestos was also judged unsuitable for use in a regenerative fuel cell.

4.6 CONCENTRATION CELLS

4.6.1 OXYGEN CONCENTRATION CELL TESTS

Because of the inconsistencies obtained in the previous cycling test another test was devised to aid in the evaluation of the results. Cell 162 was the first in a series of concentration cells that was initiated to obtain a better understanding of modes of deterioration. In oxygen concentration cell tests, both halves of the cell gas cavities were filled with oxygen to approximately 100 psig, and the gas cavities were interconnected by means of a small tube. An external power supply was provided and an 18-amp current (100 mA/cm^2) was driven through the cell. In this mode operation, the oxygen was consumed at the cathode and generated at the anode. Since the gas compartments were interconnected, no differential pressure was built up. The concentration cell, therefore, represented a steady-state situation where an O_2 electrode encountered the same reaction that would occur in a primary fuel cell mode, and the other O_2 electrode encountered the same reaction that would occur in an electrolysis mode. This type of test eliminated problems of differential pressure, drowning, and flooding, and also eliminated the H_2 electrode as a variable. It was believed that by this test technique the cause of deterioration of performance could readily be isolated.

Cell 162 consisted of gold-coated platinized EOS electrodes plus two layers of 0.030-inch asbestos material with a reference electrode located within the asbestos. The cell was run continuously over a 6-day period, at a constant current of 18 amps. During this period the cell voltage rose gradually from 0.75 to 0.92 volt, as shown in Fig. 40 indicating that even in this mode, gradual deterioration was taking place. The reference electrode indicated that the deterioration was occurring in both electrodes. After 6 days, recorded data showed that the cell voltage rose rapidly above 1.23 volts and then exhibited

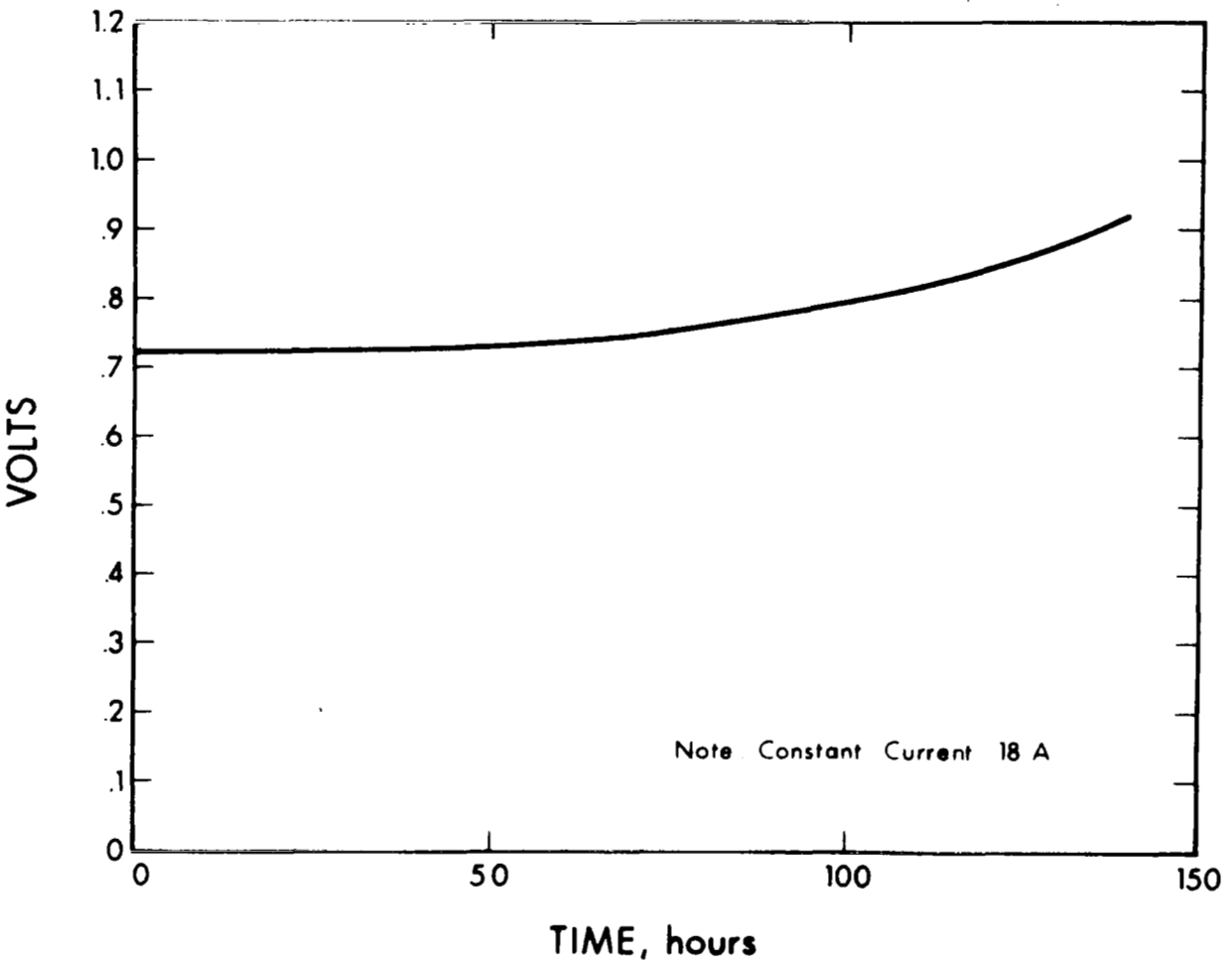

Figure 40. Continuous 0_2 Concentration Cell 162

an open circuit. Examination of the cell showed that an internal reaction had taken place, presumably at the time of the rapid rise in cell voltage. The mode of failure could be attributed to a change in the reaction mode from an oxygen concentration cell to an electrolysis cell when the cell voltage rose above 1.23 volt. Above 1.23 volts, H_2 is generated at the anode. Since the gas cavities were interconnected, the H_2 and O_2 mixture combined in an internal chemical reaction. To prevent this, the power supplies used in testing were put on a voltage limit mode so that cell voltage would not exceed 1.1 volts during these types of tests.

Cell 163 consisted of a concentration cell constructed similar to cell 162 with a new set of gold-coated, platinized EOS electrodes. However, in this case, the polarity of the current flowing through the cell was reversed every 35 minutes to simulate a cyclic mode of operation. Therefore, for a 35 minute period one electrode was consuming oxygen and the counter electrode generating oxygen, and then the reverse polarity caused the electrodes to reverse function. Cycling was continued in this manner for 34 cycles, or approximately 40 hours. During this period, the voltage rose gradually to a value of about 1 volt at which time the test was discontinued. Initially, the cell exhibited a flat voltage during a cycle. As cycling continued, the voltage performance exhibited a slope as shown in Fig. 41.

Cell 165 was a cycling concentration cell similar in construction to cell 163 utilizing a new set of electrodes and asbestos mat. The cell was cycled continuously for 146 times on the 35-minute cycle at 18 amps. During this cycling, the voltage rose gradually from an initial level of about 0.6 to 0.95 volt. Similar to cell 163, the initial voltage performance was flat and as cycling proceeded, the voltage developed a gradual slope, as shown in Fig. 42.

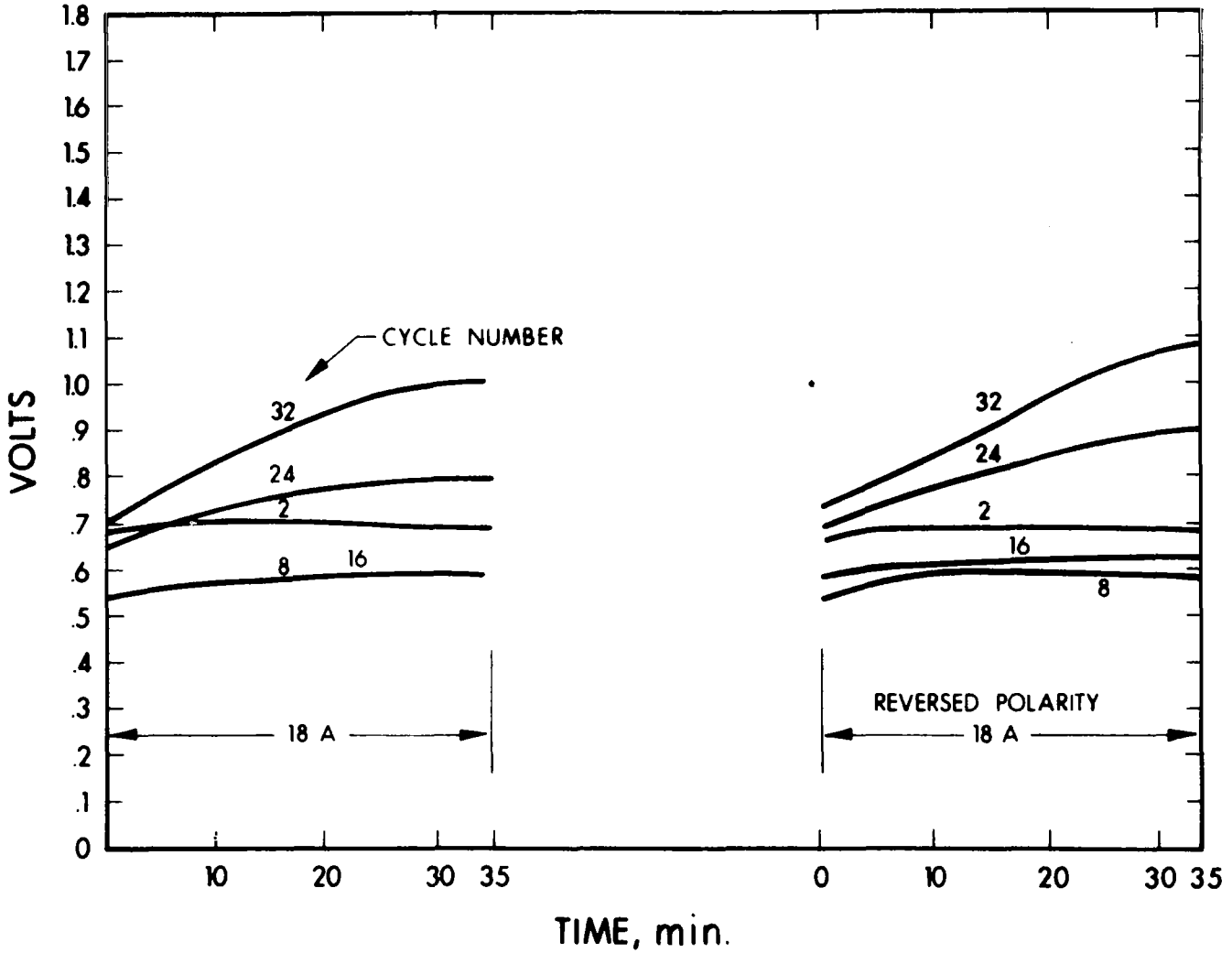

Figure 41. Cycling O_2 Concentration Cell 163

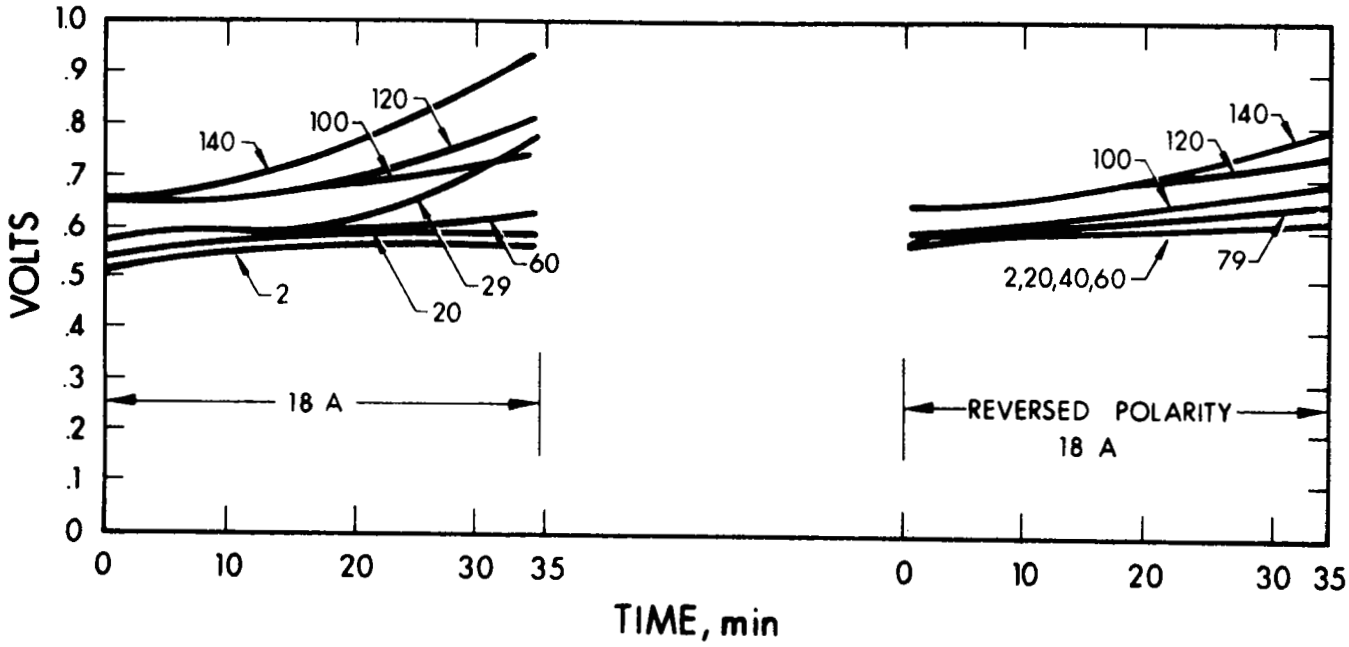

Figure 42. Cycling 0_2 Concentration Cell 165

Cell 170 was a continuous oxygen concentration cell test employing fuel cell type asbestos and gold-coated platinized electrodes. The cell was run continuously for a period of 456 hours, at which time the test was discontinued because of excessive overpotentials. During the test period there was a gradual rise in voltage with time as shown in Fig. 43. Analysis of a sample of electrolyte squeezed from the mat of the cell revealed a final KOH concentration of 26.25 percent. The electrodes and asbestos mat were relatively clean, except that the porous nickel substrate appeared oxidized, especially on the electrode that was used on the oxygen evolution side of the cell.

Cell 171 contained American Cyanamid type AB-6 electrodes and was subjected to a cycling concentration cell test. During 30 cycles, the voltage rose gradually and reached 1 volt at the end of the 30th cycle. The test was therefore discontinued. The voltage of this cell exhibited an upward slope rather than a flat characteristic during cycling.

Cell 173 consisted of gold-coated, platinized electrodes and a mat fabricated from three layers of 0.020-inch potassium titanate paper. The cell was put on test as a cycling concentration cell, with 35-minute cycles. Figure 44 shows the mid-point voltage of the cell at each direction of current flow as a function of cycling. The test was discontinued after 200 cycles due to high overpotential. As can be seen, there was a gradual rise of voltage with cycling to the end of the test. Note also the difference in voltage as the cell reversed polarity, indicating a difference in the electrode structure and performance of the electrodes within the cell. When the cell was disassembled, the mat appeared extremely dry, and a sample of electrolyte could not be obtained for analysis. This test, at conclusion, represented a maximum number of cycles or operating time achieved in a cycling concentration cell and therefore justified the pursuing of potassium titanate matrixes.

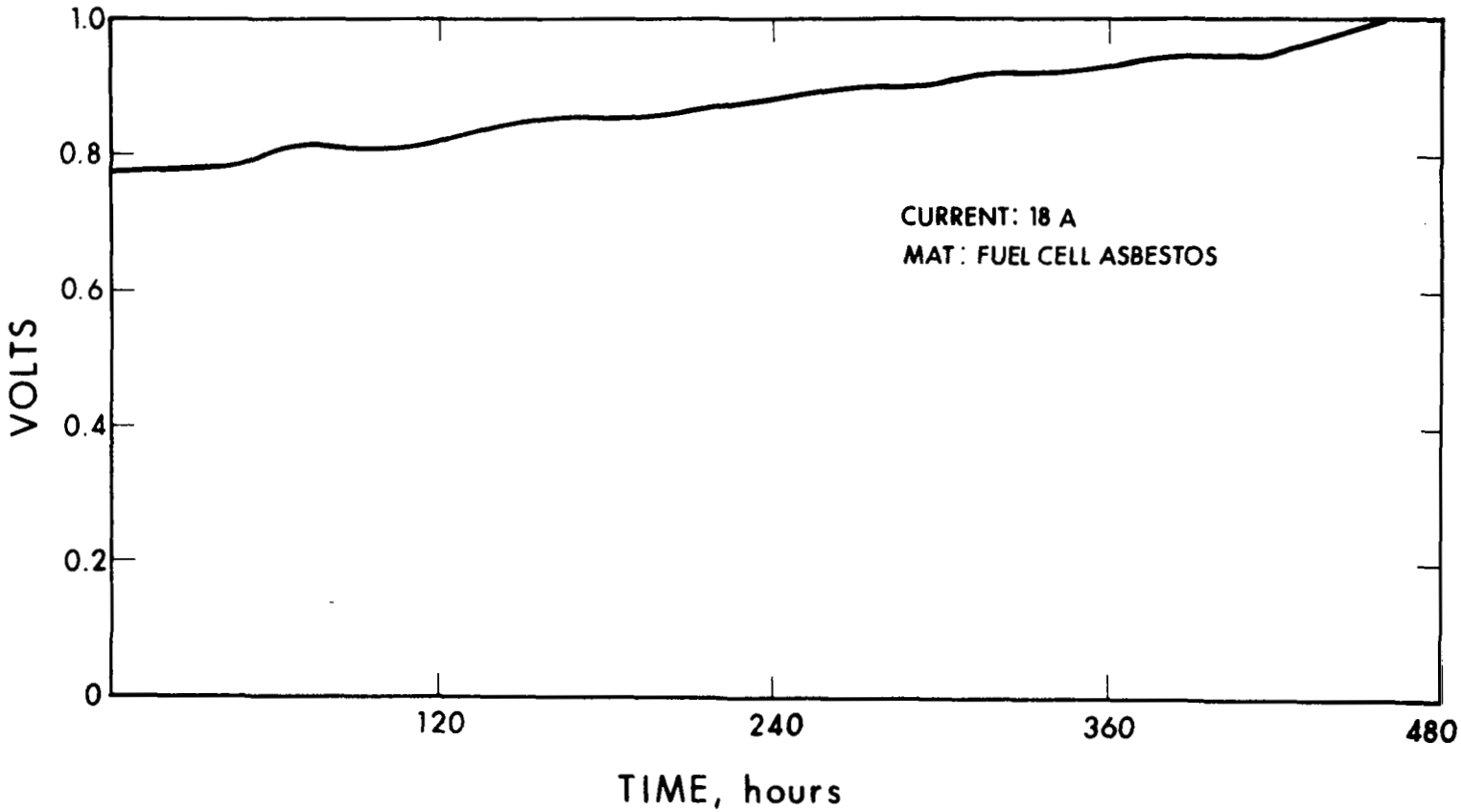

Figure 43. Continuous 0_2 Concentration Cell 170

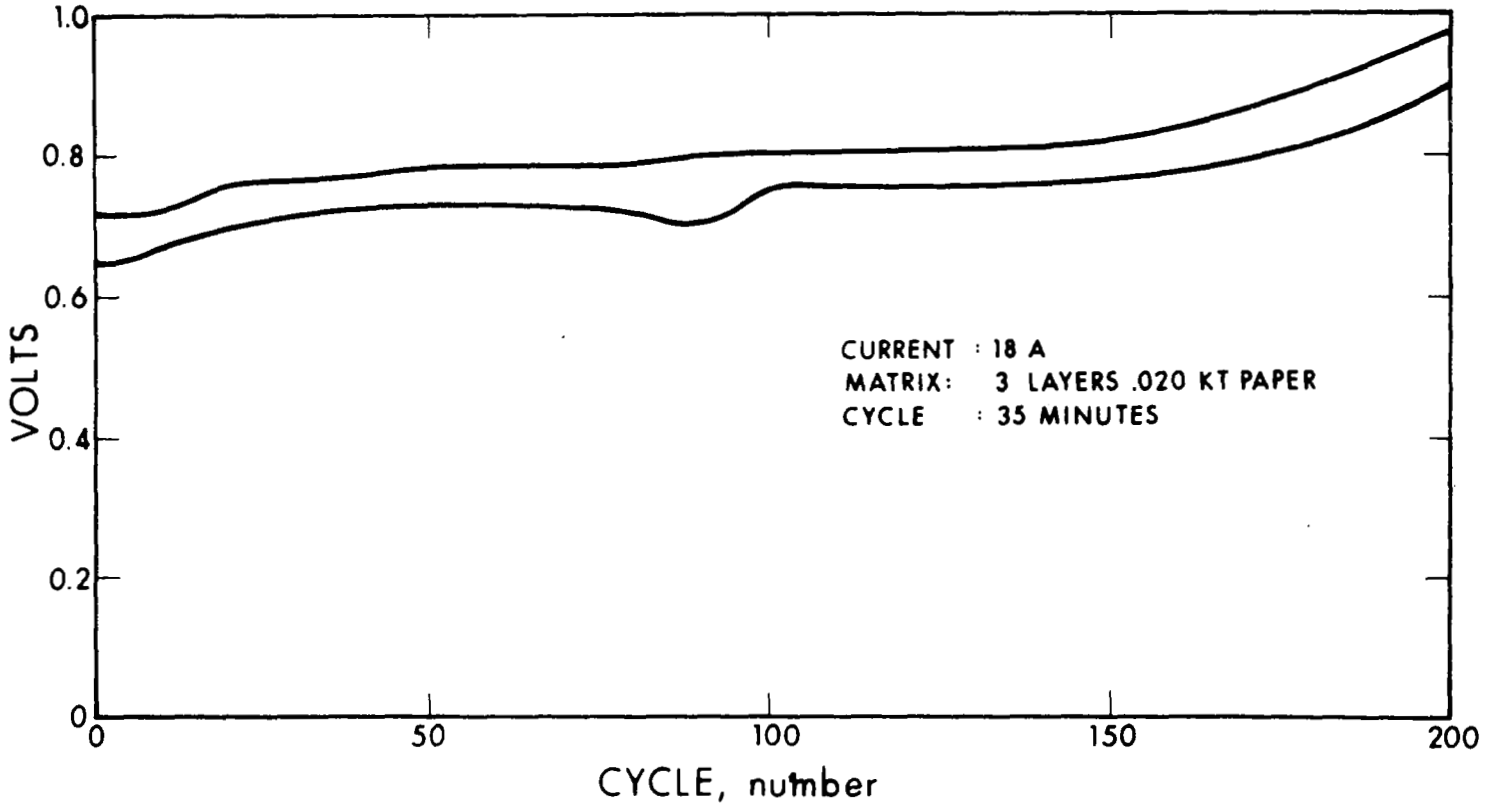

Figure 44. Cycling O_2 Concentration Cell 173 (midpoint voltage)

Cell 181 contained American Cyanamid electrodes with a mat of three layers of 0.020-inch thick potassium titanate (KT) paper. One electrode employed was new, while the other electrode was one that had been previously used in other cell tests. The cell was subjected to test in a cycling concentration cell mode, and was tested continuously for 32 cycles. During the cycling, there was a gradual increase in voltage. The test was discontinued at the 32nd cycle when the voltage reached 1 volt. The poor performance could be attributed to the previously used electrode.

Cell 183 contained American Cyanamid electrode and a fuel cell grade asbestos mat that had been acid-washed. The cell was tested in a continuous concentration cell mode and ran for a period of 140 hours to a 0.95 volt cutoff. During this period there was a gradual rise in voltage with time.

Cell 184 contained American Cyanamid electrodes and an acid-washed fuel cell grade asbestos mat identical in construction to that of cell 183. This cell, too, was run in a continuous concentration cell mode and ran for 72 hours to a 1.2-volt cutoff, showing a gradual rise in voltage with time. Final KOH concentration of the cell matrix was analyzed to be 30.5 percent.

Cell 186 was a cycling concentration cell run at 18 amps (100 mA/cm^2) for 35 minutes at each polarity. Electrodes were American Cyanamid type AB-6 with 9 mg Pt/cm^2 and the mat was 75 percent KT, 25 percent asbestos. The potassium titanate papers used in cells 173 and 181 were samples of a material manufactured by DuPont that has been discontinued. This material has been replaced by a pigmentary potassium titanate and is presently the only form of potassium titanate available. The new material is essentially a powder consisting of particles approximately 0.2 micron in diameter and 10 microns long. Mats for the cells fabricated from pigmentary KT were made from a water slurry of

the KT plus any additions desired. Forming was accomplished by filtering the slurry in a Buchner funnel. The filter cake (6-3/8 in. dia) was then pressed to compact the mat. Asbestos was employed within the KT material for cell 186 to add additional strength to the matrix since pure KT mats are extremely brittle. The cell was cycled for 320 cycles, at which point the voltage reached 1.1 volts and the test was discontinued. Additional moisture was added to the cell by filling the cell cavities with hydrogen and oxygen gas and discharging the gas into the cell. The cell was once again put on cycle and was run for an additional 10 cycles. The voltage of the cell after the addition of water dropped to a lower level and then rose rapidly over the 10-cycle period to the higher voltage level obtained when the test was stopped. The disassembled cell showed no visual signs of degradation, and the mat was clean and white in appearance throughout. The voltage performance of this cell is shown in Fig. 45. Figure 45 is a plot of the cell voltage mid-points of each cycle as a function of cycle number. As can be seen, there was a difference in the voltage of the cell as the polarity shifted. There was also a gradual increase in voltage with time, but this performance was far better than any previous performance obtained and indicated a very promising solution to degradation problems encountered in the past.

Cell 187 contained American Cyanamid electrodes and a matrix made of 100 percent KT. This cell employed electrodes that had been previously used in a number of runs and were possibly contaminated. The cell ran in a test of the continuous concentration cell type for 27 hours to 1.1 volt cutoff. The voltage of the cell was initially high and rose rapidly to the 1.1 volt level. Analysis of the KOH concentration in the mat revealed it to be 35.6 percent. The short run of this cell could be attributed to the use of old electrodes in the cell.

Cell 188 also consisted of a cell employing old American Cyanamid electrodes with a 100 percent KT mat in a continuous concentration cell mode. This cell, too, exhibited initial high voltage, and the test was discontinued.

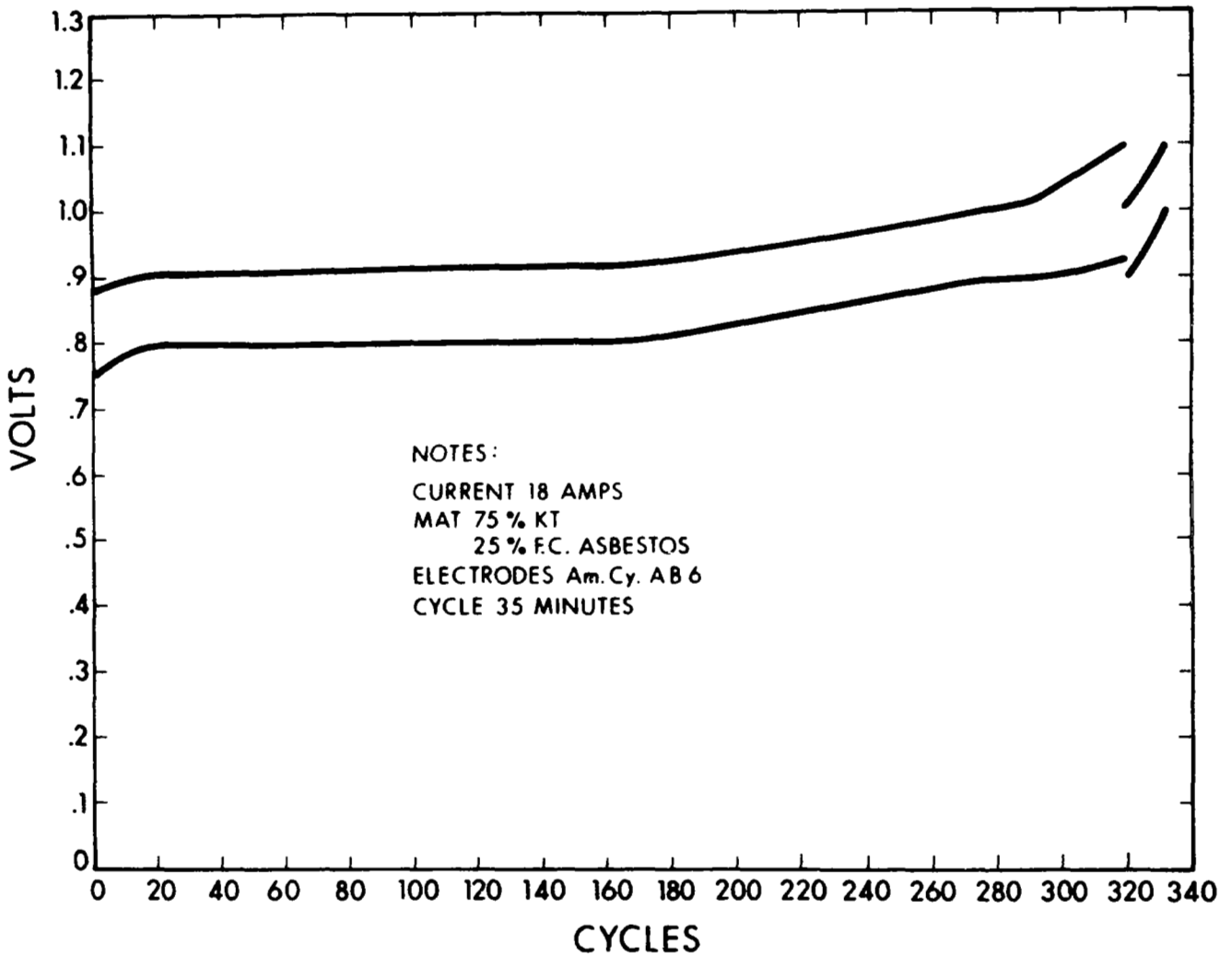

Figure 45. Cycling 0_2 Concentration Cell 186 (midpoint voltage)

Cell 189 contained new American Cyanamid electrodes with a 100 percent potassium titanate mat. This cell developed a short in assembly and was not subjected to test.

Cells 190 and 191 were continuous concentration cell tests. They both contained matrixes composed of 100 percent potassium titanate. Cell 190 contained American Cyanamid type AB-6 electrodes, and cell 191 contained felt metal nickel electrodes that had been gold coated and platinized. Cell 190 ran for 700 hours to the 1.1 volt cutoff point. Cell 191 ran for 840 hours to the 1.1 volt cutoff. The results of these tests are shown in Figs. 46 and 47. Throughout the test there was a gradual increase in voltage with time. The initial high point in voltage of cell 191 was due to a lowering of the oven temperature, which was corrected. The lives obtained with these two cells were far superior to those obtained in previous concentration cells with asbestos and demonstrated the promising nature of potassium titanate matrixes. From the results, it appeared that a deteriorating mode still existed with potassium titanate matrixes, but the rate of degradation was relatively low. It must also be considered that in the concentration cell tests, there were two functioning oxygen electrodes -- one of the discharge mode, and one in the charge mode.

Cell 193 consisted of two electrodes made by electroplating platinum black on a gold-plated nickel screen. The cell matrix was 90 percent potassium titanate and 10 percent asbestos, and it was run in a cycling concentration mode. Figure 48 shows the mid-point voltage of the cell as cycling proceeded. There was a gradual rise in the voltage with cycling, and the latter cycles showed a more pronounced upward slope in the voltage over the time period. The test was discontinued.

Cell 194 consisted of a used set of American Cyanamid electrodes with a 100 percent potassium titanate matrix. The cell was put on a

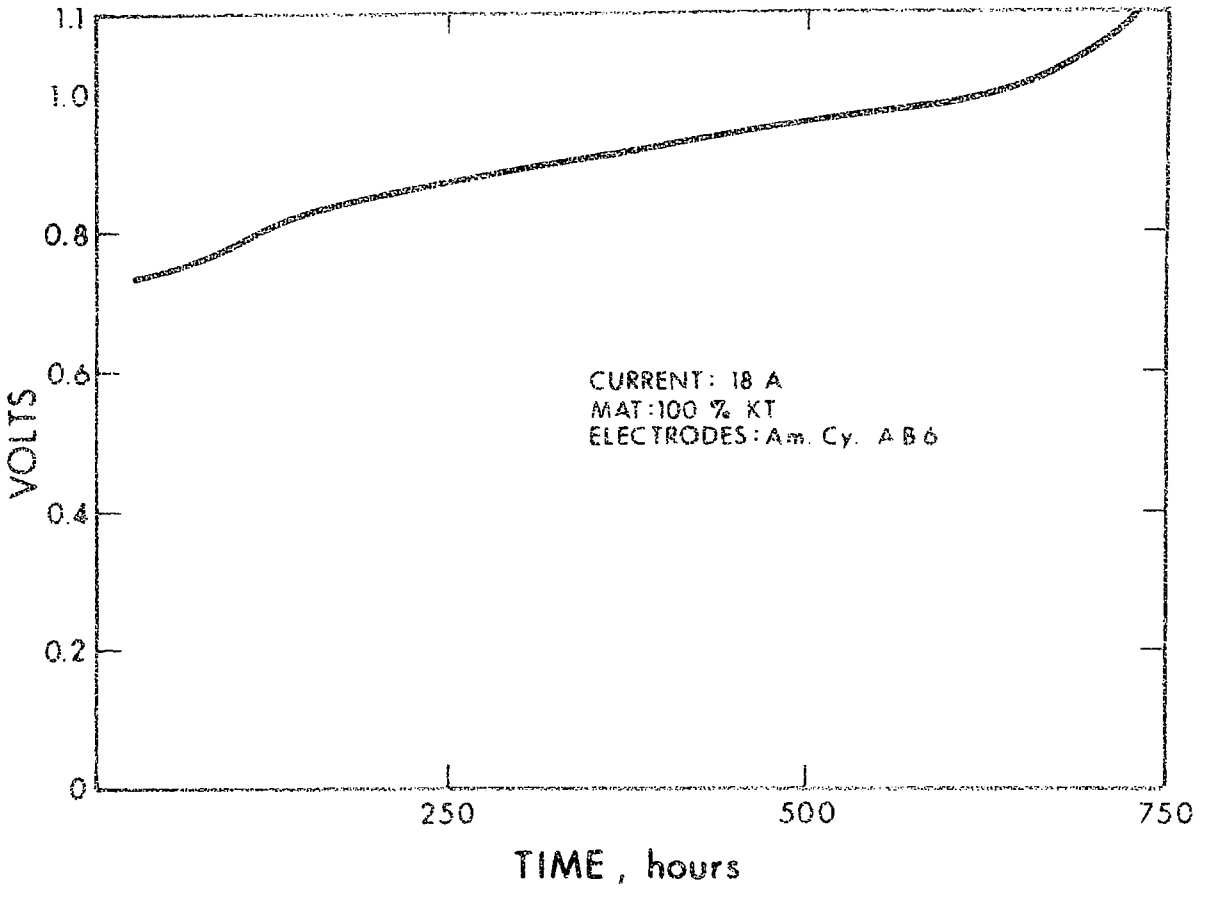

Figure 46. Continuous O_2 Concentration Cell 190

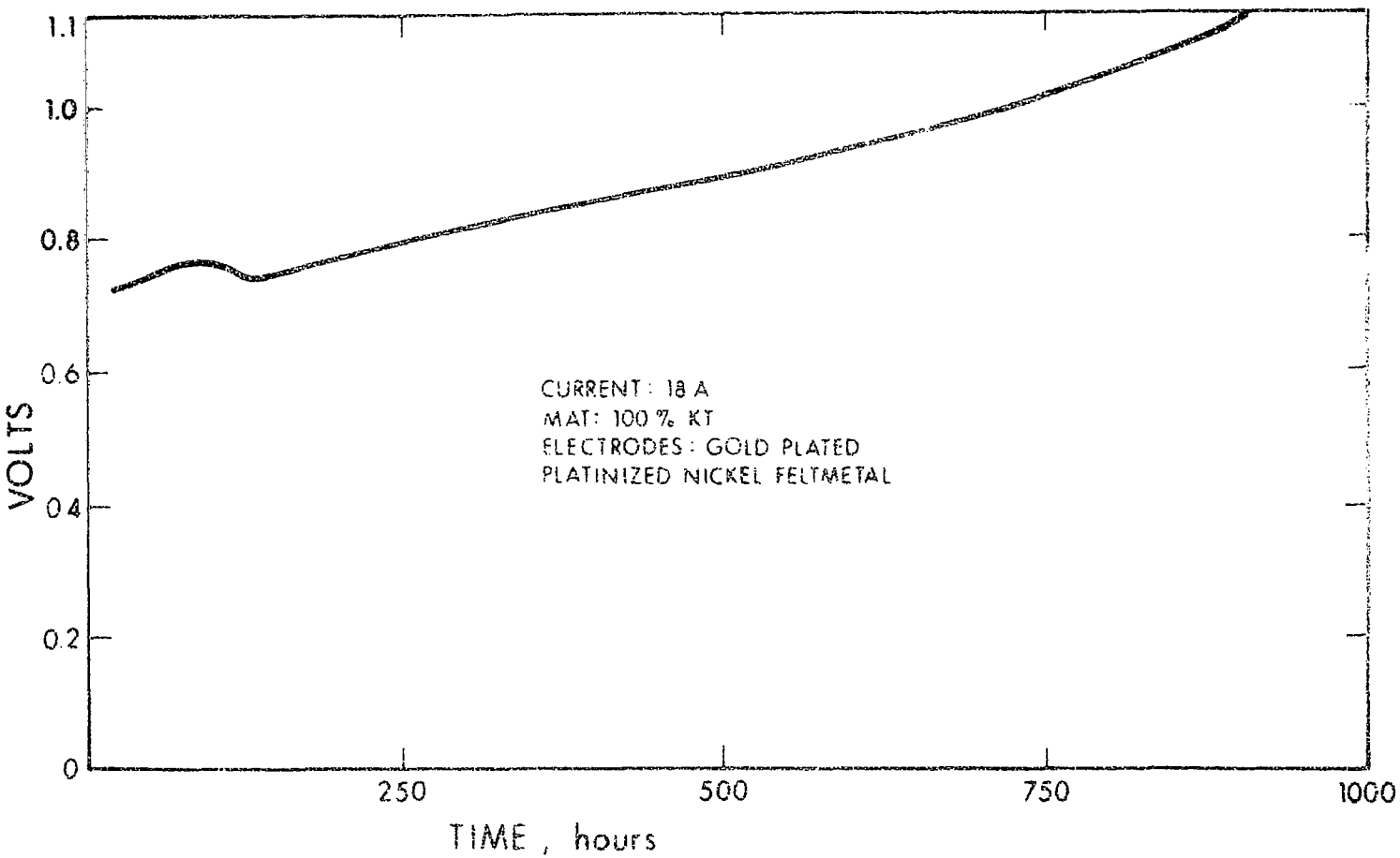

Figure 47. Continuous O_2 Concentration Cell 19i

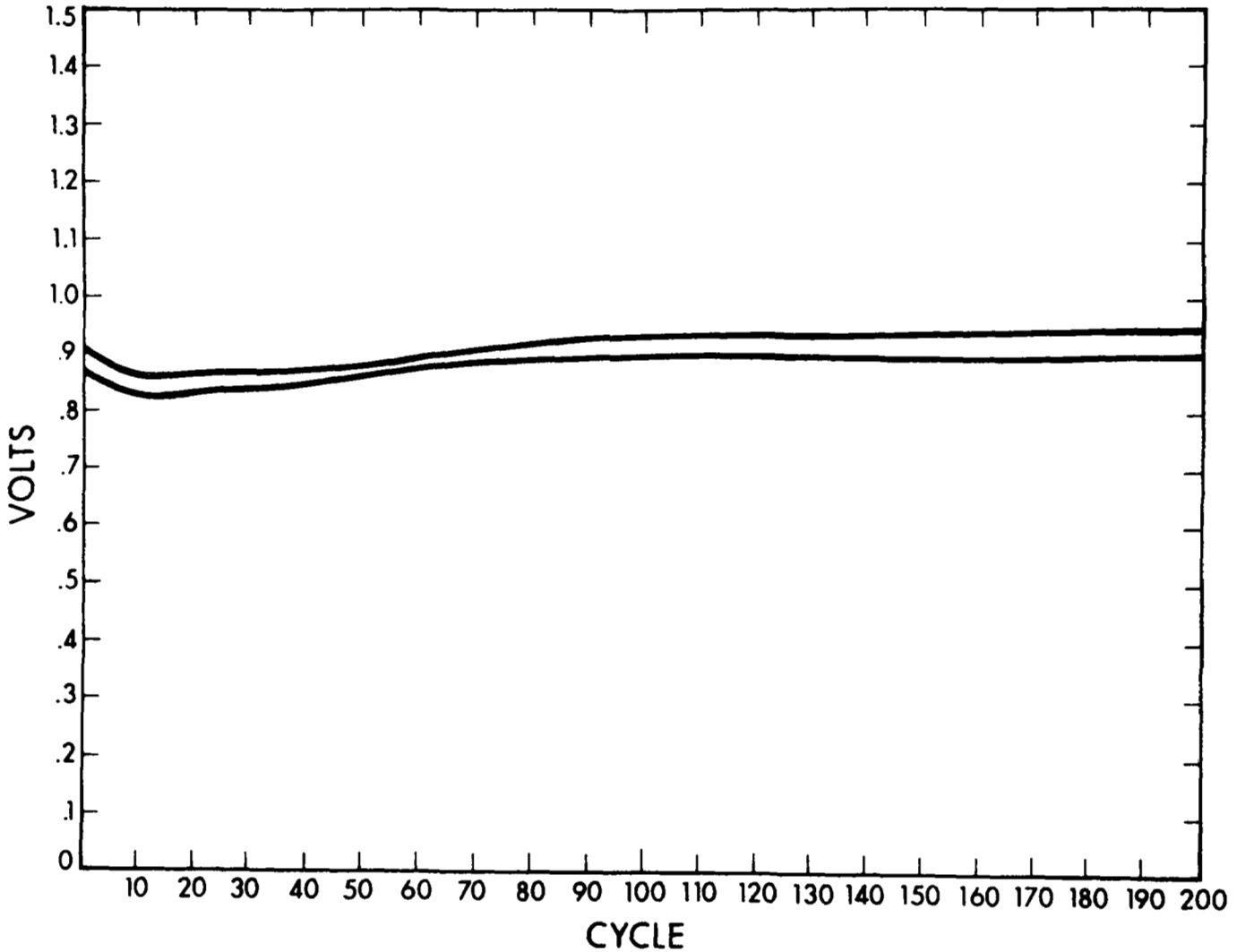

Figure 48. Single Cell 193 - Cycling Concentration Cell 193 (midpoint voltage)

continuous concentration cell test. It rose very rapidly to 1.1 volts, and the test was discontinued.

Cell 201 employed a platinized gold screen oxygen electrode and a platinized gold screen counter electrode and was tested in the oxygen concentration cell test mode. The matrix was composed of two layers of Teflon cloth that had been impregnated with potassium hydroxide electrolyte. The intent of the test was to use a completely inert matrix and determine if any degradation in performance occurred with these types of electrodes. However, when the cell was started on test, the voltage rose very rapidly to 1.5 volts, therefore, the concentration cell tests could not be conducted. The high voltage was due to the high resistance of the Teflon cloth matrixes.

Cell 248 contained two new American Cyanamid AB-6 electrodes and a 60-mil spacer. The matrix was 100% KT washed free of chlorides and sulfates. The cell was run in the oxygen concentration mode at the 18 amps rate for 1730 hours and the test was concluded. Upon disassembly the mat was examined, and no sign of platinum migration was observed. The voltage performance of this cell is shown in Fig. 49. It appears that the voltage reached a plateau and stayed there. This plateau voltage is comparable to the midpoint voltage of oxygen concentration cell 190, described previously. Cell 190 contained AB-6 American Cyanamid electrodes and a 100% KT matrix. The only difference was the fact that the KT mat in cell 190 was unwashed. This cell reached a final voltage of 1.1 volts after 700 hours, and the test was discontinued. It can be concluded that the soluble impurities in KT (chlorides and sulfates) may cause cell deterioration. Table VII is a summary of all the oxygen concentration cell tests conducted thus far. It shows that the test and cells employing potassium titanate have performed in a superior manner to asbestos type cells. Based on the satisfactory performance of the KT mats and considering the limited

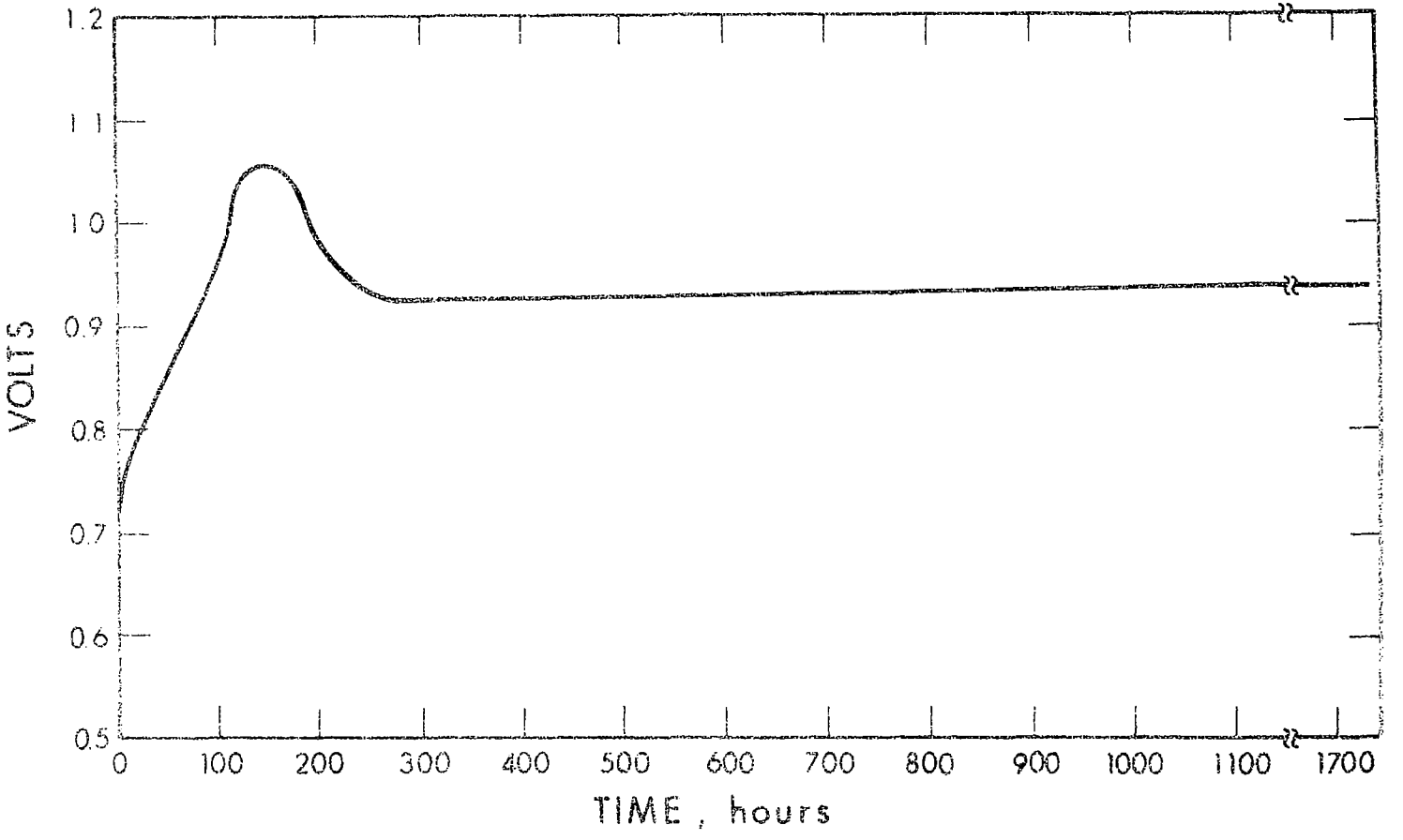

Figure 49. Cell 248 as an O_2 Concentration Cell

TABLE VII

SUMMARY OF OXYGEN CONCENTRATION CELL RESULTS

Cell No.	Electrodes	Matrix Type	Time to .9-1.1 V.	Final KOH
	Continuous			
162	Cold Coated and Pt.	F.C. Asbestos	140 hrs.	Reaction
167	" "	" "	130 hrs.	29.8%
170	" "	" "	456 hrs.	26.25%
183	Am. Cy.	Acid Washed Asbestos	140 hrs.	36.3%
184	Am. Cy.	" "	72 hrs.	30.5%
187	Am. Cy.	100% KT	27 hrs.	35.6% (Old poor electrodes)
188	Am. Cy.	100% KT	-	(Old poor electrodes)
190	Am. Cy.	100% KT	700 hrs.	
191	Felt Metal	100% KT	840 hrs.	
194	Am. Cy.	100% KT	-	(Old poor electrodes)
201	Platinized gold screen	Teflon cloth	did not work	
248	Am. Cy.	100% KT washed	1730	
	Cycling			
163	Cold coated and pt.	F.C. Asbestos	40 hrs.	-
165	" "	" "	152 hrs.	26.8%
171	Am. Cy.	" "	35 hrs.	28.8%
173	Cold coated and Pt.	KT. (3 x .020)	224 hrs.	-
181	Am. Cy.	Kt. (3 x .020)	37 hrs.	32.9%
186	Am. Cy.	75 % Kt. 25 % Asb.	372 hrs.	-
193	Platinized Screen	90 % Kt. 10 % Asb.	222 hrs.	-

test facilities available, it was decided to further test and perfect these matrixes utilizing actual fuel cell cycling tests.

4.6.2 PLATINUM ANALYSIS ON OXYGEN CONCENTRATION CELLS

To determine whether platinum migration occurs by some soluble form into the matrix where it is reduced by hydrogen, the following test was performed on cells 255, 257, and 260. The cells were flushed with oxygen gas, then 150 psi of the gas was introduced. A cycle of 18 amps forward charge for 35 minutes and 18 amps reverse charge for 35 minutes was set up. At the end of 57 cycles the cell was shut down and purged with hydrogen gas. Hydrogen gas (150 psi) was added to the cell and it was left to stand for 24 hours. At the end of this period the cell was disassembled and the membrane was analyzed for platinum. The results were:

Cell 255	0.000 mg Pt/cm^2
Cell 257	0.0088 mg Pt/cm^2
Cell 260	0.0036 mg Pt/cm^2

For comparison, a platinum analysis was performed on cell 252 which had run 567 cycles. The result was 0.115 mg Pt/cm^2. If the amount of platinum migration is dependent on cycle life this would give a figure of 0.015 mg Pt/cm^2 for 57 cycles which is almost double the highest figure given above.

4.6.3 HYDROGEN CONCENTRATION CELL TESTS

Based on some of the previous results indicating that modes of degradation encountered were caused by the matrix and/or hydrogen electrode, a hydrogen concentration cell test was set up and designated cell 209. In this case, two platinized porous nickel plaque electrodes were employed. The matrix was 90 percent KT

and 10 percent asbestos. The cell was run in a continuous concentration mode at 18 amps (equivalent to 100 mA/cm^2). Figure 50 shows the voltage performance of this cell as a function of time. As can be seen, at about the 500-hour point there was an increase in the voltage which leveled off again and remained relatively flat to the 1415-hour point where the test was discontinued. This test seems to indicate that the hydrogen electrodes are not substantially affected by long-term use in the concentration mode.

Cell 218 was a repeat of the hydrogen concentration cell test. Both electrodes were platinized porous nickel plaques and the matrix was made of 90 percent KT and 10 percent asbestos. Construction of the cell was identical to that of cell 209. The cell was put on a continuous-current load of 18 amps (equivalent to 100 mA/cm^2). Results of the test are shown in Fig. 51. The test was discontinued after 1320 hours of operation. The voltage of the cell was stable at approximately 0.1 volt which was lower than the voltage recorded with cell 209. Results of the two concentration cells showed that there was negligible deterioration of the hydrogen electrodes when operated in either the charge or discharge mode. If an electrolyte reaction did occur between the matrix and the electrolyte, this reaction did not affect the performance of the hydrogen electrodes.

Cell 265 was a cycling hydrogen concentration cell. It contained two EOS hydrogen electrodes and had a 50-percent KT/50 percent Teflon membrane sandwiched between two 90-percent KT/10-percent asbestos mats. All the KT was treated in 100°C KOH for one hour and washed with distilled water. The matrix contained 40 g of 39.7 percent KOH. A 60-mil spacer was used. The cell was flushed with hydrogen gas and then 150 psi of hydrogen was introduced. A cycle of 18 amps charge for 35 minutes was set up. The cell ran 1940 cycles and testing was discontinued. The final KOH concentration was found to be 34.8 percent. Figure 52 shows the performance. The voltage slowly rose

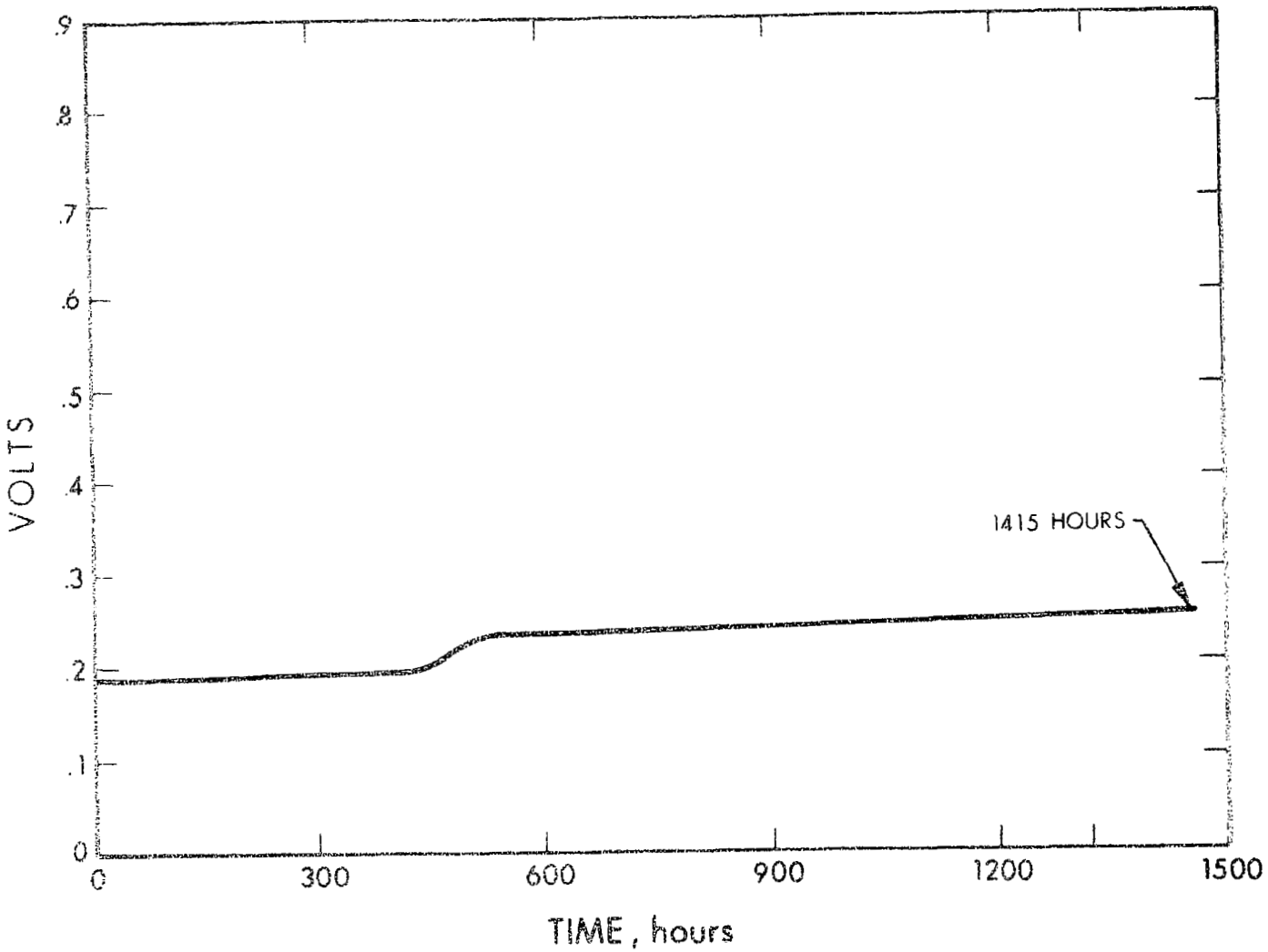

Figure 50. H_2 Concentration, Cell 20

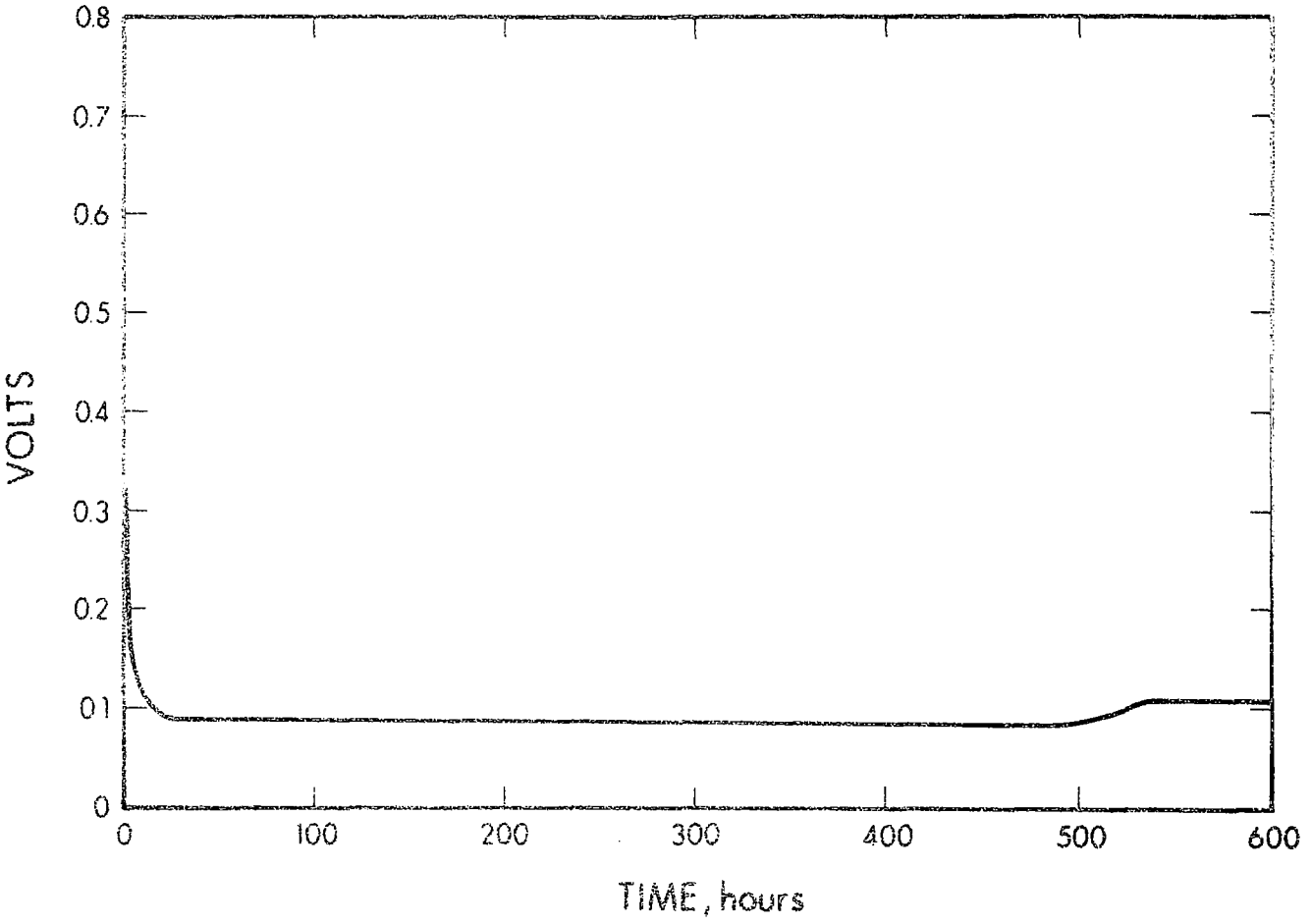

Figure 51. H_2 Concentration, Cell 218

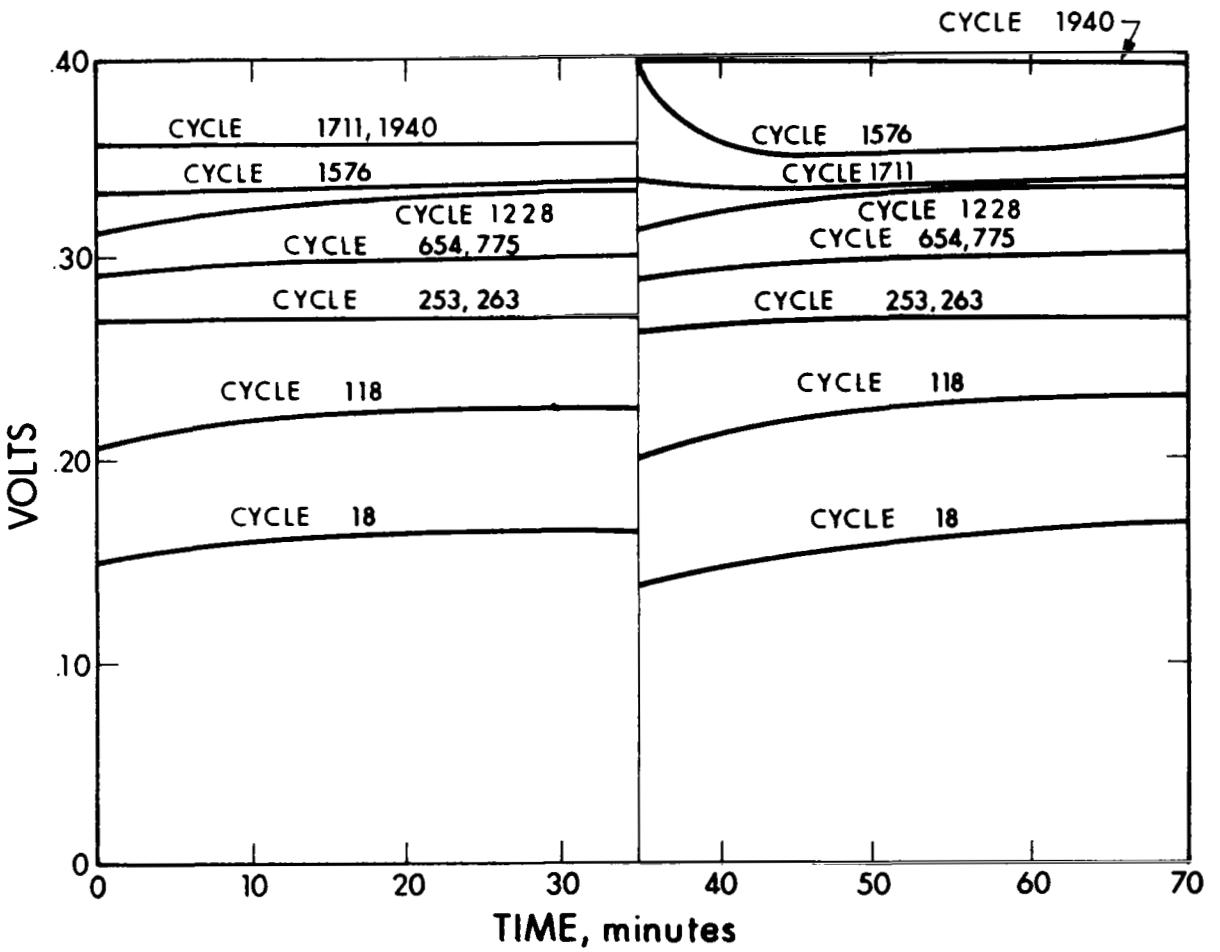

Figure 52. Cycling Performance of H_2 Concentration Cell No. 256

to between 0.35 and 0.4 volt and appeared to have stablized. This cell was cycled continuously and demonstrated a 0.25 rise in voltage in four months. It may be concluded that cycling in a hydrogen atmosphere affects the electrodes very slowly.

4.7 POTASSIUM TITANATE MATRIX CYCLING TESTS

Because of the promising characteristics of potassium titanate, a large part of the program effort was expended in the development of a matrix with this material. The final test of a matrix is in a continuously cycling fuel cell. The following tests demonstrated the feasibility of KT matrixes.

Cell 182 contained porous nickel plaques that had been chemically platinized with 20 mg Pt/cm^2 and a mat that consisted of 75 weight percent potassium titanate and 25 percent fuel cell asbestos. The cell was subjected to a standard test cycle and showed good initial performance. However, during the 12th cycle, an internal short developed in the cell. The cell was disassembled and the short traced to the outer edge of one of the electrodes. Shorting was due to an imperfection in the mat edge. Final KOH concentration of the mat was analyzed to be 35.2%.

Cell 185 consisted of a matrix made from 25 weight percent asbestos fibers and 75 percent potassium titanate pigment. Electrodes employed were porous nickel plaques that were gold coated and platinized by electrodepositing platinum black on the surface of the electrodes. Figure 53 shows the voltage performance at various cycles during the testing. As can be seen, there was a slight degradation in performance throughout the first 200 cycles, at which point the voltage performance stablized and was consistent and reproducible from cycle to cycle up to the 417th cycle. At that point, the discharge voltage exhibited a fall-off in performance towards the end of discharge. This fall-off

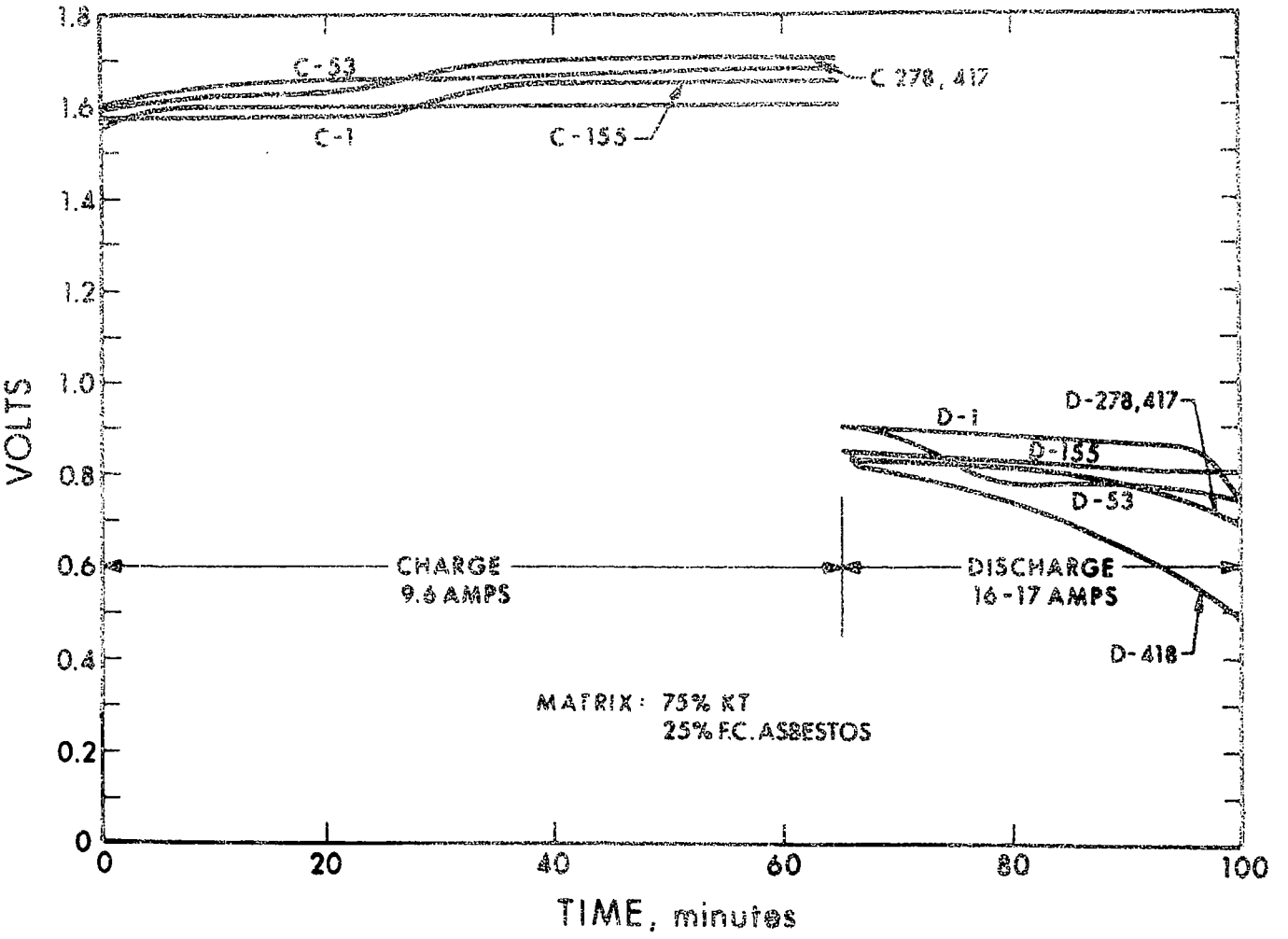

Figure 53. Voltage Performance of Cell 185

of discharge voltage was caused by the reduction in operating pressure during the cycle. On subsequent cycles it was observed that on charge it was not possible to build up pressure greater than 200 psi. Beyond the 200 psi point, apparently a slow gas diffusion and recombination was taking place so that the additional charging of the cell did not increase the cell pressure. On the discharge, the performance fell off as the pressure went below 50 psi. The inability to charge the cell beyond the 200 psi level indicated that a structural deterioration had taken place within the mat which enabled gas diffusion and recombination. This cell contained electrodes that had a porous nickel plaque substrate and oxidation of the substrate in cycling had resulted in differential pressure swings as high as 15 psi as it switched from charge to discharge. It is possible that the accumulative effects of this differential pressure pushing on the matrix from side to side resulted in its structural deterioration and enabled the cross gas leakage and diffusion. The cell was cycled an additional 10 cycles beyond the point of rapid fall-off in performance to a total accumulated cycle life of 420 cycles, and the test was stopped. Examination of the internal cell components revealed no obvious visible changes in the matrix structure. A limited amount of platinum black was observed on the matrix adjacent to the electrodes which was apparently due to mechanical adherence, but below the surface the mat was relatively clean. An analysis of final electrolyte concentration in the mat revealed 32.5 percent.

Cell 192 consisted of a new type of oxygen electrode that was made by taking a close mesh nickel screen, gold plating it, and then electrodepositing platinum black on the screen to a loading of 20 to 25 mg Pt/cm^2. The platinum black was rolled lightly to press it into the holes of the screen and make a more adherent structure. This electrode type was an attempt to make a platinum electrode that contained no wet proofing and would not be subject to oxidation of the substrate. The cell was assembled with a hydrogen electrode of the EOS standard type. The matrix was fabricated from a 90-percent

potassium titanate/10-percent asbestos mix by weight. The cycling test results are shown on Fig. 54. As can be seen, there was a gradual increase in charge voltage with cycling, and a gradual decrease in discharge voltage with cycling. On the 327th cycle, the cell started to recombine during charge, and the cell pressure only rose to 200 psi. Therefore, the test was discontinued. The results of this test and previously observed results of cell 185 indicated that the titanate asbestos matrixes were possibly too porous, and minute structural changes that occur due to differential pressures could be causing cross leakage.

Cell 195 consisted of American Cyanamid type AB-6 oxygen electrodes and EOS hydrogen electrodes. The mat was fabricated from a 90-percent KT/10-percent asbestos by weight mix. The cell was cycled continuously and showed virtually no degradation of performance up to the 278 cycle at which time the discharge voltage dropped to a very low level. The cycling performance is shown in Fig. 55. No explanation was apparent for the sharp drop in performance. This cell deterioration was different than previously observed deteriorations since over a period of one cycle that was a sharp drop in performance. Due to this type of failure, the cell was disassembled and a new matrix consisting of 90-percent KT/10 percent asbestos was inserted in the cell utilizing the same oxygen electrodes without any washing, and a new hydrogen electrode. This new cell was designated No. 202 and was put back on cycling. The cycling performance of cell 202 is shown in Fig. 56. As can be seen, there was a gradual degradation in performance with cycling, in particular, the discharge voltage. The cell reached 387 cycles and then developed an internal short. The test was discontinued and the cell disassembled. The recovery of the cell with the insertion of the new matrix indicated that possibly a high resistance contact had developed within the cell. The final electrolyte concentration in the matrix of cell 195 was found to be 30.03 percent. A 1-in^2 sample of the matrix was analyzed for platinum and found to contain

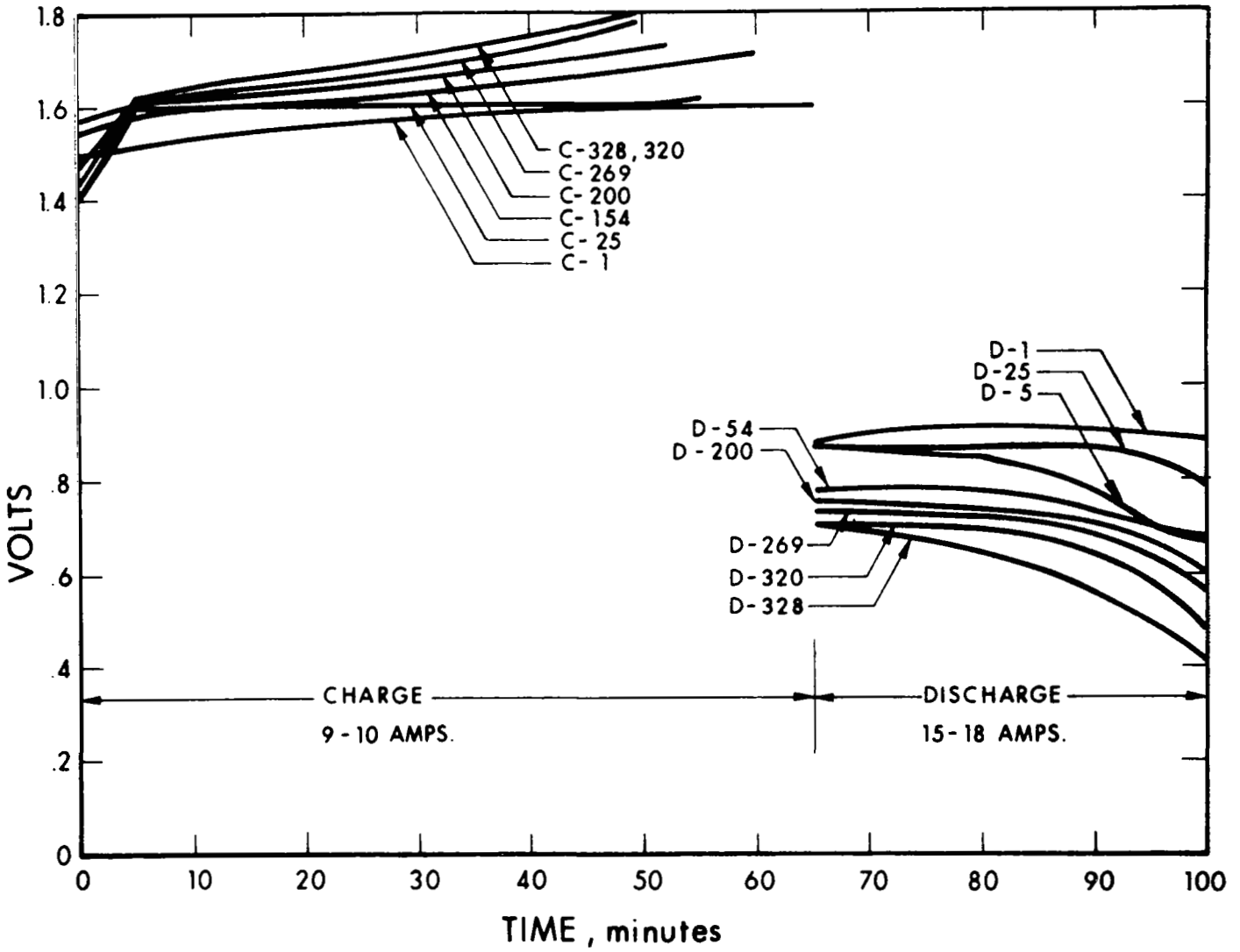

Figure 54. Cycling Performance of Cell 192

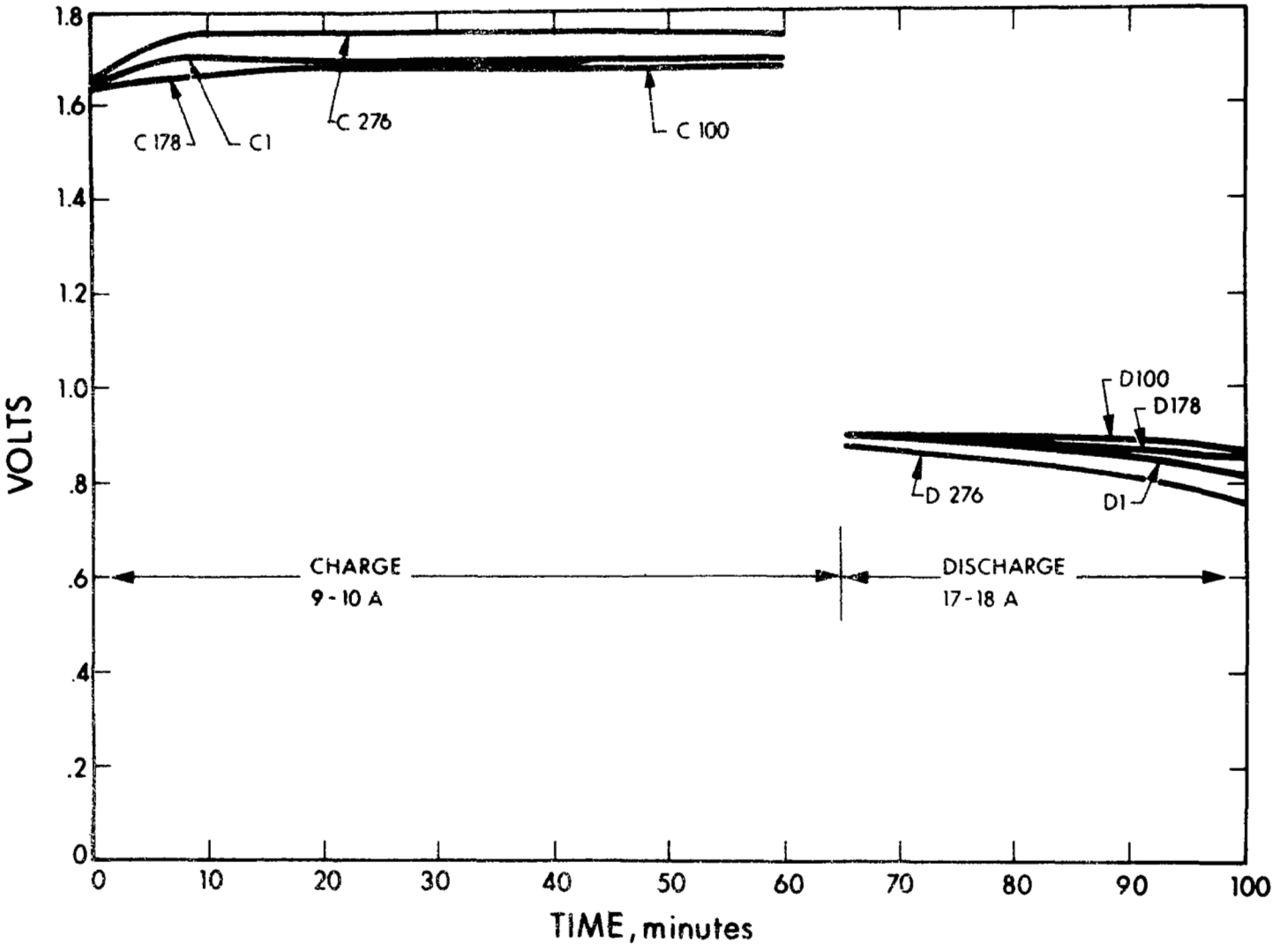

Figure 55. Cycling Performance of Cell 195

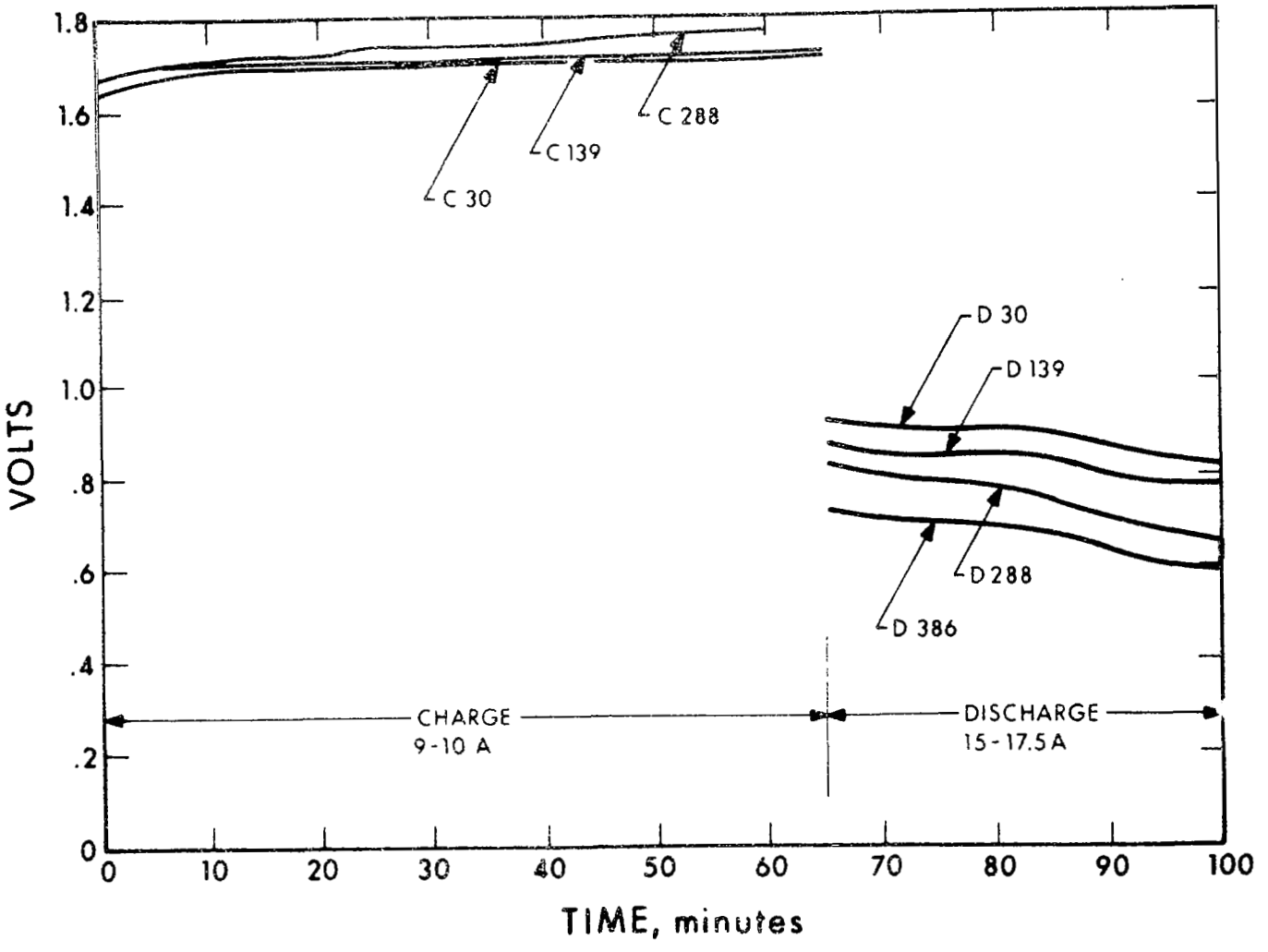

Figure 56. Cycling Performance of Cell 202

0.0078 gram of platinum which is approximately 1.2 mg platinum per cm^2. It was not established whether this platinum in the matrix was material that adhered to the surface of the matrix adjacent to the electrodes during the disassembly, or whether it had actually migrated into the matrix. This represents a relatively small quantity of platinum, and it has not been established yet whether any substantial platinum migration occurs with the use of potassium titanate matrixes.

Cell 196 showed good performance, but on the 60th cycle exhibited an internal slow initial recombination and cross leakage, and the pressure during charge did not rise above 200 psi. The cross leakage difficulty encountered with this and previous cells was fabricated potassium titanate matrixes pointed to an area of required improvement in the matrix fabrication procedure.

Cells 197 and 198 consisted of platinized nickel screen oxygen electrodes and platinized porous nickel plaque hydrogen electrodes with matrixes of 90-percent potassium titanate and 10 percent asbestos. Cell 197 exhibited a volume balance problem and the cell was only subject to a limited number of cycles and the test was discontinued.

As shown in Fig. 57 cell 198 was cycled continuously for 952 cycles. There was a gradual increase in the charge voltage and a decrease in discharge voltage. After 952 cycles a short circuit developed within the cell, causing the cell voltage to drop to zero during charge and discharge. The test was discontinued at this failure.

Since the load bank used to test the cells was a fixed resistor, the discharge current decreased as the cell voltage degraded during discharge. In the early cycling phases discharge current ranged from 15 to 18 amps, but as the voltage began to gradually drop during the latter cycling sequences, the current degraded steadily. At the start of the 952nd discharge cycle the current measured 15 amps;

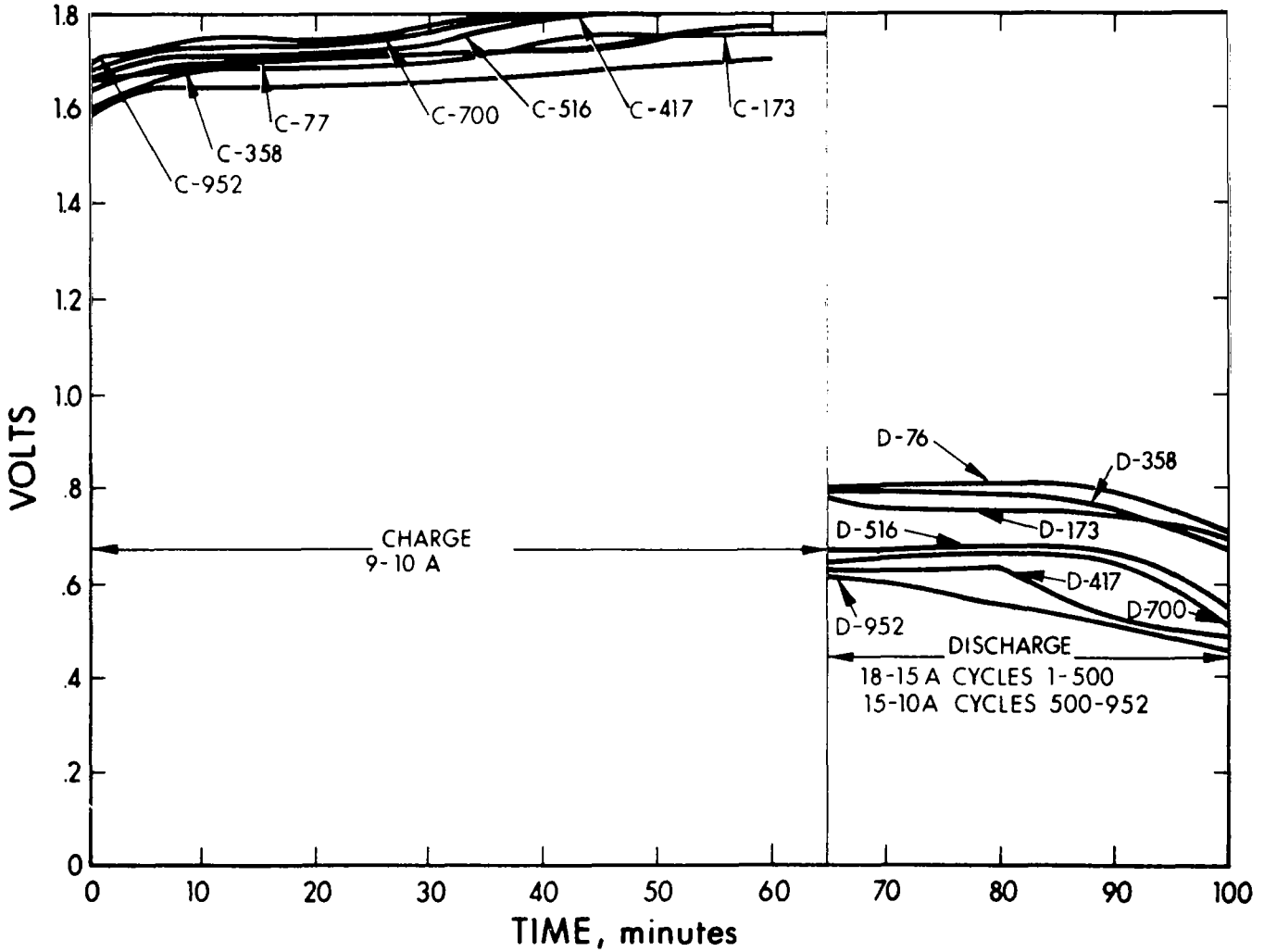

Figure 57. Cycling Performance of Cell 198

it dropped during discharge to 10 amps at the end of the cycle.

Since the ampere-hours used during the discharge cycle decreased with voltage and current falloff, the recharging time also decreased. During the charge periods of the latter cycles the pressure switch would cut off when the pressure reached 350 psi, and the cell would experience a no-charge/no-discharge open-circuit condition for 5 to 10 minutes before the next discharge cycle began. This condition was established to maintain a uniform cycling period of 65 minutes for charging and 35 minutes for discharging. Even with the considerations of degradation and reduced performance observed, this cell test represented the best performance level that had been achieved. The 952 cycles at 100 min/cycle were equivalent to 1585 hours (or a period of 66 days) -- more than two months of continuous operation.

Cells 199 and 200 consisted of American Cyanamid oxygen electrodes platinized porous nickel plaque hydrogen electrodes, and matrixes made from 90 percent potassium titanate and 10 percent asbestos by weight. In both of these cells the total weight of the matrix was increased from the previously tested 20 grams to 24.5 grams. This increase in weight was an attempt at improving the structural characteristics of the matrix since difficulties had been encountered with cross-leakage with some of the prior tests.

The oxygen electrode used in cell 199 had been previously used in cell 196 which ran 60 cycles, at which time it developed slow cross gas leakage. The cell was tested continuously for 405 cycles after which the test was discontinued. Figure 58 shows the performance of this cell. As shown, there was a gradual degradation in performance with cycling. Cell 200 was given a limited number of cycles, and the test was discontinued due to gas leakage and cell imbalance problems in the test cell set-up.

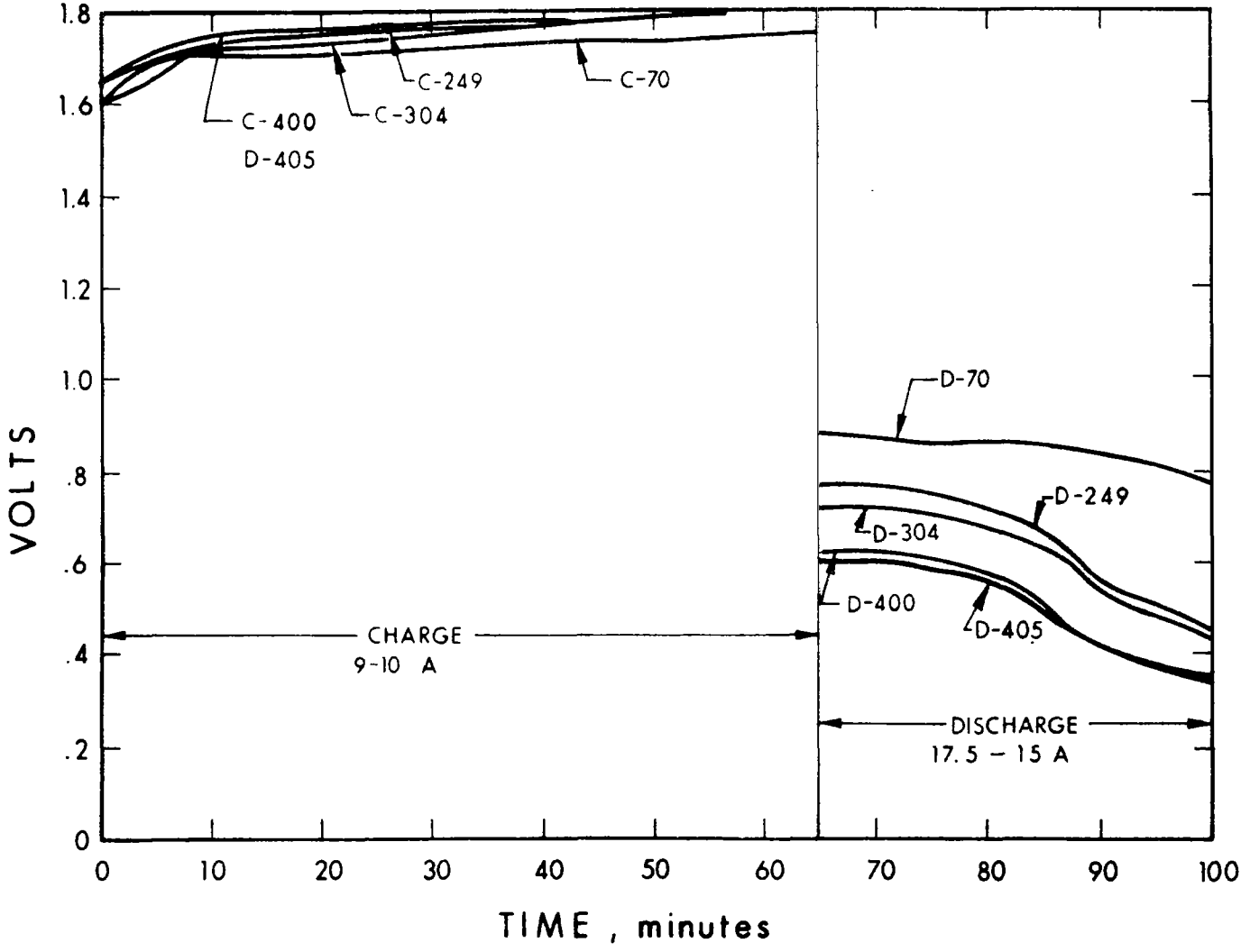

Figure 58. Cycling Performance of Cell 199

Cell 203 consisted of an American Cyanamid oxygen electrode and a platinized porous nickel plaque hydrogen electrode. The matrix consisted of a 90-percent potassium titanate/10-percent Teflon fiber mix. This matrix represented an attempt to substitute Teflon fibers for the previously used asbestos fibers to mechanically strengthen the matrix. Teflon fibers were obtained by cutting and shredding Teflon cloth that contained multi-filament threads. Initially, difficulty was had in obtaining a uniform mixture of Teflon fibers and the potassium titanate because the fibers, being nonwetting, would float to the top of the mix solution during the processing. The use of potassium hydroxide as a wetting agent enabled obtainment of a fairly uniform mix, and therefore, the matrix was made and assembled and subjected to test in this cell. The performance of this cell is shown in Fig. 59. Initial performance was fair, and as can be seen there was a rapid deterioration in performance.

Cell 205 consisted of an American Cyanamid oxygen electrode and a porous nickel plaque hydrogen electrode. The matrix was 100 percent potassium titanate, and the cell was subjected to a standard test cycle. However, during the charge, slow recombination occurred and pressures beyond 200 psi were not achieved. Therefore, the test was discontinued.

To summarize the results of the potassium titanate matrix cell test thus far, cells 185, 192 and 196 employing 20-gram mats developed cross leakage, indicating that an improvement in the process procedure was required. The 24.5-gram mats had not been fully evaluated yet.

Gradual deterioration in voltage performance was observed in the 300-500 cycle range with those cells that reached this cycle life. The component -- the hydrogen electrode, the oxygen electrode, or the matrix -- that was causing the difficulty had not been isolated yet.

Cell 206 consisted of the oxygen electrode from cell 199 and a new EOS hydrogen electrode with a new matrix composed of 90 percent KT and 10 percent asbestos. The voltage performance of various cycles of the cell, cycled 700 times, is shown in Fig. 60. As can be seen, there was a gradual increase in the charging voltage with cycling.

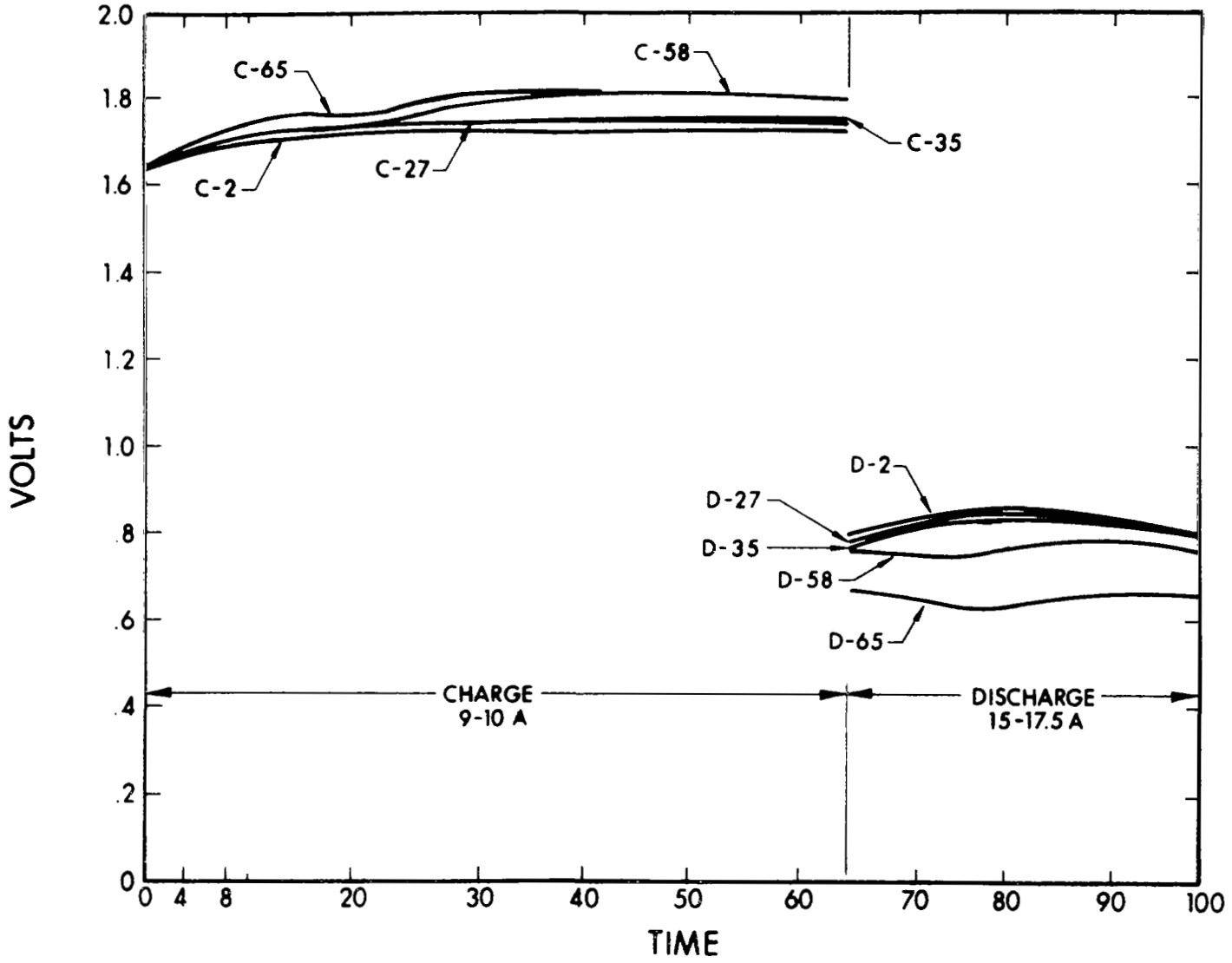

Figure 59. Cycling Performance of Cell 203

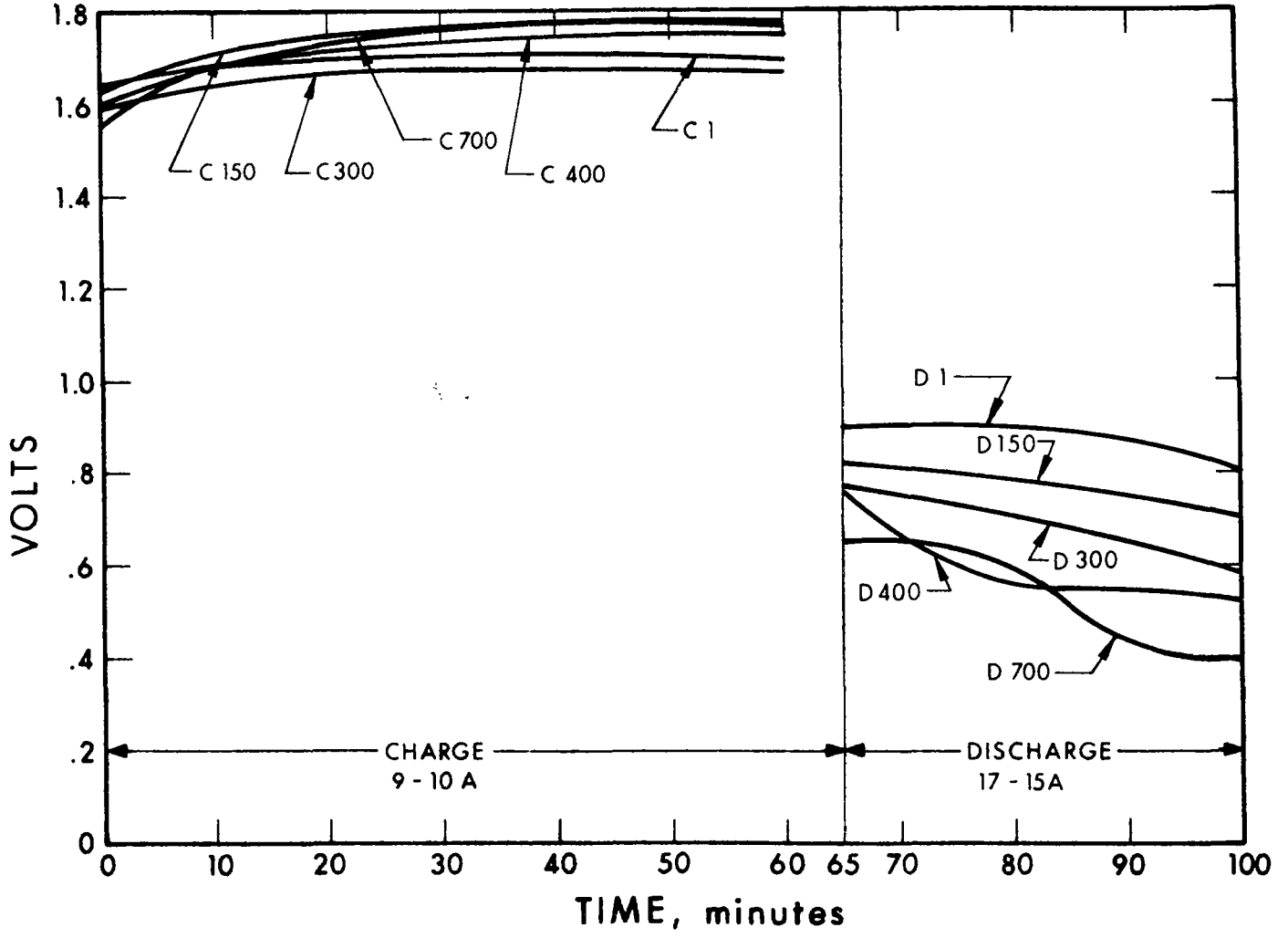

Figure 60. Cycling Performance of Cell 206

However, the initial performance of the cell showed that the oxygen electrode had not been permanently degraded as a result of its use in the previous cell tests.

Once again the oxygen electrode from cell 206 was reused and assembled in cell 214, which contained a new EOS hydrogen electrode with a new matrix of 90 percent KT and 10 percent asbestos. The hydrogen electrode of cell 206 was damaged and could not be reused. The cell was cycled continuously for 464 cycles, and then it developed a slow gas recombination. Figure 61 shows the voltage performance of the cell at various cycles. When the cell was fresh, the performance was as good as that of the original cells.

Table VIII summarizes the series of cells employing the same oxygen electrode. A total of 1629 cycles was accumulated with the same oxygen electrode; in every case the performance was equal to its original level.

TABLE VIII

PERFORMANCE SUMMARY, REUSED OXYGEN ELECTRODE

Cell	Cycles	Test Results
196	60	Developed slow gas recombination
199	405	Gradual degradation in performance
206	700	Gradual degradation in performance
214	464	Developed slow gas recombination
	Total life:	1629 cycles.

Following disassembly of cell 202, the oxygen electrode (also used on cell 195) was recovered in good condition and reassembled with a new hydrogen electrode and matrix and designated cell 207. This cell showed initial good performance, but developed a slow gas

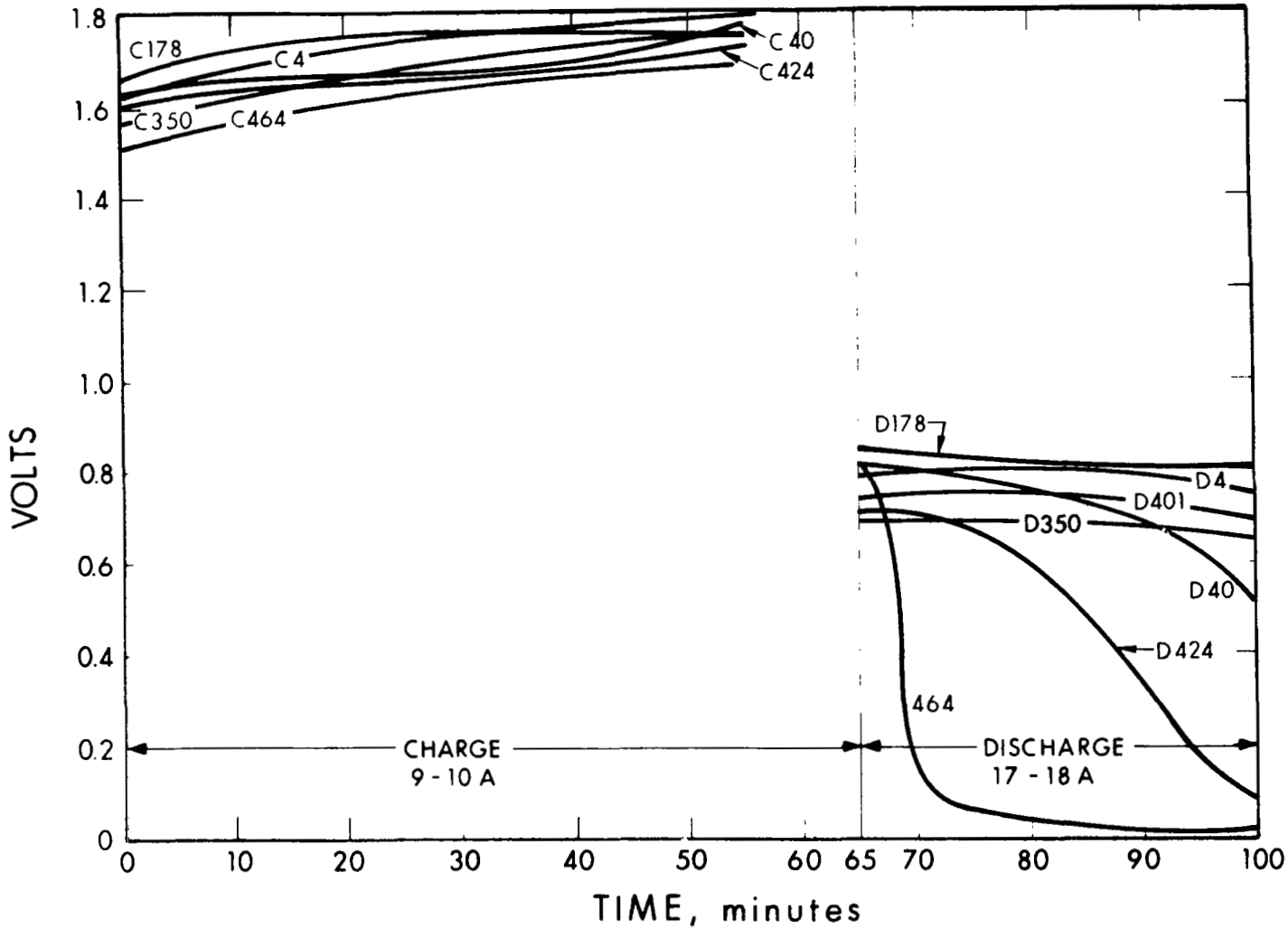

Figure 61. Cycling Performance of Cell 214

recombination on the 27th cycle and the charge pressure did not rise above 150 psi. The test was then discontinued. Since cell 195 had been subjected to 278 cycles and cell 202 to 387 cycles, the total accumulated number of cycles subjected to the oxygen electrode was 692. In each case when the cell was reassembled with a new matrix and hydrogen electrode, the initial performance returned to the original level of about 0.8 to 0.85 volt on discharge at 17 to 18 amps. The results of this and the previous series of tests indicated that the mode of deterioration encountered with the titanate matrix type cells, thus far was centered in the matrix or hydrogen electrode and not the oxygen electrode, as previously concluded in asbestos-type cells.

Cell 205 consisted of an American Cyanamid oxygen electrode and an EOS hydrogen electrode with a matrix of 90 percent KT, 10 percent asbestos. The cell was cycled 52 times and showed good initial performance. But on the 53rd cycle, it exhibited a slow recombination and was unable to recharge the cell above 200 psi; the test was discontinued.

Cell 211 consisted of an American Cyanamid oxygen electrode and an EOS hydrogen electrode with a matrix consisting of 90 percent KT and 10 percent polypropylene fibers. The substitution of polyproplene fibers for asbestos in the matrix represented an attempt to eliminate asbestos (which might have been reacting gradually with the electrolyte). The cell was cycled 50 times, showing initial good voltage performance as shown in Fig. 62. Throughout the cycling of the cell, the charge and discharge voltage remained relatively stable; during the last five cycles, however, a slow gas recombination took place within the cell such that the cell pressure did not reach the fully charged level. On subsequent discharges there was a falloff in the discharge voltage. The slow recombination that occurred in the cell was apparently due to the structural weakness and imperfection of the matrix; thus, no conclusion at this time could be drawn as to the ability of this type of matrix to enhance cycle life of the cell.

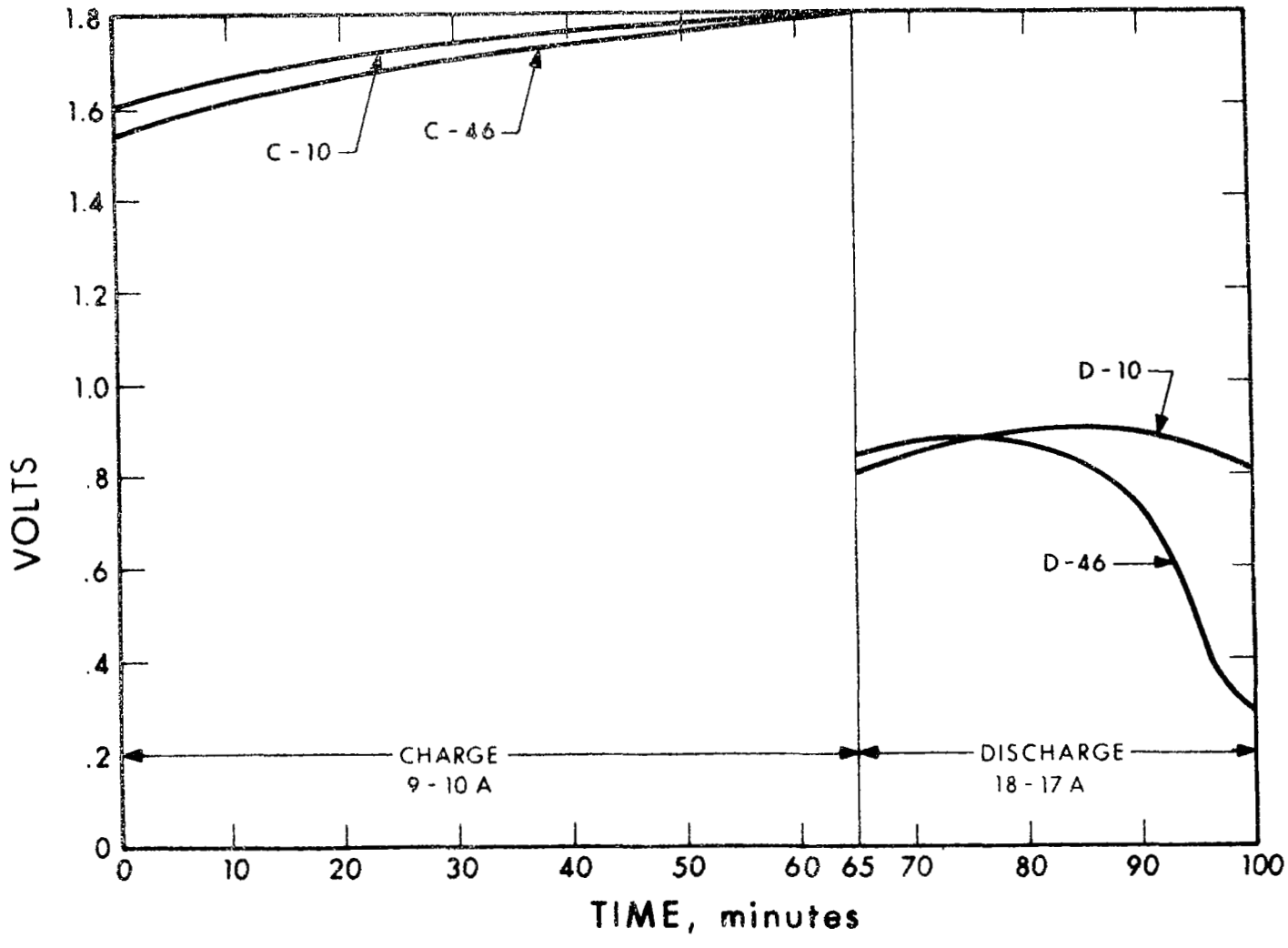

Figure 62. Cycling Performance of Cell 211

Cells 213 and 215 were additional attempts to use a matrix of 10 percent polypropylene fibers. In both cases, the oxygen electrodes were American Cyanamid types and the hydrogen electrodes were platinized nickel porous plaques. Cell 213 was cycled 82 times with relatively stable voltage performance. Beyond that point, a slow gas recombination during the charge cycle took place and the cell did not reach a full state of charge. On subsequent discharges there was a rapid falloff in discharge voltage as the cell pressure dropped to levels of 50 psi and below. Cell 215 showed initial good performance, but on the 30th cycle it also developed a slow gas recombination, resulting in a falloff in the discharge voltage as the pressure decreased below 50 psi.

Cells 223 and 224 were the final attempts with a matrix of 10 percent polypropylene fibers. Each cell was assembled with an American Cyanamid oxygen electrode and an EOS electrode. Cell 223 developed a slow gas recombination on the 22nd cycle and cell 224 developed a slow gas recombination on the 24th cycle.

The performance with the 10 percent polypropylene matrixes of the five cells resulted in a gradual slow recombination after a period of cycling. The method of fabricating these matrixes was apparently inadequate, and the resulting matrixes had flaws or pinholes that developed with cycling.

From the results obtained, it was apparent that this type of structure could not withstand cross gas leakage. Different techniques would have to be employed to fabricate chemically inert matrixes without asbestos constituents.

Many of the cell tests employing the 10 percent asbestos or polypropylene matrixes resulted in the development of cross gas leakage as cycling proceeded. This cross gas leakage apparently occurs due to structural changes in the matrix or imperfections resulting from the

processing techniques employed. To overcome this deficiency, an alternate approach was considered, which involved use of a thin membrane material that would be located between two layers of an absorbent matrix. This "sandwich" is capable of storing and holding a large quantity of electrolyte yet is resistant to cross gas leakage. Since the absorbent matrix in this configuration would not have to prevent the cross gas leakage, it would be possible to reduce matrix compression and increase the electrolyte quantity, thereby possibly increasing performance and capacity.

Cell 222 was the first attempt at such a configuration. It consisted of a membrane of radiated polyethylene (permion 300) normally employed in conventional secondary batteries and a layer of 90 percent KT and 10 percent asbestos on either side of the membrane. The compression on the membrane was reduced by eliminating the backup screens behind the gas electrodes and 25 grams of electrolyte was impregnated in each half of the matrix. The cell was put on test and subjected to five cycles. The test was discontinued because the cell exhibited very poor performance.

Cell 226 was similar in construction to cell 222 and consisted of a sandwich matrix of a radiated polyethylene membrane, and two layers of the KT with asbestos. However, in this case, the backup screens were used behind the electrodes and the electrolyte quantity was reduced to 20 grams per matrix. The cell was put on test and subjected to four cycles; the test was discontinued when the cell showed poor performance.

Cell 228 consisted of a membrane made of woven Teflon cloth between two layers of KT with 10 percent asbestos. The cell was cycled 39 times but exhibited poor performance. Apparently, the nonwetting nature of the woven Teflon material resulted in a high cell impedance.

Cell 229 consisted of an American Cyanamid oxygen electrode, an EOS hydrogen electrode, and a matrix that was made of a sandwich of two layers of KT and 10 percent asbestos with a cellulose membrane, designated FSC (also employed in conventional batteries). It was realized that this type of membrane would not withstand the high concentration electrolyte and elevated temperature conditions in the cell for very long, but it was felt that for feasibility this test should be conducted. The cell was assembled with a 0.05-inch spacer, and 20 grams of electrolyte in each of the two matrix halves. The cell was put on test and showed good performance, as shown in Fig. 63. The cell ran for 347 cycles, but cycles 276 to 347 were poor. Just prior to disassembly, it was found that the cell had been run at 115°C instead of 80°C. Analysis of the KT layers showed 20.9 percent KOH on the hydrogen side and 21.2 percent on the oxygen side, indicating a large consumption of electrolyte. It performed similarily to cells that did not contain membranes, demonstrating that the membrane approach is feasible and does not cause excessive increases in internal impedance.

Cell 224, containing the same type of electrodes and configuration as cell 229, was run at 80°C. Performance was good. After 52 cycles, the matrix was damaged by a large differential pressure.

The use of a membrane configuration offers several potential significant advantages: (1) cross gas leakage can virtually be eliminated, (2) it increases the scope of types of matrix materials that can be used for electrolyte absorbency, and (3) it reduces the stringent physical requirements on a matrix. With regard to the third advantage, matrixes inherently must have a characteristic of high quantity of electrolyte absorption, and so must be somewhat porous, yet they should be nonporous to the extent of preventing cross gas leakage.

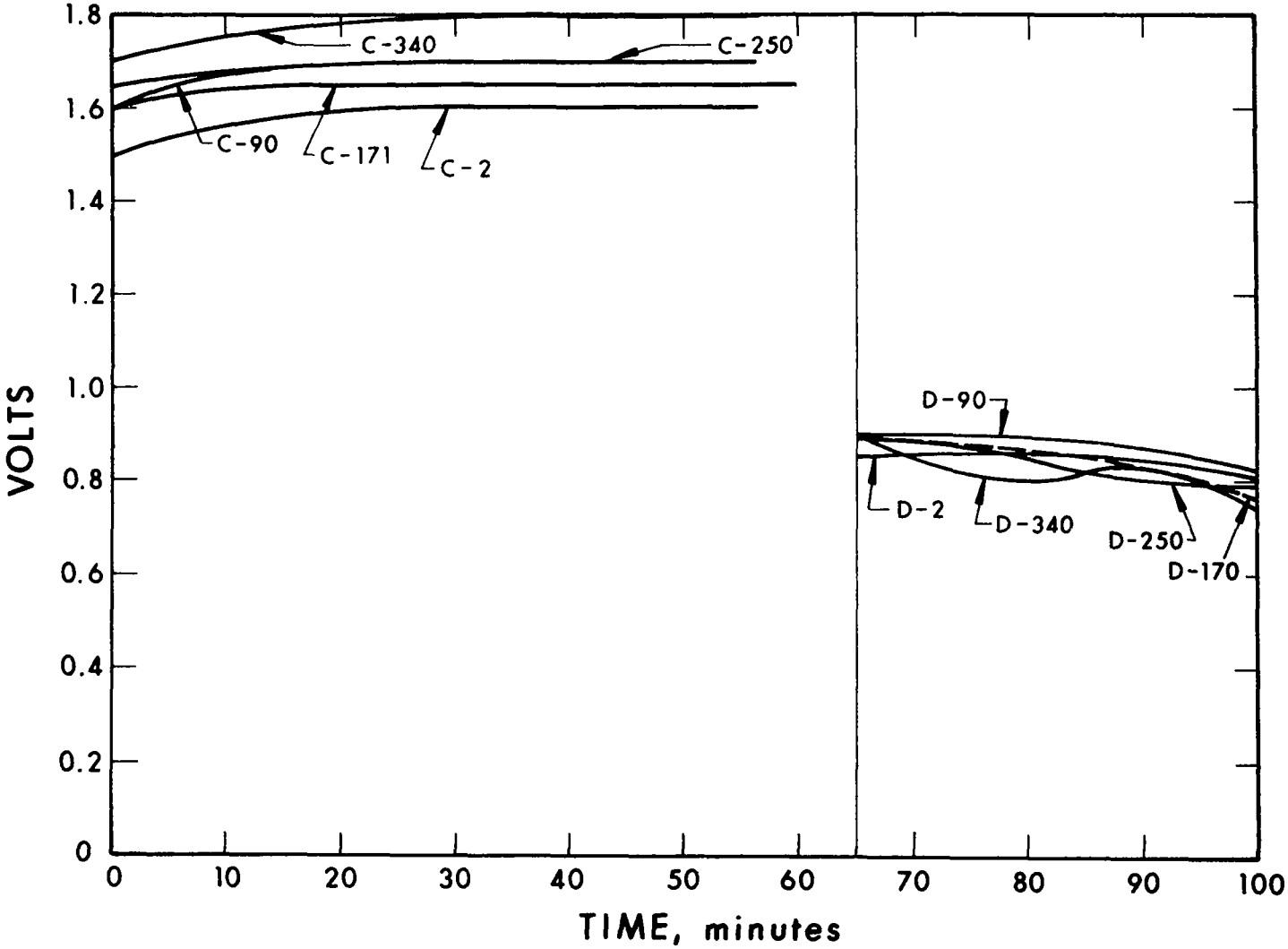

Figure 63. Cycling Performance of Cell 229

Having demonstrated the feasibility of a membrane sandwich cell by virtue of the satisfactory performance of such a cell, it was felt that the approach warranted further effort.

Cell 230 consisted of an American Cyanamid oxygen electrode and an EOS hydrogen electrode, with a sandwich matrix consisting of radiated polyethylene membrane and two layers of KT with 10 percent asbestos. This cell also contained 20 grams of electrolyte per matrix with a 0.05-inch spacer, similar to cell 229. This cell ran for 44 cycles. Performance was poor after the first seven cycles.

Cell 231 contained the same type of electrodes and matrix (eradiated polyethylene sandwiched between KT/asbestos) as cell 230 above. Twenty-five grams of 40 percent electrolyte was used on the hydrogen side and 20 grams on the oxygen side. An 0.06-inch spacer was used. The cell ran 96 cycles, 25 of which were acceptable. Results are shown in Fig. 64. The KOH analaysis showed 31.50 percent on the hydrogen side and 34.15 percent on the oxygen side.

Cell 236 was another eradiated polyethylene membrane cell deuplicating test 231. The cell ran 47 cycles and showed poor performance.

Cell 238 consisted of an American Cyanamid oxygen electrode and an EOS hydrogen electrode, with a sandwich matrix consisting of a microporous polyethylene membrane and two layers of KT with 10 percent asbestos. The cell contained 20 grams of electrolyte per KT layer and a 0.05-inch spacer. The cell ran seven cycles, then failed because of gas leakage through the matrix. Because of the poor results obtained with polyethylene membranes, it was decided to discontinue testing this type of membrane.

Cell 232 consisted of the same type of electrode with a sandwich matrix consisting of an eradiated Teflon membrane and two layers

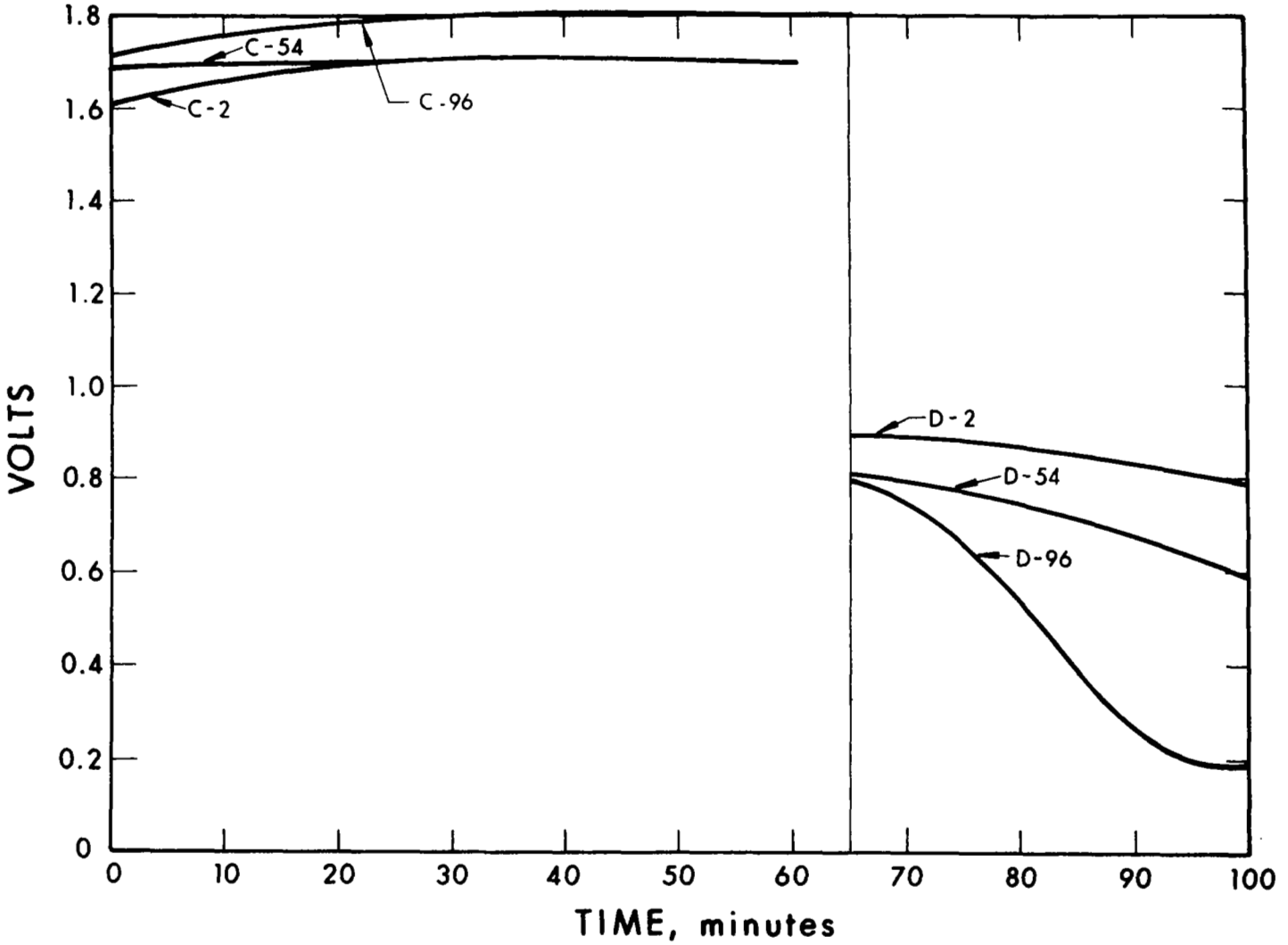

Figure 64. Cycling Performance of Cell 231

of KT with 10 percent asbestos. This cell contained 20 grams of electrolyte per KT layer and had a 0.05-inch spacer. The initial cell impedance at 80°C was 0.016 ohm which is high, the normal being about 0.008 ohm. Performance was poor, and the test was discontinued after three cycles.

Cell 233 was a duplication of cell 232 above. The cell ran poorly for 22 cycles. Results are shown in Fig. 65. Because of the poor results, testing was discontinued with the irradiated Teflon membrane.

A membrane was made by pasting a mixture of 50 percent Teflon and 50 percent KT on a 10 mil thick 100 mesh nickel screen. This membrane was sandwiched between two 13.5-gram KT and asbestos layers, wet down with 20 grams of KOH on each layer, and assembled in cell 237. This cell had the usual Cyanamid/EOS electrode configuration and a 0.050-inch separator. The cell ran well for 29 cycles but was discontinued because of high differential pressures caused by a volume imbalance. This test indicated that a pasted KT-Teflon membrane might be acceptable. Test results are shown in Fig. 66.

Cell 239 consisted of the usual American Cyanamid and EOS electrodes and a 0.06-inch spacer. The membrane was made by pasting a 50 percent KT and 50 percent Teflon mixture on a 0.010-inch thick fine mesh Teflon screen. The membrane was sandwiched between two KT asbestos layers. Twenty grams of electrolyte was put in each layer. The cell ran for 2079 cycles and the test was discontinued. Cell performance is shown in Fig. 67. As can be seen, after 1000 cycles, there was a noticeable performance degradation; however, this data represents a significant improvement in cycle life. Upon disassembly, the KOH concentration was found to be 22.55%.

Cell 246 was a duplication of cell 239 above. The cell ran well for 151 cycles and then the performance degraded. Testing was concluded

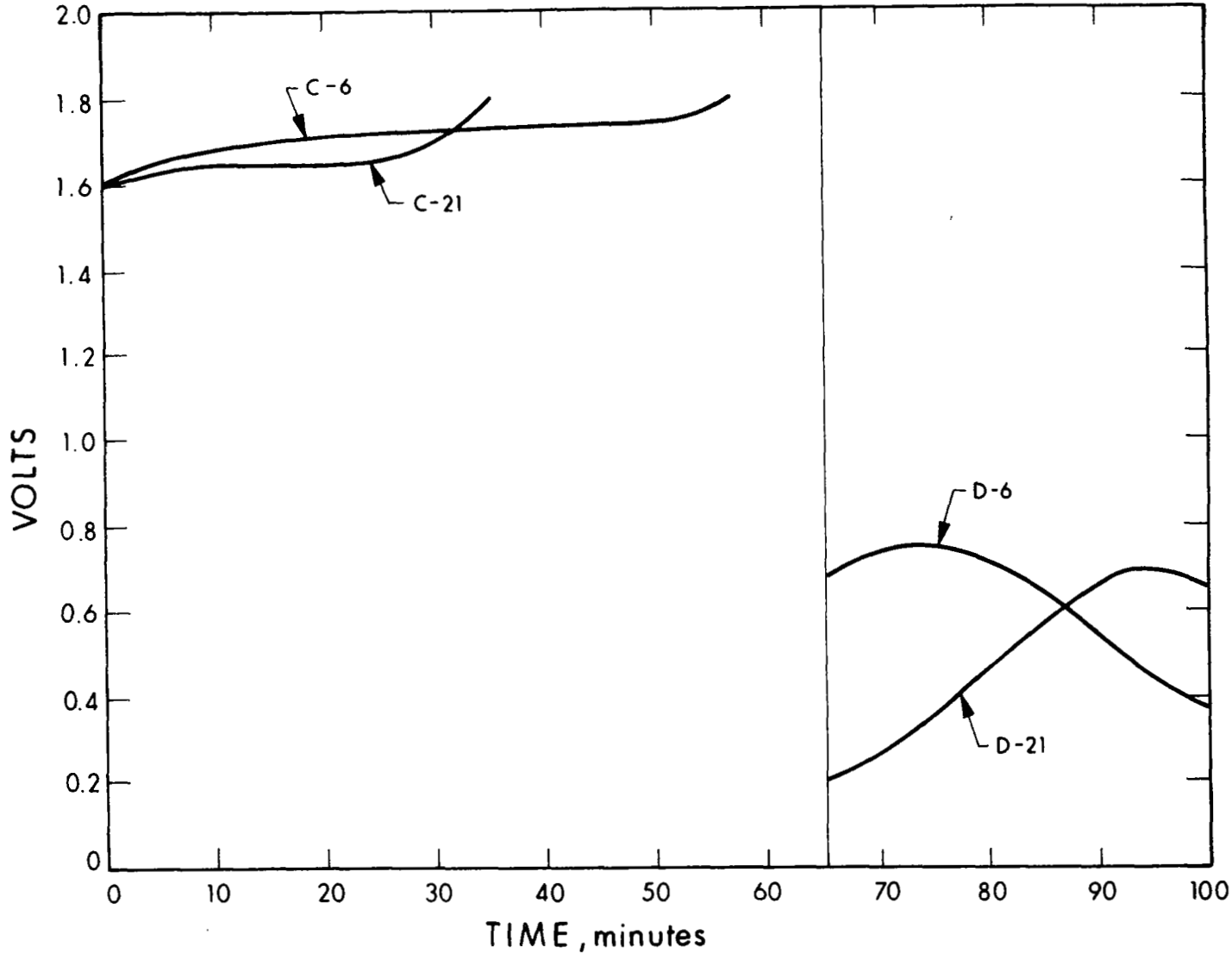

Figure 65. Cycling Performance of Cell 233

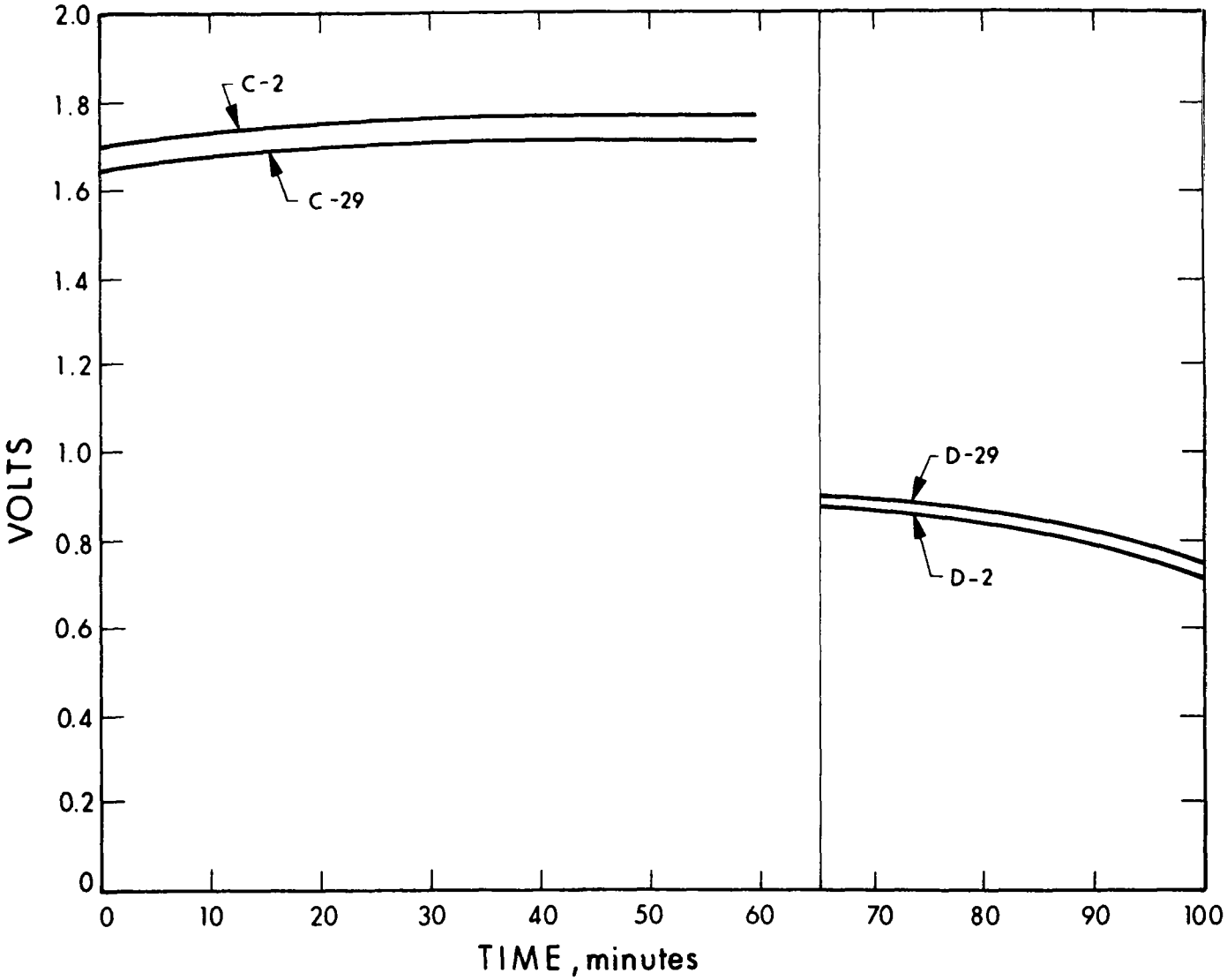

Figure 66. Cycling Performance of Cell 237

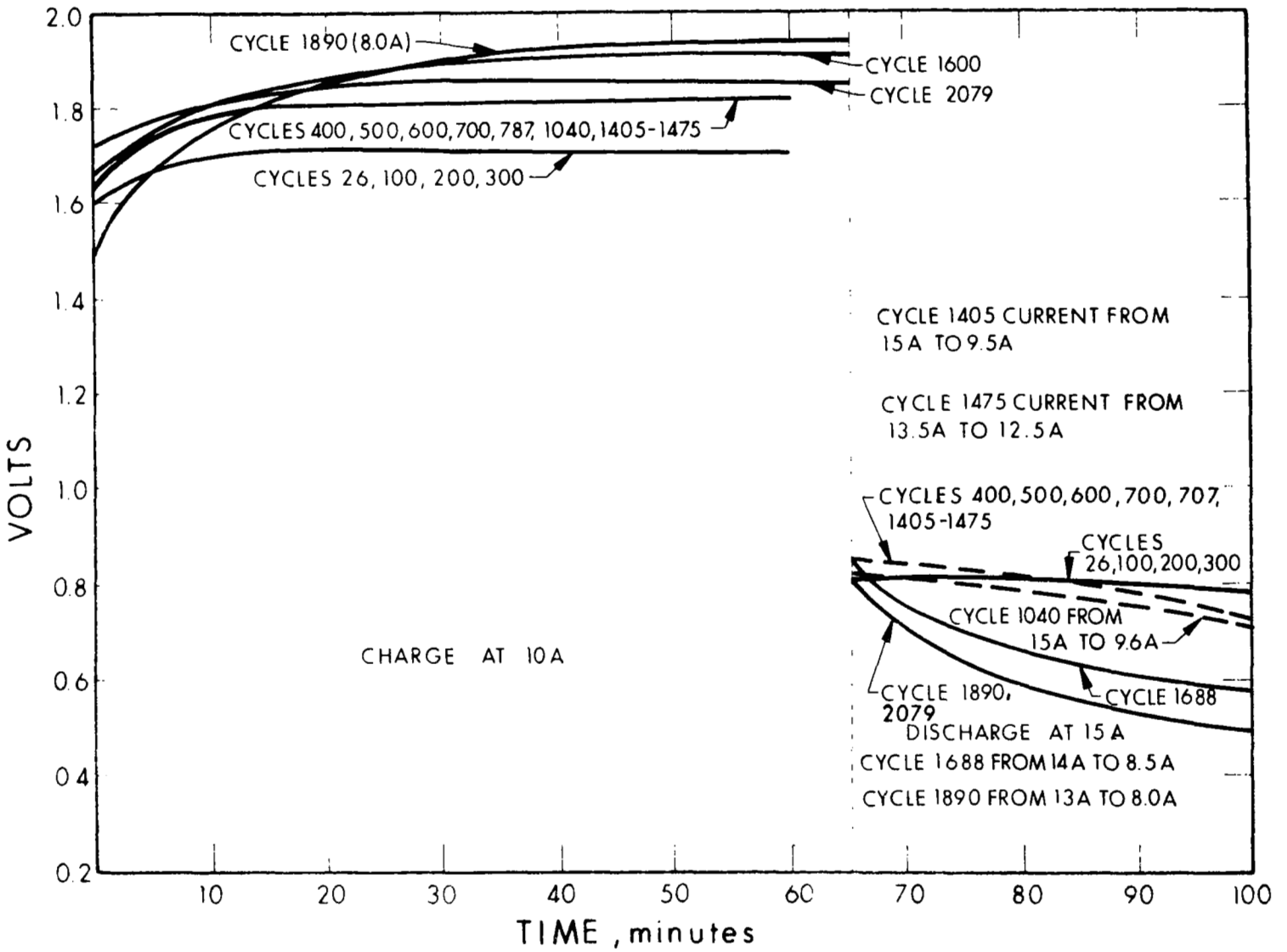

Figure 67. Cycling Performance of Cell 239

after 257 cycles. After disassembly the KOH analysis results were 32.35% on the oxygen side and 31.9% on the hydrogen side. Cell performance is shown in Fig. 68. No explanation could be given for the differences in results of this cell and those of 239.

Cell 249 consisted of two new electrodes and a 60-mil spacer. The 50-percent KT/50-percent Teflon pasted membrane was treated in 40 percent KOH at 130°C for half an hour. A matrix was made by sandwiching this membrane between two mats of 90-percent KT/10-percent asbestos. This cell performed well for 163 cycles and then was damaged from overcharging caused by a faulty transducer. After disassembly, KOH analysis showed 31 percent on the Oxygen side of the membrane and 29.5 percent on the hydrogen side. Cell performance is shown in Fig. 69.

Cell 252 was a duplication of cell 239. The cell ran 567 cycles and the test was discontinued because of cell degradation. As shown in Fig. 70 the performance degraded rapidly from cycle 500 to 567. The initial cell impedance was 0.005 ohm. At cycle 514 the impedance had increased to 0.035 ohm and at the end of the test it had increased to 0.040 ohm. This value is high enough to account for the loss in performance, since 0.6V is the IR loss for a 10 amp load. The exact cause of the IR increase was not determined, but the backup screen of the oxygen electrode was badly oxidized, which may have caused the problem.

Cell 254 differed from cell 239 in that all the components of the cell were treated in hot KOH. The electrodes were treated for one hour at 130°C in 40% KOH then washed free of KOH with distilled water. The 50% KT/50% Teflon pasted membrane was treated one-half hour at 130°C in 40% KOH. The KT in the 90% KT/10% asbestos mats were treated one hour in 100-130°C in 40% KOH and washed to a pH of 6 with distilled water. The asbestos was prepared in the usual manner using both an

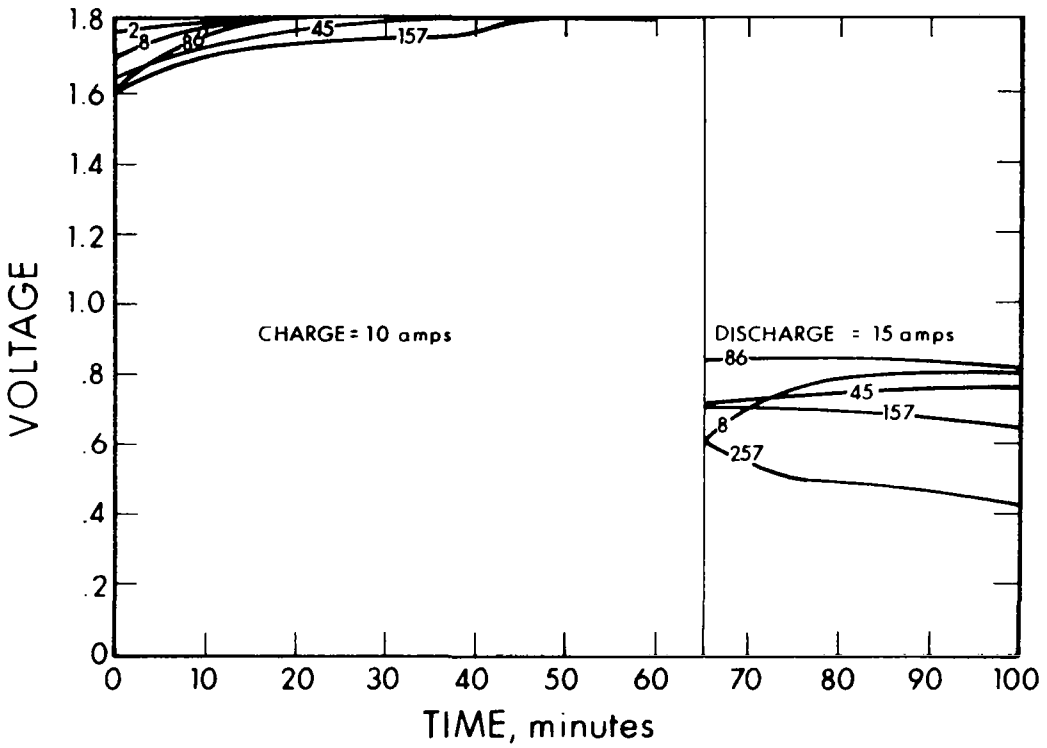

Figure 68. Cycling Performance of Cell 246

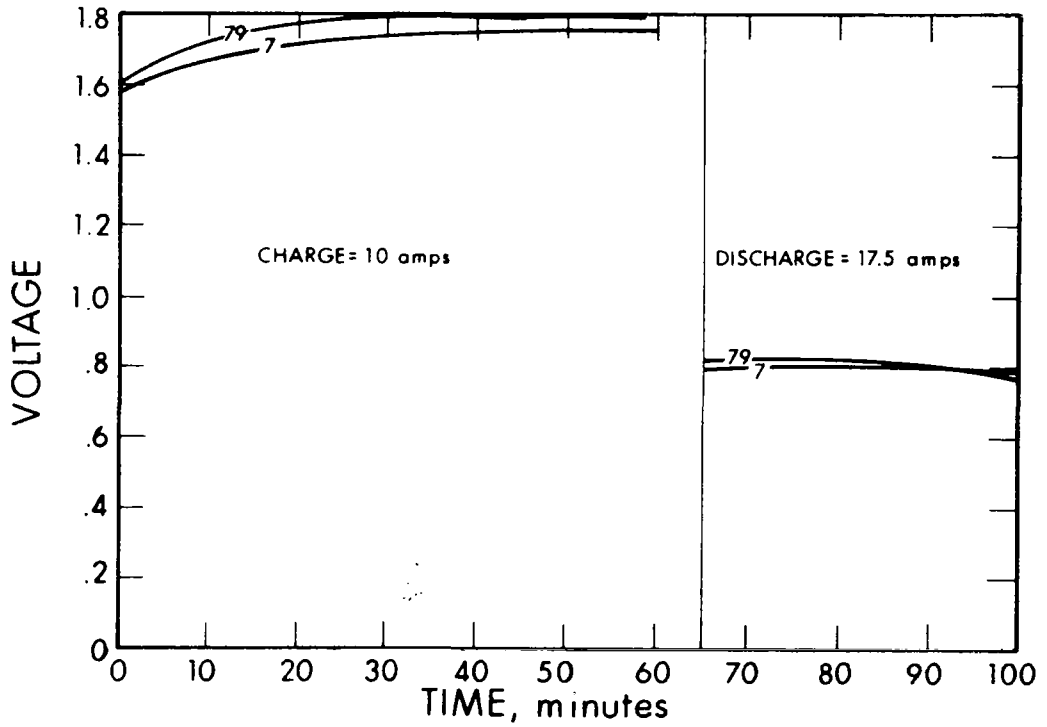

Figure 69. Cycling Performance of Cell 249

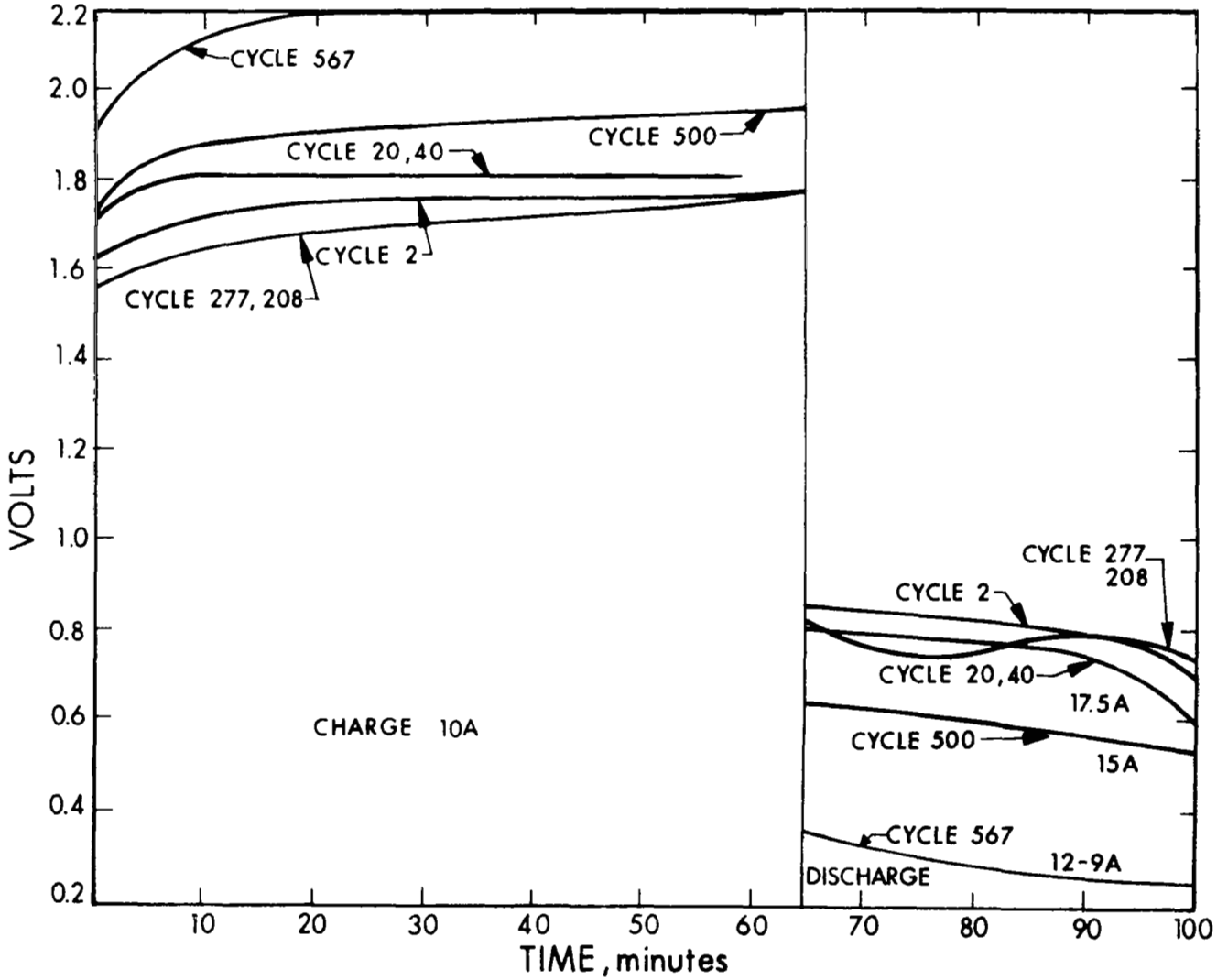

Figure 70. Cycling Performance of Cell 252

acid and a base wash at room temperature. The assembled cell contained 40 grams of 40% KOH and had a 60-mil spacer. Figure 71 shows that after 328 cycles the discharge performance stablized between 0.75 and 0.65 volt. The test was discontinued after 947 cycles since adequate information was obtained from this cell. The final KOH concentration was 31.0%.

Cell 251 consisted of used American Cyanamid and EOS electrodes and a 60-mil spacer. A 50-50 pasted membrane of Teflon and KT was treated in 40% KOH at 130°C for one-half hour. The membrane was sandwiched between two mats composed of 95% KT and 5% polyproplylene. The cell ran 593 cycles before the test was discontinued. Cell performance is shown in Fig. 72. As can be seen, there was no degradation until the 400-cycle point was approached. The operating voltage level of this cell was somewhat lower than that of other cells with asbestos/KT mats. Upon disassembly, it was found that more KOH than usual was consumed. The final KOH analysis showed 26.45% on the oxygen side and 20.7% on the hydrogen side.

Cell 256 was a duplication of cell 251; the KT in the mats of both cells were washed free of soluble chlorides and sulphates with distilled water. The polypropylene fiber was untreated. This was another EOS fuel cell without asbestos. The cell ran 443 cycles and then the test was discontinued because of performance degradation. As can be seen in Fig. 73, a sharp voltage rise occurred at the end of charge on cycle 393, the subsequent cycles demonstrated a steady degradation in performance. This phenomenon cannot be clearly traced nor explained because the data scanner was out for maintenance. A KOH analysis showed a final concentration of 31.35%.

Cell 258 consisted of the American Cyanamid and EOS electrodes and a 50% KT/50% Teflon membrane sandwiched between 100% KT mats. This was the first attempt to eliminate binders in the KT mats. The

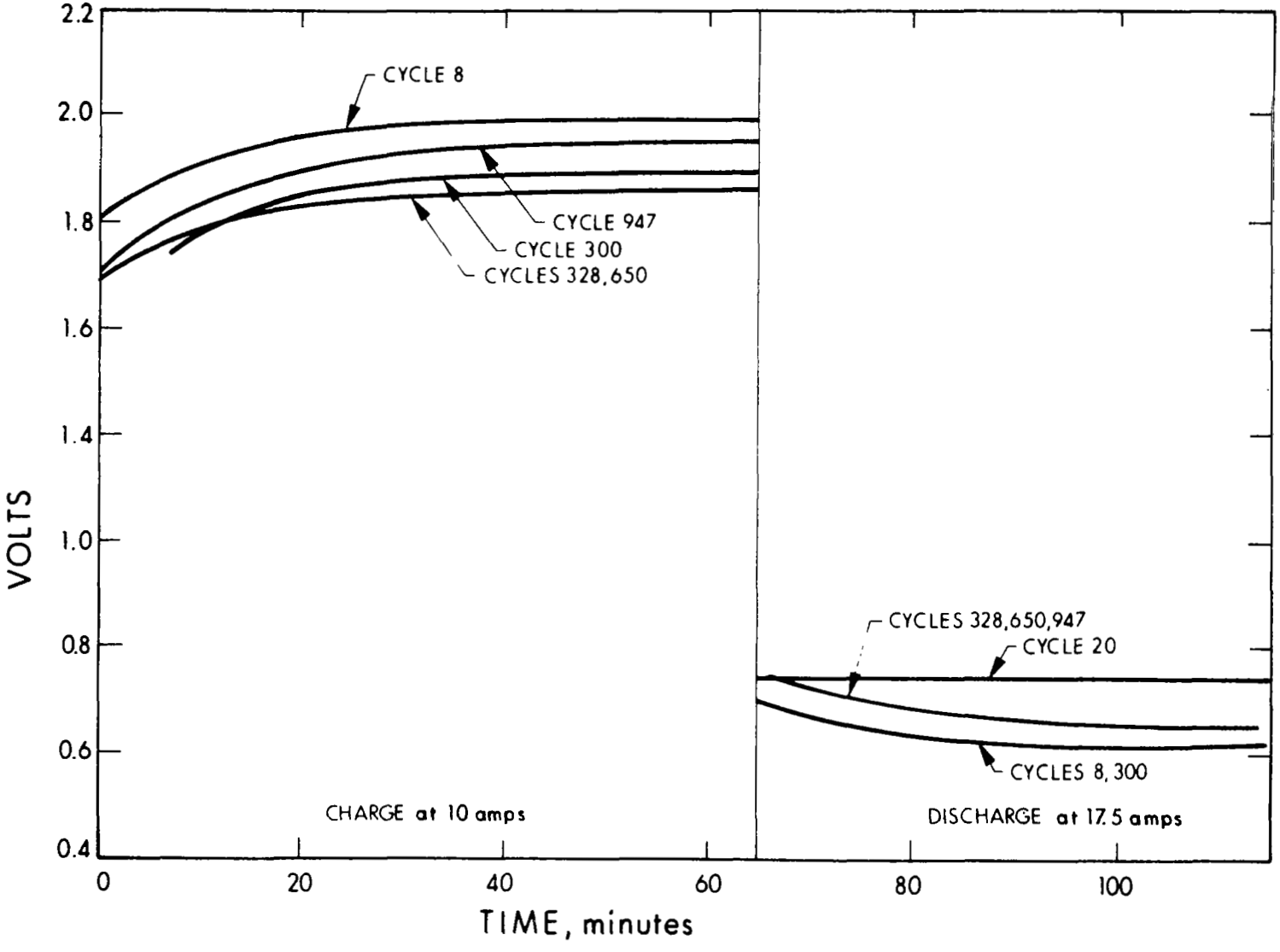

Figure 71. Cycling Performance of Cell 254

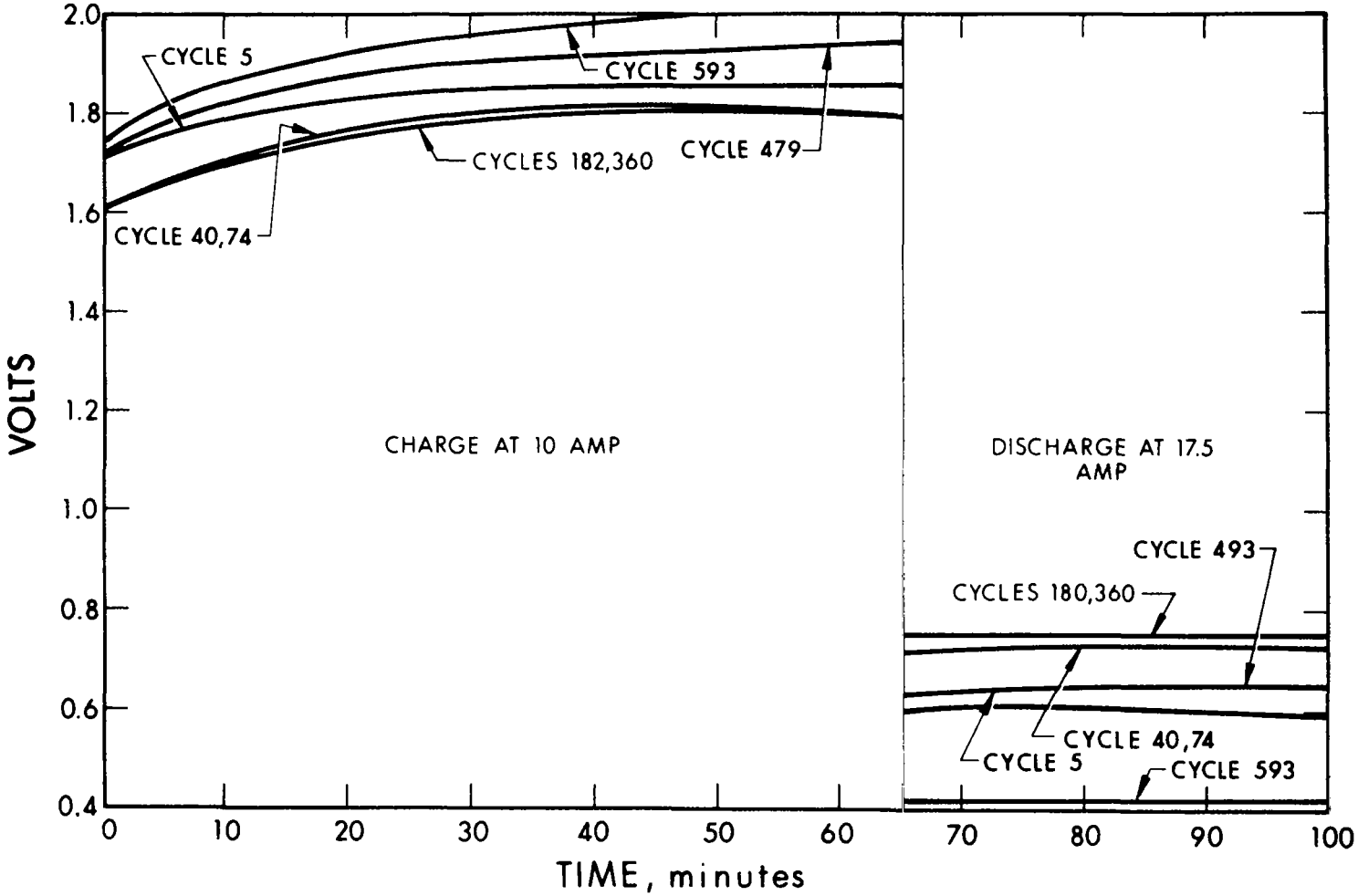

Figure 72. Cycling Performance of Cell 251

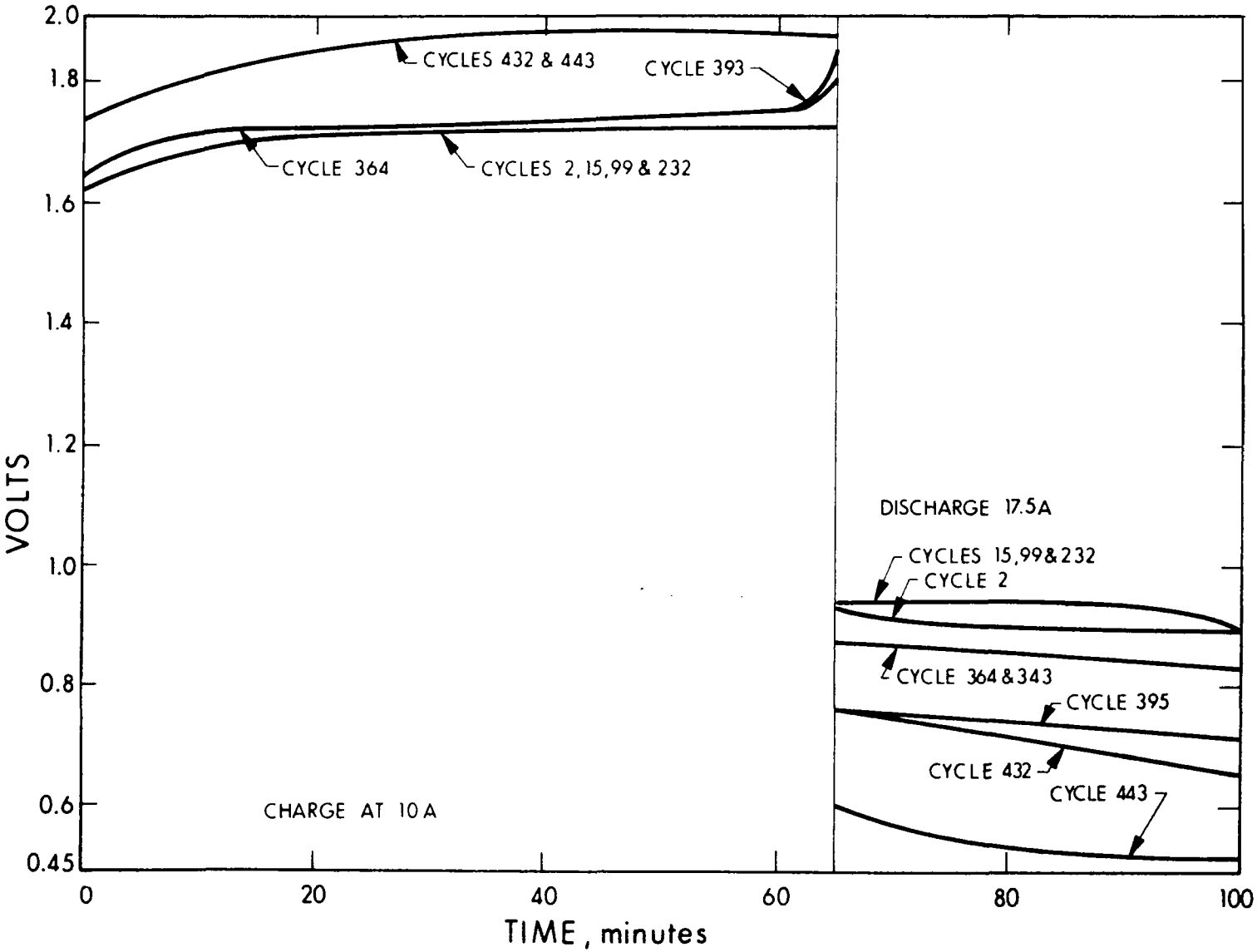

Figure 73. Cycling Performance of Cell 256

matrix contained 60 grams of 40% KOH and 60-mil spacer was used. The cell ran for 13 cycles and then failed. Failure was due to a recombination of gases leaking through the matrix.

Cell 259 was a duplication of cell 258. This cell consisted of the American Cyanamid and EOS electrodes and a 50% KT/50% Teflon membrane sandwiched between 100% KT mats. The matrix contained 40 grams of 40.2% KOH and 60-mil spacer was used. The cell ran for 36 cycles before failing. Failure was due to a recombination of gases leaking through the matrix. Apparently the pure KT mats developed leaks due to structural weaknesses.

Cell 289 was one of the last single cells built and tested on this program. It contained a matrix made by sandwiching a 50% KT/50% Teflon pasted membrane between two 90% KT/10% asbestos mats. The total weight of the matrix was 28.4 grams, and 45.5 grams of KOH was used. At 0.060-in spacer and the usual EOS/Cyanamid electrodes were used. This cell was similar to cell 276, below. From a comparison of data from long running cells the weight of matrix material and KOH loading were chosen as optimum for the given spacing and cell configuration. The cell ran for 968 cycles before testing was discontinued. As can be seen in Fig. 74 the discharge voltage remained fairly steady.

A new type of matrix was developed by rolling KT and Teflon together. This structure is referred to as a rolled matrix or membrane, depending on its use. Section 4.9 on fabrication and lab testing, is referred to for details. Using the techniques mentioned above a 0.075-inch-thick matrix was fabricated and installed in cell 262 with 51.5 grams of 39.7% KOH. A 60-mil spacer and the usual American Cyanamid/EOS electrode configuration was used. The cell was cycled while it was heating up to 80°C. It ran a total of 3 cycles and then failed because of severe gas leakage across the matrix.

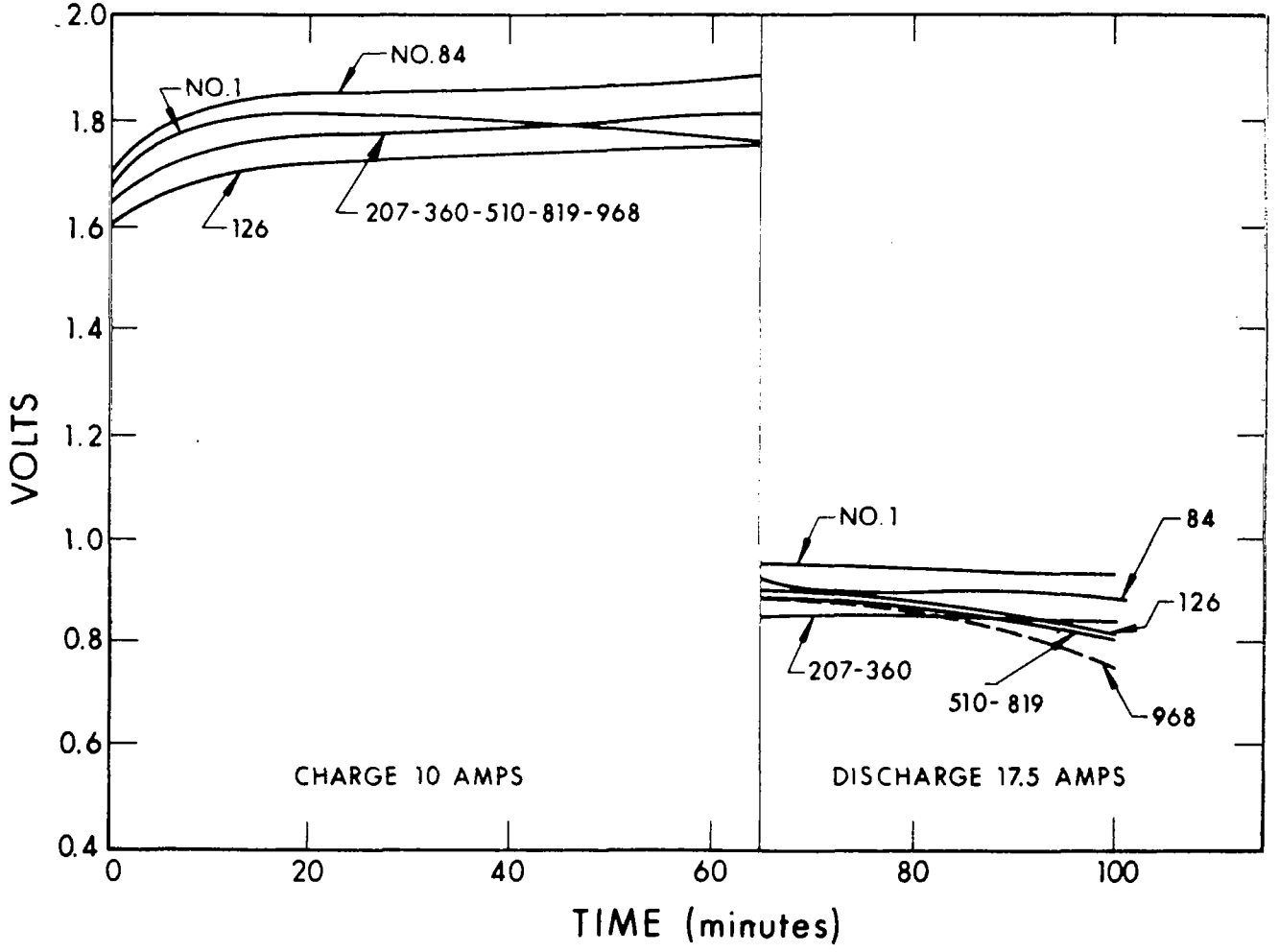

Figure 74. Cycling Performance of Cell 289

Cell 264 was a duplication of cell 262 above. It also failed because of severe cross gas leakage during the first cycle. The leakage was probably caused by Teflon flow after the matrix was heated up to 80°C. Both the bubble-through tests and preliminary differential testing of the cell at 23 to 27°C indicated that the structure was stable at room temperature.

A 35-mil KT and Teflon composite rolled membrane was fabricated using the same techniques used in cells 262 and 264 and then sandwiched between two 35-mil KT-asbestos mats. This matrix contained 65 grams of 39.7 percent KOH and was installed with a 60-mil spacer in cell 266. The cell contained the usual EOS/American Cyanamid electrodes. The cell ran for 745 cycles and the test was discontinued. As can be seen in Fig. 75, the performance was good, above 0.7 volt on discharge, for over 600 cycles and the degradation was slow. After cycle 660 the degradation in performance was more obvious. Testing was discontinued after 745 cycles. Upon disassembly it was observed that part of the KT-Teflon composite membrane had lost its latex property and appeared to have become a hard, densely packed particle structure like a porous brick. A KOH analysis showed a final concentration of 35 percent KOH. The degradation in performance may have been caused by the asbestos present in the mats. The electrolyte consumption was too small to affect performance. Dissolved asbestos in the catalyst reaction sites might have been a factor. This cell, however, did not contain an optimum electrolyte matrix spacing arrangement and the performance may have been affected by a gradual displacement of electrolyte.

A 0.075-inch thick matrix was made by forming a rolled KT-Teflon composite on both sides of a 35 mesh Teflon screen. This matrix was used in cell 268 with a 0.060 spacer. The matrix contained 37.7 grams of 40% KOH. The usual EOS/American Cyanamid electrode configuration was used. After 55 cycles the performance fell off.

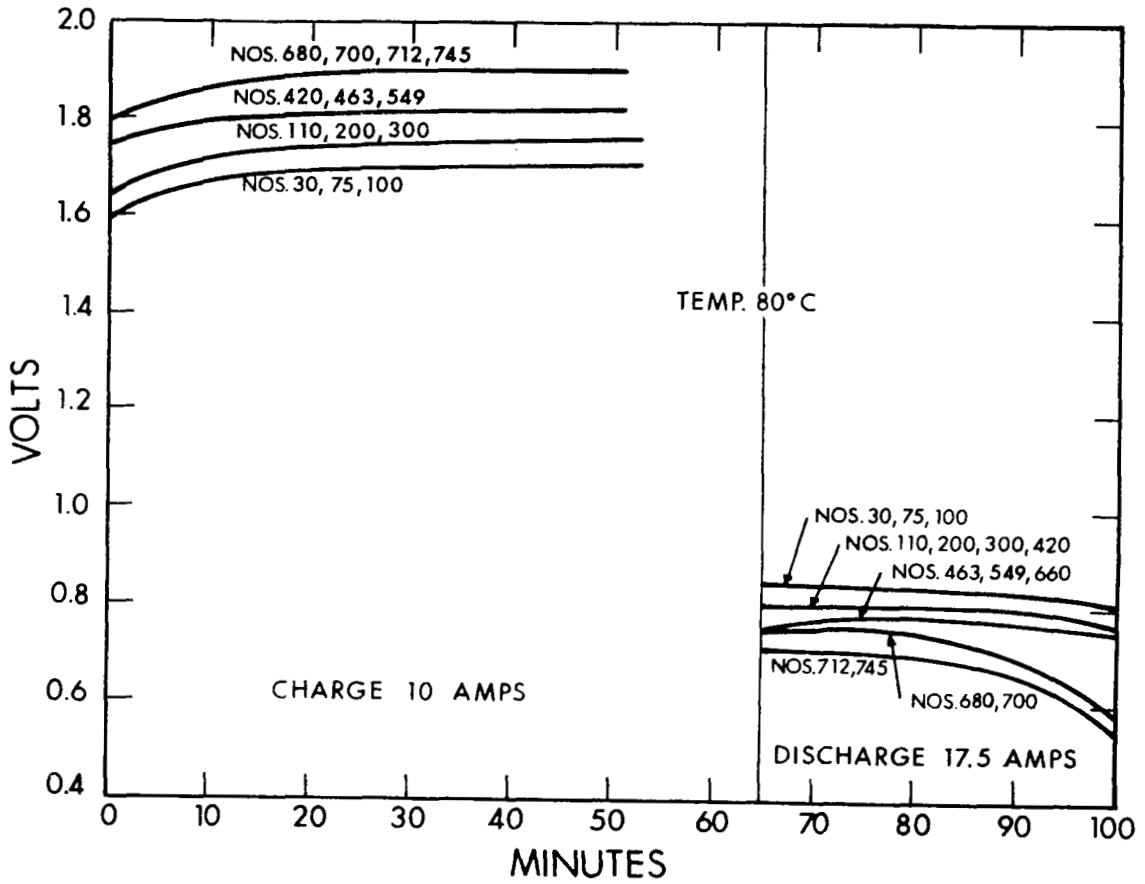

Figure 75. Cycling Performance of Cell 266

It was found that the gases had leaked through the matrix and had recombined.

A matrix was made by forming a rolled 0.030 KT-Teflon composite on each side of the membrane (50 percent KT, 50 percent Teflon pasted on 100 mesh screen). The matrix was assembled in cell 269 with a 0.060 spacer and 56.1 grams of 40 percent KOH. Both electrodes were used in a previous cell. The cell ran 676 cycles and the test was discontinued. As can be seen in Fig. 76, there was little performance degradation in the first 300 cycles. Subsequent performances, however, fell off more rapidly. Upon disassembly the final KOH concentration was found to be 35%. The performance drop could not have been caused by KOH consumption. No asbestos was used in this cell, so one variable had been eliminated. The remaining factors could have been platinum migration and/or presence of other impurities in both the KT and Teflon, or flooding of the electrodes because of improper spacing and electrolyte balance.

Cells 278, 279, and 281 were attempts to duplicate cell 269. The matrix allowed cross gas leakage to occur. Bubble-through testing showed that the formulated batch used to make these matrixes was defective.

The matrix configuration of cell 276 was similar to that of cell 266. A 0.040 in KT and Teflon composite rolled membrane was fabricated and then sandwiched between two 0.020 in KT-asbestos mats. This matrix contained 45.1 grams of 40.3 percent KOH and was installed with a 60-mil spacer. The cell contained the usual EOS/American Cyanamid electrodes. This cell ran over 875 cycles with little performance degradation. As can be seen in Fig. 77, the discharge performance dropped to a new level after 1000 cycles. The cell was accidently discharged at a high rate after 1050 cycles. The cell pressure walked

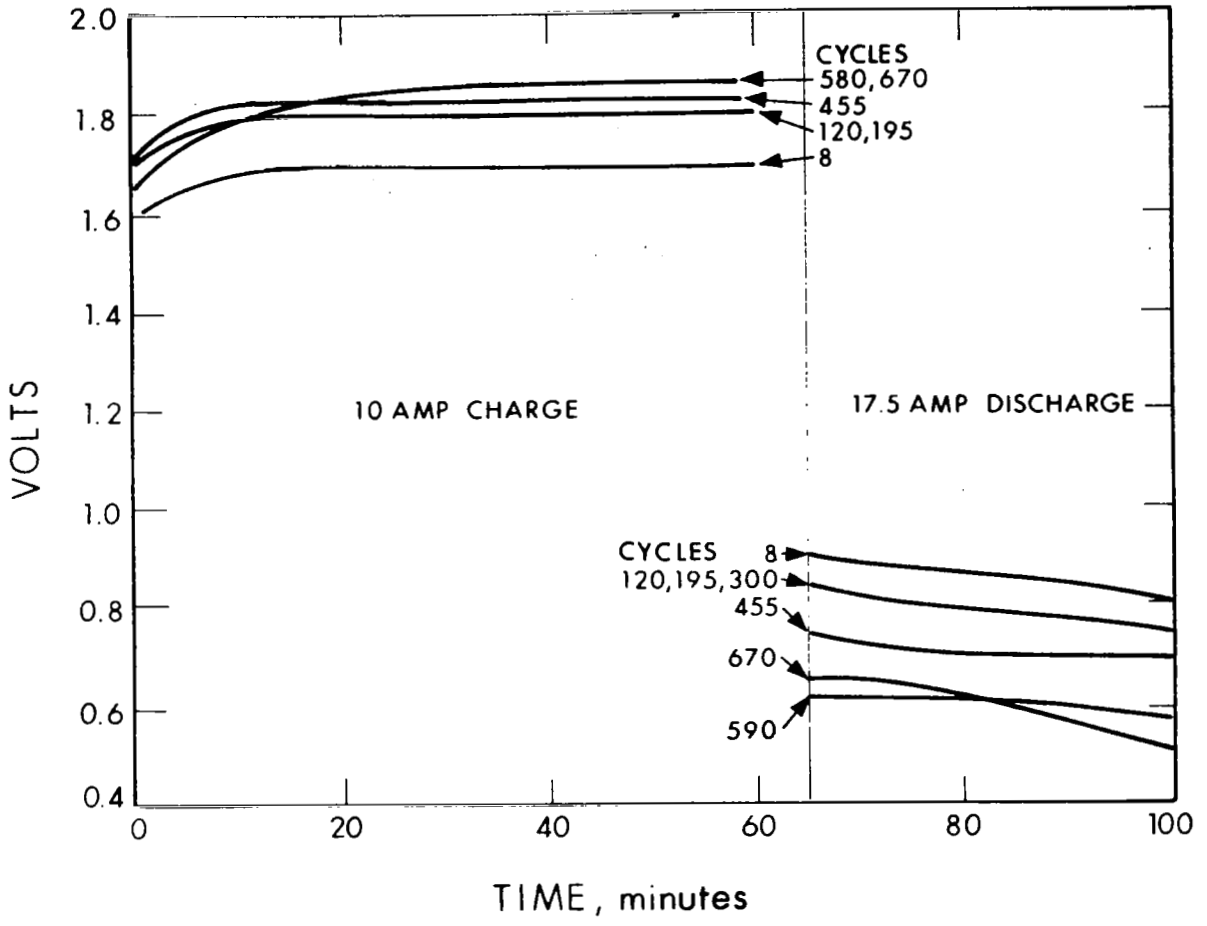

Figure 76. Cycling Performance of Cell 269

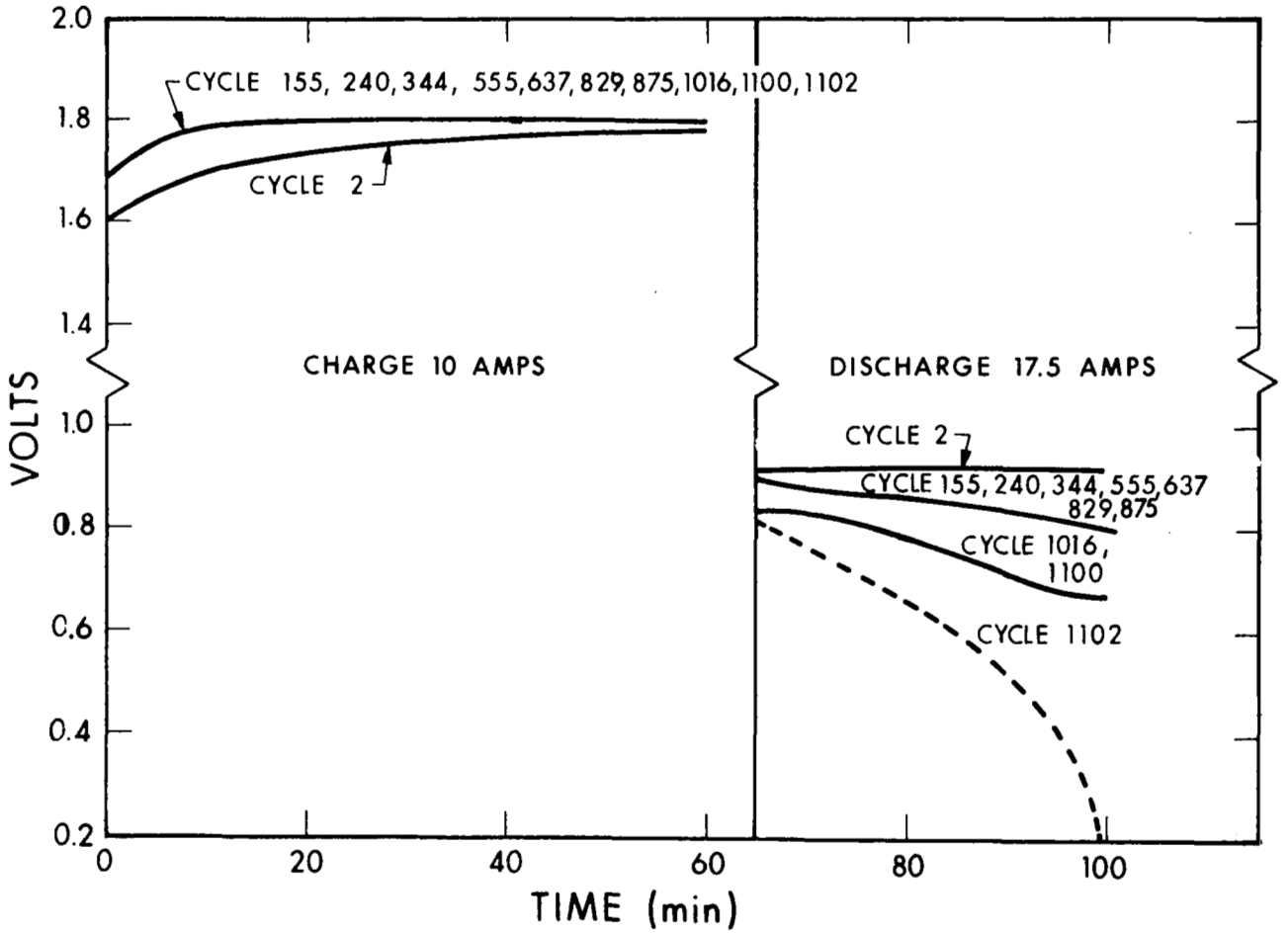

Figure 77. Cycling Performance of Cell 276

down to zero where the nickel-cadmium battery (in series) reverse-charged cell 276, causing the cell to quit functioning after cycle 1102. It can be seen in Fig. 75 that cell 266 demonstrated a poorer initial performance than cell 276 and that it exhibited a steady degradation in performance. The same KT, asbestos, and Teflon materials were used in the two cells. The difference between the two cells lay in the total mass of matrix and electrolyte. The membrane in cell 266 weighed 11.4 grams and the mats weighed 27.1 grams. The total dry weight of the matrix was 38.5 grams, and 65.0 grams of electrolyte gave a ratio of 1.69 grams KOH/gram matrix. Less matrix material was used in cell 276; the membrane weighed 8.2 grams and the mats 19.4 grams, giving a total of 27.6 grams of dry material. The electrolyte to matrix ratio was 1.635 grams KOH/gram matrix. With the larger matrix and greater amount of KOH in Cell 266 the active areas of the electrodes might have been slowly filled up with electrolyte as the cell cycled.

Another variety of KT, Teflon, and asbestos composite matrix was fabricated by pressing the material together. For details see Section 4.9 The cell matrix was composed of a pressed composite matrix fabricated from KT, asbestos, and Teflon, 0.060 inch thick, and weighing 24.8 grams. It was assembled in cell 274 with 47.0 grams of 40.3 percent KOH electrolyte and a 0.050-inch spacer. The EOS and Cyanamid electrodes had been used in previous cells. The cell ran 1120 cycles and was removed from test. Figure 78 shows that the performance was most excellent, 0.9 volt and above for the first 400 cycles. The performance may have been helped by the closer spacing, 0.050 inch. The subsequent performance degraded to below 0.8 volt. The latter cycles demonstrated a steady degradation of performance. The performance degradation may have been due to unfavorable water balance caused by the matrix-electrolyte-spacer configuration, or the electrodes may have been affected by cycling. An attempt was made to save the electrodes for further testing but pieces of the oxygen electrode stuck to the matrix.

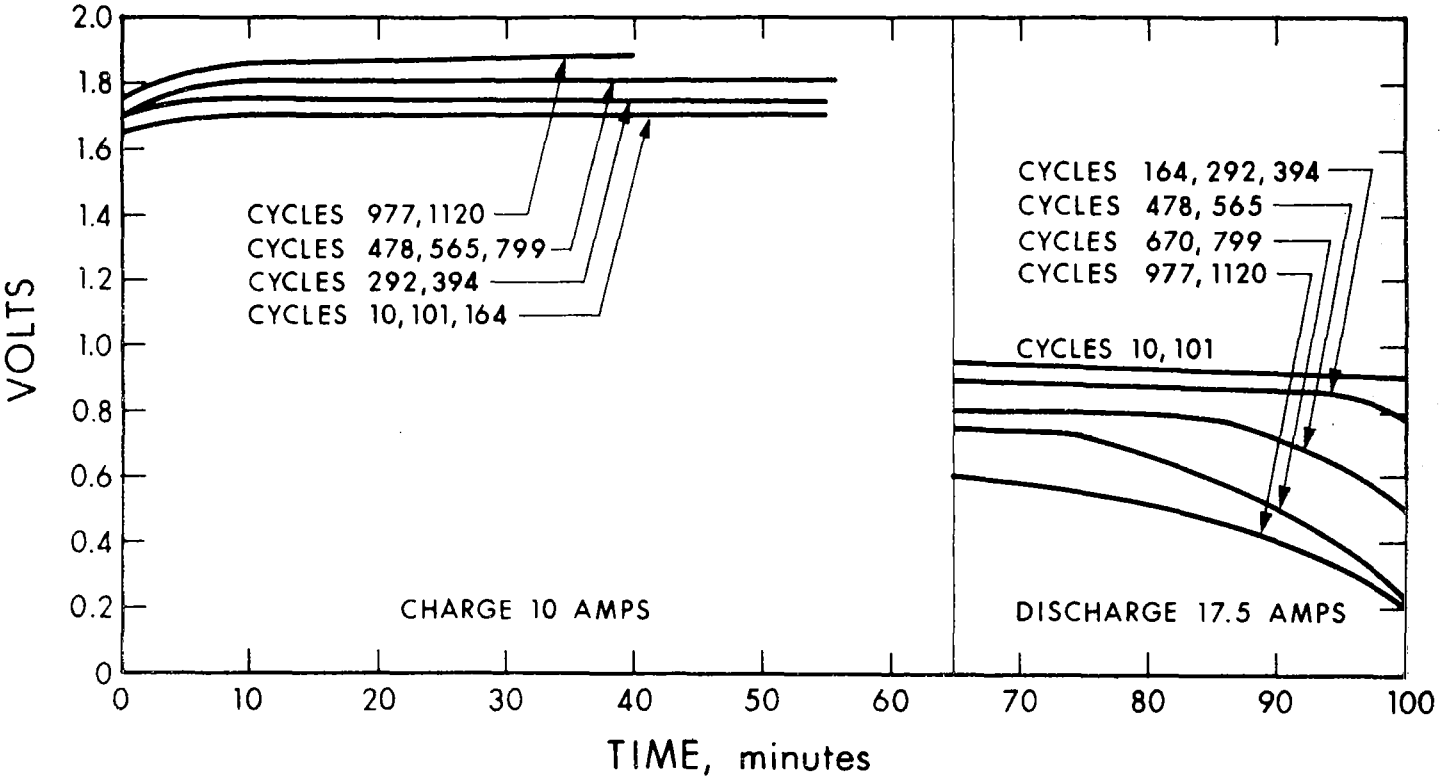

Figure 78. Cycling Performance of Cell 274

Cell 282 was similar to cell 274, aforementioned. The matrix was a pressed composite of KT, Teflon, and asbestos weighing 27.1 grams and containing 44 grams of KOH. The electrodes were the usual EOS/American Cyanamid configuration. The cell ran 488 cycles and testing was discontinued because of performance degradation. Figure 79 shows that the performance during the first 190 cycles was good (0.96 to 0.8 volt) as was the initial 400 cycles of cell 274. As can be seen a steady degradation of performance occurred and flooding effects became more noticeable as cycle life increased. The cell had a heavier matrix and more electrolyte than did cell 274. The cell performance fell off sooner than did cell 274. If the electrode reaction sites were being flooded, as had been hypothesized, the difference in performance of these two cells might be explained.

Cells 286 and 287 were both assembled with 31.8 grams pressed KT, asbestos, and Teflon composite mats wet with 40 grams of KOH. Both cells had new EOS/Cyanamid electrodes and a 0.060-inch spacer. Both cells showed signs of being too dry, i.e., high charge voltages at upper pressure levels. Gases of about 200 psig were added to each cell. This was equivalent to approximately 1.65 grams of water. Both cells appeared to function better with the gas addition. Cell 286 ran 50 cycles and cross gas leakage resulted in termination of the test. Cell 287 ran 24 cycles and then began self-discharging.

Cells 288 and 290 both contained pressed KT, asbestos, and Teflon mats, weighing 27.3 grams and contain 45.0 grams of KOH. A 0.060-inch spacer and the usual EOS/Cyanamid electrodes were used. These cells also had a configuration similar to cell 276. Cell 288 ran 853 cycles and the test was discontinued. Figure 80 shows the performance of this cell. Performance of cell 290 was good for 30 cycles; then cross gas leakage occurred and the test was discontinued.

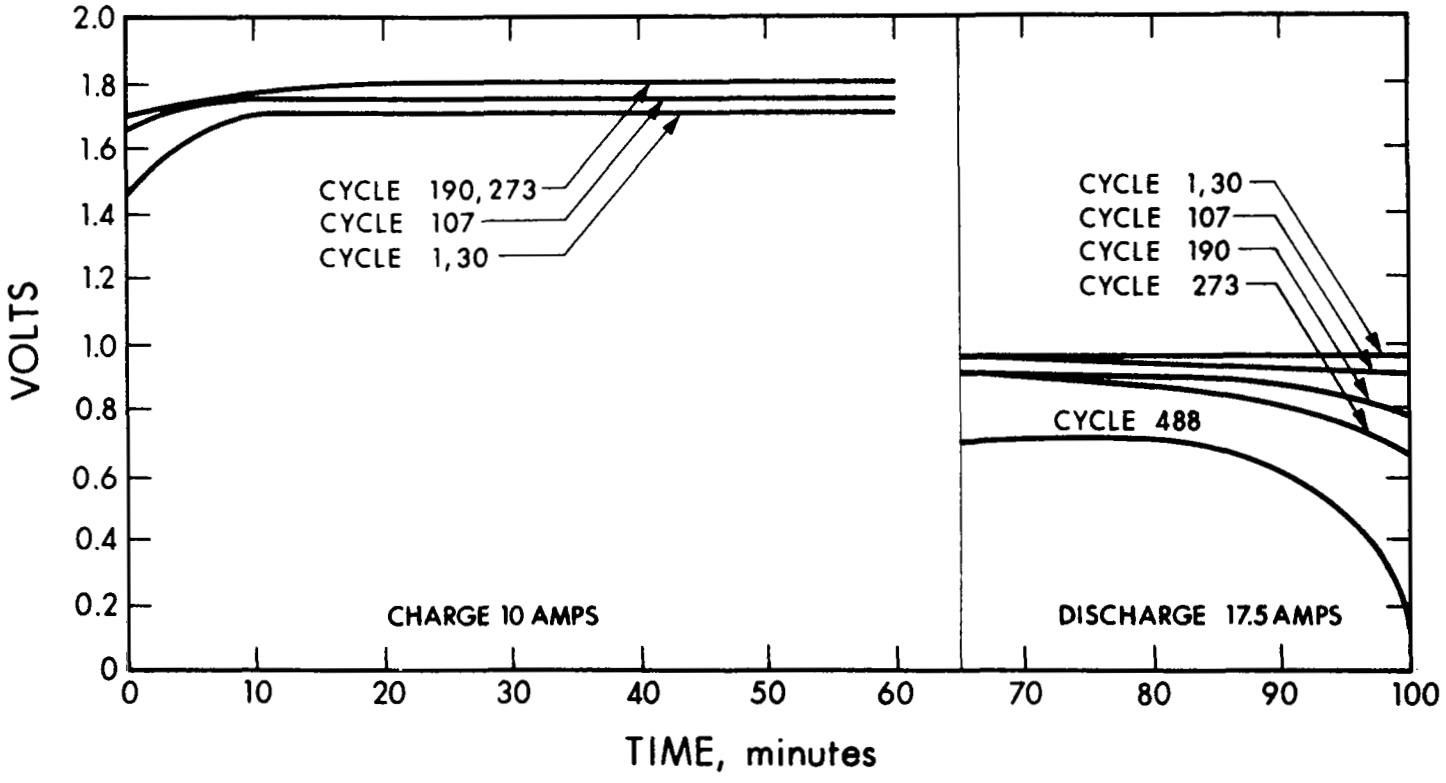

Figure 79. Cycling Performance of Cell 282

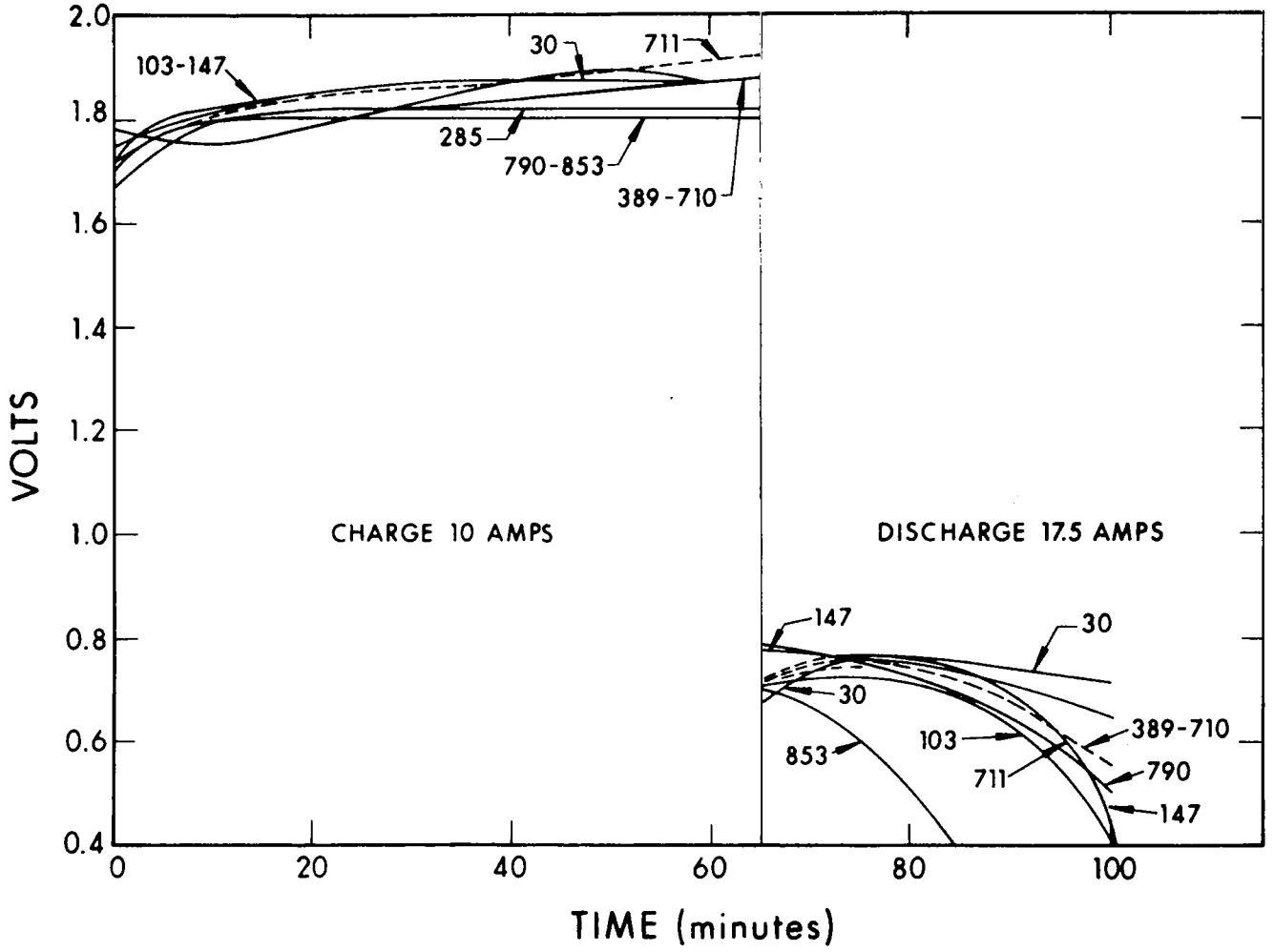

Figure 80. Cycling Performance of Cell 288

Pressed matrixes containing polypropylene were successfully laboratory tested. This type of matrix was tried in the following cells. Cell 283 contained a pressed KT and polypropylene matrix weighing 27.1 grams. The matrix contained 44 grams of 39.5% KOH. New EOS/Cyanamid electrodes and a 0.060-inch spacer were used. Cross gas leakage occurred across the matrix after the first cycle.

Cell 285 contained a pressed KT, polyproplene, and Teflon matrix weighing 23.1 grams and was wet with 40 grams of 39.7% KOH. A 0.060-inch spacer was used. The electrodes from cell 283 were used in this cell. As with cell 283, cross gas leakage occurred on the first cycle. The spacing or total mass or electrolyte ratio may have been wrong for this type of matrix or the polypropylene may have been affected by the 80°C temperature. It was concluded that more investigation of this type of matrix was required.

Matrixes utilizing zirconium oxide and cerium oxide materials were cycle tested in this program. These tests are described below.

Cell 263 consisted of the usual American Cyanamid and EOS electrodes, both new, and a 60-mil spacer. A 50% KT-50% Teflon pasted membrane was made from KT treated in KOH at 100°C for one hour and then washed. The membrane was sandwiched between two mats composed of 80% KT and 20% zirconium oxide (ZrO). This cell contained no asbestos. The cell ran 439 cycles and the test was discontinued because of degradation in performance. Cell performance is shown in Fig. 81. As can be seen, the degradation began around cycle 307. On cycles 1 to 25 the cell was discharged at 17.5 amp and the temperature was 80°C. The cycle was then changed to 10 amp charge for 65 minutes and 25 amp discharge for 22 minutes. After 108 cycles the temperature was raised to 100°C.

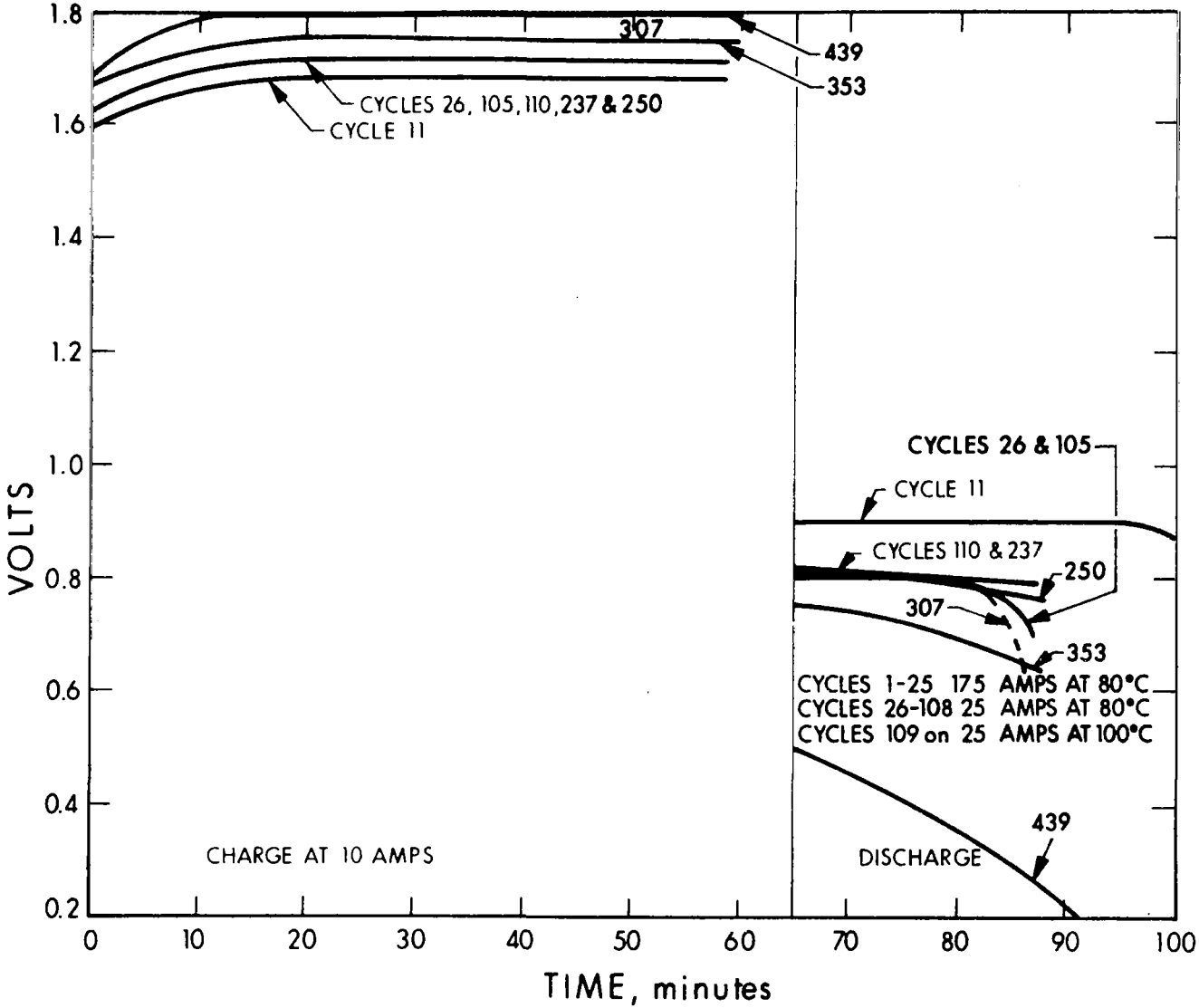

Figure 81. Cycling Performance of Cell 263

Cell 261 contained the EOS/Cyanamid electrode configuration. The matrix was assembled with a 17-mil cerium oxide (CeO) membrane supplied by American Cyanamid Co. This membrane was sandwiched between two 90% KT/10% asbestos mats and 40 grams of 40% KOH was added. The cell was cycled at 17.5 amps at 80°C on the 100 minute cycle for 36 cycles. As can be seen in Fig. 82 the performance was excellent. The cycle was then changed to 65 minutes charge at 10 amps and 24.5 minutes discharge at 25 amps. The temperature remained at 80°C. At 25 amps a lower current efficiency was observed so the discharge time was changed to 22 minutes. The temperature was left at 80°C from cycles 36 to 64, and then raised to 100°C. The performance was good until cycle 386 when it dropped off because of an internal short. Upon disassembly it was found that a fast recombination of the gases shoved a piece of the hydrogen electrode through the matrix. A KOH analysis showed the final concentration to be 33.7%.

It has been shown that cycle life of the fuel cell can be limited by the properties of the matrix material. The asbestos matrixes reacted with the KOH electrolyte. As the cell life progressed, the KOH would be consumed, the matrix weakened, and the electrodes contaminated with the reaction products. In the search for inert fibrous materials, potassium titanate, zirconium oxide and cerium oxide were investigated. All these materials appear to be compatible with aqueous KOH. Due to the lower specific gravity and high degree of chemical resistance to KOH, potassium titanate was chosen for matrix fabrication. Through the use of potassium titanate, the single cell life tests have increased from 100 cycles with asbestos to over 2000 cycles using potassium titanate matrixes. This represents over 120,000 hours of continuous fuel cell operation at high charge-discharge rates.

Potassium titanate is available in a fine pigment and must be fabricated into a useful structure to be used in the fuel cell. A number of alternate structures employing potassium titanate as the primary constituent have been developed.

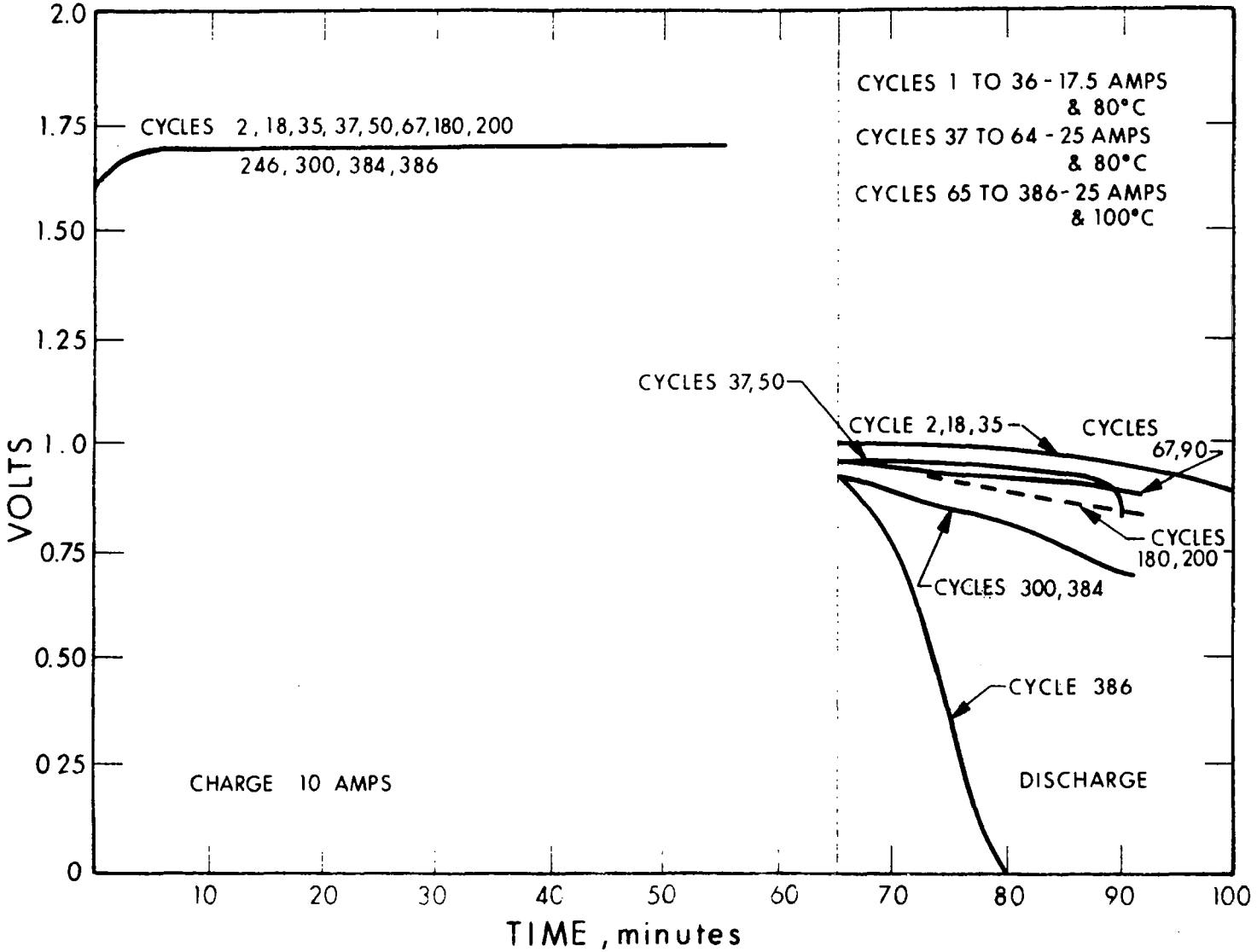

Figure 82. Cycling Performance of Cell 261

The most promising structures thus far evaluated are: (1) a three-component mix of Teflon, asbestos, and potassium titanate; (2) a three-component mix of Teflon, zirconium, and KT; (3) a sandwich arrangement of two layers of KT and asbestos with a central gas barrier membrane of Teflon and KT; and (4) a Teflon-KT mix.

4.8 POTASSIUM TITANATE STUDIES

To characterize the potassium titanate material used in the EOS matrix, stability of the KT in KOH was tested and a spectrographic analysis was performed.

4.8.1 POTASSIUM TITANATE STABILITY IN MOLTEN POTASSIUM HYDROXIDE

To determine if any reaction occurs between potassium titanate and potassium hydroxide, tests were conducted as follows:

A 0.8454-gram sample of potassium titanate was mixed with 15 cm^3 of 40.15% KOH and allowed to sit for 90-1/3 hours at 80°C. The titanate was then filtered from the solution, washed, dried, and weighed and a weight loss of 1.67% was obtained. An analysis of the sample of KOH solution, after the test period, revealed the final KOH concentration to be 40%. Both of the changes observed could be considered within experimental error. It, therefore, appears that under this type of test condition, no appreciable reaction takes place. A second sample of 0.9954 gram of KT was mixed in a 30-gram solution of molten 70% KOH in a platinum crucible. The solution was maintained in a molten state for 27 hours. (No temperature measurement was made during the molten period for fear of contaminating the solution, but in order for 70% KOH to be in a molten state, the temperature must exceed 228°C.) After the 27-hour test period, the solution was diluted and the KT was filtered, washed, dried, and weighed . The final weight indicated a weight loss of 5.6%, which is considered somewhat high for experimental error.

The above recovered sample was stored again in molten 70% KOH in a platinum crucible (greater than 228°C) for 115 hours. After the test period, the solution was diluted and KT was filtered, washed, dried, and weighed. The final weight indicated a weight loss of 11% which is above what could be considered experimental error. However, this represented only a gradual rate of reaction under a very severe set of test conditions.

An additional test to further determine the corrosion reaction rate of KT with molten KOH was conducted as follows. Three samples of KT, about 1 gram each that had been water washed, dried, and fired, were placed in platinum crucibles containing 30 grams of 70% KOH in the molten state. The samples were maintained in the molten potassium hydroxide for periods of 115 hours for sample 1, 307 hours for sample 2, and 547 hours for sample 3. At the end of these periods, the samples were removed, washed free of electrolyte, and weighed to obtain weight loss. The results for the three samples were 8.25% loss, 7.5% loss, and 8% loss, respectively. The relatively constant weight loss over this period, certainly within experimental error, indicates that there is a definite reaction which apparently occurs initially and does not proceed beyond that point. There was potentially a considerable experimental error in this test since in the washing process it would have been possible to lose a certain amount of the material. However, these results, associated with the results previously obtained and described above, were extremely encouraging and indicated that KT is relatively inert in a KOH environment.

4.8.2 POTASSIUM TITANATE STABILITY IN POTASSIUM HYDROXIDE SOLUTIONS

Stability tests of KT in 30% and 45% KOH solutions at 25°, 75°, 100°C with test times of 500 and 1000 hours were done. The tests were performed on both water-washed and as-received KT. The results obtained are tabulated in Table IX. The total results indicated that there was a 3.98% average loss of the unwashed, or as-received, KT. The loss appeared to have occurred during the first 100 hours and did not increase much with time, temperature, or KOH concentration. The washed KT averaged a 3.09% loss.

TABLE IX

KT STABILITY IN KOH SOLUTIONS

SAMPLE #	1-A	2-A	3-A	4-A	5-A	6-A	7-A
Temp. (^{o}C)	75^{o}C	75^{o}C	75^{o}C	75^{o}C	75^{o}C	75^{o}C	75^{o}C
Time (hrs.)	500	500	500	1000	1000	1000	1000
Original % KOH	30.3	30.3	30.3	30.3	30.3	30.3	30.3
Final % KOH	31.1	31.4	31.8	33.3	32.0	32.5	32.0
Washed or unwashed KT	Un	Un	Un	Un	Un	Un	-
% wt. Loss	2.39%	-	4.36%	3.79%	4.18%	3.89%	
Comments	Centrifuge aids added % wt. loss not accurate	Test ruined	Lost some of sample in washing.				

TABLE IX (Cont'd)

KT STABILITY IN KOH SOLUTIONS

SAMPLE #	8-A	9-A	10-A	11-A	12-A	13-A	14-A
Temp. (^{o}C)	75^{o}C	75^{o}C	75^{o}C	75^{o}C	75^{o}C	75^{o}C	75^{o}C
Time (hrs.)	500	1000	1000	1000	500	500	500
Original % KOH	30.3	44.7	44.7	44.7	44.7	44.7	44.7
Final % KOH	32.0	46.1	46.0	45.3	45.2	45.2	45.4
Washed or Unwashed KT	-	Un	Un	Un	Un	Un	Un
% wt. loss	-	3.43%	3.67%	5.81%	3.98%	4.06%	4.05%
Comments	KOH blank			Lost some sample in washing	good sample	good sample	good sample

TABLE IX (Cont'd)

KT STABILITY IN KOH SOLUTIONS

SAMPLE #	15-A	16-A	1-B	2-B	3-B	4-B	5-B	6-B	7-B	8-B
Temp. (°C)	75°C	75°C	100°C	100°C	100°C	100°C	100°C	100°C	100°C	100°C
Time (hrs.)	1000	500	1000	1000	1000	500	500	500	500	1000
Original % KOH	44.7	44.7	30.3	30.3	30.3	30.3	30.3	30.3	30.3	30.3
Final % KOH	46.1	45.3	37.3	33.2	34.0	31.9	32.1	31.8	32.0	35.0
Washed or Unwashed KT	-	-	Un	Un	Un	Un	Un	Un	-	-
% Wt. Loss	-	-	4.16%	4.18%	4.79%	3.88%	4.59%	4.17%	-	-
Comments	KOH Blank	KOH Blank							KOH Blank	KOH Blank

TABLE IX (Cont'd)

KT STABILITY IN KOH SOLUTIONS

SAMPLE	9-B	10-B	11-B	12-B	13-B	14-B	15-B	16-B
Temp. (°C)	100°C	100°C	100°C	100°C	100°C	100°C	100°C	100°C
Time (hrs.)	500	500	500	1000	1000	1000	500	1000
Original % KOH	44.7	44.7	44.7	44.7	44.7	44.7	44.7	44.7
Final % KOH	44.7	45.2	45.5	46.5	47.7	46.9	47.4	48.1
Washed or Unwashed KT	Un	Un	Un	Un	Un	Un	-	-
% Wt. Loss	3.88%	3.87%	4.29%	3.35%	3.63%	4.76%	-	-
Comments							KOH Blank	KOH Blank

TABLE IX (Cont'd)

KT STABILITY IN KOH SOLUTION

SAMPLE #	1-C	2-C	3-C	4-C	5-C	6-C	7-C	8-C
Temp. (°C)	25°C	25°C	25°C	25°C	25°C	25°C	25°C	25°C
Time (hrs.)	1000	1000	1000	500	500	500	500	1000
Original % KOH	30 3	30.3	30.3	30.3	30.3	30.3	30.3	30.3
Final % KOH	30.3	30.5	30.6	30.6	30.5	30.5	31.1	30.9
Washed or Unwashed KT	Un	Un	Un	Un	Un	Un	-	-
% at Loss	3.56%	4.37%	3.72%	4.01%		3.78%	-	-
Comments	Very little total wt. loss.	Very little total wt. loss.	Very little total wt. loss.	Very little wt. loss in total wt.	Total loss	No total wt loss	KOH Blank little wt. loss.	KOH Blank little wt. loss.

TABLE IX (Cont'd)

KT STABILITY IN KOH SOLUTION

SAMPLE #	9-C	10-C	11-C	12-C	13-C	14-C	15-C	16-C
Temp. (°C)	25°C	25°C	25°C	25°C	25°C	25°C	25°C	25°C
Time (hrs.)	1000	1000	1000	500	500	500	500	1000
Original % KOH	44.7	44.7	44.7	44.7	44.7	44.7	44.7	44.7
Final % KOH		44.4	44.6	44.7	44.8	44.5	45.4	45.2
Washed or Unwashed KT	Un	Un	Un	Un	Un	Un	-	-
% Wt. Loss		3.74%	3.82%	7.67%	3.49%	3.47%	-	-
Comments	Sample dried out	Very little total wt. loss.	Very little total wt. loss.	No total wt. loss. Some of sample lost in washing	No total wt. loss.	No wt. loss in total wt.	KOH Blank very wt. loss.	KOH Blank

TABLE IX (Cont'd)

KT STABILITY IN KOH SOLUTION

SAMPLE #	1-D	2-D	3-D	4-D	5-D	6-D	7-D	8-D
Temp. (°C)	75°C	75°C	75°C	75°C	75°C	75°C	75°C	75°C
Time (hrs.)	500	500	1000	1000	500	500	1000	1000
Original % KOH	30.3	30.3	30.3	30.3	44.7	44.7	44.7	44.7
Final % KOH	32.0	32.2	33.5	35.2	44.9	44.9	46.5	45.3
Washed or Unwashed KT	Washed	Washed	Washed	Washed	Washed	Washed	Washed	Washed
% Wt. Loss	2.68%	2.55%	2.66%	3.14%	3.48%	2.79%	2.34%	2.62%
Comments	Good sample	Good sample			Good sample but a little loss in washing	Good sample		

TABLE IX (Cont'd)

KT STABILITY IN KOH SOLUTION

SAMPLE #	9-D	10-D	11-D	12-D	13-D	14-D	15-D	16-D	17-D	18-D
Temp. (°C)	125°C	125°C	125°C	125°C	125°C	125°C	125°C	125°C	100°C	100°C
Time (hrs.)	500	500	1000	1000	1000			1000	1000	1000
Original % KOH	30.3	30.3	30.3	30 3	44.5	44.5	44.5	44.5	44.5	44.5
Final % KOH	-	-	-	-	50.2%			53.3	45.3%	45.5
Washed or Unwashed KT	Washed	Washed	Washed	Washed	Washed	Washed	Washed	Washed	Washed	Washed
% Wt. Loss	-	-	-	-	4.59%			2.88%	3.81%	
Comments	Dried out in oven	Dried out in oven bottle leaks.	Dried out in oven	Dried out in oven						Ruined

TABLE IX (Cont'd)

KT STABILITY IN KOH SOLUTION

SAMPLE #	19-D	20-D	21-D	22-D	23-D	24-D
Temp. (^{o}C)	100^{o}C	100^{o}C	100^{o}C	100^{o}C	100^{o}C	100^{o}C
Time (hrs)	1000	1000	1000	1000	1000	1000
Original % KOH	44.5	44.5	44.5	44.5	44.5	44.5%
Final % KOH	45.3%	44.8%	45.2%	45.7%	45.6%	45.6%
Washed or Unwashed KT	Washed	Washed	Washed	Washed	-	-
% Wt. Loss	3.68	3.39	3.77	3.45	-	-
Comments					KOH Blank	KOH Blank

TABLE IX (Cont'd)

KT STABILITY IN KOH SOLUTION

SAMPLE #	1-E	2-E	3-E	4-E	5-E	6-E	7-E	8-E
Temp. (^{o}C)	125^{o}C	125^{o}C	125^{o}C	125^{o}C	125^{o}C	125^{o}C	125^{o}C	125^{o}C
Time (hrs.)	1000	1000	1000	500	500	500	500	1000
Original % KOH	30.3	30.3	30.3	30.3	30.3	30.3	30.3	30.3
Final % KOH	-	-	48.2	45.7	35.0	35.1	56.1	54.8
Washed or Unwashed KT	Un	Un	Un	Un	Un	Un	-	-
% wt. Loss	-	-	4.51%	4.52%	3.09%	3.13%	-	-
Comments	Sample dried out in oven	Sample dried out in oven					KOH Blank	KOH Blank

TABLE IX (Cont'd)

KT STABILITY IN KOH SOLUTION

SAMPLE #	9-E	10-E	11-E	12-E	13-E	14-E	15-E	16-E
Temp. (°C)	125°C	125°C	125°C	125°C	125°C	125°C	125°C	125°C
Time (hrs.)	1000	1000	1000	1000	1000	1000	1000	
Original % KOH	44.5	44.5	44.5	44.5	44.5	44.5	44.5	44.5
Final % KOH	52.4%	46.1%	52.4%	48.2%	51.1%	50.5%	47.8%	
Washed or unwashed KT	Un	Un	Un	Un	Un	Un	Un	Un
% Wt. Loss	4.07%	4.19%	4.28%	4.21%	4.09%	4.51%	-	
Comments							KOH Blank	

TABLE IX (Cont'd)

KT STABILITY IN KOH SOLUTION

SAMPLE #	1-S	2-S	3-S	4-S	5-S	6-S	7-S	8-S
Temp. (°C)	75°C	75°C	75°C	75°C	75°C	75°C	75°C	75°C
Time (hrs.)	150	150	150	150	150	150	150	150
Original % KOH	45.5	45.5	45.5	45.5	45.5	45.5	45.5	30.3
Final % KOH	43.3	-	43.7	-	-	-	44.5	28.8
Washed or unwashed KT	Un	Un	Un	Un	Un	Un	Un	Un
% Wt. Loss	3.81%	-	3.89%	-	-	-	3.80%	3.82%
Comments	Oven was heated to 150°C at 150 hrs. test time accid-ently	Test ruined when bottle collap-sed from over heat-ing.	Oven was accid-ently over heated at 150 hrs.	Test ruined	Test ruined	Test ruined	Oven was accid-ently over heated at 150 hrs.	Oven was accid-ently over heated at 150 hrs.

4.8.3 SPECTROGRAPHIC ANALYSIS OF POTASSIUM TITANATE

Upon inquiry to the E.I. DuPont Company, the following chemical composition of pigmentary potassium titanate was obtained:

TiO_2	81 - 83.5%
K_2O (Net)	14 - 15%
KCl	0.5% max.
K_2SO_4	2.0% max.
Al_2O_3	0.2 - 0.4%
H_2O	2.5 - 4.0%
Fe	60 - 80 ppm
Pb	10 - 20 ppm
As	10 - 20 ppm

They indicated that the KCl and K_2SO_4 are surface salts associated with the pigmentary KT processing and are removable by washing.

To obtain a better understanding of the composition and impurities in the pigmentary KT used in the matrixes, a sample was submitted to an outside testing laboratory for spectrographic analysis; the results are shown below:

SPECTROGRAPHIC ANALYSIS OF PIGMENTARY POTASSIUM TITANATE

Titanium	47%	Aluminum	0.071%	Calcium	0.11%
Potassium	17%	Silicon	0.042%	Lead - less than	0.02%
Magnesium	0.020%	Other elements - nil			

This analysis confirmed roughly the composition of KT as supplied by DuPont.

4.9 MATRIX FABRICATION AND LAB SCREENING

At the time the KT material was judged acceptable for use in the fuel cell matrix, a fabrication and screening program was implemented.

4.9.1 SCREENING APPARATUS

Figure 83 is a cross section drawing of the apparatus used to test the amount of differential pressure that a matrix can withstand. As can be seen in the illustration a wetted matrix was mounted in the cell and the N_2 pressure was increased until a bubble of N_2 gas broke through the mat.

One of the screening tests defined for fuel cell matrixes was electrical resistance. Since the fuel cell matrix differs from battery separators in that it is compressed when assembled in a cell, a special testing cell was designed and built. Figure 84 illustrates this cell mounted in a hydraulic press. With this test unit we could measure matrix thicknesses, compressive load, and resistance simultaneously. Thickness of the matrix under variable compressive loads could be correlated while the resistance was read on a General Radio Type 1650-A ac impedance bridge. The ac type of measurement was preferred because polarization effects were eliminated.

4.9.2 PASTED MEMBRANE

One of the more successful matrixes was a membrane of KT and Teflon pasted on a Teflon screen sandwiched between two mats composed of KT and asbestos. Fabrication techniques of the pasted Teflon/KT membranes were investigated. Membranes 3 inches in diameter were fabricated varying both the ratio of Teflon to KT and treatment after pasting. The membranes were tested in a bubble-through apparatus as shown in Fig. 83. The results of testing are shown in Table X.

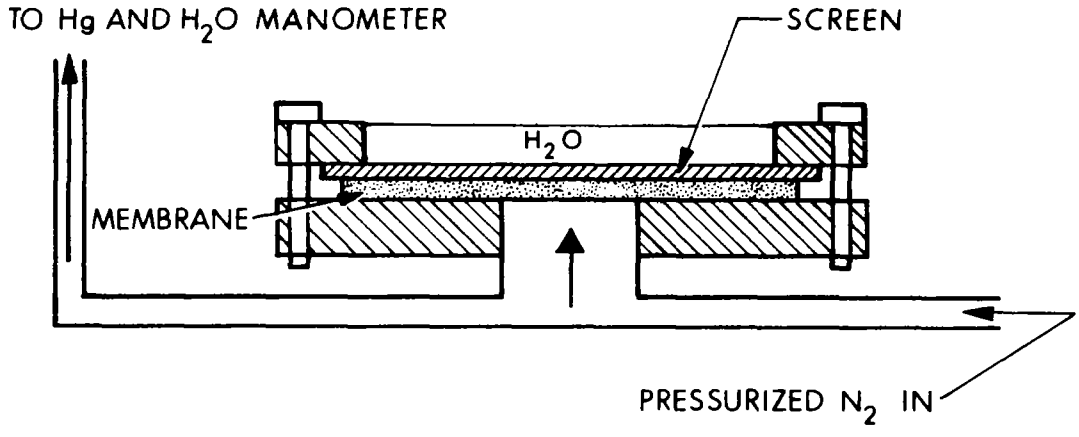

Figure 83. Bubble Cell Cross Section

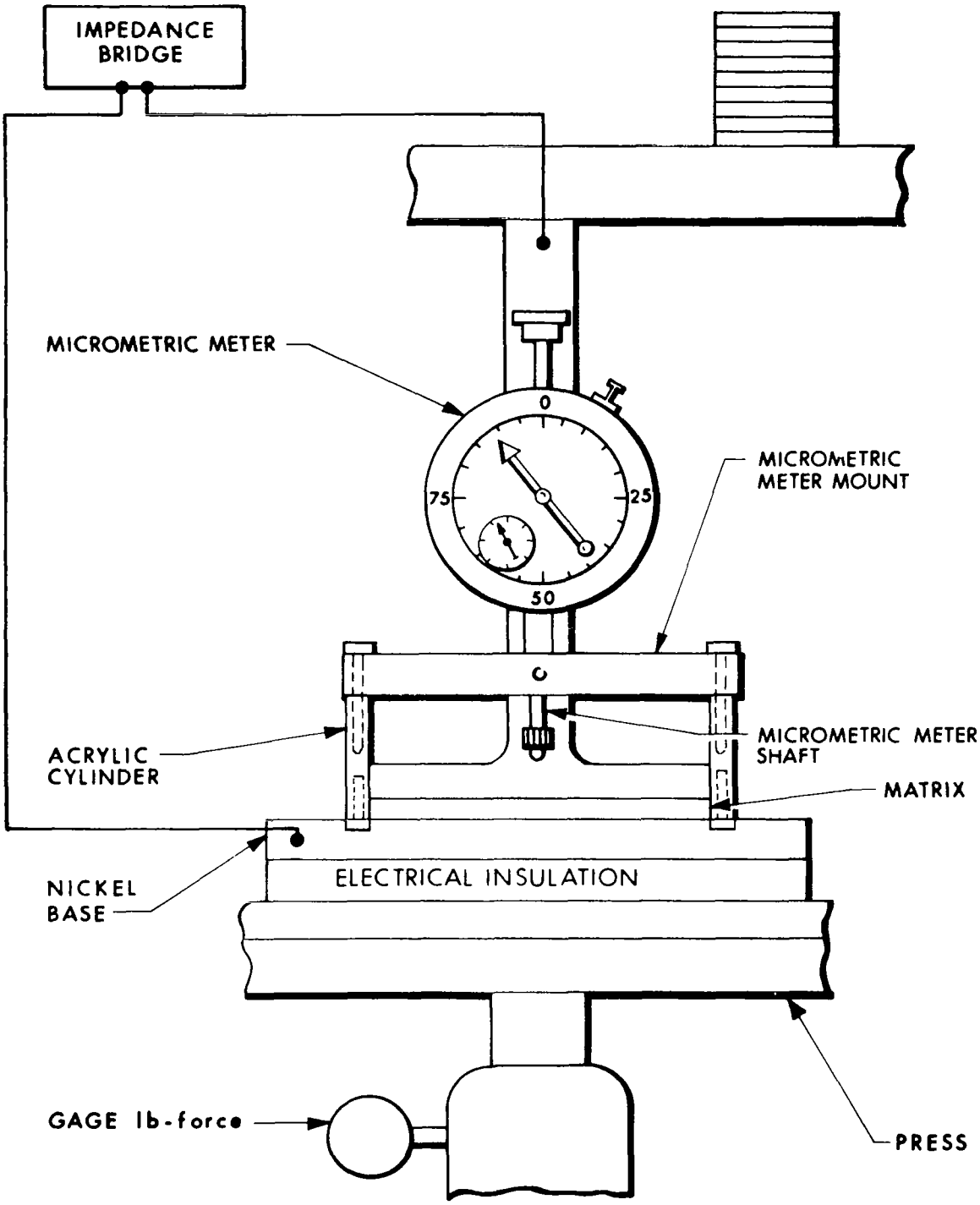

Figure 84. Impedance-Thickness-Compression Measuring Cell

4110-Final

TABLE X

BUBBLE-THROUGH TESTS

Test No.	Composition of Membrane	Treatment	psi Held
1	50% Teflon/50% KT	1 hr in 40% KOH at 135°C - washed and dried.	0.7
2	50% Teflon/50% KT	1/2 hr in 40% KOH at 115°C - washed and dried.	1.0
3	50% Teflon/50% KT	1/2 hr in 40% KOH at 130°C - washed and dried.	1.0
4	50% Teflon/50% KT	1/2 hr in 40% KOH at 105°C - washed and dried.	0.2
5	50% Teflon/50% KT	1/2 hr in 40% KOH at 115°C - washed and dried.	0.5
6	50% Teflon/50% KT	1/2 hr in 40% KOH at 127°C - washed and dried.	1.1
7	50% Teflon/50% KT	1/2 hr in 40% KOH at 150°C - washed and dried.	0.5
8	50% Teflon/50% KT	1/2 hr in 40% KOH at 105°C - washed and dried.	1.0
9	50% Teflon/50% KT	1/2 hr in 40% KOH at 115°C - washed and dried.	0.5
10	50% Teflon/50% KT	1/2 hr in 40% KOH at 130°C - washed and dried.	0.1
11	50% Teflon/50% KT	1/2 hr in 40% KOH at 150°C - washed and dried.	0.1
12	50% Teflon/50% KT	1/4 hr in oven at 400°C - decomposed.	-

TABLE X (Cont'd)

BUBBLE-THROUGH TESTS

Test No.	Composition of Membrane	Treatment	psi Held
13	50% Teflon/50% KT	1/2 hr in oven at 190°C - washed and dried.	0.3
14	50% Teflon/50% KT	10 min in oven at 300°C - decomposed.	-
15	50% Teflon/50% KT	1/2 hr in oven at 220°C - washed and dried.	0.01
16	50% Teflon/50% KT	1/2 hr in 40% KOH at 115°C - tested without wash or drying.	1.9
17	50% Teflon/50% KT	1/2 hr in 40% KOH at 130°C - tested without wash or drying.	2.7
18	50% Teflon/50% KT	1/2 hr in 40% KOH at 130°C - tested without wash or drying.	2.5
19	50% Teflon/50% KT	1/2 hr in 40% KOH at 150°C - tested without wash or drying.	3.7
20	50% Teflon/50% KT	1/2 hr in 40% KOH at 130°C - washed and dried.	1.15
21	50% Teflon/50% KT	1/2 hr in 40% KOH at 130°C - washed and dried - then soaked in H_2O for 1.2 hr before testing.	2.0
22	60% Teflon/40% KT	No treatment - wet for 1/2 hr.	1.2
23	60% Teflon/40% KT	1/2 hr in 40% KOH at 100°C - washed, then tested while wet.	3.0

TABLE X (Cont'd)

BUBBLE-THROUGH TESTS

Test No.	Composition of Membrane	Treatment	psi Held
24	60% Teflon/40% KT	1/2 hr in 40% KOH at 130°C-washed then tested while wet.	3.2
25	70% Teflon/30% KT	No treatment, wet for 1/2 hr	2.5
26	60% Teflon/40% KT 100 mesh 10 mil screen.	Treated 1/2 hr at 150°C in 40% KOH, washed and tested wet.	3.3
27	70% Teflon/30% KT mesh 10 mil screen.	Treated 1/2 hr at 100°C in 40% KOH, washed and tested wet.	4.5
28	70% Teflon/30% KT mesh 10 mil screen.	Treated 1/2 hr at 130°C in 40% KOH, washed and tested wet.	3.8
29	70% Teflon/30% KT 100 mesh 10 mil screen.	Treated 1/2 hr at 130°C in 40% KOH, washed and tested wet.	3.1
30	50% Teflon/50% KT 100 mesh 10 mil screen.	Screen was preshrunk 1/2 hr at 150°C in 40% KOH then pasted, treated 1/2 hr at 130°C in 40% KOH, washed, dried, wet before test.	3.4
31	50% Teflon/50% KT 100 mesh 10 mil screen.	Treated 1/2 hr at 115°C in 40% KOH, washed, dried, wet before test.	4.0
32	50% Teflon/50% KT 100 mesh 10 mil screen.	Treated 1/2 hr at 150°C in 40% KOH, washed, dried, wet before test.	2.0
33	50% Teflon, 60 mesh screen, 45 mils thick.	No treatment, wet before test.	0.5

TABLE X (Cont'd)

BUBBLE-THROUGH TESTS

Test No.	Composition of Membrane	Treatment	psi Held
34	70% Teflon, 60 mesh screen, 45 mils thick.	No treatment, wet before test.	3.0
35	50% Teflon/50% KT 100 mesh 10 mil screen.	No treatment	Not bubble tested
36	50% Teflon 100 mesh 10 mil screen.	Treated 1/2 hr at 115°C in 40% KOH, washed, dried resoaked in 40% KOH 22 hr pressed to 3400 psi.	3.5
37	50% Teflon 100 mesh 10 mil screen.	Treated 1/2 hr at 130°C in 40% KOH, washed, dried, resoaked in 40% KOH 48 hr pressed to 3400 psi.	3.5
38	50% Teflon 100 mesh 10 mil screen.	Preshrunk screen 1/2 hr at 150°C in 40% KOH then pasted, treated 1/2 hr at 130°C in 40% KOH, washed, dried, resoaked in 40% KOH 3 days and pressed to 3400 psi.	3.5
39	70% Teflon/30% KT 60 mesh 0.045 in. thick.	Treated by pressing between two hot plates temperature 140°C for 15 minutes at 3400 psi	1.5
40	50% Teflon/50% KT 60 mesh 0.045 in. thick.	Treated by pressing between two hot plates, temperature 140°C, for 15 minutes at 340 psi.	4.0

TABLE X (Cont'd)

BUBBLE-THROUGH TESTS

Test No.	Composition of Membrane	Treatment	psi Held
41	60-mil fuel cell grade asbestos.	Wet and tested	better than 25.0
42	60-mil fuel cell grade asbestos.	Not bubble tested	

The first 15 samples tested gave low results. Samples 16 to 19 were taken right from the KOH bath and tested. The higher results led to the conclusion that the previous samples were not wetted sufficiently. Samples 20 and 21 were treated in the same manner except that sample 21 was soaked for half an hour in water before being tested. Sample 21 gave the higher result in the bubble-through pressure test. Subsequent samples were thoroughly wetted before testing and showed more reasonable values. The data from Table X indicates that the bubble-through pressures of the pasted 100 mesh, 10-mil Teflon screens vary between 2 and 4 psi and are independent of treatment. The treatment in KOH was continued to remove objectionable impurities. Membranes were fabricated using 60 mesh, 45-mil-thick Teflon screens. The bubble-through results were poor until this type of membrane was treated by pressing between two hot platens at 3400 psi. It is interesting to note that a sample of 60-mil asbestos showed a bubble-through pressure of 25 psi.

Some resistance test results are tabulated in Table XI. In all the tests the resistivity decreased and then increased with compression. This phenomenon was probably due to a decrease in pore size and subsequent removal of KOH. The resolution of the readout on the impedance bridge was hazy in this group of readings. Despite this, the test results showed fair reproducibility. It was suggested that the hazy resolution of the impedance bridge readings was due to low cell capacitance caused by the smooth nickel plates in the test cell. Asbestos sample 42 was tested between nickel carbonyl plates which had rough surfaces. The resistance readings were consequently sharper and the resistivity values were lower. It can be noted from the results in Table XI that the resistivity increased with the amount of Teflon used in the membrane. Although it would be expected that the bubble-through characteristic should improve with an increase of Teflon this does not seem to be true.

TABLE XI

RESISTANCE TEST RESULTS

Sample No.	Type and Treatment *	Resistivity Ω/cm	Resistance Ω	Compression, psi	Thickness (wet) mils	Thickness (dry) mils	Electrolyte Ratio gm of 40% KOH/gm sample
35	50% KT/50%	710	0.388	0	9.8	9.5	0.507
	Teflon No	270	0.128	284	8.5		
	treatment	242	0.108	570	8.0		
		298	0.108	1420	6.5		
		375	0.098	3400	4.7		
36	50% KT/50%	575	0.320	0	10	10.3	0.262
	Teflon	242	0.108	570	8.0		
	Treated 1/2	263	0.098	1420	6.7		
	hr. at 115°C	316	0.088	3400	5.0		
	in 40% KOH						
37	50% KT/	480	0.308	0	11.5	10.5	0.242
	50% Teflon	195	0.098	284	9.0		
	Treated 1/2	208	0.098	570	8.5		
	hr at 130°C	205	0.088	1420	7.7		
	in 40% KOH	314	0.103	3400	5.9		
38	50% KT/	875	0.488	0	10.0	9.4	0.229
	50% Teflon	450	0.238	284	9.5		
	Treated 1/2	342	0.168	570	8.8		
	hr at 130°C	306	0.128	1420	7.5		
	in 40% KOH	450	0.138	3400	5.5		
41	Asbestos	110	0.478	0	78	60	1.51
	fuel cell	27.2	0.093	284	61		
	grade	23.0	0.073	570	57		
		24.3	0.073	1420	54		
		38.4	0.078	3400	36		

* See Table X for details

TABLE XI (Cont'd)

RESISTANCE TEST RESULTS

Sample No.	Type and Treatment*	Resistivity Ω/cm	Resistance Ω	Compression psi	Thickness (wet) mils	Thickness (dry)mils	Electrolyte Ratio gm of 40% KOH/gm sample
42	Asbestos fuel cell grade	8.17	0.036	284	79	60	1.51
		9.75	0.036	570	66		
		12.3	0.033	1420	48		
		22.6	0.044	3400	35		
43	60% Teflon 100 mesh 10-mil screen No treatment.	550	0.1105	0	14.2		0.349
		668	0.1085	284	11.5		
		512	0.0725	570	10.0		
		350	0.0415	1420	8.4		
		427	0.0350	3400	5.8		
		520	0.0665	0	9.0		
		547	0.0525	1700	6.8		
		433	0.0350	3400	5.7		
48	70% Teflon/ 30% KT 100 mesh, 10-mil No treatment Tested with Ni sheets	1280	0.2085	0	11.5		0.216
		1025	0.1485	284	10.2		
		955	0.1285	570	9.5		
		1040	0.1235	1420	8.4		
		1182	0.1290	2270	7.7		
		1440	0.1385	3400	6.8		
49	70% Teflon/ 30% KT 100 mesh 10-mil screen No treatment No plates, sheets, or anything else used in this test.	608	0.688	0	8.0		0.218
		376	0.388	284	7.3		
		141	0.138	570	6.9		
		121	0.103	1420	6.0		
		138	0.108	2270	5.5		
		167	0.113	3400	4.8		
		493	0.488	0	7.0		

TABLE XI (Cont'd)

RESISTANCE TEST RESULTS

Sample No.	Type Treatment	Resistivity Ω/cm	Resistance Ω	Compression psi	Thickness (wet) mils	Electrolyte Ratio gm of 40% KOH gm Sample
50	70% Teflon/30% KT 100 mesh 10-mil screen treated 0.5 hr. at 100°C in 40% KOH. Tested with carbonyl nickel plaques	1005	0.2135	0	15	0.118
		703	0.1095	284	11	
		430	0.0595	570	9.8	
		1675	0.0190	1420	8.0	
		1280	0.0125	2270	6.9	
		1113	0.0090	3400	5.7	
		2400	0.2785	0	8.2	
51	60% Teflon/40% KT 100 mesh 10-mil screen No treatment	546	0.788	00	10.2	0.340
		1925	0.248	284	9.1	
		1005	0.118	570	8.3	
		852	0.088	1420	7.3	
		900	0.088	2270	6.9	
		1230	0.103	2400	5.9	
		976	0.108	0	7.8	
52	60% Teflon/40% KT 100 mesh 10-mil screen. No treatment. Tested with Ni plaques	550	0.1105	0	14.2	0.348
		667	0.1085	284	11.5	
		512	0.0725	570	10.0	
		349	0.0418	1420	8.4	
		382	0.0390	2270	7.2	
		427	0.0350	3400	5.8	
		523	0.0665	0	9.0	
		434	0.0350	3400	5.7	
		543	0.0675	0	8.8	

4.9.3 EVALUATION OF ZIRCONIA AS A FABRICATION MATERIAL

Zirconia is an oxide of zirconium having a probable formula of ZrO_2 and a specific gravity of 4.5, which is higher than the KT (specific gravity of 3.66). The zirconia was obtained from H.I. Thompson Company, Gardena, California. A weighed portion of this compound was subjected to 40.3% KOH at 100°C for 340 hours. At the end of the test, the zirconia lost 3.14% in weight. Subsequently, mats of the following composition were formed: 100% zirconia, 50% zirconia/50% KT, 80% KT/20% zirconia. Although the zirconia appears to have a longer fiber than KT, the 100% zirconia mat fell apart easily when dry. This may have been due to the high specific gravity of the compound which resulted in too much weight to be supported by a fibrous mat structure. The 50% KT/50% zirconia held together, but the resulting weight of 12 grams for a 3-in. diameter 50-mil mat was much too high to be practical. The 80% KT/20% zirconia mat was judged to have about the same structural strength as the 50% KT/50% zirconia mat and, of course, resulted in a more advantageous bulk density. Two 6.25-in. diameter, 35-mil mats of 80% KT and 20% zirconia were made and successfully tested for over 400 cycles in cell 263. This mat weighed 17.5 grams whereas 100% KT weighed 14 grams; considering this, the 100% KT mat was the favorable one. A membrane was fabricated by pasting a 50-50 zirconia/Teflon mixture on a 10-mil, 100 mesh screen. It gave a bubble-through test result of 3.5 psi. Unless a higher bubble-through result can be obtained, the zirconia shows no advantage over KT in a membrane.

4.9.4 ROLLED KT-TEFLON STRUCTURES

A new KT/Teflon structure was developed. A mixture of KT and Teflon emulsion was dried and then worked with a roller on a hot plate. The resulting structure was mechanically stronger than the KT/asbestos mats.

It could be bent 90° without breaking or distorting while dry. Two 3-inch-diameter mats were fabricated and tested. The results are shown in Table XII. The bubble-through and KOH retention figures indicated that this KT structure may be used for the whole matrix. Full-size matrixes were fabricated and tested in cells. It was found that when used as a matrix the Teflon would flow at 80°C and allow cross leakage of the gases in the cell. However, some success was obtained using it as a membrane.

TABLE XII

SCREENING TESTS OF ROLLED KT STRUCTURES

Sample	Diam.	Thickness	Dry Wt.	40% KOH Retention	Resistivity at 20 psi	Imped. Compr.	Bubble-through
1	3 in.	50 mils	5.19 g	After 1 hr soak: 5.3 g	107.5Ω-cm	0.3Ω	> 20 psi
2	3 in.	40 mils	4.90 g	After 48 hr soak 6.56 g	35.9Ω-cm	0.08Ω	10 psi

4.9.5 PRESSED COMPOSITE MATRIXES

Fabrication of composite matrixes using KT, asbestos, and Teflon pressed together was explored. Table XIII summarizes the screening test results. Sample M-1 was the standard sandwiched matrix used in many of the tests. Sample M-2 was a standard 90 percent KT/10 percent asbestos mat. The bubble-through pressure of 15 psi for matrix M-1 and 5 psi for mat M-2 along with the respective resistivity data gave a baseline to compare the new structures with. Samples M-3 and M-4 were KT/asbestos/Teflon composites. The variable in fabrication was that sample M-4 was unpressed. The pressed matrix demonstrated a superior bubble-through test of 20 psi. The unpressed matrix gave a result of 10 psi, which was below that of the sandwiched matrix but better than the pressed KT/asbestos mat (M-2). Pressed matrixes similar to sample M-3 have been used in cycling cells with excellent results.

Fabrication of composite matrixes using KT, polypropylene, and Teflon pressed together was also explored. Table XV summarizes these screening test results. Sample M-5, composed of 95% KT and 5% polypropylene, pressed one half-hour at 124 psig, gave the highest bubble-through result of 25 psig. Samples M-6 and M-7 both had 5% Teflon added but gave lower bubble-through test results of 10 psig. This result may have been because the mats containing Teflon were thinner.

Samples M-9 and M-10, composed of 85 percent KT, 5 percent polypropylene, and 10 percent Teflon, pressed one half-hour at 124 psig, gave high bubble-through results. Sample M-8 gave a lower bubble-through test result of 7 psig. This result may have been because the mat was thinner. Samples M-11 and M-12 were both as thick as M-8 and M-4 but did not contain Teflon. No positive results using polypropylene in cycle tests have been obtained.

TABLE XIII

SCREENING TEST RESULTS

Sample	Composition	bubble-through psig.	Resistivity Ω-cm	Resistance	Compression psig	Thickness (wet)	Thickness (dry)
M-1	Sandwich two 90/10 KT and asbestos mats, 50/50 KT and Teflon 100 mesh screen membrane between mats pressed ½ hour at 124 psi	15	32.4	0.136	0	0.071"	0.076"
			46.8	0.126	71	0.051	
			40.8	0.116	142	0.041	
			37.4	0.096	213	0.031	
M-2	90/10 KT and asbestos mat pressed at ½ hour 124 psi	5	77	0.137	0	0.082	0.034
			105	0.117	213	0.020	
			122	0.102	355	0.015	
			218	0.097	390	0.008	
M-3	Matrix consisting of 82% KT, 10% asbestos and 8% Teflon pressed at ½ hour 124 psi	20	37.0	0.167	0	0.081	0.067
			27.7	0.117	160	0.076	
			24.6	0.097	284	0.071	
			23.7	0.087	390	0.066	
			21.2	0.072	710	0.061	
			25.2	0.067	850	0.048	
M-4	Matrix consisting of 83.5% KT 8.25% asbestos 8.25% Teflon not pressed.	10	16.5	0.137	0	0.148	0.145
			19.3	0.137	178	0.128	
			19.4	0.127	213	0.118	
			19.5	0.117	213	0.108	
			20.6	0.112	248	0.098	
			32.7	0.157	284	0.088	

TABLE XIII (Cont'd)

SCREENING TEST RESULTS

Sample	Composition	bubble through- psig.	Resistivity Ω-cm	Resistance	Compression psig	Thickness (wet)	Thickness (dry)
M-5	95% KT 5% polypropylene pressed one half hour at 124 psig.	25.0	35.1	0.137	0	0.070"	0.060"
			38.2	0.127	178	0.060"	
			35.1	0.107	188	0.055"	
			38.8	0.097	284	0.045"	
			43.5	0.097	284	0.040"	
			51.5	0.097	284	0.034"	
			78.0	0.117	284	0.027"	
M-6	90% KT 5% polypropylene 5% Teflon pressed one half hour at 124 psig.	10	55.2	0.138	0	0.045"	0.040"
			53.2	0.118	117	0.040"	
			45.3	0.098	213	0.039"	
			40.3	0.083	284	0.037"	
			36.1	0.068	427	0.034"	
			38.1	0.068	710	0.032"	
			40.7	0.068	1142	0.030"	
M-7	90% KT 5% polypropylene 5% Teflon	10	184.0	0.438	0	0.043	0.040"
			77.7	0.168	177	0.039	
			51.2	0.108	284	0.038	
			44.0	0.088	356	0.036	
			37.6	0.073	568	0.035	
			34.4	0.063	780	0.033	
			45.3	0.078	923	0.031	
M-8	80% KT 10% asbestos 10% Teflon solution	7					0.032"
M-9	5% polypropylene 10% Teflon solution 85% KT	80					0.070"

TABLE XIII (Cont'd)

SCREENING TEST RESULTS

Sample	Composition	bubble-through psig	Resistivity Ω-cm	Resistance	Compression psig	Thickness (wet)	Thickness (dry)
M-10	5% polypropylene 10% Teflon solution 80% KT	25					0.072"
M-11	1.3 g polypropylene, 22.8 g KT	10					0.060"
M-12	1.3 g polypropylene, 22.8 g KT	15					0.060"

SECTION 5

SIX-CELL ASSEMBLY - FIRST GENERATION

5.1 SIX-CELL DESIGN

The first design of the six-cell prototype was completed in November, 1963. Figure 85 is an assembly drawing of the design, and Figs. 86 and 87 are photos of it. The fuel cell portion of the assembly contained six series-connected cells. Both hydrogen and oxygen electrodes were platinized porous nickel discs 6 inches in diameter and 0.022 inch thick. The design was based on a stack capable of 75-watt discharge for 35 minutes and recharge in 65 minutes.

The hydrogen electrodes contained a mixture of 5 mg/cm^2 of platinum and 5 mg/cm^2 of palladium, and the oxygen electrodes contained 10 mg/cm^2 of platinum. The matrix had electrolyte content of 0.7 gram of 35 percent KOH solution per gram of dry asbestos.

Cell separators (Fig. 88) were made of nickel-plated magnesium and served a threefold purpose. First, they provided recessed areas to contain the electrodes; second, they provided gas manifolds and ports to transport the gases from the gas containers to their respective electrodes; and third, they served to connect adjacent cells in series. The end plates of the cell stack were also made of nickel-plated magnesium. Bolts were passed through each of the end plates and separators to provide a means for compressing the cell stack. Gas storage containers were made of nickel-plated aluminum and formed an integral part of the assembly.

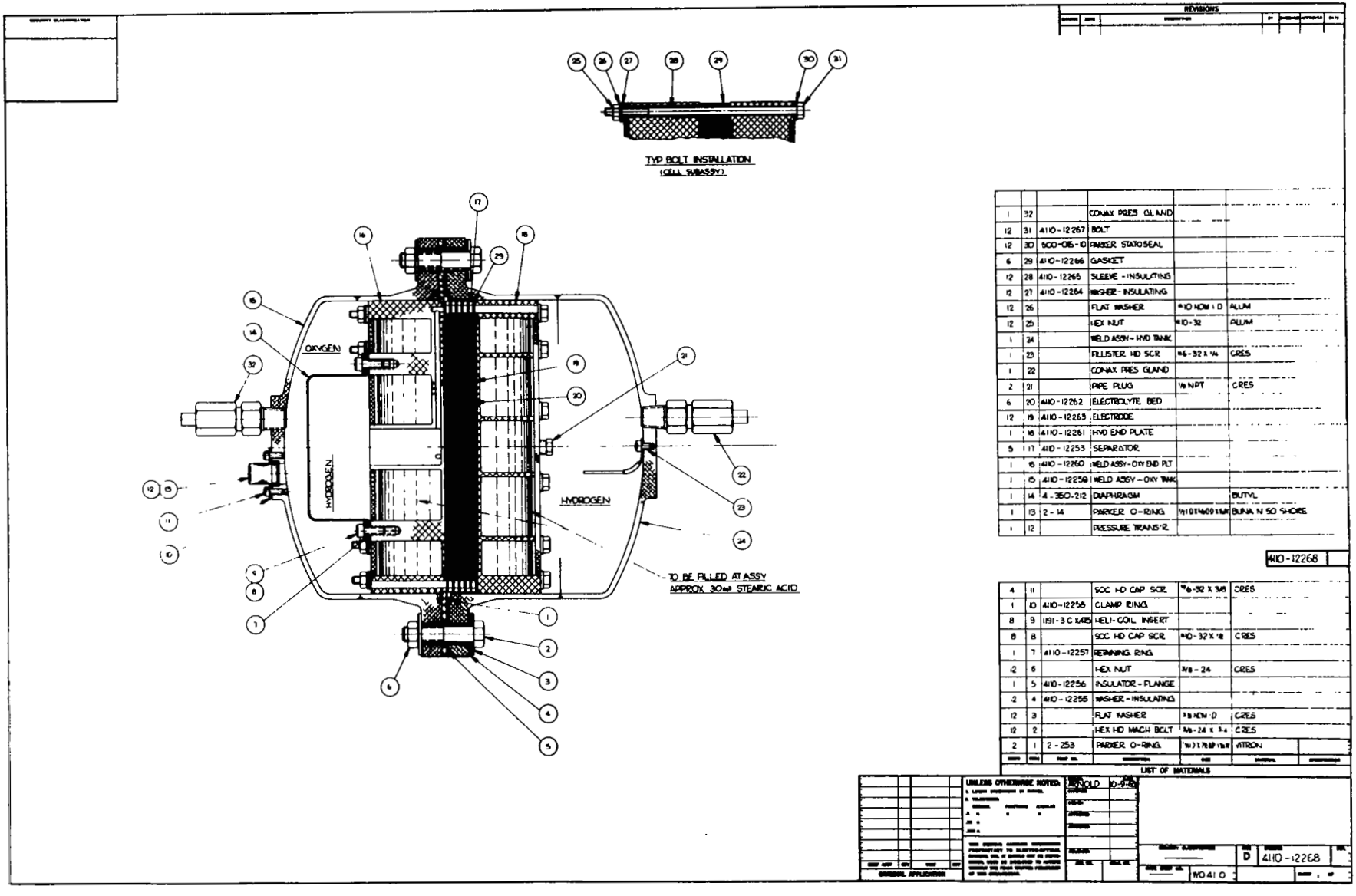

Figure 85. Six-Cell Fuel Cell Assembly

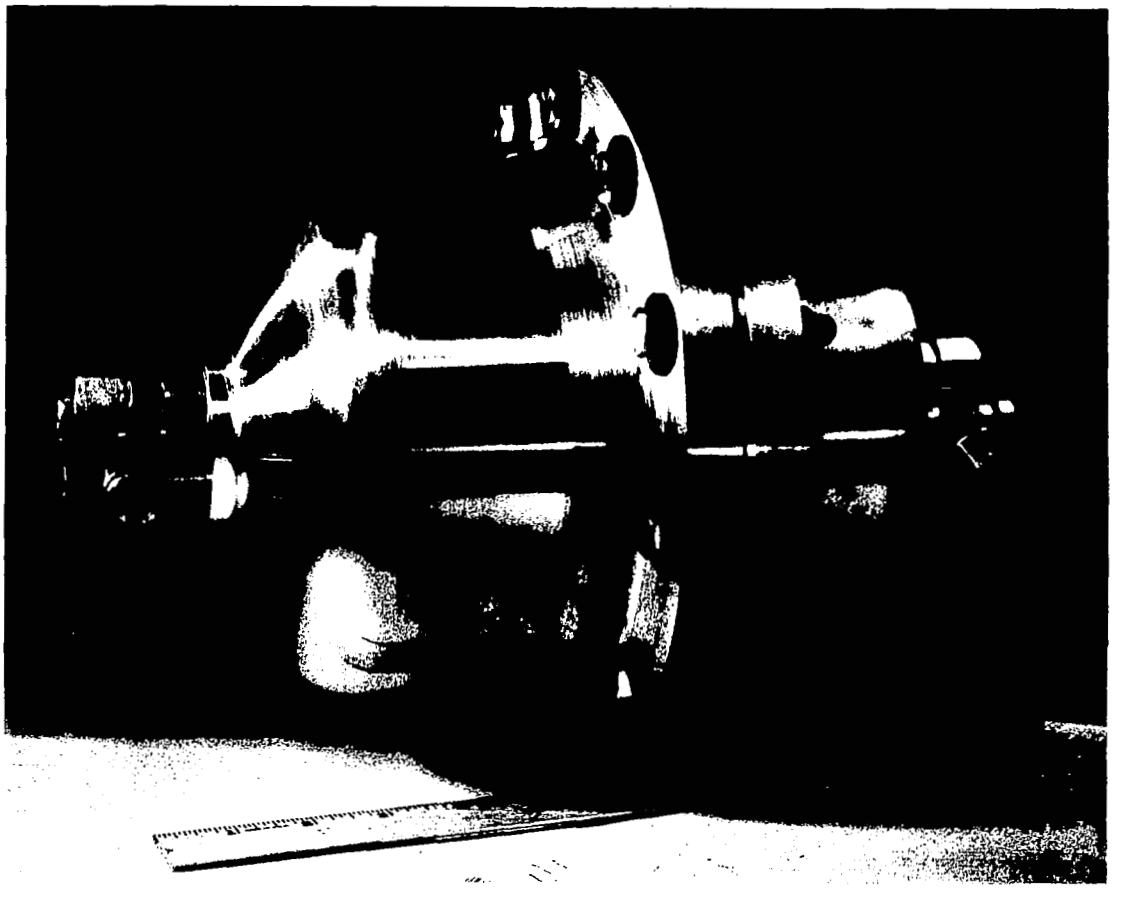

Figure 86. Six-Cell Fuel Cell Assembly

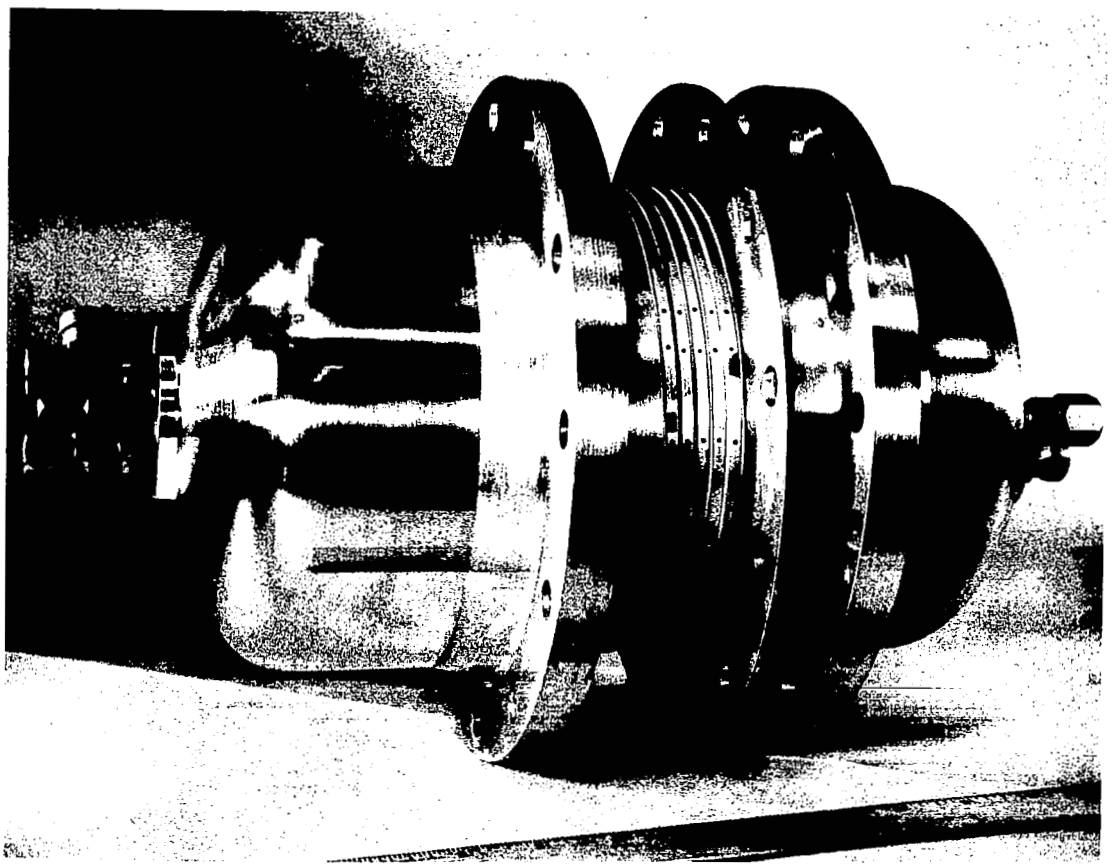

Figure 87. Six-Cell Fuel Cell Assembly Partially Disassembled

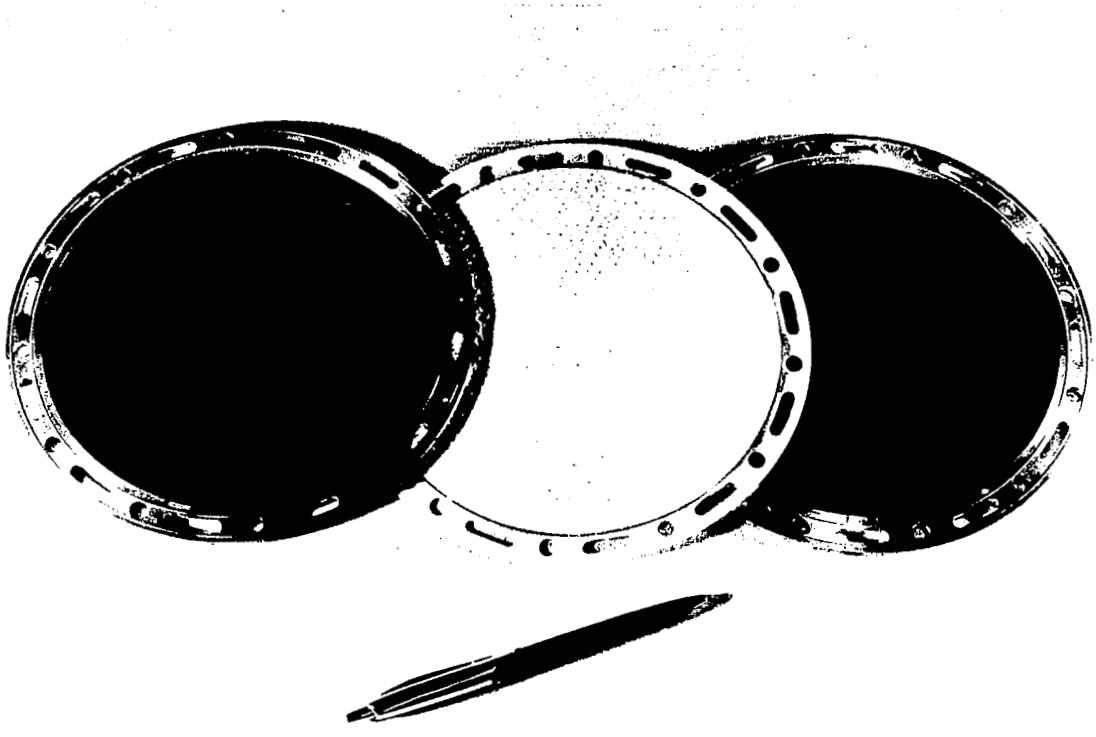

Figure 88. Electrode and Separator of Assembly

The gas storage volume ratio was 2/1 (hydrogen and oxygen, respectively). Gas containers with a volume ratio of 2/1 respectively for hydrogen and oxygen were integral, and were of such size that the maximum gas pressure was 400 psig at the full state of charge. Cylinder flanges contained bolt holes to compress O-rings located within each flange, thereby sealing both halves of the assembly. Pressure balance between the hydrogen and oxygen gas chambers was accomplished by means of a rubber diaphragm. This diaphragm would either expand or shrink if a slight differential developed between the two chambers and thereby balance the pressure.

The original cell specifications called for isothermal operation, Therefore, tankage for a heat of fusion thermal storage material (stearic acid) was incorporated into the design. This tankage was made an integral part of the end plates. During the test program, the desirability of using stearic acid was found to be questionable, and it was eliminated.

Instrumentation on the unit consisted of thermocouple leads to measure internal temperatures and voltages, a pressure transducer, a visual gage for internal gas pressure, and a differential transducer to monitor pressures between the gas chambers. Continuous cycling was carried out by means of a tandem recycle timer which switched from charge to discharge at the appropriate times. Charge current was set on the constant current power supply and discharge current was set by a rheostat. A multipoint recorder was employed to record voltage, current, temperature, and pressure data during operation.

5.2 ASSEMBLY AND START-UP

Nickel gas distribution screens and catalyzed electrodes were spot welded to the cell separators. The electrolyte bed was prepared by adding the required amount of KOH solution to the asbestos discs. Next, the cell stack was assembled and compressed by tightening the 12 insulated bolts on its periphery. A torque wrench was used here to obtain uniform compression. Gas ports leading to the diaphragm pressure equalizer were blocked off for initial tests. The complete cell stack was then installed inside the gas containment cylinders. Insulated bolts on the flanges of the gas cylinders were uniformly tightened, and the unit was readied for test.

Residual air within the assembly was removed by a purging process. This process consisted of repeated pressurization of the cylinders with their respective gases, and subsequent venting to the atmosphere. Gases were admitted to and released from the cylinders simultaneously and slowly, using needle valves. A differential pressure gage, connected across the cell, was employed to keep the differential pressures to a value less than 1.0 psi during the purging operation. After completion of this operation, the unit was ready for electrical testing.

5.3 CYCLE TESTS

This section presents the results of the cycle tests conducted on the unit. Table XIV gives a brief summary of each of the tests. A considerable amount of difficulty was experienced throughout the testing because of the cross gas leakage and other mechanical problems. However, a great deal of information and a better understanding of the operating parameters was obtained. Figure 89 shows typical performance data obtained on the first five cycles during Run 7. Electrical performance (Fig. 89) indicates a relatively constant charge voltage

TABLE XIV

SUMMARY OF CYCLE TESTS

Run No.	Date	Cycles	Temp. °C	Press. (psig)	Charge		Discharge		Purpose and Comments
					Volts	Amps	Volts	Amps	
1	2/13	4	28-64	0 Ch 100 Dis. 150 Dis.	10-12	9.6-10	3.0-4.8	10-15	Checkout test while operating in "quasi-secondary" mode of operation. Ignition occurred while adjusting pressures.
2	2/18	3	28-42	52-200	10.4-12.2	10	3.2-4.8	8-10	First run in actual secondary operation. Low power output indicated contaminated electrodes.
3	2/27	1	30	-	9.5-12.5	9.6	-	-	First run with complete instrumentation. Ignition occurred at beginning of discharge.
4	3/1	1	35-40	-	9-18.7	2-8	4.5	10	Test with new viton bellows and new set of electrodes. Ignition occurred on discharge. Found internal crack in O_2 end plate.
5	3/25	6	30-60	50-200	9.6-11	9.6	2.7-5.0	10-30	Test with new electrolyte layer and differential pressure transducer. Found build up in excess H_2 pressures. Ignition occurred at beginning of 6th discharge.
6	4/7	7	27-50	40-240	-	-	-	-	Adjusted gas volumes for each cycle until proper volume ratio was obtained.

TABLE XIV (contd)

Run No.	Date	No. Cycles	Temp. °C	Press. (psig)	Charge		Discharge		Purpose and Comments
					Volts	Amps	Volts	Amps	
7	4/9	5	29-57	55-320	9.8-10.2	9.6	3.9-4.5	15.8-16.7	Began final continuous cycle test. Ignition occurred in middle of 5th discharge period.
8	4/29	6	31-60	50-302	8.9-10.1	9.6	3.5-4.8	16-18	Began another continuous cycle test. Internal short circuit developed during 5th discharge period. Turned off.
9	5/5	1	28-46	50-287	9.8-10.5	9.6	4.3-4.5	17.7-18.2	Began another continuous cycle test. Ignition occurred during first discharge period.
10	5/15	19	28-70	50-380	9-10	10	3.6-4.5	16-19	Longest cycle test of 36 hr. Performance dropped near end.
11	5/25	5	30-63	50-270	10-13	10	3-4	10-11	Cycle test with new set of electrodes and gaskets and electrolyte. Low performance throughout.
12	5/27	1	28-37	50-265	10.0-10.6	9.6	3.4	5	Check out test. Found two reversed cells.
13	6/8	4	62-83	54-315	9.0-9.3	8	5.0-5.1	12-13	Replaced electrodes of reversed cells and began cycle test. Started cycle test at higher temp. Good performance until sudden combustion.

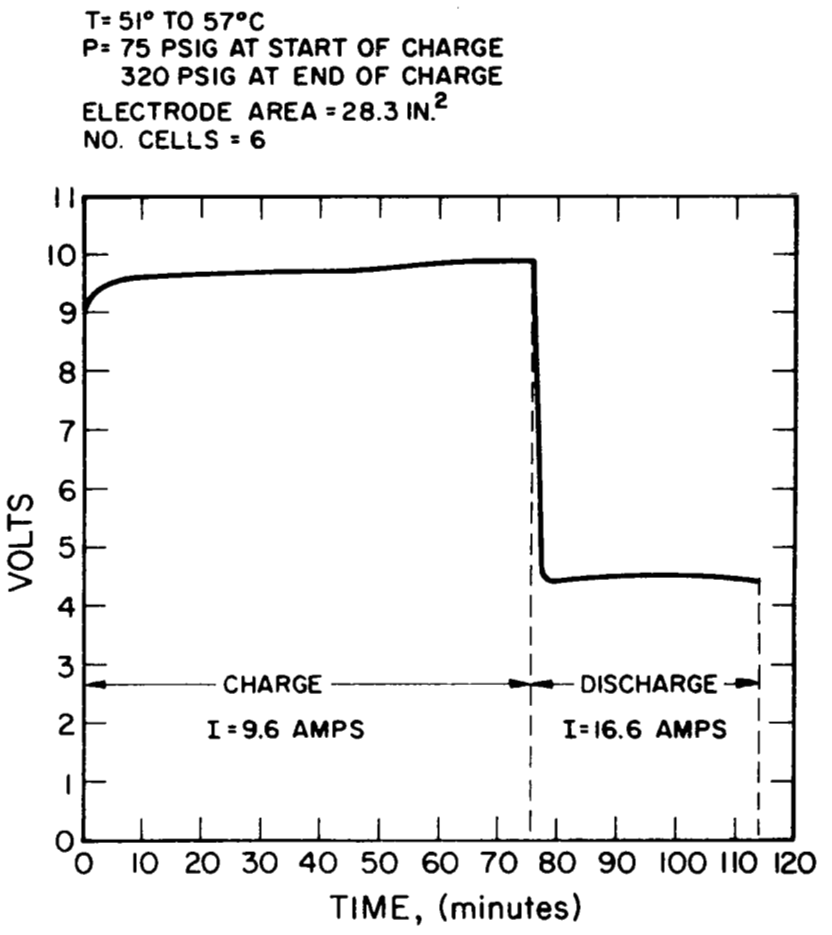

Figure 89. Electrical Performance in Run No. 7

near 9.6 volts during charge at 9.6 amps and a relatively constant discharge voltage at 4.5 volts at a current of 16.6 amps. Internal temperature (Fig. 90) (measured on the hydrogen end plate) indicated a temperature rise during discharge and a fall during charge. This result can be explained by the thermodynamics of the hydrogen-oxygen reaction. During discharge, the unit generates heat from internal polarization losses as well as from the entropy change, "$T\Delta S$", of the reaction for the formation of water. During charge the unit generates a much smaller amount of heat from polarization losses and absorbs heat from the entropy change accompanying the decomposition of water. For a more detailed analysis of the thermodynamics of the hydrogen-oxygen reaction in the fuel cell, see Subsection 3.3.1. The steady state temperature range appeared to be 58°C at the end of discharge and 54°C at the end of charge.

5.4 ANALYSIS OF RESULTS

The test program yielded significant results and a much better understanding of the operating parameters was obtained. Six critical factors not previously fully understood were defined, and design criteria were established:

a. Asbestos type requirements.
b. Asbestos compression requirements.
c. Electrolyte requirements.
d. Gas port requirements.
e. Separator seal requirements.
f. Operational procedures.

Each of these factors is discussed in the following subsections.

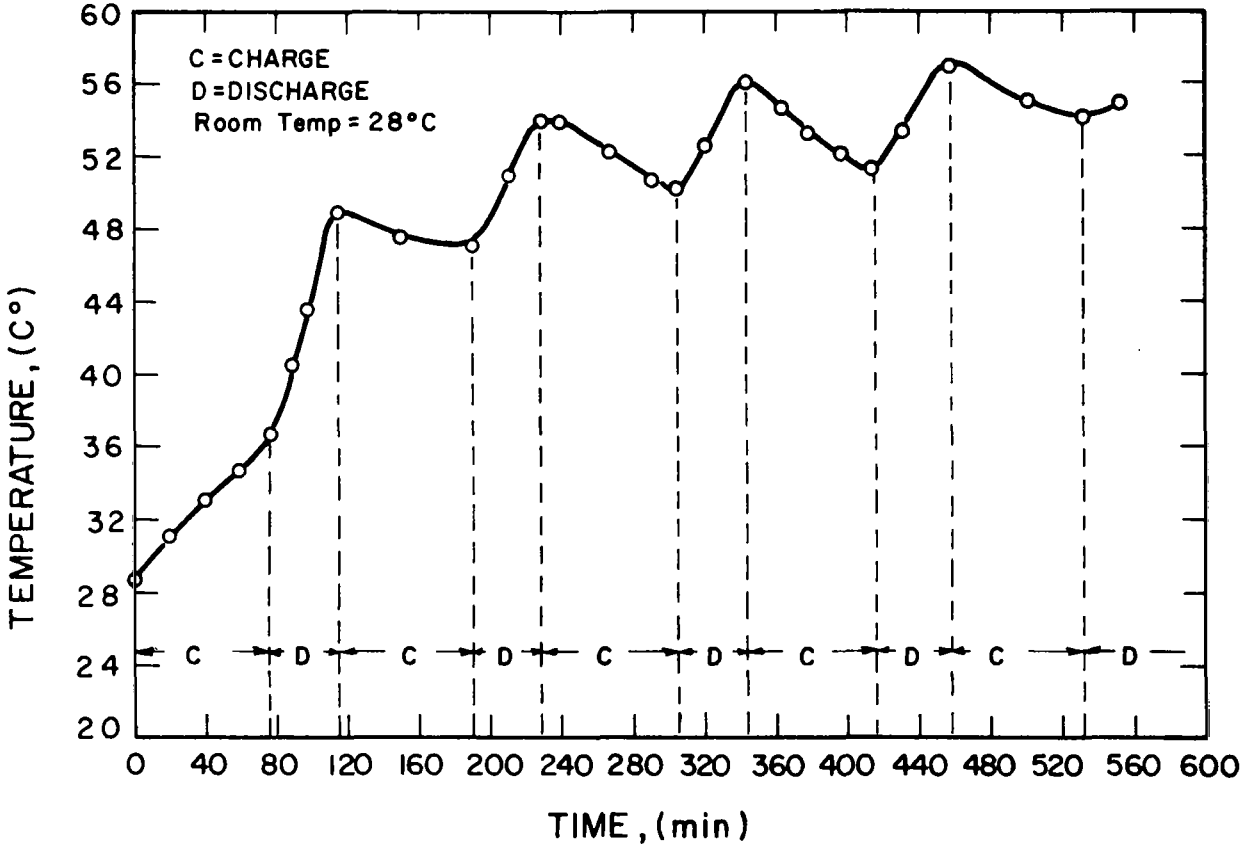

Figure 90. Internal Temperature in Run No. 7

5.4.1 ASBESTOS TYPE REQUIREMENTS

As a result of the thermochemical failures and poor performance exhibited by the 0.070 in. and 0.020 in. asbestos materials, it was readily apparent that an asbestos material must be carefully chosen. Highly porous materials (such as the 0.070 in.) led to mixing and subsequent reaction. Low porosity materials caused concentration polarization and resulted in poor performance.

Results indicated that a multilayer asbestos of medium porosity (i.e., similar to the 0.035 in. material) would provide adequate performance and storage capability and would effectively prevent gas mixing. (The term effective, as used here, is defined as the prevention of bulk mixing. Gas diffusion, however, will occur. Such diffusion mixing will only result in minor chemical recombination and formation of water at the electrode).

Two candidate materials appeared useful at that time. These were the 0.035 in. commercial and 0.060 in. electrolytic grades of asbestos. It was anticipated that other thicknesses of the electrolytic grade material would also be suitable and these other thicknesses were evaluated later in the program.

Prior to the present program, various materials such as polypropylene, pure asbestos, and various felt materials were evaluated. All of these were eliminated due to poor electrolyte retention characteristics. Although other absorbent porous products might have been suitable, work was limited to asbestos.

5.4.2 ASBESTOS COMPRESSION REQUIREMENTS

To prevent leakage through any of the electrolyte retention materials, a certain compression of the material is required. As a result of previous tests, a 7/4 compression ratio appeared to be a satisfactory value. Above this ratio, electrolyte is squeezed out of the separator material and into the electrode area. This tends to flood the electrode. Below this ratio, gas leakage occurs, as was evidenced by Run. No. 12.

Further testing of this factor, to determine allowable tolerances on the 7/4 ratio, was conducted.

5.4.3 ELECTROLYTE REQUIREMENTS

Optimum conductivity of aqueous solutions of KOH occur at roughly 30 weight percent KOH. It was apparent that this value represented a desirable concentration. Since the regenerative mode of operation used in the EOS design requires the removal and addition of water from the electrolyte as a function of charge and discharge, a 30 percent concentration cannot be held constant. However, the variation in concentration can be such as to minimize the change in conductivity. By maintaining an initial concentration of $\simeq$25% KOH, the concentration at full state of charge becomes $\lesssim$35%. Therefore, only minor changes in cell impedance occur as a function of state of charge.

The quantity of electrolyte is the other important requirement. If insufficient electrolyte is initially charged into the asbestos matrix, gas leakage will occur. Conversely, too much electrolyte will cause electrode flooding. Tests conducted, using 0.035 in. commercial asbestos, indicated that a 0.7/1 initial weight ratio of electrolyte to asbestos was optimum. At full state of charge (for a 750 n.mi. orbit) this results in an $\lesssim$0.5/1 ratio, which is quite satisfactory

to prevent gas mixing. For higher orbits, i.e., those requiring longer discharge times and larger capacities, additional layers of asbestos would be required to maintain the 0.5:1 final ratio.

5.4.4 GAS PORT REQUIREMENTS

During the test program, there were indications that 100-150 mA/cm^2 represented a limiting current density. It was believed that this limit was imposed by insufficient gas port area, in effect starving the electrodes and resulting in extreme concentration polarization. A new gas port design was prepared which both increased the gas port area, and better distributed the flow of gas.

5.4.5 SEPARATOR SEAL REQUIREMENTS

Two failures could be directly attributed to gasket and seal problems. In addition, unsatisfactory tolerances on rubber gaskets contributed to two other failures. Therefore, a new type of seal, eliminating extrusion, cold flow, and critical dimensional tolerances, was designed. This design incorporated a continuous rubber compression seal integral with the separator plates. Insulation and cell spacing were accomplished using a rigid flat plate spacer with appropriate ports and bolt holes.

SECTION 6

SIX-CELL ASSEMBLY - SECOND GENERATION

6.1 SIX-CELL DESIGN

Based on the results of the first six-cell design and certain single cell tests, a redesign of the six-cell unit was undertaken. The design contained certain changes from the design previously evaluated and described in Section 5. These changes were made to improve reliability and performance and are listed below.

a. Replacement of the rubber pressure balancing diaphragm by a stainless steel bellows.

b. Incorporation of an improved bipolar plate containing an integral gas port seal.

c. Incorporation of improved gas distribution by elimination of bipolar plate external drill holes.

d. Elimination of thermal storage tanks.

e. Incorporation of unipotential tankage.

Each of these changes was made along with other modifications to simplify fabrication and assembly, to increase gas porting area to the pressure balancing bellows, and to minimize the hazards involved in testing. Figure 91 is a photo of the assembled 75-watt unit and Figure 92 is an assembly drawing of the unit giving details of internal construction.

As in the previous 75-watt model, six series-connected cells using 6-inch diameter electrodes were employed. Assembly was accomplished

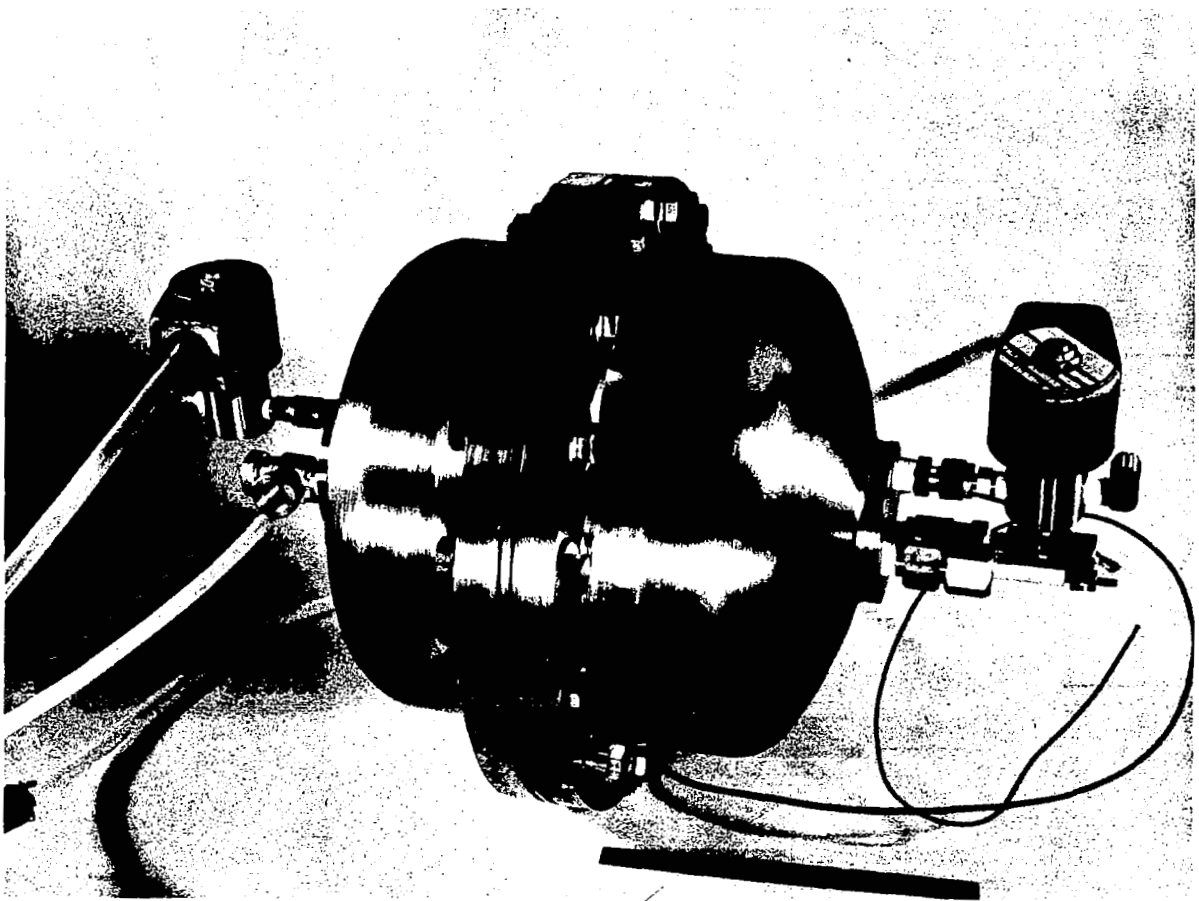

Figure 91. 75-Watt Fuel Cell Assembly

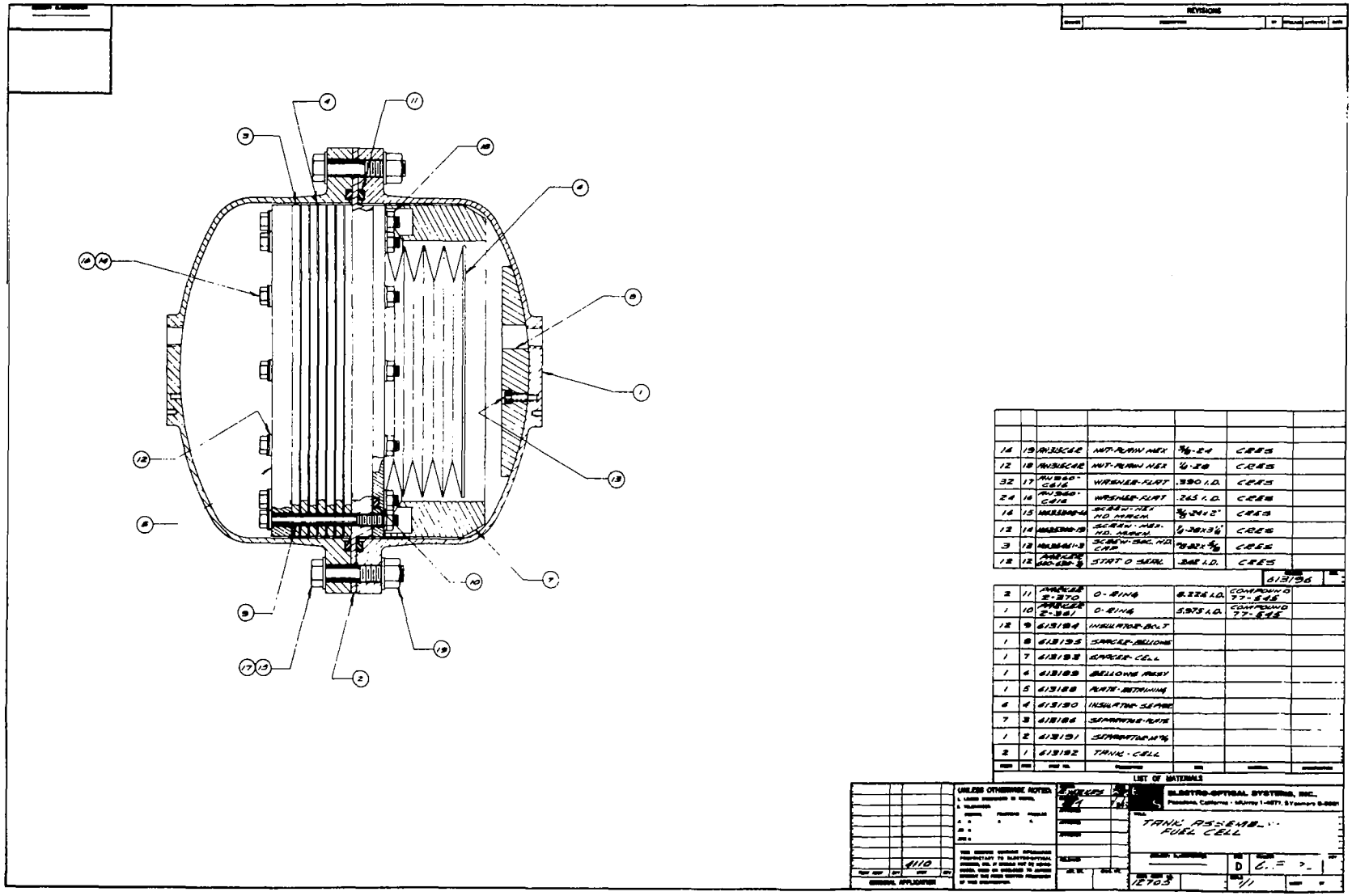

Figure 92. Tank Assembly - Fuel Cell

by stacking the individual bi-polar plates containing the electrodes and asbestos mats. A stainless steel bellows, which acted as a volume compensation device, was attached to the oxygen end plate. This volume compensation was required for two purposes: first, to correct any errors in volume due to design of machining errors, and second, to compensate for nonstoichiometric evolution of hydrogen and oxygen during the initial portions of the charge and discharge cycle. Nonstoichiometric evolution resulted from electrochemical oxidation of uncatalyzed portions of the nickel in the nickel plaque oxygen electrode. On discharge, this nickel oxide was reduced prior to the consumption of gaseous oxygen.

Once the cell stack, including the bellows, was assembled, the negative lead from the high pressure feed-through was attached to the stack along with an iron-constantan thermocouple. The integral tanks were then installed and bolted externally. To simplify tank construction, both gas tanks were made identical. Volume adjustment was made by installing two Teflon spacers, one of which was also used as a bellows extension stop.

6.2 INSTRUMENTATION

For both single and multi-cell tests, readout and control instrumentation was assembled in one test cabinet for consolidation and ease of handling (see Fig. 93). The test unit consisted of a load bank with variable resistors to control discharge current, a power supply to supply charging current, a power supply for the two pressure transducers, and two vacuum tube volt meters for total and differential pressure readout. A recycling timer was also included to automatically switch the cell from charge to discharge. (It was set for a 65 minute charge and a 35 minute discharge cycle.) The unit also contained outputs to a multipoint recorder for recording cell voltage, cell discharge current, and total cell pressure. Cell temperatures were also recorded on a

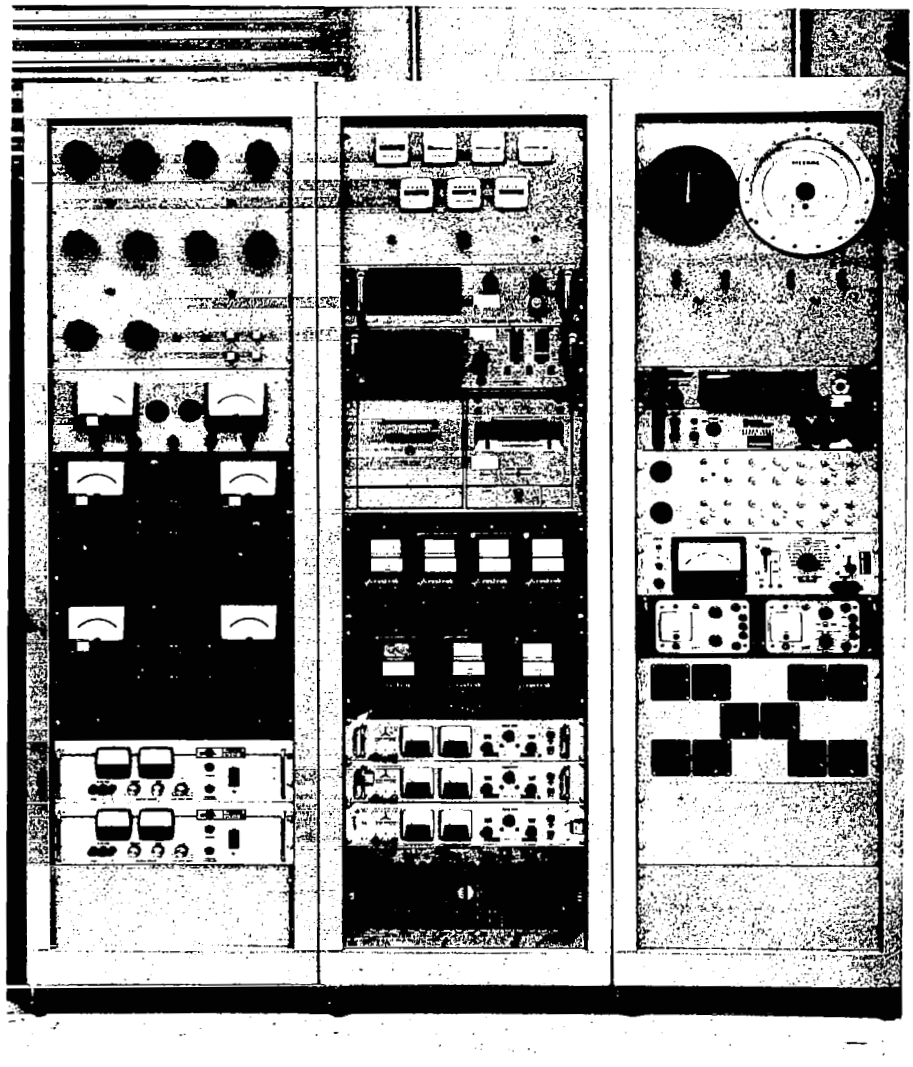

Figure 93. Fuel Cell Test Console

multipoint recorder, using a thermocouple located inside and on the external periphery of the cell. Differential pressure was recorded on a continuous strip chart recorder.

6.3 TEST AND EVALUATION

The second generation six-cell design, as basically described above was used in the conduction of a series of tests as surveyed in Table XV. The following paragraph describe the construction details and results obtained from these six-cell units during the program.

S/N 101

The electrodes employed contained 20 mg/cm^2 of catalyst (platinum) rather than the 10 mg/cm^2 as used previously. Fuel cell millboard asbestos was used in this 75-watt assembly test. The matrixes were 50 mils thick, weighed 22 grams, and were compressed to 40 mils in the cell stack. Twenty-nine grams of 40 percent KOH was added to the mat as the electrolyte.

After initial assembly and check out, the first redesigned six-cell unit was installed and tested in the new fuel cell testing facility. Appropriate feed-throughs for electrical and pneumatic connections had been installed in the test facility, and were connected to the cell. The unit was flushed 10 times by pressurizing with hydrogen and oxygen to 50 psig and then venting the gases. The ambient temperature in the test oven was then raised to 70°C, and the cell was put on cycle. The cycle consisted of 65 minutes charge at 9.6 amps, and a discharge load of 0.33 ohm set to give 75 to 80 watts during discharge. In the initial cycles, the performance of the unit appeared to be stable and satisfactory. Therefore, it was decided to continue cycling and conduct a continuous 48-hour test, which represented a major test

TABLE XV

SUMMARY OF TESTS ON 6 CELL NOMINAL 75 WATT UNITS

Construction								Results		
			Avg. Matrix		Avg. KOH					
S/N	O_2 Electrode	H_2 Electrode	Dry Wt. (gms)	Type Thickness	Wt. (gms)	%	Comments	Total # cycles	Final KOH(%)	Comments
101	20 mg. Pt./ cm^2	20 mg.Pt./ cm^2	22	.050" asbestos	29	40.5	Viton rubber edging on Mats	39	13	Exhibited gradual deterioration in charge and discharge voltage.
102	10 mg.Pt./ cm^2 + 10 mg.Pd./ cm^2	"	22	.050" asbestos	29	40.5	No rubber edging stack bolts insulating washer glass epoxy	16	33-34%	Stack bolts had relaxed and cell could not hold differential pressure
103	"	"	26.5	.060" asbestos	31	40.5	Following units had poly-prop. edging on mats, Belleville Springs on stack bolts	-	-	Found gas leakage through stat seals due to undersides bolt shank.
104	"	"	26.5	.060" asbestos	31	40.5		-	-	Found gas leakage through stat seal due to scratches on bolt shank.

TABLE XV (Cont'd)

SUMMARY OF TESTS ON 6 CELL NOMINAL 75 WATT UNITS

Construction								Results		
			Avg. Matrix		Avg. KOH					
S/N	O_2 Electrode	H_2 Electrode	Dry Wt. (gms)	Type & Thickness	Wt. (gms)	%	Comments	Total # cycles	Final KOH(%)	Comments
105	10 mg. Pt./ cm^2 + 10 mg. Pd./ cm^2	20 mg. Pt./ cm^2	26.5	.060" asbestos	31	40.5		-	-	Unit developed two internal cell shorts on first charge.
106	"	"	26.5	.060" asbestos	31	40.5		70	34.2, 34.4 %	Developed Oxygen leak through pressure switch during cycling.
107	"	"	26.5	.060" asbestos	31	40.5	Aluminum gas tanks .040" spacers	343	23 to 25	Test ended when internal reaction took place.
108	Au plated Ni plaques with 14 mg Pt/cm^2	Au plated Ni plaques with 14 mg Pt/cm^2	27.5	.060" asbestos		40	1. Bipolar plates & screens Au plated. 2. New end plates that acc-omodate electrodes	150	26.9 to 28.9	Discontinued test because of perform-ance degradation.

TABLE XV (Cont'd)
SUMMARY OF TESTS ON 6 CELL NOMINAL 75 WATT UNITS

Construction								Results		
			Avg. Matrix		Avg. KOH					
S/N	O_2 Electrode	H_2 Electrode	Dry Wt. (gms)	Type & Thickness	Wt. (gms)	%	Comments	Total # cycls.	Final KOH(%)	Comments
109	Au plated Ni plaques with 14mg pt/cm^2	Au plated Ni plaques with 14 mg pt/cm^2	27.5	0.060" asbestos		40	Attempted to electrically isolate bolts	22	23 to 28.4	Exhibited poor performance from the start to end of test
110	American Cyanamid AB-6 9 mg Pt./cm^2	EOS - 20 mg Pt/cm^2	20.5	0.065" 90% KT and 10% asbestos	34	40	0.050 spacer	175	26.35 to 32.75	Test stopped because of performance degradation caused by extreme corrosion of bipolar plates
111	Electrodes taken from unit 110	EOS 20 mg Pt/cm^2	20.5	0.065 90% KT 10% asbestos	34	40	"	79		Poor performance O_2 electrodes may have been poisoned by corrosion products.
112	American Cyanamid AB-6 9 mg Pt./cm^2	"	20.5	0.065" 90% KT 10% asbestos	35	40	"	0		Cell stack leaked because of faulty matrixs.

TABLE XV (Cont'd)
SUMMARY OF TESTS ON 6 CELL NOMINAL 75 WATT UNITS

Construction								Results		
			Avg. Matrix		Avg. KOH					
S/N	O_2 Electrode	H_2 Electrode	Dry Wt. (gms)	Type & Thickness	Wt. (gms)	%	Comments	Total cycles	Total KOH(%)	Comments
113	American Cyanamid AB-6 9 mg Pt/cm^2	EOS 20 mg Pt/cm^2		50% KT 50% Teflon membrane sandwich between two 90% KT 10% asb. mats.	40	40				Leak between bipolar plate seals
114	American Cyanamid AB-6 9 mg Pt/cm^2	EOS 20 mg Pt/cm^2	31	Same type as unit 113	45	40	0.060" spacers	55		Unit failed because of recombination of gases
115	"	"	31.0	"	45	40	"	23.5		Unit failed when defective end plate allowed gases to mix.

objective. Data for cell voltage, cell pressure, and temperature during the continuous 48-hour test is shown in Figs. 94 through 98. Throughout the entire testing period, the differential pressure swing did not rise more than 0.2 to 0.3 psi. When the cell pressure reached 380 to 390 psi, the charger was automatically shut off, and the cell allowed to sit on open circuit until the cycling timer (set at a 65-minute charge duration) switched the unit to discharge.

After the 48-hour test, the cell was vented and allowed to sit at temperature on open circuit. In the following days, a number of other charge-discharge cycles were conducted to determine various performance capabilities, and to see if any deterioration in performance would occur. Figure 99 shows a series of discharge curves at different temperatures and loads. As can be seen, at a slightly higher temperature, the unit was capable of discharging continuously at 25 amps.

Figure 100 shows a test of cell capacity. The unit was charged until the cell pressure reached 350 psi, and then continually discharged at 15 amps until the cell voltage reached 3 volts. (It should be noted that at the end of charge period, the cell voltage was still relatively low, indicating that the mats contained additional water that could have been utilized for additional capacity.) Figure 101 shows a voltage vs. current curve for the unit, and the accompanying power output curve for this test. After 39 cycles, the unit exhibited slightly deteriorated performance on both charge and discharge. The unit was then disassembled and examined. The individual mats had gray to black discoloration adjacent to the hydrogen electrode and the rubber on the matrix edges had turned from green to black. Electrolyte squeezed from samples of two of the cells showed that the KOH concentration had dropped to approximately 13 percent from the 40 percent level. This drop in KOH concentration was later determined to have been caused by a combined reaction of the electrolyte, the asbestos, and oxidizable nickel.

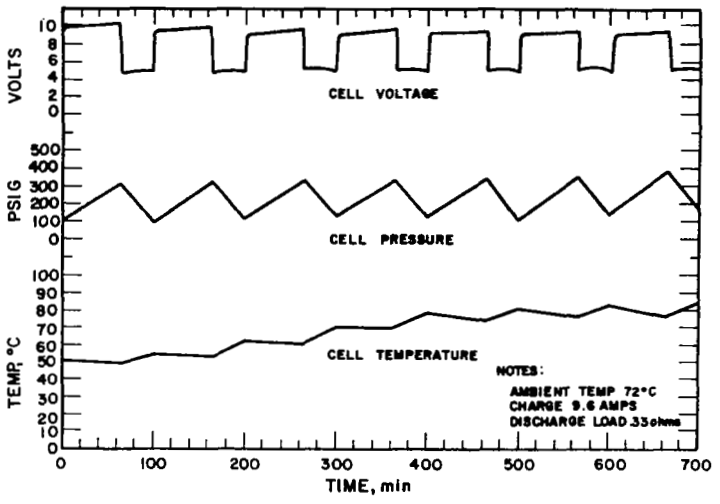

Figure 94. Continuous 48-Hour Cycling of 75 Watt Electrolytic Regenerative H_2-O_2 Fuel Cell

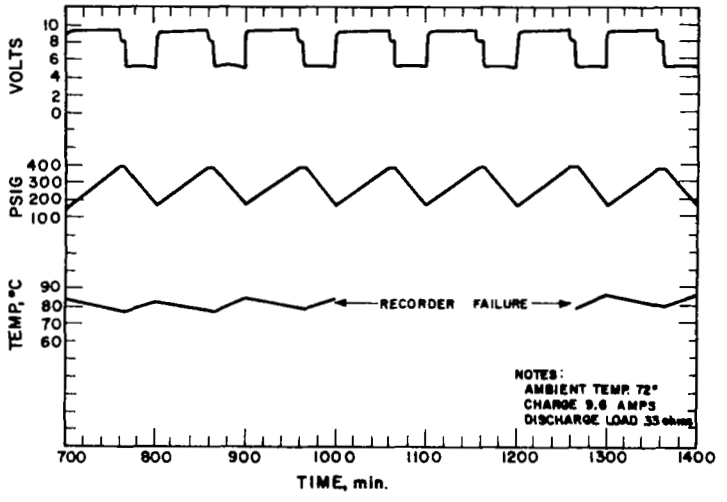

Figure 95. Continuous 48-Hour Cycling of 75 Watt Electrolytic Regenerative H_2-O_2 Fuel Cell

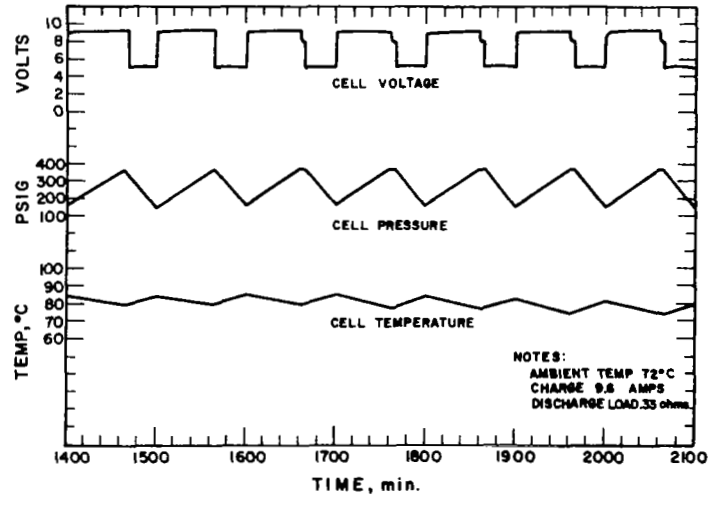

Figure 96. Continuous 48-Hour Cycling of 75 Watt Electrolytic Regenerative H_2-O_2 Fuel Cell

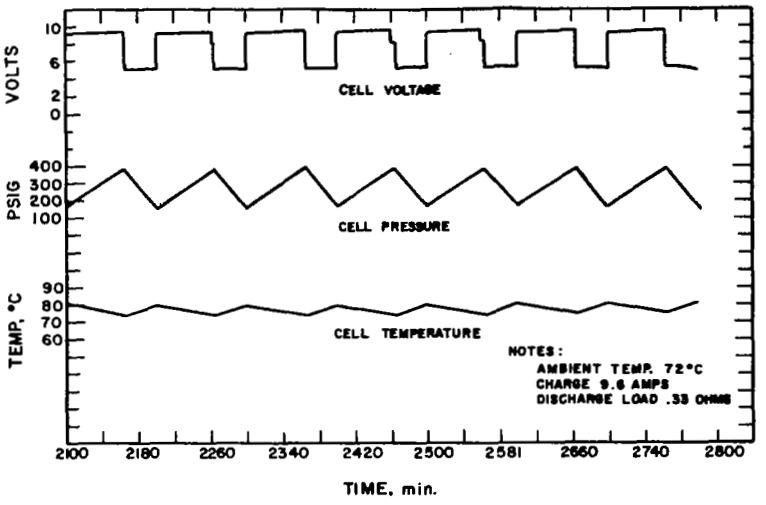

Figure 97. Continuous 48-Hour Cycling of 75 Watt Electrolytic Regenerative H_2-0_2 Fuel Cell

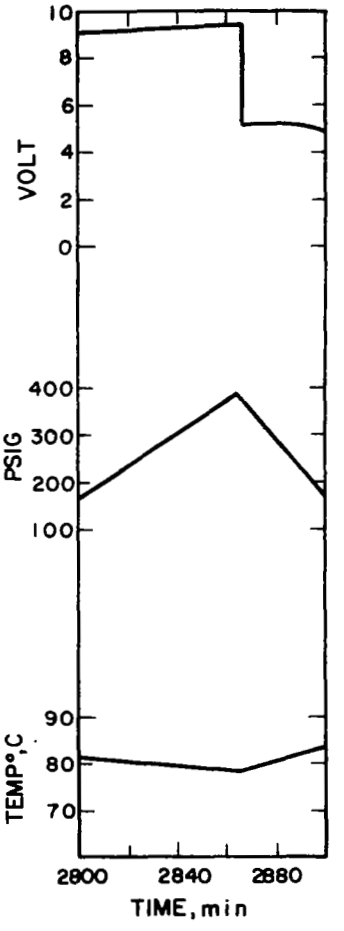

Figure 98. Continuous 48-Hour Cycling of 75 Watt Electrolytic Regenerative H_2-0_2 Fuel Cell

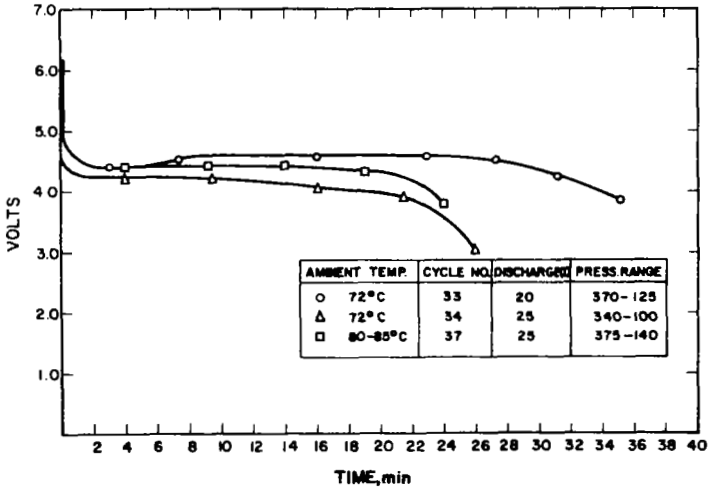

Figure 99. Discharge Data 75 Watt Electrolytic Regenerative H_2-0_2 Fuel Cell

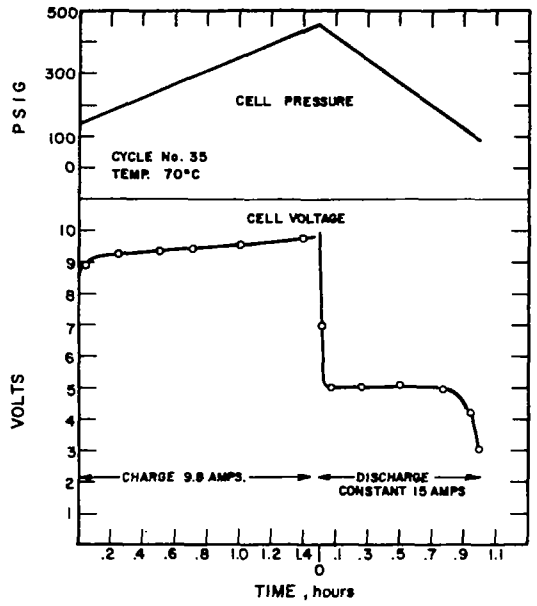

Figure 100. Capacity Test Cycling Data H_2-0_2 Electrolytic Regenerative Fuel Cell

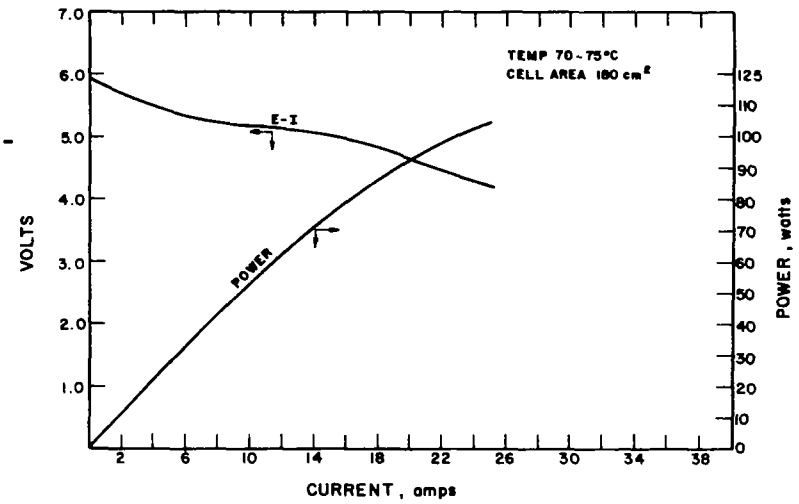

Figure 101. Performance Data 75 Watt (6 Cell) Electrolytic Regenerative H_2-0_2 Fuel Cell

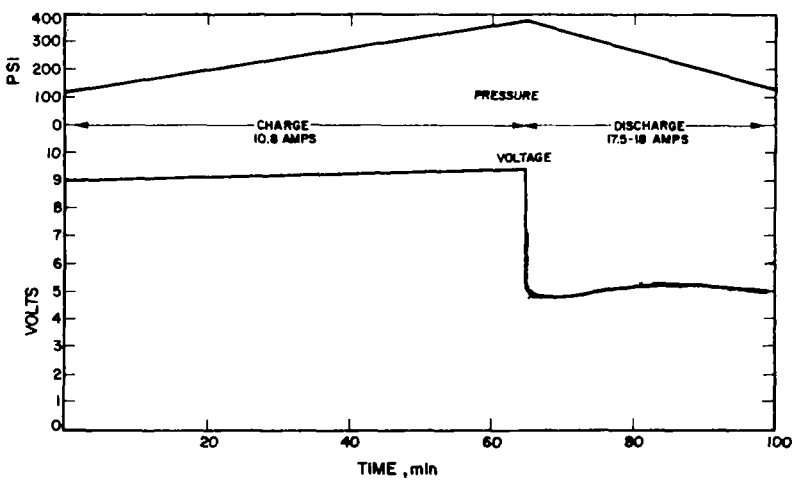

Figure 102. H_2-0_2 Regenerative Fuel Cell Cycle Performance of Six-Cell Unit S/N 102

S/N 102

A second multi-cell unit was later assembled using components identical with the first, with the following exceptions: (1) the oxygen electrodes consisted of a mixed catalyst, i.e., 10 mg of platinum, and 10 mg of palladium per sq. cm.; (2) insulating washers used on stack bolts were fabricated from glass epoxy rather than the previously used nylon to prevent relaxing of the washers during load at elevated temperatures; and (3) the mats contained no edge sealant.

The unit was cycled in the normal manner, i.e., 35-minute discharge, 65-minute charge. During the first two cycles, the temperature was gradually raised, and the unit discharged at about 18 amps. The unit was cycled only during an 8-hour day. Overnight the unit was kept at elevated temperature. Prior to shutdown, the unit was vented of all pressurized gas, and the following morning was repressurized to the final pressure level of the previous evening. Figure 102 shows a typical charge-discharge curve of the cell during the cycling period.

On the morning following the 16th cycle, when the cell was being pressurized to be put into service, it was noted that there was cross leakage between gas compartments and the cell was not capable of holding a differential pressure. A slight rise in internal temperature was also recorded (15°-20°) during this filling period. The unit was therefore disassembled and examined.

Examination of the disassembled unit revealed that the stack bolts had relaxed considerably. These bolts were initially torqued to 75 inch-pounds. Inspection of the unit revealed that the bolts were essentially at zero torque after the testing period. A relaxation of this type most probably released the compression on the mats and allowed gas leakage between cell compartments at the matrix periphery. Considering

this difficulty, it was decided to use some form of compression loading springs on the stack bolts to eliminate the relaxation problem in the future. The mats had a gray discoloration adjacent to the hydrogen electrode but were otherwise satisfactory, and they did not stick to the electrodes within the entire assembly. Analysis of electrolyte concentration, within two of the matrixes of the disassembled cell, revealed concentrations of 33 and 34 percent KOH.

S/N 103

Difficulties were encountered in the assembly of the six-cell unit due to leakage through the seals around the stack bolts. (A stat seal washer is used on the shank of the stack bolt to provide a seal between the hydrogen and oxygen compartments where the bolts go through the stack.) New bolts were used in assembly S/N 103 and were found to have undersized shanks, providing an inadequate seal along the shank. This leakage was determined in the standard checkout of the cell during assembly.

S/N 104

Different bolts were used in assembly of S/N 104 and were found to have scratches and imperfections along the shank which also resulted in leakage through the stack bolts. Finally, a set of specially machined bolts, with ground shanks, had to be fabricated to eliminate this difficulty.

S/N 105

After eliminating the leakage problem, SN 105 was assembled and installed in the test chamber. About 10 minutes after starting to charge the unit, a sharp drop in charge voltage of 1.5 volts was noted,

followed shortly thereafter by another 1.5 volt drop. This decrease was indicative of cell shorting. The unit was therefore disassembled and inspected. Two cells in the center of the stack were found to have shorted, but the cause of the short could not be determined. An interesting sidelight noted in the disassembly was the fact that the four cells that did not short had asbestos mats that were impregnated with the normal black discoloration. The shorted cells were not discolored. This implied that some electrochemical phenomenon had caused the discoloration.

S/N 106

Cell S/N 106 was reassembled without any further problems and subjected to test. The cell was cycled during the working day and was allowed to sit at temperature and pressure over night. A total of 70 cycles was accumulated. During the cycling period, there was a degradation in performance, as observed by an increase in charging voltage and a decrease in discharge voltage. Initial cell performance had an average discharge voltage of 4.9 volts and a charge voltage of 9.4 volts. At the 70th cycle, the performance had deteriorated to a point where the discharge voltage was 4.2 to 4.4 volts, and the charging voltage had increased to approximately 9.7 volts. This deterioration in performance is shown in Fig. 103. In addition, the cell exhibited a sharp dip in voltage at the start and end of discharge. To determine if the fall-off in performance was caused by gas mixing, gas samples from the hydrogen and oxygen compartments were taken at the end of the 70th discharge. Analysis for hydrogen in the oxygen sample and oxygen in the hydrogen sample by a gas chromatographic technique, showed that essentially no mixing had taken place.

Throughout the cycling, there was a gradual drift in differential pressure towards an increase in hydrogen pressure, indicating a

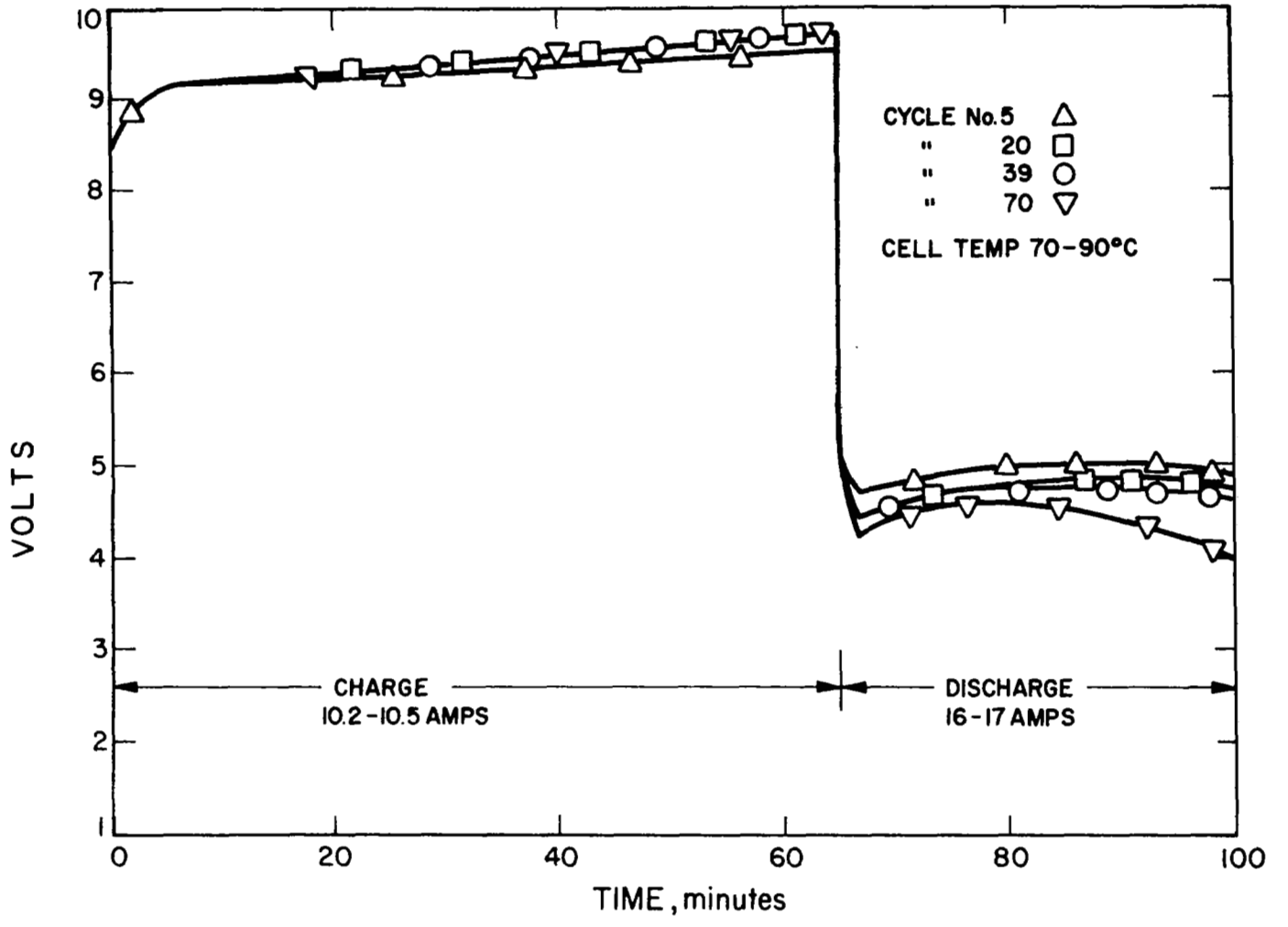

Figure 103. Performance of S/N 106, Six-Cell Regenerative H_2O_2 Fuel Cell

possible oxygen leak. On the 71st charge, an abrupt shift in the differential pressure was encountered. This was traced to a gross leak that had developed in the diaphragm of the pressure switch (located on the oxygen tank), which is used to shut off the charger when the cell comes up to pressure. Apparently, this diaphragm had a pinhole which allowed oxygen to escape during the early cycles. The pressure switch contained a brass pressure-sensitive diaphragm, which closed a set of contacts when the pressure acting on the diaphragm reached a pre-set level. A 110-volt source was applied across the contacts of the pressure switch, and was used to activate a relay which shut down the charger. Most probably, the hot oxygen that leaked into the pressure switch in conjunction with the arcing of the contacts increased deterioration of the diaphragm. The cell was at approximately 100 psi when the oxygen gas vented. However, the bellows and stack held the differential pressure that was created, and no other reactions took place. Considering the deteriorated performance, and the difficulties with the pressure switch, it was decided to discontinue the test and examine the cell stack.

Examination of the internal components of the multi-cell unit revealed moderate mechanical deterioration of the Pd/Pt oxygen electrodes. Analysis of samples of electrolyte, obtained from two cell mats, showed KOH concentrations of 34.2 and 34.4%. As in the past, the asbestos mats were substantially discolored with a blackish-blue color adjacent to the hydrogen electrode. There was no free liquid in the gas storage tanks, and no discoloration of the tank walls was noted. The deterioration in performance observed could have been the result of excessive handling of this particular cell assembly since it had been assembled, disassembled, and reassembled a number of times due to the gas leakage problems around the stack bolts.

S/N 107

Considering the results of S/N 106, an identical cell assembly (S/N 107), was constructed and put on test. The only difference between this unit and the prior unit, was that this unit was assembled in the nickel-plated aluminum gas tanks. This cell was cycled continuously on the standard 65 minute charge, 35 minute discharge regime for 353 cycles. The test set-up contained a pressure switch, which automatically shut down the cell charger when the cell pressure reached approximately 385 psi. Throughout the first 200 cycles, there was only a slight change in performance, with voltage on charge increasing slightly, and voltage at the end of discharge decreasing slightly. From the 200th to the 342nd cycle, charge voltage increased gradually and discharge voltage decreased gradually. This change in voltage performance is shown in Figs. 104 and 105. Figure 104 is a family of curves at various cycles. Figure 105 is a plot of the extreme voltage points to show the rate of deterioration as a function of cycles. Up to the first 200 cycles, the deterioration rate appeared to be at one level. Beyond that cycle, there was a more rapid fall-off in performance, with the slope for the end of discharge voltage being greater than the other deteriorating modes.

At the 343rd cycle, which occurred in the middle of the night, data indicated that an internal reaction took place. From that point on, the performance was considerably worse, as shown in Fig. 104. After 353 cycles, the test was discontinued, and an impedance measurement was made of the cell at operating temperature. It was found to be 0.034 ohm. The assembly was allowed to cool to room temperature, and another resistance measurement was made. In this case, it was found to be 0.098 ohm. This value was considerably larger than the initial resistance at room temperature which was 0.057 ohm.

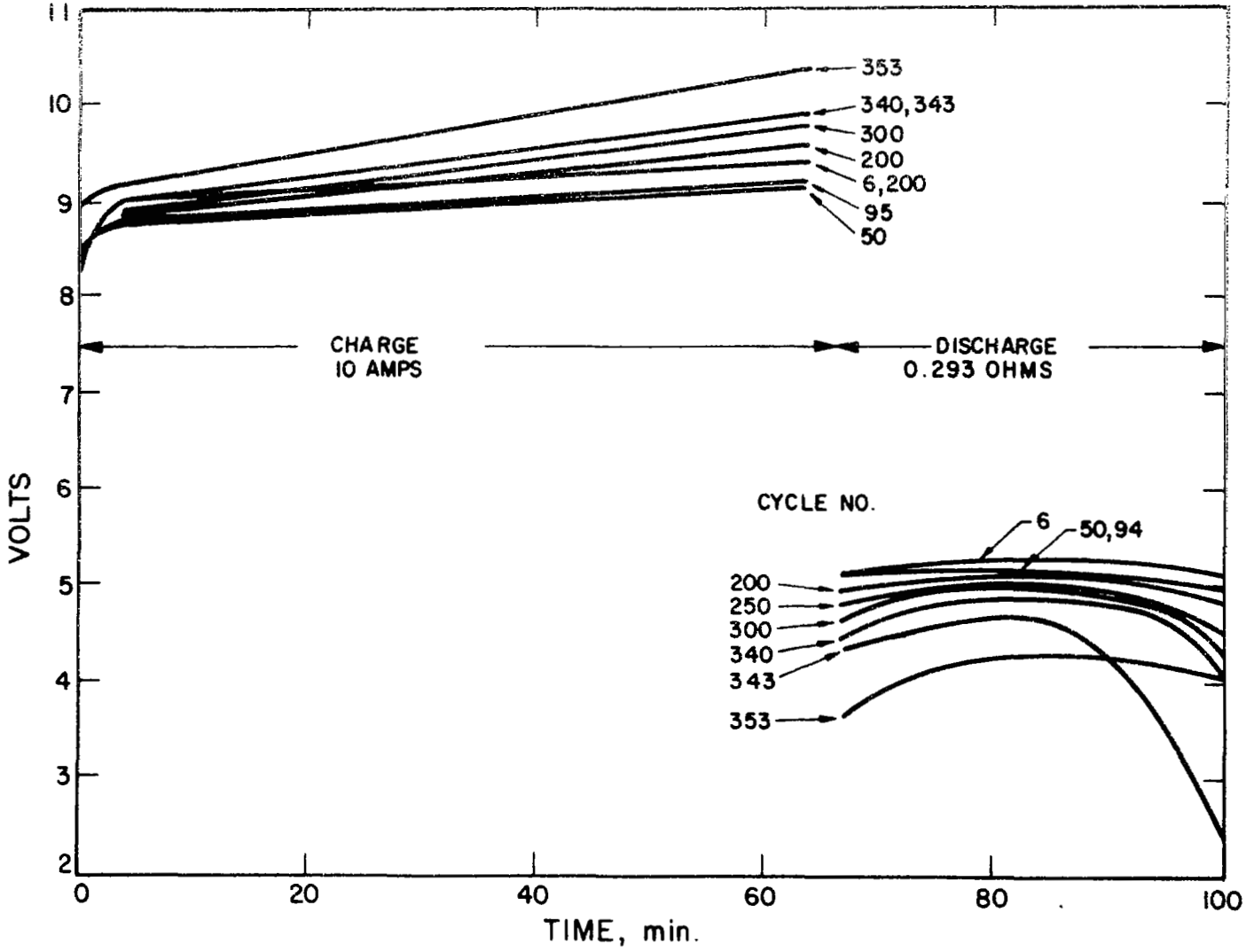

Figure 104. Voltage Performance Data at Different Cycles of Regenerative Fuel Cell (S/N 107)

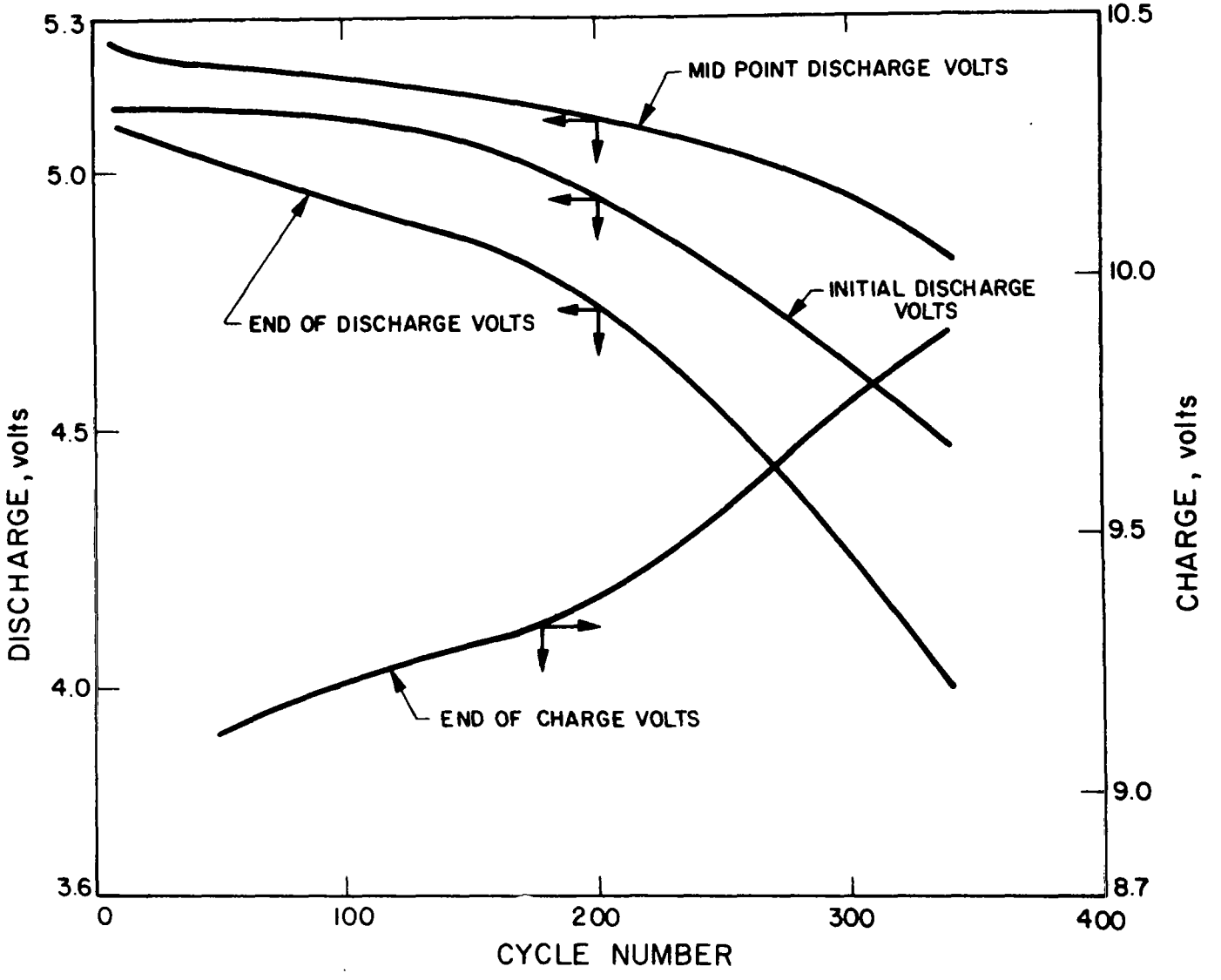

Figure 105. Effect of Fuel Cell Voltage as a Function of Cycling (S/N 107)

Examination of the internal components revealed that the inside of the bellows, which contained hydrogen, had rusted on the surface, apparently due to long term contact with KOH vapors. The outside of the bellows and the oxygen compartment showed a black to green dis - coloration, indicating that a chemical reaction took place in that compartment. The stack bolts had residual torques of 25 to 30 inch-pounds. Initially, these bolts had been torqued to 70 inch-pounds. The Belleville springs on the ends of the stack bolt were still fully compressed.

Taking apart the cell stack, it was found that the oxygen back-up screen and bipolar plate had a black discoloration. The bipolar plates and screen from the hydrogen electrodes looked perfectly clean. The oxygen electrodes in four of the cells had crumbled away along the edge, which probably was due to chemical deterioration. However, in other areas the structure of the oxygen electrode appeared fine. The asbestos mats had a black discoloration adjacent to the hydrogen electrodes and were relatively clean facing the oxygen electrodes. Analysis of all the mats in the cell stack revealed final KOH concentrations to be in the range of 23 to 25 percent.

The performance data showed two problem areas: (1) gradual degradation in performance, and (2) long-term gas mixing that led to an internal reaction that further degraded performance. Gradual degradation in performance could have been caused by a number of problems. Most probably the gradual degradation was caused by structural deterioration of the oxygen electrode, and/or gradual loss of KOH, due to reaction with asbestos matrixes and a nickel hydroxide side reaction within the cell. The cause of the slow gas mixing that lead to the chemical reaction was believed to have been due to leakage through the spacers.

Cycle life performance was considered very encouraging, and indicated certain modes of deterioration that were investigated further. It

appeared that additional studies on the asbestos mat were justified. For long term use, a nickel substrate for the oxygen electrode was not desirable, since it apparently gradually oxidizes with cycling and structurally deteriorates. It also can be related to the electrolyte consumption, since the formation of certain nickel oxides could tie up OH^- ions. These possibilities were investigated further in single cell tests.

S/N 108

The 6-cell unit, designated S/N 108, was similar in construction to S/N 107 with the following exceptions:

a. The electrodes on both the hydrogen and oxygen sides were gold plated nickel plaques platinized to 14 mg/cm^2.

b. The backup gas distribution screens behind the electrodes and the bipolar plates were gold plated to prevent possible oxidation of the nickel surfaces

c. The hydrogen and oxygen end plates employed were of the type used in the 34-cell design that allowed for the incorporation of the end stack electrodes directly on the end plate.

d. A bellows with a modified flange to accommodate this end plate.

e. A new Teflon bellows stop to compensate for stack length changes due to the above modifications.

The cell was operated for 10 cycles, at which time a short developed that fully discharged the unit to 0 volts. The short was traced to a failure of the insulation on the main feed-through terminal through the stack. This terminal consisted of a 1/4-inch copper rod that was sealed and insulated from the tank by means of a Teflon ring. Apparently, this ring gradually flowed, allowing the copper rod shank to short out. Difficulties with this fitting had been encountered in the past, and it was decided to replace this with a different feed-through that employed a 1/8-inch copper rod and allowed for a much thicker Teflon insulation ring.

The feed-through terminal was replaced and the cell was once again subjected to test. The cell was operated on an intermittent basis due to gradual differential pressure buildups that indicated possible gas leakage. The voltage performance of the unit is presented in Fig. 106. As can be seen, there was a gradual degradation in performance as the cycling continued.

Testing of the unit was stopped after 150 cycles at which point the unit was disassembled and examined. It was found that a buildup of corrosive products had developed on the end of one of the stack bolts, which was moist with liquid. Apparently, liquid was squeezed out of the stack and collected across the insulating washer between the bellows flange and the stack bolt. The stack is designed such that the stack bolts are electrically in contact with the opposite end plate and the full stack potential exists between the bellows flange and the bolts, which is insulated by a fiber-glass washer. Apparently, moisture bridged this washer and set up local corrosion and electrolysis in this area. The source of the moisture was not determined, but it was decided in future units to insulate the stack bolts on both ends of the stack to prevent this. All other internal components appeared clean and showed no visual signs of corrosions. Gold plating of the bipolar plates and internal hardware apparently quite effectively prevented any oxidation or corrosion. As in the past, the asbestos matrixes had a gray to black discoloration adjacent to the hydrogen electrode. Samples of asbestos from the 1st, 2nd and 5th cells were analyzed for KOH concentration and were found to be 26.9%, 28.9%, and 29.5%, respectively.

S/N 109

To evaluate the new insulated bolts and to obtain additional test data, a second six-cell unit utilizing the same type of electrodes, S/N 109, was assembled and subjected to test. The only difference

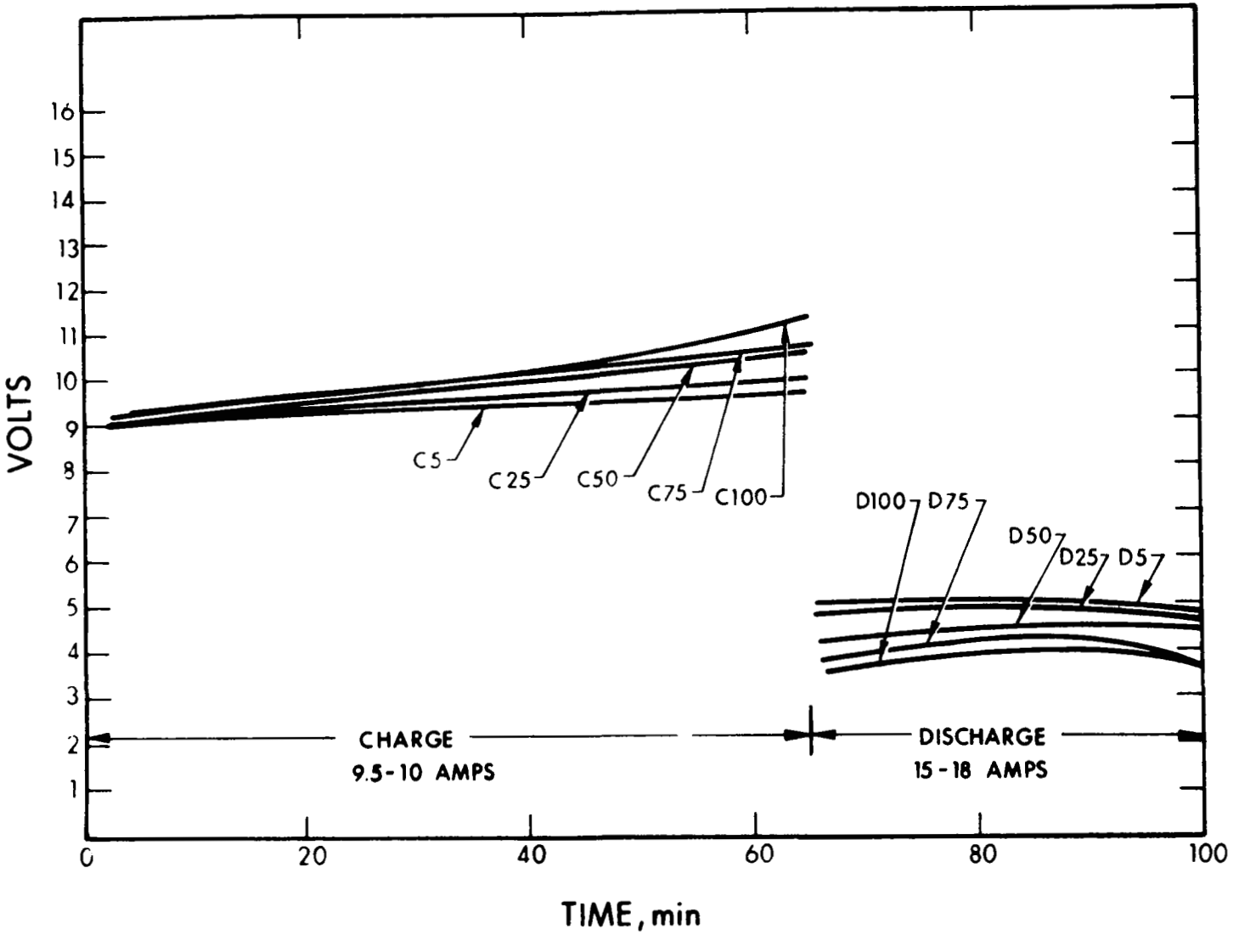

Figure 106. Cycling Performance of Six-Cell Regenerative Fuel Cell S/N 108

between multicells 108 and 109 was that a thin Teflon sleeve was used on the stack bolts where they fed through the hydrogen end plate to isolate the stack bolts electrically. The unit was subjected to the standard test cycle, and from the start exhibited poor performance. The unit was cycled 22 times and the test was stopped to evaluate the cause of the poor performance. An examination of the disassembled unit revealed no obvious defects that could have caused the low performance. Analysis of the final electrolyte concentrations in the matrixes revealed the following:

Cell No. 1 - 27.9%
Cell No. 2 - 27.0%
Cell No. 3 - 23.3%
Cell No. 4 - 23.0%
Cell No. 5 - 26.35%
Cell No. 6 - 28.4%

The variation in final electrolyte concentration and the relatively low values obtained in cells 3 and 4 indicated the possible cause for the poor performance. Once again, the asbestos matrix material had reacted with the electrolyte and probably caused the poor performance.

S/N 110

Based on the satisfactory results with the potassium titanate matrixes in the single cell tests, a new six-cell unit S/N 110, was assembled for test with these types of mats. The individual cells were made up of American Cyanamid AB-6 oxygen electrodes, EOS platinized nickel plaque hydrogen electrodes, and 90 percent KT, 10 percent asbestos mats.

The cycling performance of this unit is shown in Fig. 107. As can be seen, there was a gradual increase in the charging voltage and a decrease in the discharge voltage. The rate of degradation observed was considerably greater than that observed with single cells employing the electrode/matrix combination that was utilized in this unit. Due to the degradation in performance, the test was stopped at the 175th cycle and the unit was disassembled. An examination of the internal components of the cell revealed that a number of the bipolar plates had areas where severe corrosion had taken place. Apparently, there were imperfections in the electroless nickel and gold plating that was employed over the magnesium plates, KOH had contacted the magnesium, resulting in corrosion and pitting of the plates. There were substantial quantities of a corrosion product throughout the backup screens behind the oxygen electrodes. This muddy sludge could possibly have reduced gas access to the back side of the electrodes. In addition, the corrosion and reaction of the electrolyte with the bipolar plates could consume electrolyte which also would result in poor performance. A chemical analysis of the sludge revealed that the heavy metal content was primarily nickel, copper, and magnesium; this confirmed the observations that the sludge resulted from the corrosion of the bipolar plates. In the plating of the magnesium plates, a copper flash is employed prior to the electroless nickel plate. The matrixes from the unit were analyzed for final KOH concentration and were found to be as follows:

No. 1 - 27%
No. 2 - 26.35%
No. 3 - 30.25%
No. 4 - 32.75%
No. 5 - 29.35%
No. 6 - 26.9%

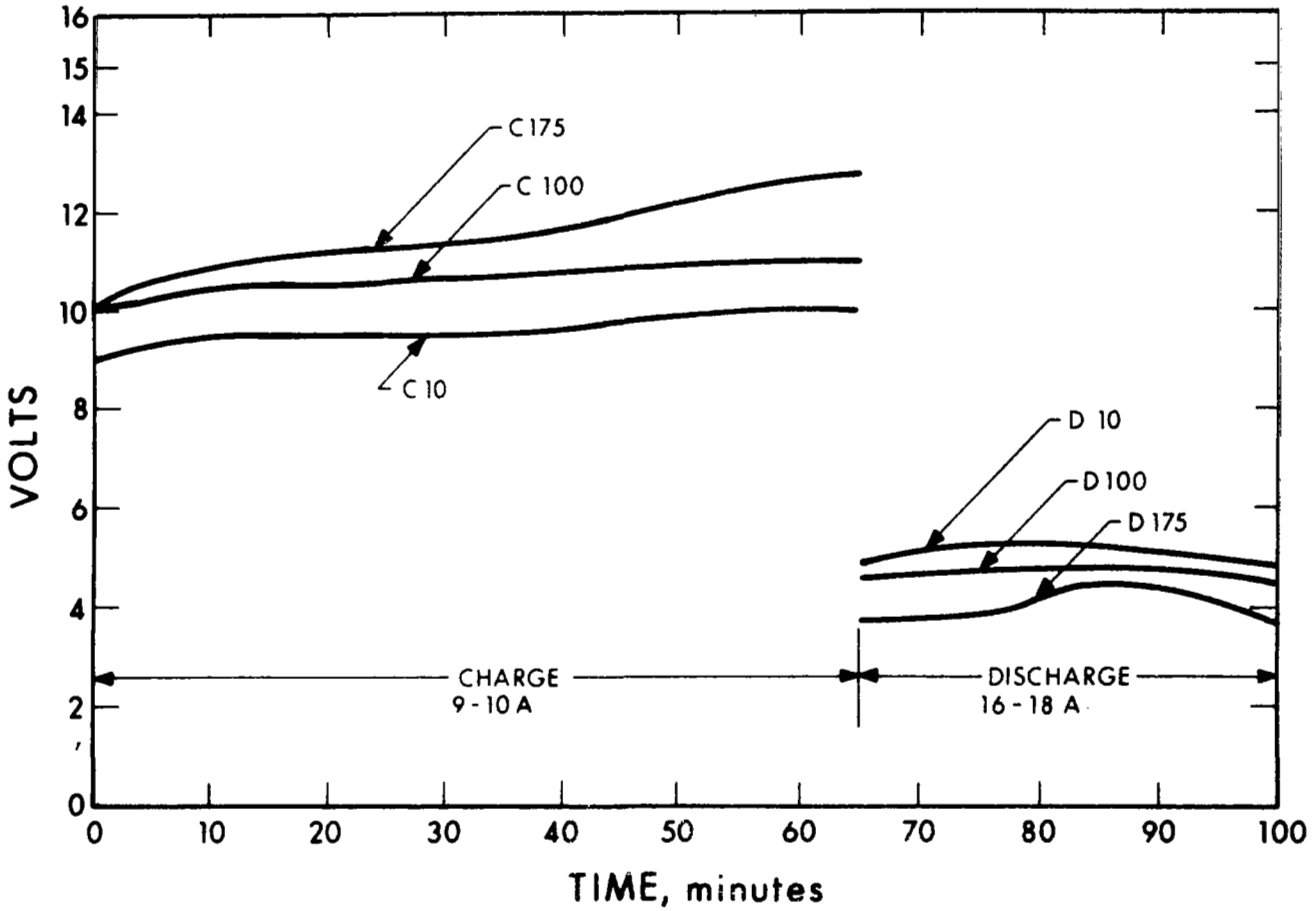

Figure 107. Cycling Performance of Six-Cell Unit S/N 110

The variation and also reduction in the electrolyte concentration observed in these tests indicated that the corrosion reaction resulted in some electrolyte consumption.

S/N 111

To further evaluate the cause of deterioration, the American Cyanamid oxygen electrodes were salvaged from the unit and reassembled in a new 6-cell unit, S/N 111, with new matrixes and hydrogen electrodes. This unit was put on test and on initial charge rose rapidly to 12 volts (2 volts per cell) and on discharge ran at 4 volts at 10 amps. The extremely poor performance of this unit indicated that the oxygen electrodes had somehow been poisoned in the prior cell. This poisoning could have been a result of the corrosion products of the bipolar plate.

S/N 112

Platinized nickel plaque hydrogen electrode configuration and a matrix of KT with 10 percent asbestos, a new 6-cell unit, S/N 112, was built to be subjected to test. During checkout of the cell stack, the unit was subjected to slight differential pressure to determine if any cross leakage existed. This checkout revealed an appreciable cross gas leakage through the matrixes which would have resulted in a slow recombination within the stack; the unit was therefore disassembled. An examination of the matrixes revealed no obvious area where the cross leakage was occurring, except that many of the matrixes were found to be thinner in the center than on the edges. A review of the process technique of the matrixes revealed that a slight convex Buchner funnel was utilized in the filtrate formation of the matrixes which would result in less material being in the center of the matrix. To alleviate this problem, a new funnel with a flat inner plate was used for fabrication of future matrixes.

S/N 113

At this time, a sandwich matrix had been developed and had shown good performance in single cell tests. Therefore, the next six-cell unit contained this structure. The oxygen electrodes were American Cyanamid type AB-6, and the hydrogen electrodes were EOS 20 mg Pt/cm^2 carbonyl nickel plaques. The matrixes consisted of 50-percent KT/50-percent Teflon pasted membrane sandwiched between two 90-percent KT/10-percent asbestos mats. The assembled stack failed to pass the leak test; gas leakage occurred at the seal between two bipolar plates and separators. The cell was disassembled and the components cleaned. Components were then prepared for another six-cell assembly.

S/N 114

To retest the sandwich matrix, S/N 114 was assembled. The oxygen electrodes were American Cyanamid type AB-6, and the hydrogen electrodes were EOS 20 mg Pt/cm^2 carbonyl nickel plaques. The matrixes consisted of 50-percent KT/50-percent Teflon pasted membrane sandwiched between two 90-percent KT/10-percent asbestos mats. Forty grams of 40-percent KOH was added to the matrixes and 60-mil spacers were used. As Fig. 108 shows, the cell ran well for 51 cycles then the performance became erratic and the voltage dropped to zero after cycle 55. This occurred over a weekend while the cell was unattended. Upon disassembly it was ascertained that a fast recombination of gases occurred on the oxygen side of the cell. No cause for this gas leakage was determined.

S/N 115

The final six-cell unit, S/N 115, was assembled and consisted of oxygen electrodes of the American Cyanamid AB-6 type, and EOS hydrogen electrodes of 20 mg Pt/cm^2 carbonyl nickel plaques. The matrixes

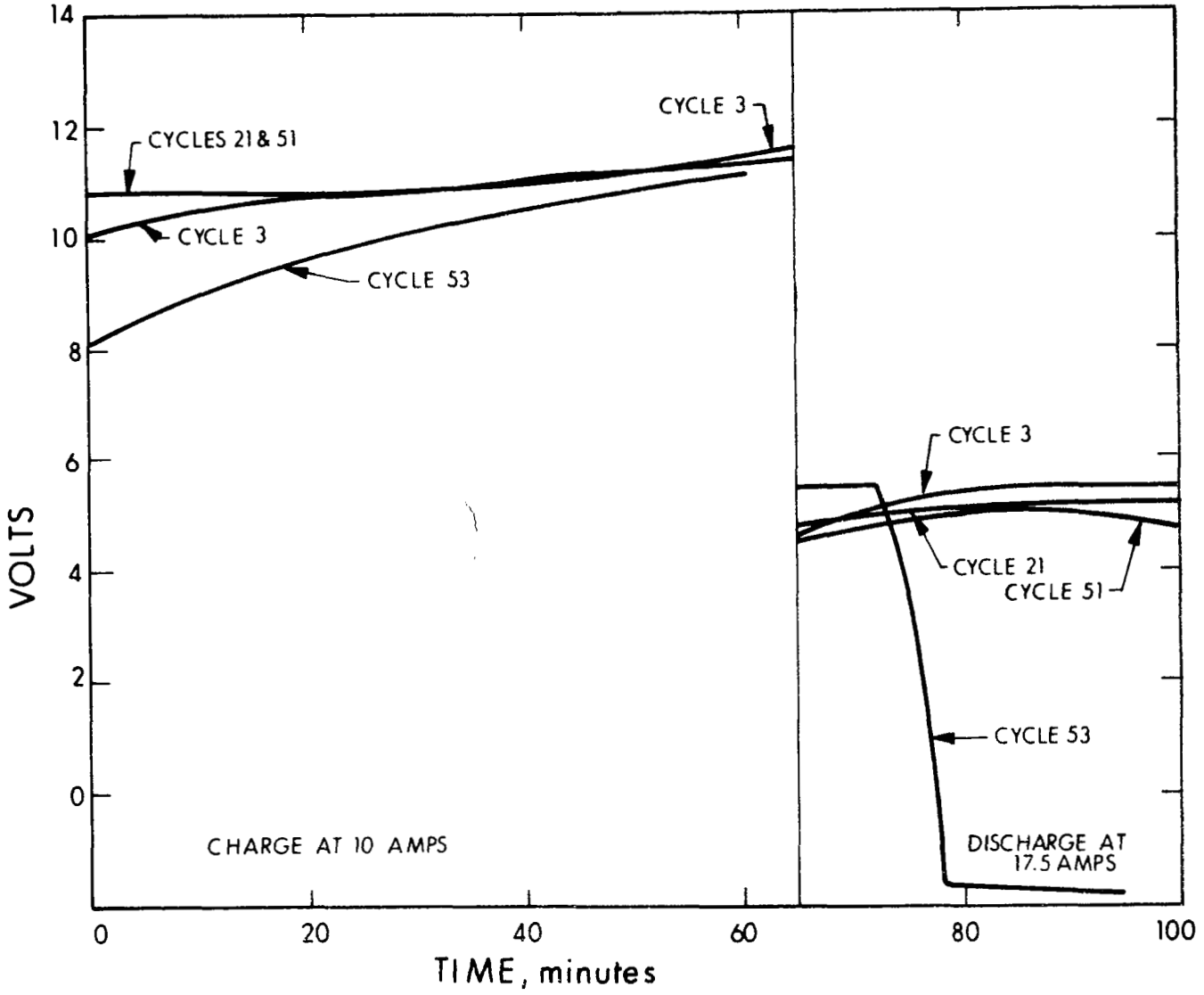

Figure 108. Cycling Performance of Six-Cell Unit S/N 114

consisted of 50-percent KT/50-percent Teflon pasted membrane sandwiched between two 90-percent KT/10-percent asbestos mats. Forty grams of 40-percent KOH was added to the matrixes and 60-mil spacers were used.

As can be seen in Fig. 109, the cell ran well with no degradation for 235 cycles. Near the end of charge, at cycle 236, the cell pressure rose from 350 psi to 450 psi in less than a second. The cell voltage rapidly fell to zero. When taken apart, it was evident that the cell stack was damaged by an extremely fast recombination of the gases. Upon inspection the cause of failure was found in the hydrogen end plate. In Fig. 110, a photograph of the end plate, the arrow indicates the spot on the inside sealing edge of the plate that is warped upward. The warp was caused by the formation of magnesium oxide from exposed magnesium and KOH. The swelling forced the end plate and bipolar plate apart, eventually allowing the gases to rapidly mix and recombine. This plate had been previously used and reworked by patching holes in the nickel plate with silver epoxy, and then plating gold over the patch. Figure 110 shows that not one of the patches held and corrosion occurred at all the spots repaired.

This ended the six-cell tests for the program and pointed up that significant progress had been made. A number of mechanical difficulties were encountered with the six-cell assemblies, but through an evolutionary process, improvements had been made.

The internal gas leakage problem was eliminated by the use of integral gas port seals on the bipolar plates, incorporation of rigid flat plate spacers, and replacement of the rubber pressure balancing diaphragm by a stainless steel bellows. Enlarging the gas ports and providing gas distribution paths behind the electrodes eliminated large concentration polarization effects at high current densities. The replacement of the asbestos matrix with potassium titanate

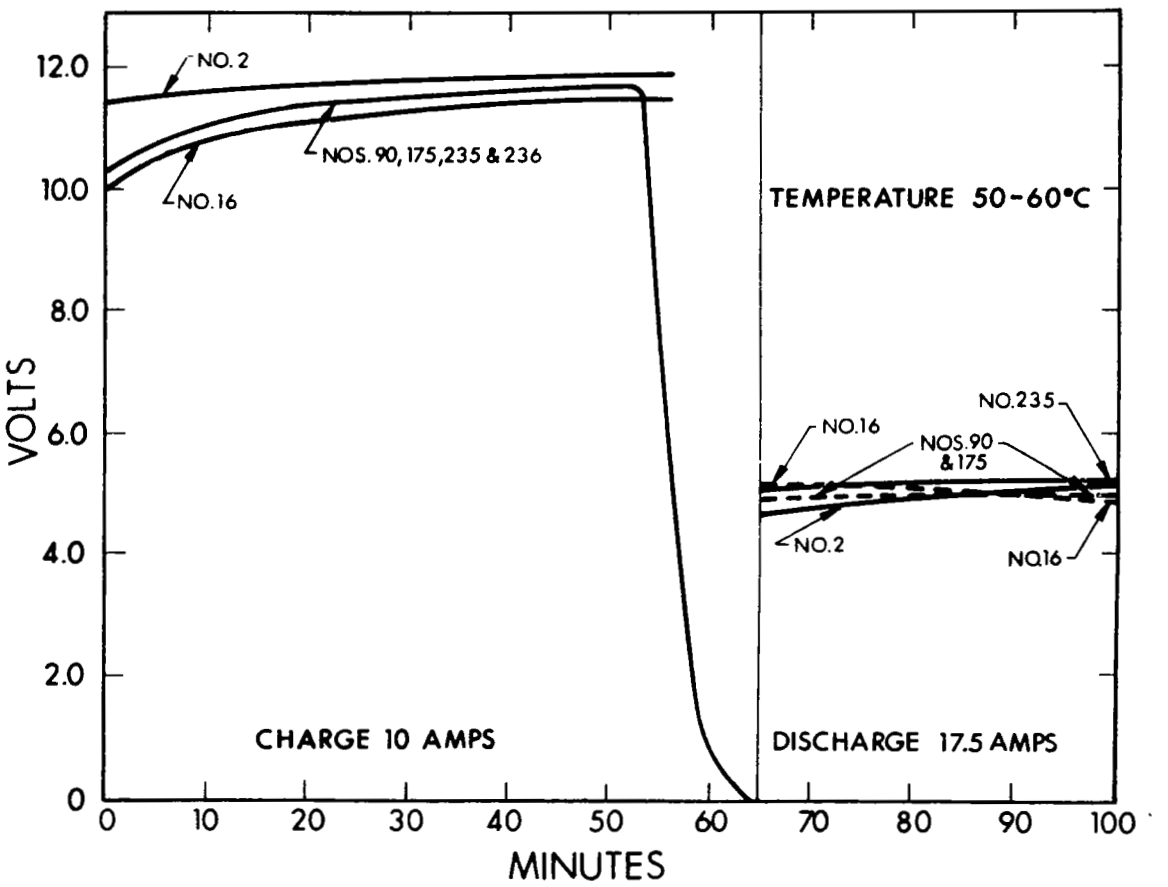

Figure 109. Cycling Performance of Six-Cell Unit S/N 115

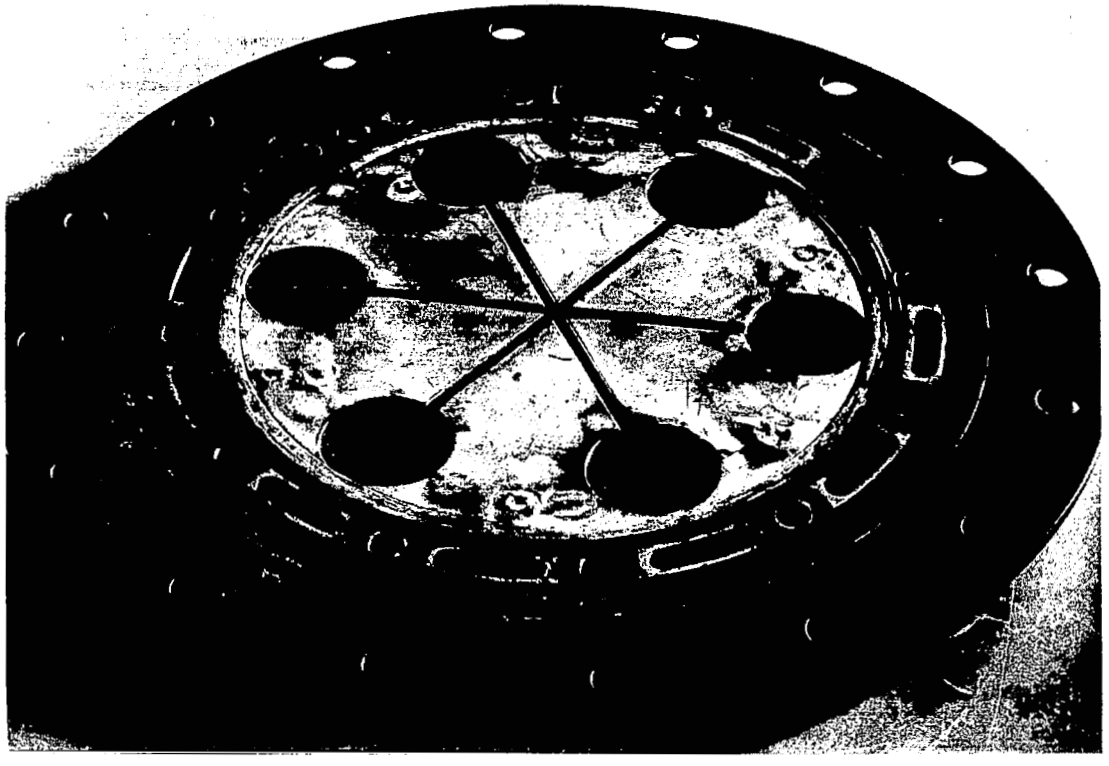

Figure 110. H_2 End Plate From Six-Cell Unit S/N 115

matrixes was the most significant improvement. Utilization of new matrixes should extend cell life beyond the loss cycles. The final unit, S/N 115, cycled for 235 cycles with virtually no degradation in performance. The cells with asbestos matrixes characteristically began to degrade in performance after the first 10 cycles and degradation was extreme after the first 100 cycles. Corrosion of the bipolar plates and other components continues to be a problem that needs further work. This problem might be eliminated by fabricating the bipolar plates from a suitable plastic material.

SECTION 7

MULTI-CELL 500-WATT DESIGN AND TEST

7.1 FIRST GENERATION

The first prototype design for the 500-watt, 600-watt-hour multicell unit consisted of 34 series-connected cells employing the bipolar plate stack arrangement developed in Phase I of the program. Figure 111 is an assembly drawing of the complete unit. The self-contained unit utilizes tanks that contain the stored hydrogen and oxygen. The tanks are capable of storing sufficient gas to deliver 21.5 ampere-hours. The design is based on a pressure cycle of 50-500 psig. Also included within the cell is a pressure compensating bellows to minimize differential pressures between the hydrogen and oxygen compartments. The first prototype tankage was fabricated from stainless steel. The second prototype incorporated nickel-plated aluminum tanks of the same geometry as that shown in Fig. 111. The gas tanks were hydrostatically tested to 800 psig and found to be acceptable. The components and a stack assembly are shown in Figs. 112 and 113.

A 500-watt, 34-cell battery was assembled and no problems were encountered during the assembly. However, during a routine checkout for cell stack gas leakage, a number of very small leaks were noted on the external diameter of the stack. Attempts to stop the leakage by compressing the cell stack further were unsuccessful. Visually, it appeared that the leaks were in the glass Teflon insulating spacers. To evaluate this possibility, several tests were made using both new and used spacers. It was definitely established that certain of the spacers leaked, probably due to poor glass-Teflon bonding.

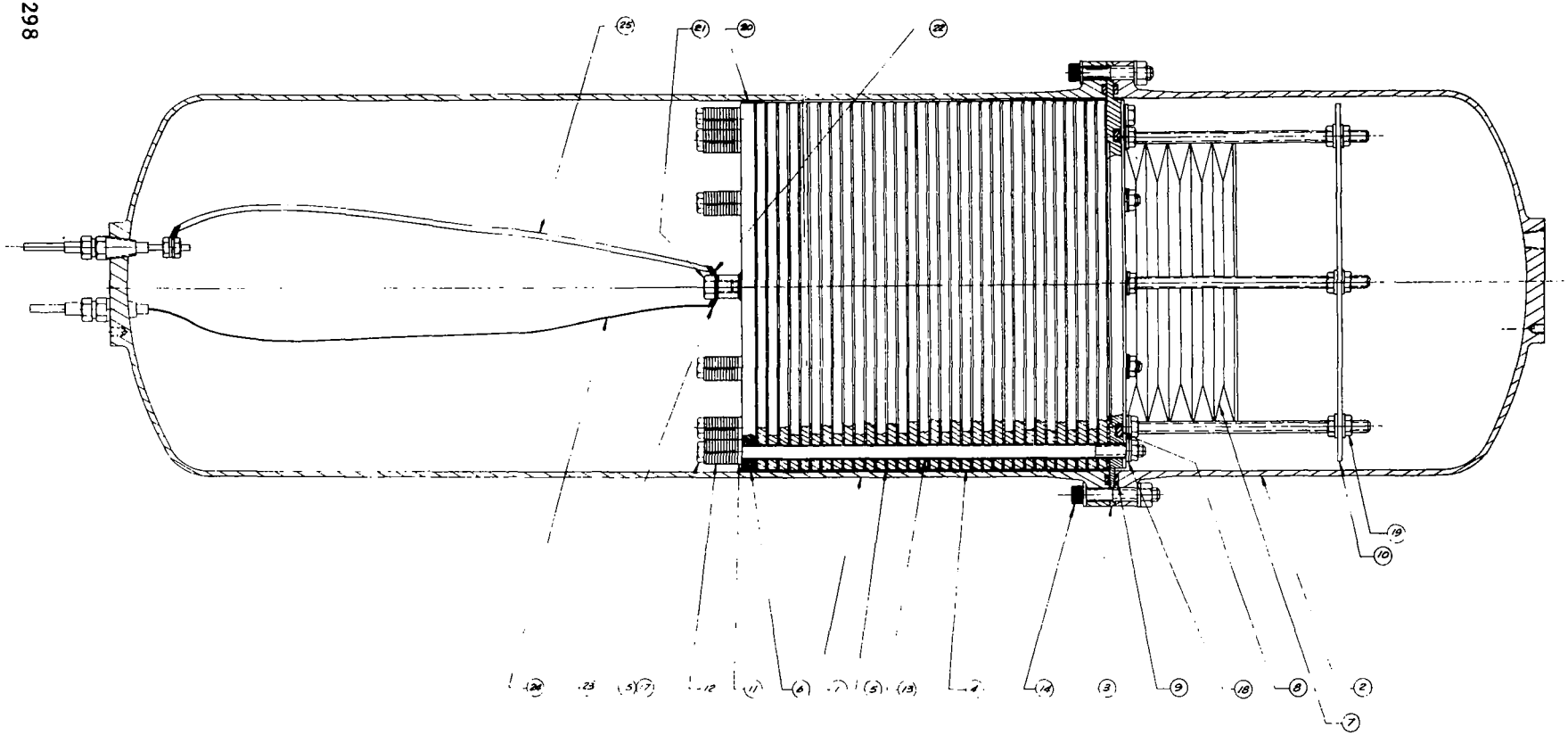

A/R	25		WIRE	#8		
A/R	24		I.C. THERMOCOUPLE WIRE			
1	23	MS25036-54	TERMINAL LUG	1/4		
2	22	MS20659-9	TERMINAL LUG	1/4		
1	21	MS35314-1	SCREW-HEX HD MACH	1/4-28 x 3/8	ALUM	
A/R	20		INSULATOR	5 MIL	TEFLON MESH	
30	19		NUT-PLAIN HEX	1/4-28	TITANIUM	
12	18		WASHER, INSULATING	.265 I.D.	FIBERGLASS	
74	17	AN960-D416	WASHER, FLAT	.265 I.D.	ALUMINUM	
3	16	G13651-2	STACK BOLT	1/4-28 x 1 1/2	GOLD-Tg Alum. Alc.	
3	15	G13651-1	STACK BOLT	1/4-28 x 9/16	GOLD-Tg ALUM. AL.	
16	14		SCREW, ALLEN HD MACH	1/4-28 x 1-3/4	TITANIUM	
12	13	G13564	BOLT INSULATOR		TEFLON	

120	12	85/8-1/4 O.S.	BELLEVILLE SPRING			
2	11	PARKER 2-247	STAT-O-SEAL	.247 I.D.	CR65	
1	10	W36146	BELLOWS STOP	.437 x .875 DIA	GOLD-Tg ALUM. AL.	
2	9	PARKER 2-247	TANK O-RING	8.234 I.D.	COMPOUND 77-545	
1	8	PARKER 2-361	END PLATE O-RING	5.975 I.D.	COMPOUND 77-545	
1	7	G13650	BELLOWS ASSY			
1	6	W3047	H_2 END PLATE		AZ31B	
34	5	G13652	SEPARATOR		.010 FILLED TEFLON	
33	4	W3045	BI-POLAR PLATE		AZ31B	
	3	G13651	O_2 END PLATE			
1	2	W3556-2	O_2 TANK		GOLD Tg	
1	1	G13556-1	H_2 TANK		GOLD-Tg	

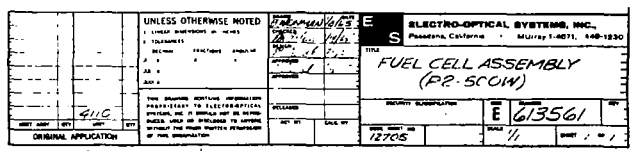

Figure 111. Fuel Cell Assembly

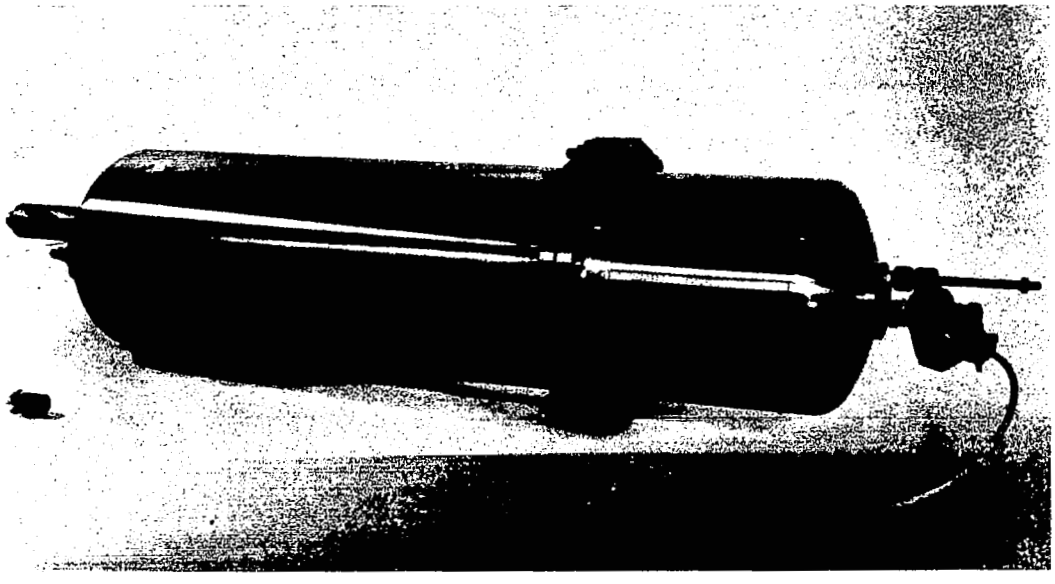

Figure 112. 500-Watt Regenerative Hydrogen-Oxygen Fuel Cell Assembly

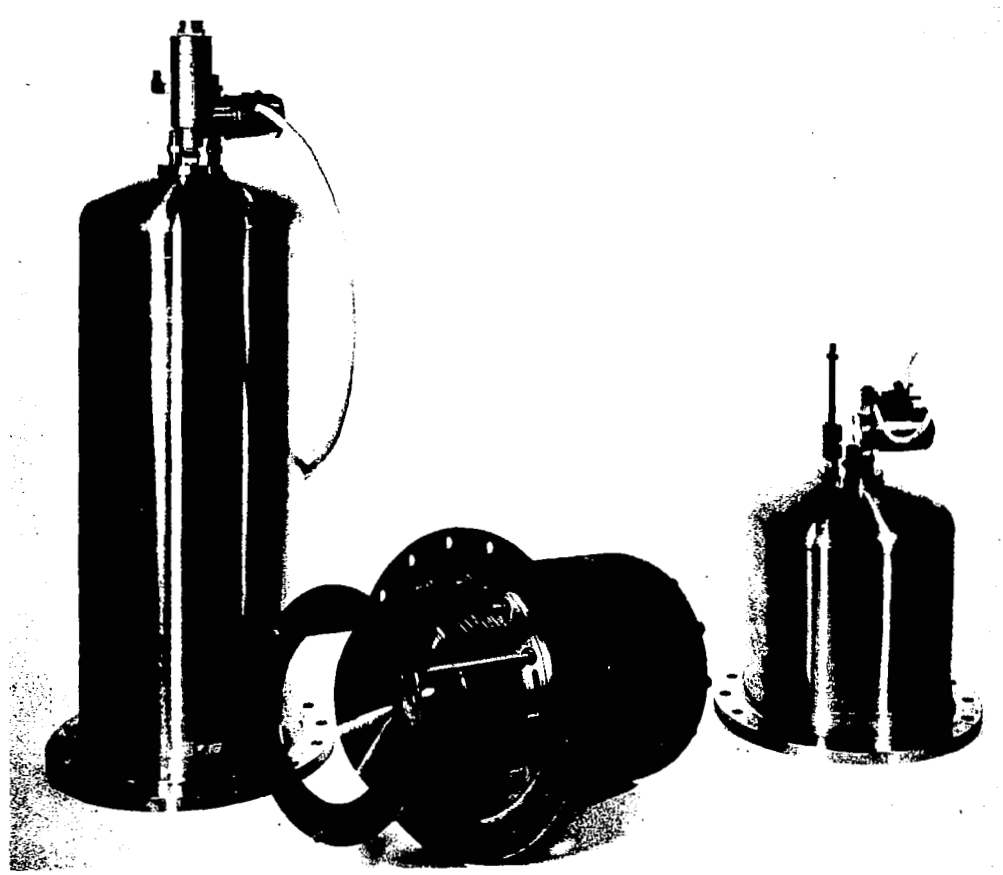

Figure 113. 500-Watt Regenerative Hydrogen-Oxygen Tanks and Cell Stack

Due to this leakage problem, glass-Teflon spacers were eliminated. Instead, a glass-epoxy material which had been used successfully in single cell tests was substituted.

A new 34-series cell, 500-watt prototype was assembled incorporating these separators. Standard EOS platinized porous nickel plaque electrodes were used. The intent of the assembly was to use existing hardware to check out the mechanical, thermal, and electrochemical characteristics of the 500-watt design, and to debug the readout instrumentation. This unit, designated cell 1002-34, incorporated stainless steel gas tanks.

The cell was placed in the test chamber and put on standard cycle, 65 minutes charge at 10 amps, and 35 minutes discharge at a nominal current of 17.5 amps. The cell performed satisfactorily during the initial cycles; however, during the 7th and 8th cycles a wiggle in the cell voltage was observed. In the middle of the 8th discharge, an internal short developed. It was later found that the short was between the positive terminal bus and the negative tank wall at the insulated feed-through connector.

During cycling, substantial temperature gradients ($\approx 40^{\circ}C$) were encountered between the cell stack and the end of the hydrogen tank where the feed-through was located. Typical temperatures during discharge were $110^{\circ}C$ at the hydrogen end of the cell stack and approximately 70° at the tank end. This temperature gradient apparently caused condensation of moisture in the cool end of the tank. The condensed water apparently caused arcing at the copper bus, resulting in a metallic short from the bus to the grounded feed-through connector. Figure 114 shows data for saturation pressure of KOH solutions vs. temperature and concentration. It shows that approximately $30^{\circ}C$ temperature differences can be tolerated without exceeding the saturation pressure of 40 percent KOH solution and water, and therefore,

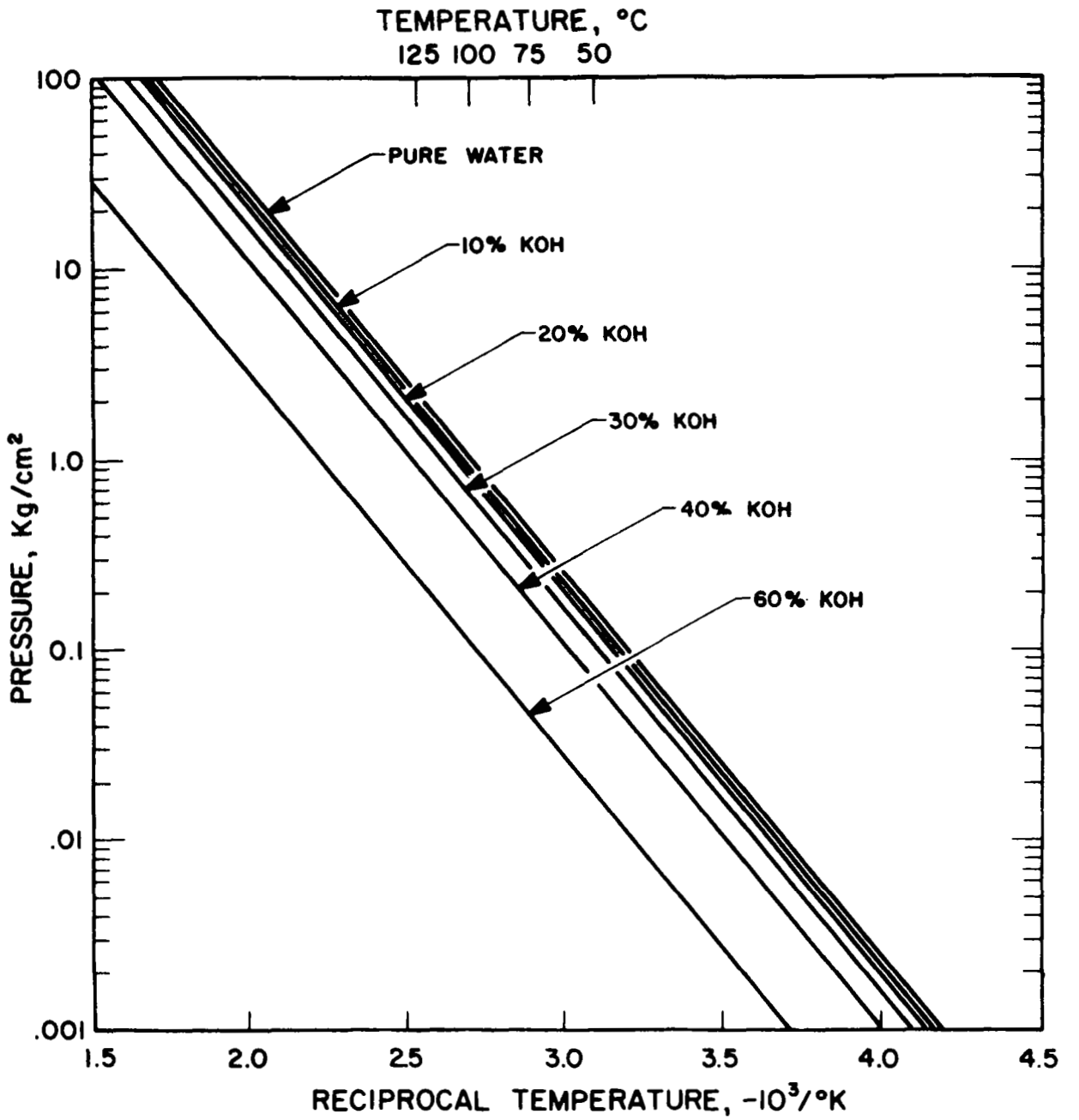

Figure 114. Saturation Pressure of KOH Solutions versus Temperature and Concentration

avoiding condensation. However, since all the heat is generated by the cell stack, and the stainless steel tank is a poor conductor, the rate of heat transfer was such that the end of the hydrogen tank did not heat up sufficiently during discharge.

Figure 115 shows typical voltage performance of the unit during its initial cycles. Since the performance of the cell stack was quite good when the short developed, the tanks were disassembled and a new insulated feed-through was installed. Asbestos insulation was wrapped around the hydrogen end of the tank in an attempt to keep the end hot enough to prevent additional condensation. The unit was subsequently cycled through the 26th discharge. During the second cycling period, a degradation in discharge voltage was observed similar to that recorded in the early single and 6 cell tests. The discharge voltage during the initial and end portions of discharge was 10 to 20 percent lower than at the mid-point. This performance data is also shown in Fig. 115. Large temperature gradients were again observed between the cell stack and the hydrogen tank end, and it was assumed that additional condensation within the unit was occurring due to this temperature gradient. Considering the gradual degradation of performance and the substantial temperature gradient encountered, it was decided to discontinue the test and to modify the unit to eliminate the temperature problems.

Examination of the disassembled unit showed all aspects of the internal components in good condition and revealed that additional condensation had taken place in the end of the hydrogen tank.

To determine overload capabilities of the unit during the 12th discharge, voltage vs. current data was obtained, and is presented in Fig. 116. This showed considerable overload capabilities with minimal polarizations. This data was also utilized in plotting power vs current data which is presented in Fig. 117. Line resistance between the cell

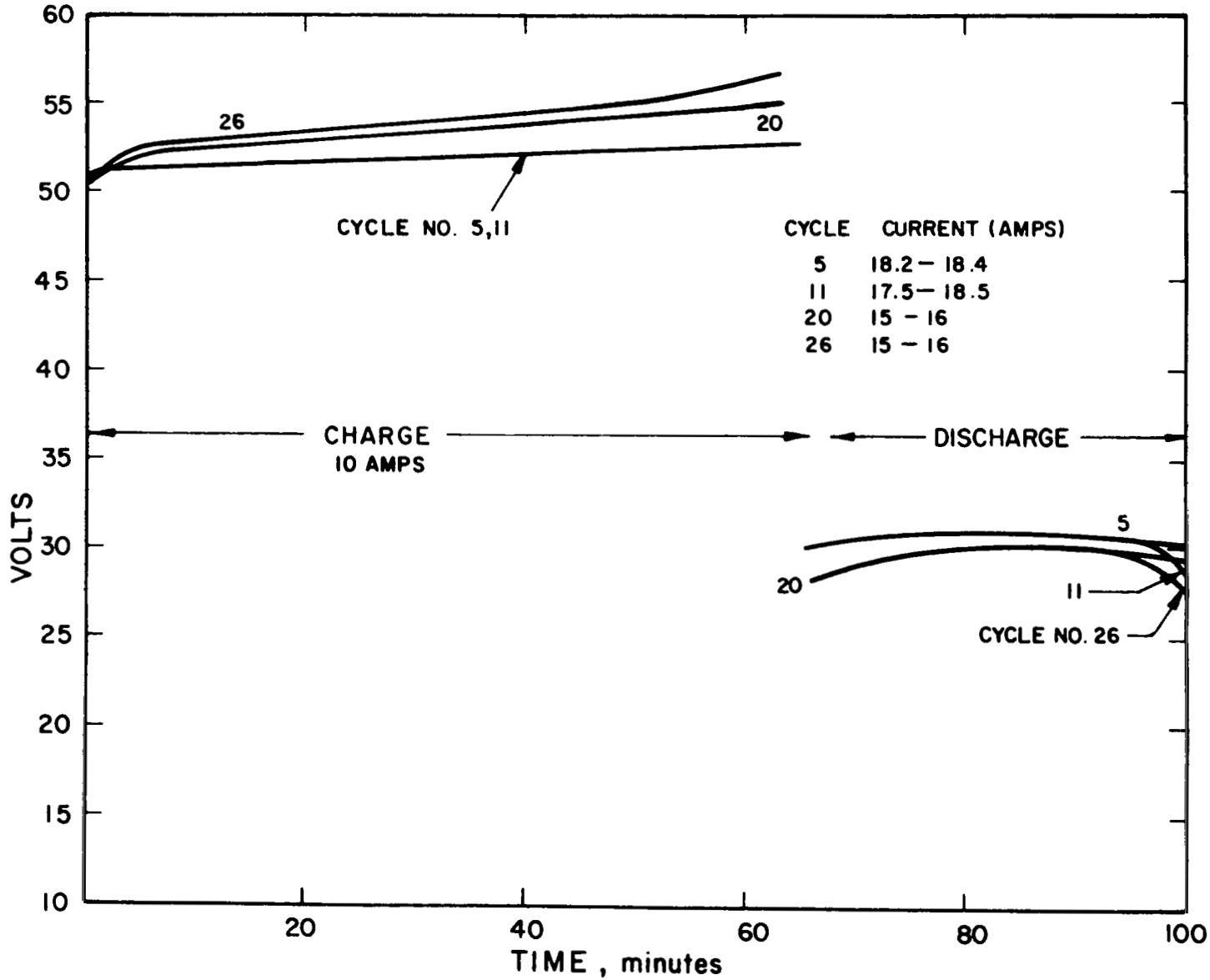

Figure 115. Cycling Performance of 500-Watt Regenerative Hydrogen-Oxygen Fuel Cell S/N 1002-34

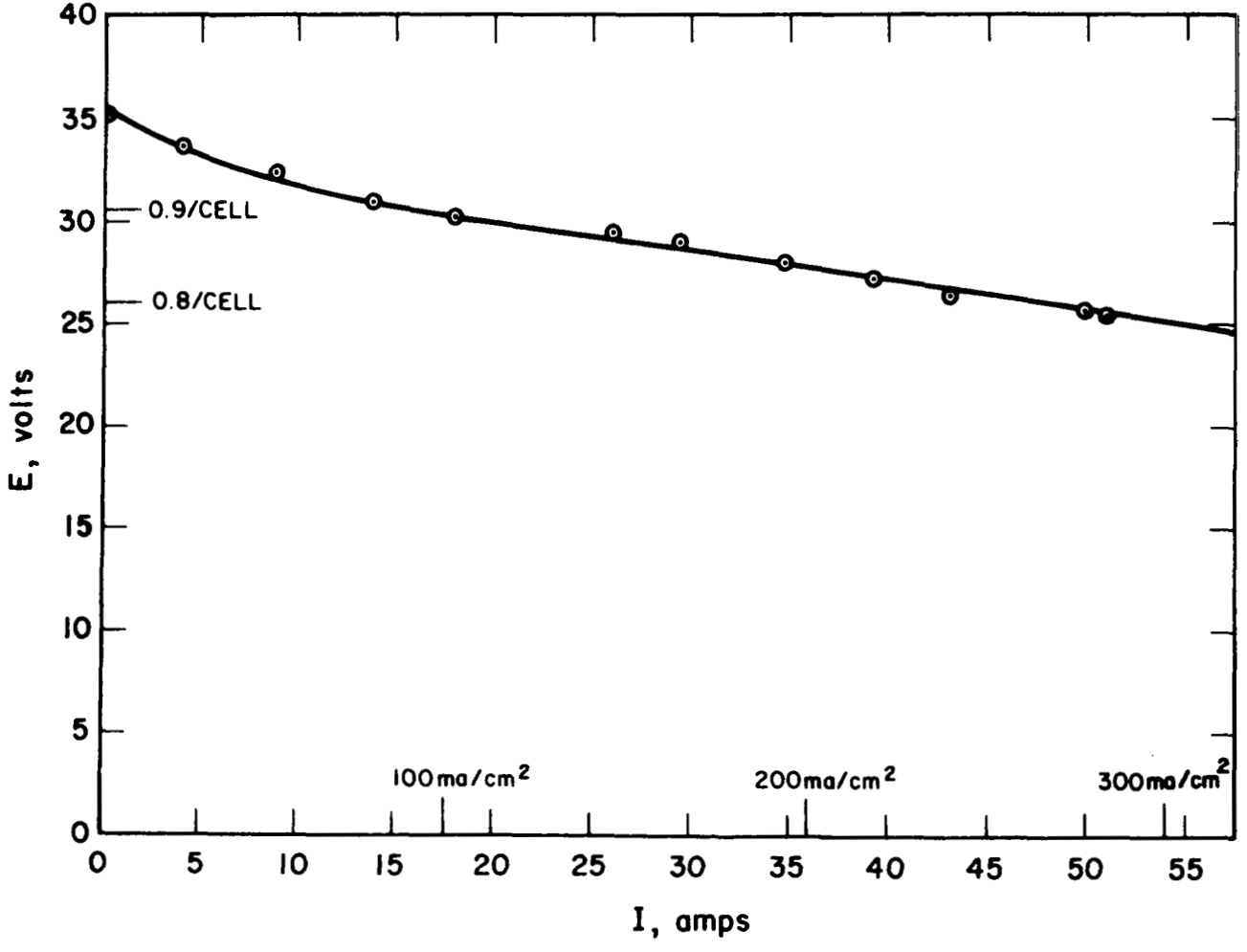

Figure 116. Voltage versus Current Data for 500-Watt Regenerative Hydrogen-Oxygen Fuel Cell S/N 1002-34

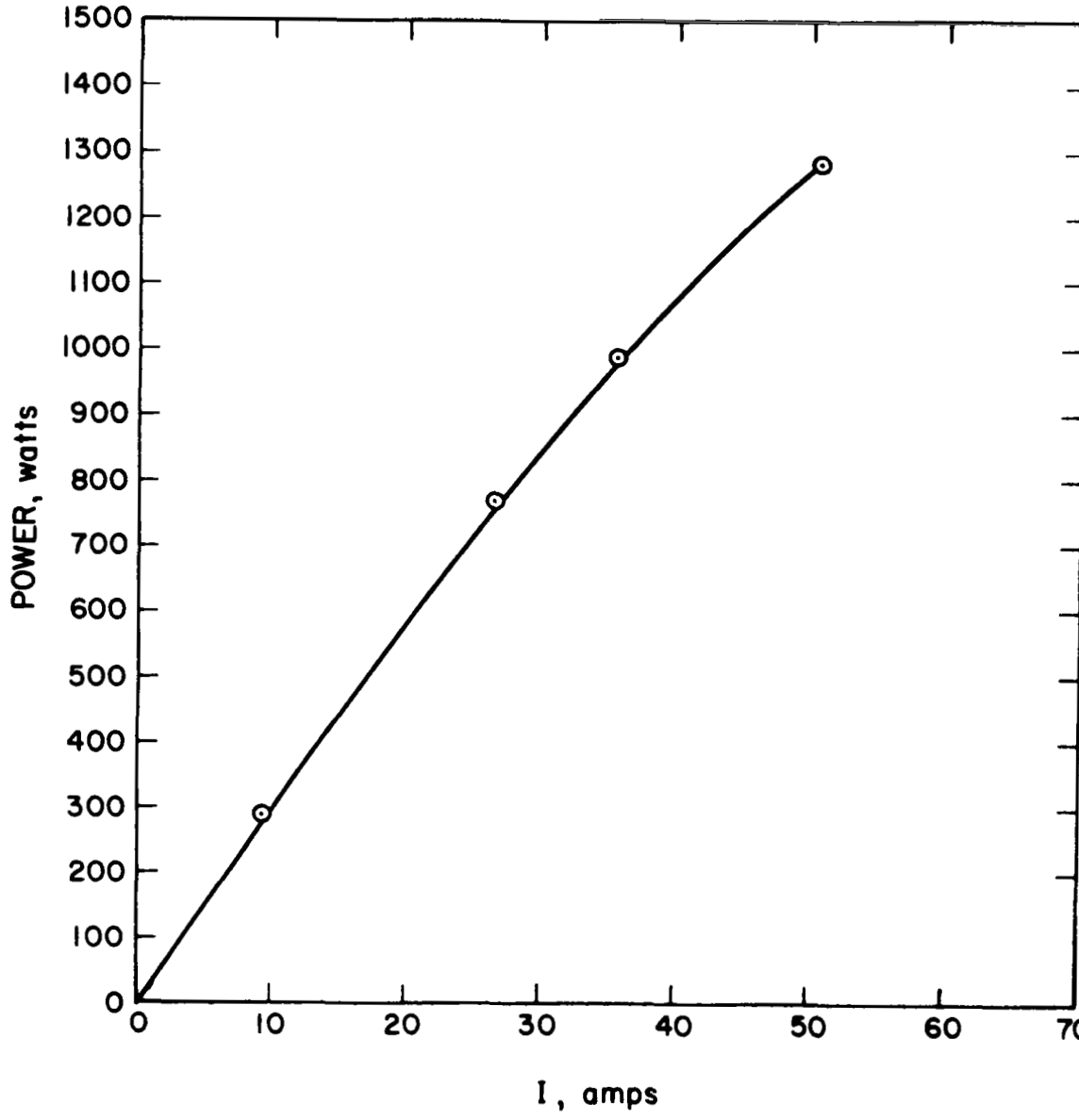

Figure 117. Power versus Current for 500-Watt Regenerative Hydrogen-Oxygen Fuel Cell S/N 1002-34

and the load bank limited the maximum current drawn to ≈ 50 amps. It is believed that powers to ≈ 2000 watts could have been achieved with larger size power lines.

These tests of the 500-watt unit showed that the mechanical design, including compensating bellows, tank volumes, etc., was proper, and that the unit was capable of running continuously in excess of 500 watts and had an overload capability 2.5 times nominal. Temperature gradient and condensation problems encountered can be attributed primarily to the poor thermal conductivity of the stainless steel tank used.

To study the above difficulties, and to obtain additional test information from the unit, the unit was rebuilt and designated cell 1003-34. This unit contained the same electrodes that were used in the previous unit, except that the bi-polar plates were reversed; i.e., the old oxygen electrodes became the hydrogen electrodes, and the old hydrogen electrodes became the oxygen electrodes. The single cell tests had shown that the degradation in performance occurs on the oxygen electrode, and by reversing the electrodes, recovery and good performance could be obtained. The following changes were also made in the new assembly and test setup.

a. An electrical heating band was placed on the end of the hydrogen gas tank. The heater was connected to a Variac for controlling the temperature of the hydrogen end tank to prevent large gradients and water condensation.

b. The new asbestos mats were impregnated with 50 percent potassium hydroxide to decrease vapor pressure, and to further reduce possibilities of condensation within the gas tanks.

c. The previous unit contained a 5-mil strip of Teflon wrapped around the fuel cell stack to prevent vibration shorting of the stack to the walls of the hydrogen tank. This continuous strip was replaced by bands of glass tape that were placed longitudinally down the stack. This change was incorporated to improve the conduction of heat (generated within the stack during discharge) to the outer walls of the hydrogen tank.

d. The internal thermocouple that is connected to the hydrogen end plate was electrically insulated from that plate by means of a mica washer. This thermocouple had caused an instrumentation problem due to being at the cell stack potential. By insulating the couple, the problem was eliminated.

e. To further reduce the temperature gradient of the unit, the entire assembly was inverted such that the hydrogen end was up and the oxygen end was down. It had been observed in the previous test that substantial temperature gradients due to poor circulation existed within the test chamber that was being used to control ambient temperature.

The 34-cell unit was placed in the oven, flushed, and cycled three times to check out instrumentation and temperature gradients. The unit was allowed to sit overnight at open circuit, and the following morning a continuous 72 hour cycling test was initiated. The test regime consisted of the standard 100 minute cycle, 65 minutes charge and 35 minutes discharge. During the cycling a gradual degradation in discharge voltage was observed. This degradation was similar to performance previously observed, and could be attributed to the gradual oxidation of the porous nickel substrate used on the oxygen electrode.

The purpose of the test was not to obtain long term life data since this type of degradation was predictable from previous data. However, since these types of electrodes were available, it was deemed desirable to assemble the unit and run the electrical tests to determine if any other difficulties or deficiencies would become apparent. Aside from the gradual voltage decay, the unit performed satisfactorily. The temperature gradient problem was considerably reduced, and typical gradients between stack and the oxygen tank end, which now exhibited the lowest temperature, were 80 to 100°C.

Figure 118 shows performance of various cycles throughout the test period. At the completion of the 72-hour test, the unit was allowed to sit at open circuit for about three hours, and then a new test was started at a slow rate of charge and discharge. This test consisted of a charge of 4 amps to 500 psi, and then a discharge of one hour at 200 watts, and the remainder of the discharge at 50 watts to exhaustion. The test was conducted to study the effects of a slow cycle. Performance is shown in Fig. 119. On this slow charge/discharge test regime, the unit was capable of delivering in excess of 700 watt-hours.

After completion of this test, the unit was put back on the 100-minute cycle, 35 minutes discharge and 65 minutes charge. However, due to the degradation in performance that was observed during the 72-hour test, the load levels were reduced and the charge was conducted at 4 amps and the discharge at approximately the 200-watt level. At this load level, the unit was cycled continuously unattended for 48 additional cycles. During that period, there was a slight, almost negligible, decrease in the discharge voltage. This performance can be seen in Fig. 120.

At the start of the 95th charge, recorded data showed a substantial drop in the internal pressure of the unit and in the operating voltage.

CYCLE NO.	DISCHARGE CURRENT	DISCHARGE PRESSURE RANGE
6	17 - 17.5	310 - 120
25	16.5 - 17	385 - 195
47	15 - 16	380 - 205

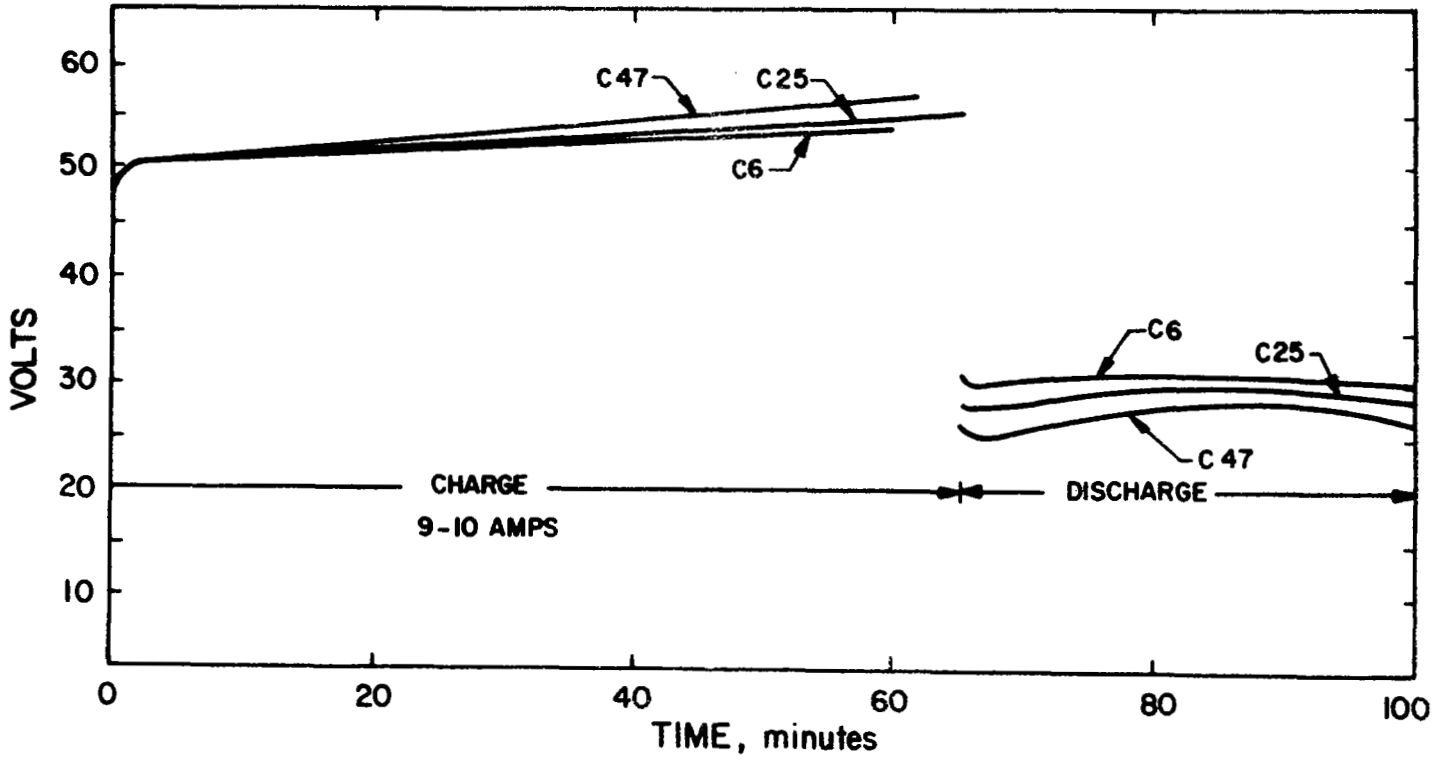

Figure 118. Cycling Performance of 500-Watt Regenerative Fuel Cell S/N 1003-34

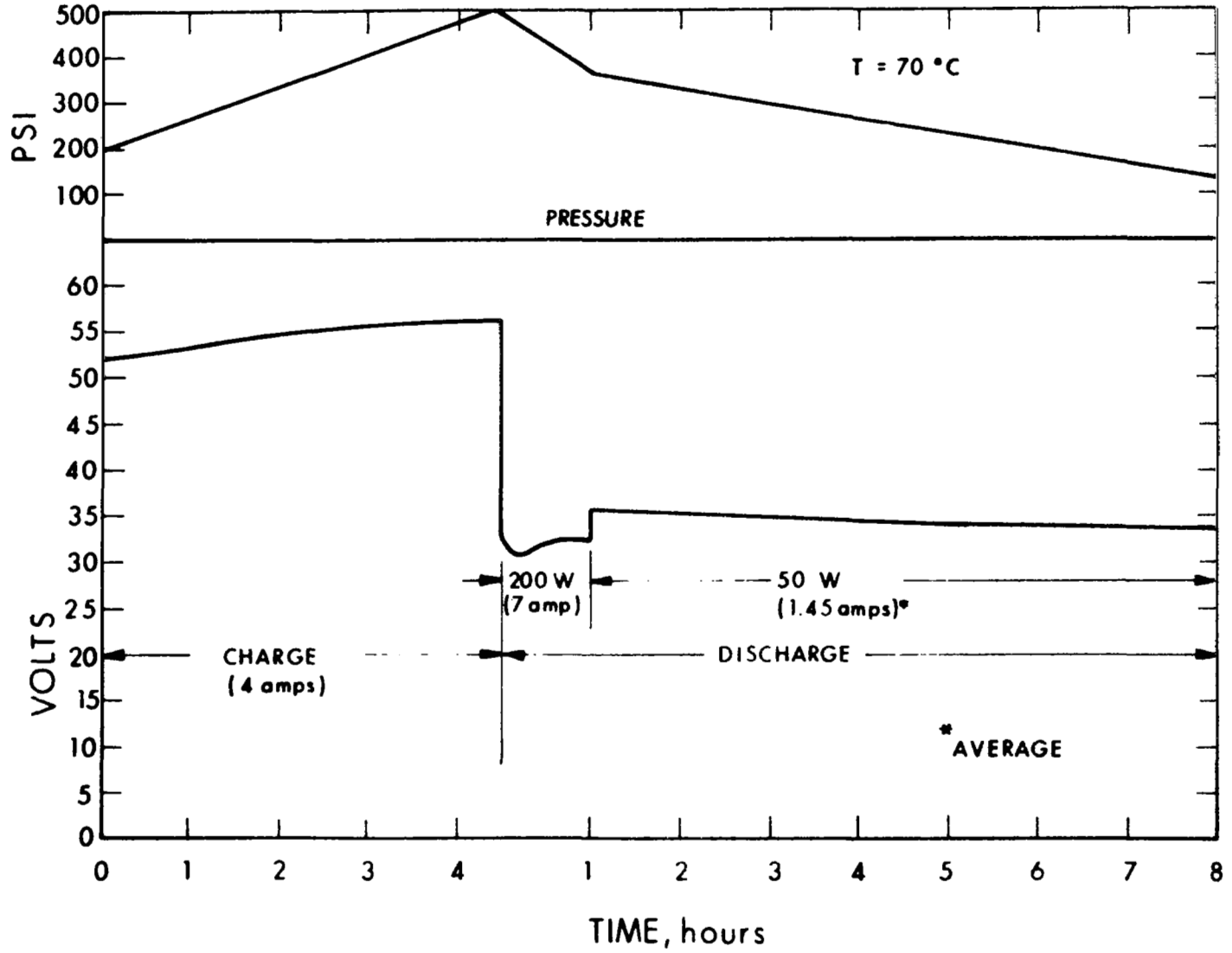

Figure 119. 34 Cell Performance for 600-Watt Hour Discharge as Per JPL Specification GMP-50-136-DSN-A

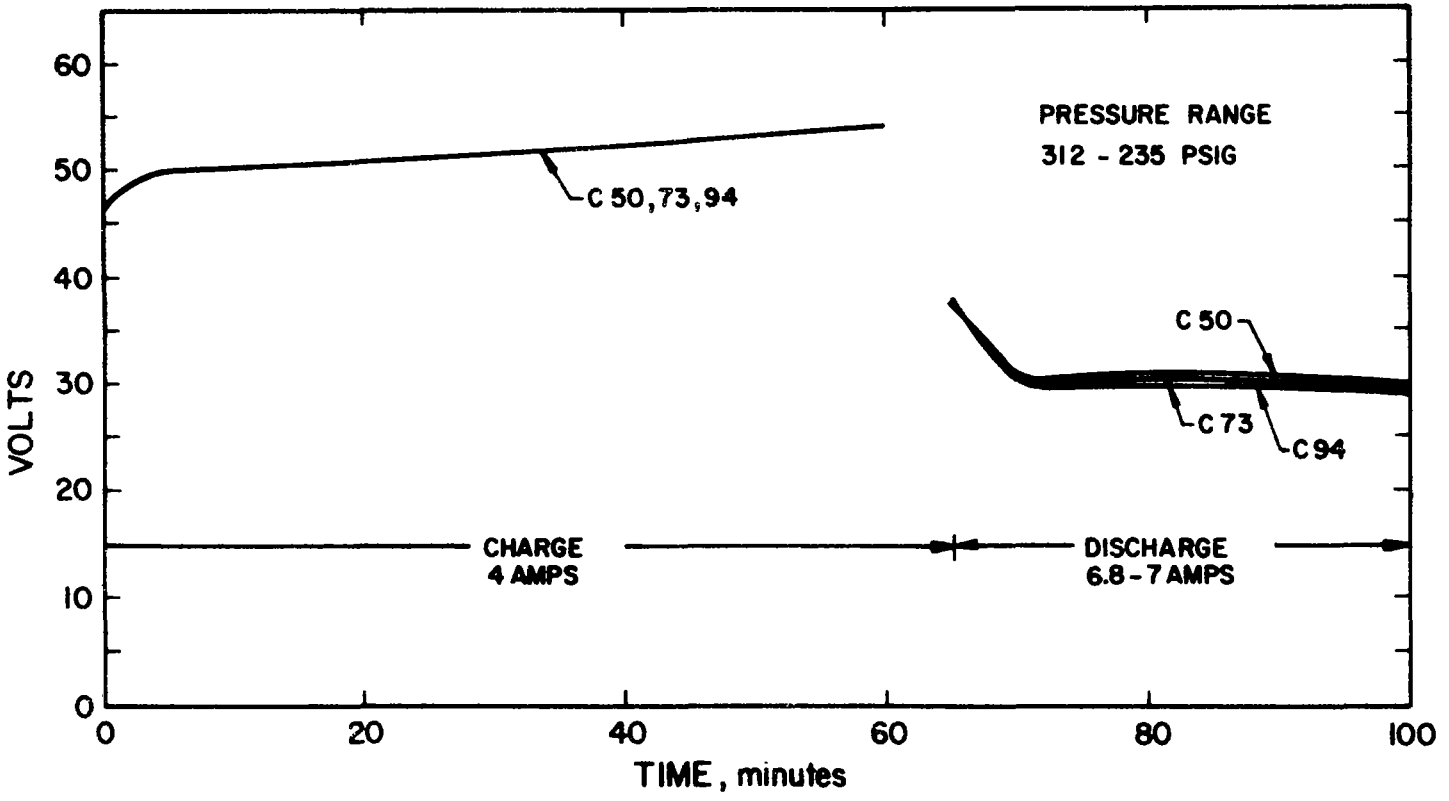

Figure 120. Low Level Cycling Performance of Regenerative Fuel Cell S/N 1003-34

The differential pressure was off scale during this period, and then dropped to 0 differential. Examination of cycle data showed that substantial differential pressures built up rapidly at the start of each charge, and gradually reduced as the charge proceeded. This magnitude of the differential pressure apparently increased gradually as cycling proceeded. The differential was due to an excess hydrogen pressure, causing the bellows to reach its fully extended position. Recorded temperature data during the drop-off in pressure point showed a substantial rise in internal temperature of the unit.

Due to this difficulty, the test was stopped and the unit was disassembled. Examination revealed that the excessive differential pressure had caused one of the welded seams on the bellows to split. This resulted in gas mixing and chemical recombination in the oxygen compartment. The hydrogen compartment was perfectly clean while the oxygen tank and external surfaces of the bellows were oxidized. In addition, the oxygen tank, directly opposite the rip in the bellows, exhibited a highly heated zone indicating that this was the point of high temperature recombination.

All other aspects of the unit were in excellent condition. The fuel cell stack was clean, and showed no obvious effects of the chemical reaction.

The cause of the gradual build-up in hydrogen differential pressure with cycling was not readily apparent. It could have been caused by a slow oxygen leak in the tankage. However, pressure testing of the tankage prior to the disassembly did not reveal any leakage. Another possible explanation could be some irreversible combination of oxygen with the porous nickel electrode, or any of the materials in the oxygen side of the system.

7.2 SECOND GENERATION

The last effort of the program was devoted to the building and testing of a 34-cell unit with the best components developed throughout the program. The first such unit was designated S/N 1004-34 and incorporated a matrix and the type of electrodes developed for long cycle life in the single cell program. The matrixes were composed of a 50% KT and Teflon pasted membrane sandwiched between two 12.5-gm 90% KT/10% asbestos mats. American Cyanamid AB-6 electrodes were used as oxygen electrodes and the standard EOS 20 mg Pt/cm^2 electrodes were used for hydrogen. The cell spacers were 0.060 inch thick.

The purpose of the test was to evaluate the fuel cell battery mechanical and operational performance. After flushing with H_2 and O_2 gases ten times the cell was placed on a 100 minute cycle. The cycle was the standard 35 minute charge at 10 amps and 35 minute discharge at 19.5 amps. The battery shorted out in the middle of the third cycle. The tanks were removed and it was discovered that the Teflon screen wrapped around the cell stack shrunk. The shrinkage allowed the cell stack to short against the tank. Upon further inspection of the cell stack it was discovered that the stack leaked. The cell was disassembled and all the components washed.

A new 34 cell 500 watt fuel cell was assembled utilizing the bipolar plates and electrodes from battery S/N 1004. This assembly was designated S/N 1005-34. The matrixes were composed of 80% KT, 10% asbestos, and 10% Teflon pressed together. The cell stack was wrapped in Teflon sheet.

The cell was flushed and put on the standard 100 minute cycle. During the first charge the cell stack shorted out. The short was caused by a glass epoxy washer breaking, thus allowing a stack bolt to short out.

It was also discovered that the bolts were loose. The bolt was reinsulated and the stack retorqued. The fuel cell was then reassembled, reflushed, and put on the 100 minute cycle.

During the next charge cycle the fuel cell demonstrated extreme gas recombination. After the tanks were removed it was observed that the glass epoxy washers had allowed the cell stack to relax. Further examination revealed that combustion had occurred, allowing the gases to leak freely through the matrixes. The cell stack was taken apart and all the cell components were washed.

Another 34-cell 500-watt prototype, designated S/N 1006-34, was assembled. This unit incorporated the same bipolar plates and electrodes used in prototypes S/N 1004 and S/N 1005. New matrixes were made using the EOS pressing technique. The matrixes were composed of 80% KT, 10% asbestos, and 10% Teflon. The cell spacers were 0.060 inch thick. Again, the purpose of the test was to evaluate mechanical and operational performance. The cell was cycled for 72 hours using the 65 minute charge at 10 amps and 35 minute discharge at 17.5 amps. As can be seen in Fig. 121 the performance degradation was quite small. At the end of the 72 hour period a polarization test was performed at 50^{o}C and is shown in Fig. 122. The battery was allowed to cycle continuously after the 72 hour period. At cycle 63 it shorted out. It was discovered that the stack bolts were shorted across the stack. All of the polysulfone washers used as insulation had crazed and split, allowing many of the stack bolts to come into contact with the end plate. The polysulfone washers were replaced with ceramic washers and the cell put on cycle. At cycle 76 the cell shorted out again. It was found that the ceramic washers had soaked up moisture and were eroded away by electrolysis. The fuel cell is repairable but due to lack of time has not been prepared for testing again.

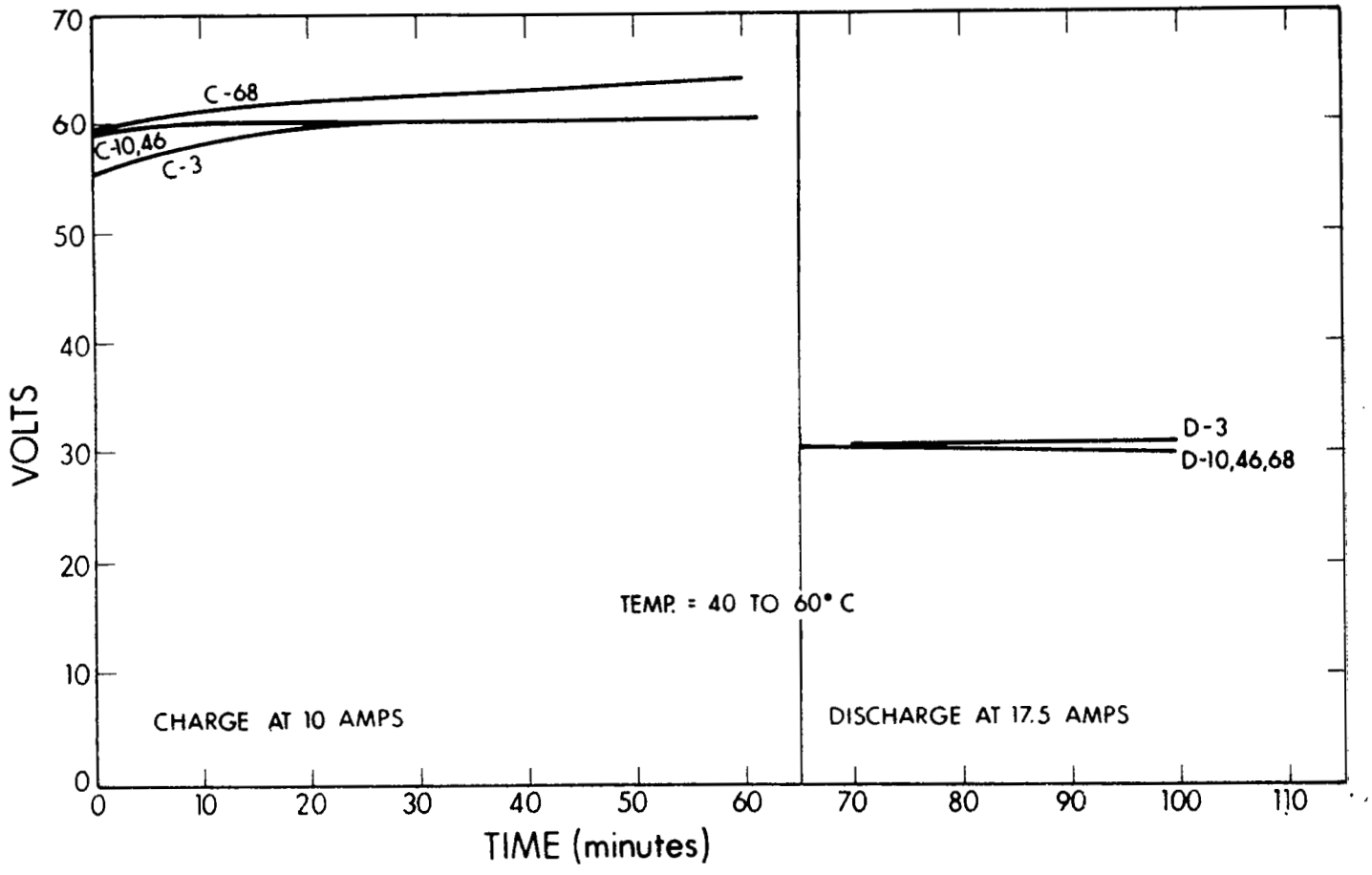

Figure 121. Cycling Performance of 500-Watt Regenerative Cell S/N 1006

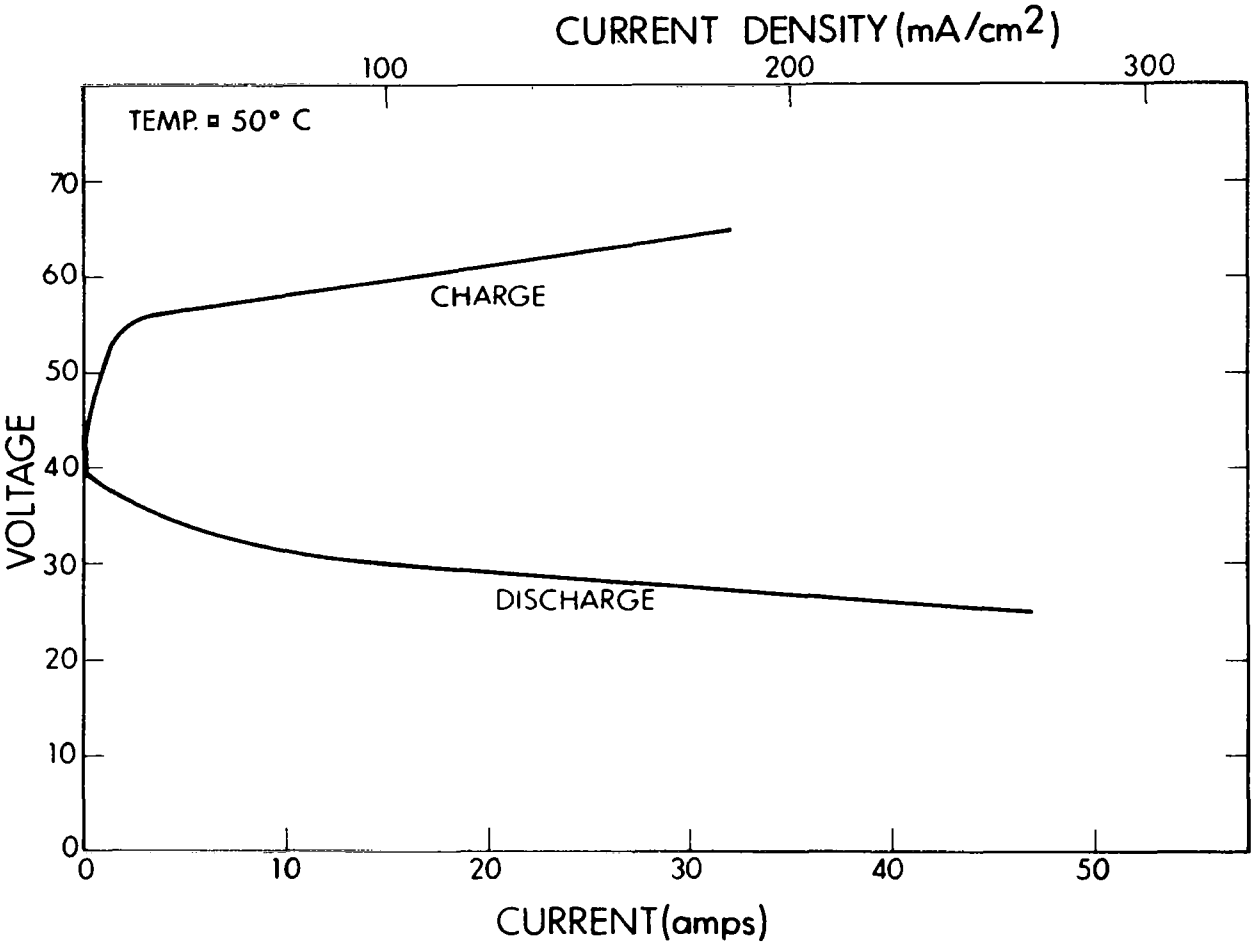

Figure 122. Polarization Curve of 500-Watt Regenerative Cell S/N 1006

It can be concluded that the electrochemical performance of the fuel cell has improved since very little performance degradation occurred. However, the mechanical design is limiting the fuel cell life. The stack bolts need to be completely insulated from the cell stack to prevent shorting and insulated from the end plates to prevent the bolts from becoming polarized with respect to the cell stack. The insulating washers at the ends of the bolts need to be of sufficient mechanical strength to retain the stack compression and be able to withstand a moist oxygen environment.

SECTION 8

CONCLUSIONS

The regenerative hydrogen oxygen fuel cell employing a capillary matrix for water storage has been demonstrated as a practical concept for a secondary battery. The use of integral tankage around the fuel cell stack results in a self-contained sealed unit that can be utilized as a conventional secondary battery. Studies of the oxygen electrode, hydrogen electrode, and matrix have revealed the following:

It is necessary to employ an oxygen electrode that contains no oxidizable materials since in the charge, oxygen generation, mode of operation oxidation of many materials occurs very rapidly. The best oxygen electrode structure consisted of a gold-plated nickel screen, on which a platinum black Teflon mix is applied. Electrodes of this type, manufactured by the American Cyanamid Corporation (AB-6, 9 mg platinum per cm^2), were found to be stable. The hydrogen electrode does not present oxidation problems and a porous nickel electrode impregnated with platinum black was found to be very suitable. This type of porous electrode allowed for storage of a certain amount of water within the electrode. Studies of fuel cell grade asbestos as a matrix material in the regenerative fuel cell revealed that it slowly reacts with the potassium hydroxide electrolyte which results in performance degradation. Utilizing asbestos, 100 to 200 charge/discharge cycles was the maximum reproducibility obtainable. Screening of substitute matrix materials for the regenerative fuel cell revealed that potassium titanate was a superior material. Fuel cell matrixes made with mixtures of potassium titanate, Teflon, and/or

asbestos were found to be chemically stable and comparable to asbestos in resistance and bubble-through pressure. Single cell tests employing the potassium titanate matrixes achieved cycle life [65 minute charge, 35 minute discharge] of 500 to 1000 cycles.

Slight degradation with the potassium titanate matrixes was still observed and additional research and development will be necessary to optimize the matrix structure and pinpoint the causes of observed deteriorations.

A number of six-cell prototypes were tested throughout the program and demonstrated the feasibility of the multicell concept employing common gas storage. Continuous difficulties were encountered with the bipolar plates employed, which consisted of a magnesium plate, electroless nickel and gold plated. Improved plating techniques or a change to a less corrosive material will be necessary for long life applications. Thirty-four-cell units capable of 600 watt hours of storage energy at a nominal 28 volts were also built and subjected to test. These units demonstrated the ability of such a large unit to perform satisfactorily. A substantial effort was not carried out in the mechanical design of these units and repeated difficulties occurred with shorting of the stack bolts and relaxing of the stack compression. These tests also revealed that uniform temperature throughout the assembly is necessary to avoid water condensations in the extreme lower temperature ends of the tankage. Therefore, additional thermal analysis and design modifications will be necessary for reliable continuous cyclic operation of a large regenerative fuel cell assembly.

The 34-cell unit with lightweight aluminum tankage was capable of delivering approximately 15 W-hr/lb.

The program has resulted in the development of a fuel cell matrix and a set of electrodes that are quite stable for fuel cell applications. The multicell mechanical design and tests demonstrated the feasibility of the regenerative fuel cell and pointed out some mechanical design weakness. It is projected that with additional development efforts, substantial increases in cycle life and energy density will be attained and the regenerative fuel cell will take its place as an available secondary battery with many advantages.

APPENDIX A

SCOPE OF WORK

PHASE I 28 June 1963

TASK I - System Optimization Studies

1. Contractor shall perform system studies to determine the optimum parameters for operating a hydrogen-oxygen fuel cell battery regeneratively for the following orbital missions.

   (a) 300-mile orbit

   (b) range of orbits from 300 to 22,400 miles

   The evaluation should be made for mission requirements of 0.1, 0.5, 1.0, 5.0, and 10.0 kw at a nominal 28 volts.

2. The system studies will be based primarily on previous experimental results in regenerative hydrogen-oxygen fuel cell technology and one appropriate empirical relationships.

3. In cases where necessary information for the system studies is not available from previous experimental results, and empirical relationships cannot be established, the Contractor will conduct single cell experiments.

4. The fuel cell design will be based on a static electrolyte system, whereby the electrolyte is held by an asbestos capillary membrane.

TASK II - Design and Development of Multi-cell Regenerative Hydrogen-Oxygen Battery.

1. Within ten (10) days of notification by the Contractor of completion of Task I, the NASA Technical Manager will designate the oribital mission which will serve as the basis of the design and development of a multi-cell electrolytic regenerative hydrogen-oxygen fuel cell battery.

2. The fuel cell battery should be capable of producing a minimum of 75 watts electrical output in a range of 3.5 to 4.5 volts, and charged and discharged over the appropriate cycle.

3. Since this fuel cell battery is not intended for flight tests, but strictly as a demonstration unit, it need not be optimized in regard to weight; but must duplicate operating and design features optimized in Task I.

TASK III - Test and Evaluation

1. Before the fuel cell stack is assembled into the complete demonstration unit, it will be instrumented to supply the following data.

   (a) Discharge current and voltage.
   (b) Charging current and voltage.
   (c) Cycle time.
   (d) Tank pressures, O_2 and H_2.
   (e) Individual cell temperature.
   (f) Individual cell voltage.

2. The charge-discharge tests for the fuel cell stack will be operated as a closed cycle. In other words, gas storage cylinders will be incorporated with the fuel cell stack to supply and store the gases at the required pressure during the cycle test.

3. After the fuel cell stack has been tested and evaluated, it will be incorporated into the complete demonstration unit, This unit will be instrumented to supply the following:

   (a) Discharge current and voltage.
   (b) Charging current and voltage.
   (c) Cycle time.
   (d) Tank pressures, O_2 and H_2.
   (e) Fuel cell battery voltage.
   (f) Minimum of five temperatures on outside wall of battery casing.

4. The demonstration fuel cell battery will undergo the following tests in order to evaluate its mechanical and operating performance.

   (a) Mechanical design test considerations - As proof of material selection and sealing of gases and electrolyte, cell will be pressurized with inert gas and pressure loss checked.

   (b) Polarization characteristics during charge and discharge cycle.

   (c) Charge retention characteristics - Cell will be charged to desired level, and its open circuit and

reactant pressures monitored. Loss of pressure and decrease in open circuit voltage over a twenty-four (24) hour period will indicate self discharge.

(d) Cycle tests - The regenerative fuel cell system will be placed on an automatic charge-discharge cycle simulating the power requirements and charge-discharge times specified. In order to prove out design and operating characteristics, the system should be cycle tested continuously for a minimum time of forty-eight (48) with no degradation in performance.

The electrolytic regenerative fuel cell will be operated isothermally without any auxiliary cooling coils or radiators. The passive thermal control and heat rejection system concept will be based on the use of the heat of fusion of a suitable compound, with a melting point at the operating temperature of the fuel cell. This compound will be contained in the annular space between the fuel cell and an appropriate casing material. During the charge-discharge cycle, heat will radiate at a constant rate to space from the compound "heat-sink" through the casing wall. In the discharge portion of the cycle, heat must be absorbed by the compound, via its heat of fusion, in order to maintain a constant fuel cell temperature. In the charge portion of the cycle, heat will be rejected by the compound in order to supply the heat required for radiation into space. The overall design concept will be based on operating a relatively low temperature cell with no moving parts within the system. These features will provide an electrolytic regenerative fuel cell of increased energy density and high reliability.

5. The operating and design parameters to be optimized will include at least the following:

   (a) Electrode spacing.
   (b) Operating temperature and pressure.
   (c) Operating charge and discharge current density.
   (d) Operating electrolyte concentration range during charge and discharge cycle.
   (e) Radiator surface temperature.
   (f) Heat rejection rates.
   (g) Selective coating for radiator surface.

(h) Heat storage material.

(i) Materials of construction.

(j) Gas storage tanks.

(k) Overall configuration of complete regenerative assembly.

6. For this evaluation the system components will be optimized to achieve a composite system having minimum weight and volume characteristics, based on the existing state-of-the-art. The performance of the regenerative fuel cell should either have been demonstrated or appear feasible as a result of preliminary development experience.

7. The fuel cell will provide the power needed by the satellite during the shade portion of the orbit. Primary solar cells will provide power during the sunlight portion of the orbit and the power necessary to regenerate the fuel cell reactants.

8. The system optimization studies will be made for the complete regenerative powerplant which will be composed of at least the following sub-systems:

(a) Fuel cell battery.

(b) Electrolyte and gas storage systems.

(c) Power conditioning equipment and controls.

(d) Solar energy converter.

(e) Other required auxiliary systems.

For items (c), (d), and (e) specify assumptions made, and maintain consistency in all calculations.

AMENDMENT No. 3 2 July 1964

Fabricate two (2) six cell units and one (1) single cell unit utilizing design improvements recognized during the performance of the program. These improvements will be in the following areas:

a. Separator gasket design.
b. Elimination of stearic acid tankage.
c. Modification of gas port design.
d. Increase cell stack bolt diameter and compressive loading.
e. Improve design of pressure balancing diaphragm.
f. Eliminate plastic pressure tubing.
g. Eliminate magnesium in critical structural portions of cell.
h. Improve external "O" ring seal design.

The following tasks, Phase II, will be initiated upon completion of Phase I and the Contracting Officer's approval.

PHASE II

1. Construction of a 28-Volt, 500-Watt Test Unit - Assembly No. 1 - The contractor shall construct a regenerative H_2-O_2 fuel cell battery based on the cell design developed under Phase I. The fuel cell battery shall be so constructed as to provide minimum weight and volume.

   (a) Fuel Cell Design Description - The fuel cell design shall be based on a static electrolyte system whereby the electrolyte is held by an asbestos capillary membrane. The overall design concept will be based on operating a relatively low-temperature cell with no moving parts

within the system. These features will provide an electrolytic regenerative fuel cell of increased energy density, and high reliability. It is required that the fuel cell shall be operated with gases stored in pressure tanks designed for this application, that the tanks shall be replenished by the electrolysis of the water contained in the asbestos pad, and that the cyclical operation will be obtained from the reaction and electrolysis of this stored water.

(b) Fuel Cell Design Specifications - The design of the 500-watt system shall be based upon the following operating characteristics:

Operating Temperature	70°C
Design Power Output	500 watts
Design Battery Voltage	28 volts +0.5 volts at 500 watts
Active Cell Diameter	6 inches
Gas Storage	Common External Cylinder
	H_2 and O_2 Separated by Flexible Pressure Balancing Diaphragm
	Pressure (Discharged) - 50 psig
	Pressure (Charged) - 400 psig
Normal Operating Cycle	Charge - 65 minutes
	Discharge - 35 minutes
Design Capacity	600 Watt Hours
Capacity at Normal Operating Cycle	290 Watt Hours

Design power is 500 watts at 28 volts in an orbit of 300 miles. The 600 watt-hour capacity will allow the fuel cell to be tested in any orbit up to 22,400 miles at the design power and voltage.

This range is from 65 minutes charge-35 minutes discharge to 22.8 hours charge-1.2 hours discharge.

(c) The contractor shall construct a fuel cell battery whose performance characteristics are outlined in the preceding design specification. In addition, the contractor shall provide the following:

1. Charging Equipment - The contractor shall supply an external electrical power source capable of supplying the necessary direct current electrical power to fully charge the fuel cell battery in a minimum of sixty-five minutes. The charger shall have a variable control so that the charging period may be varied from fifty minutes to twenty-three hours.

2. Load Bank - The contractor shall supply a resistive load bank capable of dissipating the power output of the fuel cell battery. A fixed resistor may be used for the 500 watt load, but ; the bank should provide a means for loading the cell at approximately 100-watt increments from zero to 2000 watts output.

3. Control Equipment - The contractor shall supply the components and control circuits necessary to operate the fuel cell battery automatically through repeated charge/discharge cycle tests. A variable time shall be included which will allow variation of the charge/discharge cycles to simulate operation at orbital altitudes from 150 to 22,400 miles.

4. Fuel Cell Battery Instrumentation - The fuel cell will be instrumented to supply the following data:
   (a) Discharge current and voltage
   (b) Charging current and voltage
   (c) Gas Storage Pressure
   (d) Temperature of fuel cell, at least four points on outside wall of battery casing. A temperature sensor will also be placed on each end plate.

5. Design Changes - The contractor may recommend changes in the design specification, based upon experimental results from Phase I and the contractor's own engineering judgement, to the NASA Project Manager. These recommendations will be reviewed and approved in whole, or in part, by the NASA Project Manager. Only those recommendations, or portions thereof, which are specifically approved may be incorporated into the design by the contractor.

(d) Fuel Cell Studies - The objective of this task is to study the operating characteristics of the multiple-cell regenerative fuel cell system in order to verify the soundness of the design and indicate improvements which could be made. To this end, the following studies shall be made:

1. The effect of overload on performance and materials shall be determined. Under overload conditions, a thermal strain is placed on the materials of construction in addition to the possible disruption of the

membrane. Tests shall be run at 150, 200, 250, and 300%, for a minimum of three continuous cycles for each drain. Voltage, current and temperatures shall be monitored continuously during the tests. Run will be terminated upon the cell voltage reaching one-half open circuit voltage or when tank pressure reaches 50 psig.

2. Materials compatibility in the actual unit should be checked whenever the unit is dismantled through visual examination of the unit.

3. Study shall be made of the loss of water as a function of cycle life. This would be determined by the loss of capacity with time.

4. When specific tests are not being performed, the fuel cell shall be run at the design cycle and power to obtain operating time on the unit. Operation will be carried out during the normal eight-hour working day, rather than continuously. As a goal, a minimum of 60 cycles is required.

(e) Construction of a 28-Volts, 500-Watt Flight Prototype FC-Assembly No. 2 - Build a 500-Watt, 28-Volt regenerable hydrogen-oxygen fuel cell. On the basis of the results obtained from Phase I of Task I(single cell and diffusion studies), and Phase I of Task II (multiple cell fabrication, testing, and optimization), design and build a 28-volt, 500-watt electrically regenerable hydrogen-oxygen fuel cell for use in an application. Its capacity should be that of the 22,400-mile orbit (600-watt hours) (as set

forth in Task 1.(b)). The goal of Task 1(a) shall be an electrolytically regenerable fuel cell with an energy density of 15-watt hours per pound based on the 300-nautical mile orbit. Studies from the first two tasks shall be performed with this goal in mind. The fuel cell shall be optimized from a weight standpoint. At the end of twelve months, a meeting shall be arranged between the contractor and the Government for the express purpose of reviewing the project to date and the contractor shall submit a design of the 500-watt, fuel cell. At this time, the size, number of cells, operating temperature, gas storage method, capacity and power output will be finalized. The contractor will then proceed with the fabrication of a regenerable fuel cell after approval of the design by the Project Manager.

1. Specifications for the final unit will remain the same unless changes are approved as set forth in Task (c) 5. The same accessories and instruments can be used as set forth in Tasks 1.(a), 1.(b), and 1.(c).

2. With the completion of the final unit, an acceptance test will be run. The test will consist of continuous operation for a period of seventy-two hours at design conditions specified in Task 1.(b). The fuel cell battery shall undergo the following tests in order to evaluate its mechanical and operational performance. The charge-discharge tests will be operated as a closed cycle. Gas storage tanks will be incorporated with the fuel cell to supply and store the gases at the required pressure during the cycle test.

(a) Polarization characteristics during charge and discharge will be monitored.

(b) Charge retention characteristics - cell will be charged to desired level (21 amp hours) and its open circuit voltage and reactant pressures monitored. Any loss of pressure greater than 10% over a twenty-four hour period will indicate self-discharge and will be unacceptable.

(c) Cycle tests - the regenerative fuel cell system shall be placed on an automatic charge-discharge cycle simulating the design orbit (Task 1.(b)) under design specifications. In order to prove out design and operating characteristics, the system should be cycled continuously for a continuous period of seventy-two (72) hours with no physical failures or performance variations greater than 45% of nominal.

3. Leakage of any sort, i.e., gas, electrolyte, either from the cells or the complete unit will constitute an unacceptable fuel cell battery. Fuel cell stack shall be checked for electrolyte leaks under charged and discharge conditions. Pressure tests will again be made after the complete unit is assembled.

4. The Project Manager or a representative designated by the Project Manager will be in attendance during all acceptance tests.

MODIFICATION No. 5 6 October 1965

*As part of Phase II of Task I, the contractor shall conduct the following described experiments and tests prior to commencing the work called for under paragraph 1(e) of Amendment No. 3, Phase II, Task I:

1. The contractor shall conduct experiments to determine the chemical and electrochemical reactions which occur between the KOH electrolyte and the asbestos mat. These experiments shall not be evaluated in extended life tests, but rather shall be chemical tests or electrochemical tests of short duration (1-50 hours). The following shall be determined:

   a. Chemical and/or electrochemical reactions that occur between the electrolyte and the asbestos, if any.

   b. Determine the identity of the black deposits found in asbestos after electrochemical processes have occurred, and determine how they occur.

   c. Determine whether there is deterioration due to temperature in an electrolyte soaked mat at temperatures up to 150°C. The contractor shall determine these effects with fuel-cell-grade asbestos and KOH electrolyte concentrations between 30 to 45 percent.

   d. The asbestos and KOH shall be chemically analyzed before and after each test.

2. The contractor shall perform tests set forth in subparagraph e. to evaluate electrode structures with the objective of improving the operating life of oxygen electrodes. The following four electrode structures shall be evaluated, and any additional electrodes to be evaluated shall be subject to prior approval of the Contracting Officer:

   a. Standard nickel plaque electrode which has been gold plated and then platinized.

   b. Nickel fiber metal plaques which have been gold plated and then catalyzed. Gold plating shall be applied to sintered plaques made by Huyck Metals Corporation. In addition, plaques may be prepared from nickel fibers which have been plated prior to sintering, with prior approval of the NASA Project Manager.

   c. American Cyanamid electrodes, platinum catalyzed, teflon bonded, with gold plated collector.

   d. Teflon bonded non-sintered type of electrode with compatible metal collector, of the Monsanto Research Corporation MD-Series.

   e. Electrodes of the types specified above shall be tested in single-cell fixtures and shall show promising performance levels before testing in multicell units. Promising performance is considered to be indicated by a minimum of 0.84 volts at 100 mA/cm^2 at 70 to 90^{o}C for operation periods of at least 100 hours. In addition to the above performance requirement, an acceptable

electrode shall be one that does not show signs of physical degradation due to chemical or electrochemical attack, such as cracking, erosion, and loss of physical integrity.

3. The Contractor shall build two additional single-cell tests fixtures and test stands for life testing of single-cell fuel cells. He shall also build an additional six-cell test fixture and test stand for life testing. These test stands shall be instrumented to record voltage, current, gas pressure, and temperature. The necessary monitoring equipment, charging equipment, and load bank shall also be provided.

   a. Using the new test fixtures and stands specified above, as well as those already available, the contractor shall perform continuous life tests of at least two single-cell fuel cells and one six-cell fuel cell at the thirty-five minute discharge, sixty-five minute charge duty cycle. This is not to be construed as a requirement for continuous operation of two specific fuel cells or a specific six-cell fuel cell, but that the contractor shall have the test facilities in operation on a continuous basis with replacement of failed cells permitted. A minimum of at least 2000 hours of six-cell fuel cell testing and 4000 hours of single cell testing shall be accumulated during the period of performance. Fuel cells shall be discharged at current density of 100 mA/cm^2 and at 70 to 90^{o}C. Acceptable performance shall be defined as follows:

      Charge: A minimum of 8 amperes at a maximum of 1.7 volts/cell.

Discharge: A minimum of 14.0 amperes at a minimum of 0.70 volts/cell.

The contractor shall submit a detailed test plan outlining the life tests to be performed, test conditions, and anticipated number of tests within ten (10) working days after date of this Modification. At the completion of the testing required herein, the contractor shall recommend the type of electrode or electrodes to be used in the construction of the 500-watt fuel cell.

MODIFICATION No. 7 15 November 1966

Under Article I of the contract schedule, Phase II of Task I, as last changed by Modification No. 5, the contractor shall conduct the following described tests and experiments prior to commencing the work called for under paragraph 1 (e) of Amendment No. 3, Phase II, Task I:

4. The contractor shall conduct experiments to determine the proper matrix composition for use with the regenerative fuel cell. Potassium titanate fibers shall be used as the major matrix component. A non-reactive fibrous binder of organic or inorganic origin shall be used only if necessary to form a physically stable matrix.

   A mat six inches in diameter and 0.060 ± 0.003 shall be used as the standard. These compositions shall not be evaluated in extended life tests, but rather in chemical tests and electrochemical tests of short duration (1-72 hours). The following tests shall be performed.

   a. Chemical Tests
      (1) analysis and characterization of Potassium titanate as received, including trace elements
      (2) stability tests of potassium titanate in 30 and 45% KOH solutions at 75°C, 100°C, and 125°C (test times are 500 and 1000 hours)

   b. Determination of proper mat composition using potassium titanate fibers as the basic constituent.

Any binder used shall be inert in KOH and shall not react when used in the fuel cell. The binder should not represent more than 25% of the mat by weight. The performance and physical properties shall be compared to fuel cell asbestos board, the 75%-25% potassium titanate-asbestos mat, and the 90%-10% potassium titanate-asbestos mat compositions for which preliminary screening tests were run (EOS - QL, Nos. 1,2, and 8, Contract NAS3-2781).

Prior to running electrochemical tests, the following physical tests shall be performed on the mats:

(1) porosity (dry)
(2) density (dry)
(3) electrolyte absorption
(4) conductivity (wet)
(5) gas permeability (wet)

c. The mat shall then be subjected to electrochemical single cell tests to determine the optimum electrolyte-mat ratio for use in the fuel cell. Weight ratios shall range from 1:1 electrolyte-mat to saturation. These electrochemical tests shall be run with the standard hydrogen electrode and the American Cyanamid 20 mg/cm^2 platinum oxygen electrode. Test conditions shall be those described in Item 6. Cycle time ratios can be varied with the prior approval of the NASA Project Manager.

5. The contractor shall obtain a teflon ceria matrix as fabricated by American Cyanamid, and evaluate the matrix to determine whether it can be used in the regenerative hydrogen-oxygen cell. To

accomplish this, the contractor shall perform the physical tests outlined in Item 4.b above. If the mat looks promising, the tests in Item 4.c. above shall then be performed. Cells shall be allowed to continue cycling until performance drops below values outlined in Item 7 below. At the conclusion of the tests outlined in this paragraph, a decision shall be made by the NASA Project Manager whether to continue work on the teflon ceria matrix or the potassium titanate matrix. Based on this decision of the NASA Project Manager, the remaining life tests called for in Item 6 below shall be run with the selected matrix.

6. The American Cyanamid electrode with gold plated collector screen and 9 mg/cm^2 platinum loading has been found, during the preliminary screening, to be the most acceptable for an oxygen electrode. This electrode shall be used in all single and six cell tests. In an effort to completely characterize the electrode, the following tests shall be run on single cells. The contractor shall construct three single cells containing potassium titanate mat with reference electrodes, standard hydrogen electrode and the American Cyanamid oxygen electrode. The cells shall then be placed on continuous life cycle tests, except when performing the following experiments.

   a. Obtain a polarization curve at current densities of 25, 50, 100, 300, and 500 mA/cm^2 for each cell before and after completion of the life test.

   b. In order to determine the various sources of polarization within the cell, the contractor shall imbed reference electrodes within the mat. For these tests, the mat can be composed of three layers of 20 mil material with

reference electrodes between each layer. The purpose of this construction shall be to determine the division of polarization within the cell before, during, and after life cycle tests. In addition, the contractor shall determine the potential with respect to electrolyte resistance as the cell is charged and discharged. The measurements shall be made:

(1) at standard charge discharge conditions, 9-10 amps charge - 18 amps discharge.

(2) at 10 amps charge - 10 amps discharge

(3) at 18 amps charge - 18 amps discharge

An AC bridge shall be used to make the measurements. Other methods of measurement may be used with the prior approval of the NASA Project Manager.

c. After failure on life cycling of the three cells, as defined in Item 7 below, the contractor shall perform the following tests. The oxygen electrodes shall be removed from the cells and washed with hot (75°C) 5 N KOH for 2 hours. The electrodes shall then be rinsed with distilled water and dried. The electrodes shall be placed back in the cell and a polarization curve determined as specified in 6.a. above. The curves shall then be compared to the initial tests. If electrode performance improves due to the wash, the wash solution will be analyzed spectrographically along with the standard pre-electrolyzed 40% KOH solution.

d. The six electrodes from the tested cells plus two samples of electrode material not tested shall be examined to determine whether there has been a change in the catalyst surface area. The B.E.T. method of measurement shall be used for this determination.

e. In order to determine whether platinum migration occurs by some soluble form into the mat where it is reduced by hydrogen, the following test shall be run. An oxygen concentration cell shall be run for 50 cycles. At the end of this time the cell shall be purged of all oxygen and filled with hydrogen. After an overnight stand, the cell shall be disassembled and examined. If no visible change in the mat is noticable after stand, the cell shall be run for two cycles and then re-examined for precipitated platinum in the membrane which is characterized by a black discoloration. The material, if any, shall also be analyzed chemically to determine its identity.

At the completion of the testing required herein, the contractor shall proceed to Task II, Phase II of this contract.

7. Using the test fixtures and stands available, the contractor shall perform continuous life tests of at least two single cell fuel cells and one six cell fuel cell containing the best combination of components at the thirty-five minute discharge, sixty-five minute charge duty cycle or any other regime, as approved by the NASA Project Manager. This is not to be construed as a requirement for continuous operation of two specific fuel cells or a specific six cell fuel cell, but that the contractor shall have the test facilities in operation on a continuous basis with replacement of failed cells permitted. A minimum of 32,000 cell hours of testing in single or six cell configurations, with at least 10,000 of the hours in six cell stacks are to be accumulated during the period of performance of the contract which includes the testing previously conducted under paragraph .3 of Amendment No. 5. Fuel cells shall be

discharged at current density of 100 mA/cm^2 at 70°- $100^{\circ}C$. Acceptable performance shall be defined as follows:

Charge: A minimum of 8 amperes at a maximum of 1.7 volts/cell.

Discharge: A minimum of 14 amperes at a maximum of 0.7 volts/cell.